University of Southern Queensland

School of Engineering

Advanced Numerical Simulation of Rock Joints Load Transfer Mechanisms Under Various Geotechnical Conditions

A dissertation submitted by

Niraj Nitesh Kumar

in fulfilment of the requirements of

ENP4111 Professional Engineer Research Project

towards the degree of

Bachelor of Engineering (Honours) (Civil)

Submitted November 2024

This page intentionally left blank

University of Southern Queensland

School of Engineering

ENP4111 Dissertation Project

(This is a 2-unit research project in Bachelor of Engineering Honours Program)

Limitations of Use

The Council of the University of Southern Queensland, its Academic Affairs, and the staff of the University of Southern Queensland, do not accept any responsibility for the truth, accuracy or completeness of material contained within or associated with this dissertation.

Persons using all or any part of this material do so at their own risk, and not at the risk of the Council of the University of Southern Queensland, its Faculty of Health, Engineering and Science or the staff of the University of Southern Queensland.

This dissertation reports an educational exercise and has no purpose or validity beyond this exercise. The sole purpose of this dissertation project is to contribute to the overall education within the student's chosen degree program. This document, the associated hardware, software, drawings, and other material set out in the associated appendices should not be used for any other purpose: if they are so used, it is entirely at the risk of the user

CERTIFICATION

I certify that the ideas, designs and experimental work, results, analyses and conclusions set out in this dissertation are entirely my own effort, except where otherwise indicated and acknowledged.
I further certify that the work is original and has not been previously submitted for assessment in any other course or institution, except where specifically stated.

Student Name: Niraj Nitesh Kumar
Student Number: [redacted]

[redacted]

Signature

4th November 2024
Date

Abstract

Joints in a rock mass have a significant effect on the shear strength and deformation properties of the rock mass. Different experimental research projects have been performed since the last decades on the rock joints using the conventional direct shear apparatus under constant normal load (CNL), where the normal stress which acts on the joint was assumed to be constant during the shearing process. Moreover, recently a number of experimental research studies have been dedicated to shear strength of rock joints under constant normal stiffness conditions (CNS) where the dilation is not freely permitted during shearing. Despite the significant number of experimental studies on this topic, yet and to the best of authors' knowledge, there is no holistic and systematic numerical studies to investigate the shear load transfer mechanisms of rock. Hence, this project aims to investigate shear strength properties of rock joints under various geotechnical conditions for joints having various roughness distribution. The following items are studies numerically as part of this investigation:

- Effects of normal load on shear strength of rock joints
- Effects of joint roughness on shear strength of rock joints
- Effects of boundary conditions on shear load transfer mechanisms of rock joints
- Effects of shearing rate on shear strength of rock joints
- Effects of meshing size on shear strength of rock joints
- Scale and model size effects on shear strength of rock joints, and
- Effects of rock bolts on shear strength of rock joints

The study is conducted using two-dimensional distinct element code known as UDEC. Initially, available experimental data sets in literature are digitised. Subsequently, the collected data sets are simulated numerically using the developed subroutine programs. The above-mentioned items then will be investigated once the numerical model is calibrated using the digitised data from literature.

Acknowledgements

My heartfelt appreciation to my supervisors, to whom this thesis is dedicated: Prof. Ali Mirzaghorbanali. I owe a particular debt of gratitude to Prof. Ali for inspiring me to carry out a dissertation on a subject of my interest.

Prof. Ali had been generous with his time and guidance, despite having to contend with the numerous administrative duties required of as for the Professor. His suggestions with regard to mathematics, classic elastic solutions and addressing numerical artifacts, and advice on managing the overall progress of the project, are particularly appreciated.

They had been invaluable in overcoming the obstacles and difficulties that I had encountered throughout this dissertation. I am indebted to Prof. Ali for their encouragement and enthusiasm, which helped me persevere with the numerous numerical iterations.

Prof. Ali's advice on the expression of ideas, and persistent questions concerning the technical content of my work throughout this dissertation taught me to be meticulous and ensured that I had given the best of my ability, and more.

As he had continued to follow the progress of my dissertation closely, even after he had been very busy with major projects at work. Prof. Ali had also advised and made constructive comments on the draft of this thesis, for which I am extremely grateful. I also would like to thank my families, especially to my mother for her support which is unrepayable debt.

Contents

Figures

Tables

Glossary of Abbreviations and Symbols

Abbreviation		Meaning
a	-	Mean Asperity Height
A	-	Fracture surface area of the test
a_{max}	-	Maximum Amplitude or Offset
ASTM	-	American Society for Testing and Materials
B-B	-	Barton-Bandis Joint Model
c	-	Cohesion
c	-	Constant
CNL	-	Constant Normal Load
CNS	-	Constant Normal Stiffness
coh	-	Cohesion value in units of force per unit of area
CS	-	Coulomb Slip
C-Y	-	Continuously Yielding Joint Model
dens	-	Density
di	-	Initial dilation angle
dn	-	Peak dilation angle
E	-	Young's Modulus of Rock Mass
FISH	-	programming language embedded within UDEC
fric	-	friction angle
G	-	Shear Modulus
h	-	Upper block thickness
ISRM	-	International Society for Rock Mechanics and Rock Engineering
jcoh	-	Cohesion Value
JCS	-	Joint Wall Compressive Strength
jcso	-	Joint Compressive Strength
jfric	-	Friction Angle
jfric	-	Intrinsic Friction Angle
jifric	-	Initial Friction Angle
jkn	-	Normal Stiffness
jks	-	Shear Stiffness
JMC	-	Joint Matching Coefficient
join_contact	-	Command for individual joints or set of joints
jR	-	Joint Roughness Factor
JRC	-	Joint Roughness Coefficient
jrco	-	Joint Roughness Coefficients
jrough	-	Joint Roughness Value
js	-	Smoothness Factor
jtens	-	Tensile Strength
jw	-	Waviness Factor
K	-	Bulk Modulus
K_n	-	Normal Stiffness
L	-	Length of a Rectangular Jointed Block
L	-	Spacing between joints in the rock mass
L_j	-	Length of the edge should match that of the joint
M-C	-	Mohor Coulomb Joint Model
mm/min	-	Millimetre per minute

mm/sec	-	Millimetre per second
MPa	-	MegaPascal
N	-	Applied Normal Stress
N_0	-	Initial Applied Normal Stress
OCR	-	Overconsolidation Ratio
Pa/m	-	Pascal per meter
Q System	-	Classification system for rock masses with respect to the stability of tunnels and rock spaces
R	-	Rebound number on dry joint surface
RMR	-	Rock Mass Rating
sigmac	-	Uniaxial Compressive Strength
t	-	Thickness of infill
U	-	Waviness of the joint wall
u	-	Undulation
UCS	-	Uniaxial Compressive Strength
UDEC	-	Universal Distinct Element Code
v	-	Poission's Ratio
KNM	-	Machine's Normal Stiffness

Symbol		**Remarks**
ϕ	-	Joint Friction Angle
τ	-	shear strength
σ	-	Normal Stress
ϕ	-	Internal Friction Angle
σ_{n0}	-	Initial Normal Stress
σ_c	-	Compressive Strength of joint surface/intact rock
ΔF_n	-	Applied Normal Load
$\Delta\delta_n$	-	Change in Normal displacement
$\boldsymbol{\sigma_1}$	-	Maximum Principle Stress
$\boldsymbol{\sigma_3}$	-	Minor Principle Stress
$\boldsymbol{\tau_m}$	-	Designated Shear Strength
γ	-	Density of rock (kN/m³)
$\boldsymbol{\sigma_{peak}}$	-	Peak Shear displacement
δtot	-	Total sliding displacement
δp	-	Axial
δs	-	Shear displacement

1 Introduction

1.1 Background to the Study

Rock mechanics focuses on understanding the mechanical properties of rocks and the methods needed to design rock structures. In many rock engineering projects, such as those involving slopes and underground excavations, it's crucial to account for the impact of discontinuities on rock mass behaviour. This is especially important when the stability of infrastructure is affected by the shear behaviour of individual joints or multiple discontinuities in the surrounding rock, (Richard E. Goodman, 1991).

The overall strength of a discontinuous or jointed rock mass is governed not by the strength of the intact rock, but by the relatively weak shear strengths of the discontinuities. Accurately determining the shear strength of these discontinuities is crucial for designing safe and economical excavations within a fractured rock mass. The shear strength of discontinuities in rock masses is typically assessed using the standard Mohr-Coulomb strength parameters such as the joint friction angle and joint shear strength intercept (cohesion). These parameters are most often determined through direct shear tests conducted at a minimum of three different normal stresses on a single joint specimen, in accordance with ASTM and ISRM standards, (ASTM, 2016).

The issue with determining the shear strength parameters of a rock joint using the current standard method, is that specimens are sheared beyond their peak strength. This repeated shearing of a single damaged specimen damages the joint surface asperities, resulting in less accurate test results, (ASTM, 2016).

This testing-induced damage has been recognised in both the current standards (ASTM, 2016) as well as in previous research (Manuel J.A. Leal Gomes, 2009). Damaged surface asperities lead to lower observed peak shear stress values under successive normal stresses, which in turn causes underestimation of friction angle and overestimation of joint shear intercept (N. Barton, 1982).

1.2 Aims and Objectives

The objective of this study is to:

- Conduct an extensive review of literature pertaining to past research on the mechanical behaviours of rock joints, encompassing both experimental and numerical studies.
- Identify the optimal constitutive models for utilisation within Itasca's UDEC software (including options such as Mohr-Coulomb, Continuously Yielding and Barton-Bandis models) to effectively capture shear load transfer mechanisms in jointed rocks under both constant normal load (CNL), ensuring computational efficiency.
- Numerically analyse the impact of loading conditions (including dynamic loading) on shear load transfer mechanisms of rock joints.
- Investigate the influence of shear rate on the shear behaviour of rock joints.
- Explore the effects of scale size on shear load transfer mechanisms of rock joints.
- Examine the impact of rock bolts on shear load transfer mechanisms of rock joints.
- Investigate the effects of pre-tension values applied to rock bolts on their respective shear load transfer mechanisms.

1.3 Thesis Outlines

This thesis consists of (number) Chapters followed by a list of References and Appendices, including this Introduction (Chapter 1).

Chapter 2 presents a summary of literature review on the shear behaviour of rough joints. This chapter discusses the factors that controls the shear behaviour of rough rock joints. Subsequently, existing joint surface roughness characterisation methods, including joint surface measurement techniques and quantification approaches are briefly summarised. The highlights and limitations that existing methods have in characterising asperity deformation are also presented. Finally, a detailed review of the development of existing models that focus on CNL and CNS boundary conditions is also described.

Chapter 3 describes the Numerical modelling of rock joints shear behaviour under Constant Normal Loading (CNL), which is detailed using UDEC software program undertaken to study the shear behaviour of rough natural joints. This chapter includes the simulation of rock joint using UDEC 7.0 software for direct shear test and a brief description and modification of the model incorporating rock bolt to see the behaviour of the stress and displacement and, and also the data acquisition and process.

Chapter 4 provides the conclusion of this thesis which descriptions the shear behaviour of rock joints is substantially influenced by factors such as joint roughness, joint friction, dilation, compressive strength, UCS, velocity, normal load, and shear and normal stresses. Experimental data and results for the numerical simulations indicate that increased roughness and normal stress enhance shear strength.

2 General Review of Literature

2.1 Introduction

A rock mass is deemed discontinuous if it is intersected by any type of geological disruption (Goodman, 1993). According to (Gonzalez de Vallejo, 2011), intact rock which does not intersect by discontinuity is defined as rock mass or rock block. He also stated that discontinuity refers to a plane, created from mechanical or sedimentary processes, which divides that blocks of intact rock within the rock mass. Some examples of discontinuities includes:

- bedding planes
- foliation surfaces
- joints
- faults and
- dikes

Furthermore, (Gonzalez de Vallejo, 2011) stated that some of the properties of discontinuities can be determined by the impact on a rock mass which includes:

- shear strength
- roughness
- spacing
- persistence
- aperture
- infilling and
- orientation

(Gonzalez de Vallejo, 2011), expressed that the existence of discontinuities has a substantial influence on the strength and mechanical properties of the complete rock mass, and makes it problematic to assess its engineering capabilities.

(Barton, N & V. Choubey, 1977) stated that in a discontinuous rock mass, shear strength can be evaluated for both the intact rock and the features of the discontinuities.

He further highlighted that at shallow excavation depths of typical geotechnical engineering projects which has the low normal stresses, the shear strength along an unfilled discontinuity will be notably lower than the shear strength of the intact rock. Thus, the joint surfaces are known as the areas within the rock mass most prone to commence potential failure (Barton, N & V. Choubey, 1977).

2.2 Shear Behaviour of Rock Joints

As stated in (Stout, 1975) rock mechanics, shear stress refers to the stress acting parallel to a plane, while shear strength denotes the maximum measured stress that a discontinuity or solid rock can endure before experiencing failure.

In (Adachi, 1999), the primary factors influencing the shear strength of a solid jointed rock mass are as:

- in-situ normal stress
- strength of the undamaged rock material
- composition of joint infilling, and
- roughness of the joint surface

Studies carried out in (Tanimoto C, 1996), determines the shear strengths of the discontinuities by analysing the peak shear stress values. It refers to the maximum shear stress value exhibited by a discontinuity, or a solid intact rock just before the shear failure, to the point at which the discontinuity or the intact rock, starts to reduce the gathered shear stress.

In (ASTM, 2016) when the rock reaches its post-peak shear strength, it is often termed as the **residual strength**, which can be observed within materials and rock discontinuities. Post-peak shear strength refers to the stable (or the equilibrium) strength preserved by the material or discontinuity once it has sheared far off initial peak shear stress.

In this research, while the post-peak shear strength is not of main focus, the data is gathered from prior technical reports and conference presentations.

Referring to (Barton, N & V. Choubey, 1977), the primary parameters utilised to define the shear strength of geological materials typically includes the friction angle and cohesion values in the Mohr-Coulomb criterion. specifically, failure associated with:

- pre-existing joint surfaces
- parameters used are joint friction angle (φ), and
- joint shear strength intercept (c).

These parameters serve as indicators of a rock's ability to withstand shear stress. Figure 1 shows the Mohr-Coulomb Chart and the theory states that, shear strength (τ) is dependent on the normal stress (σ), internal friction angle (φ) and the cohesion (c) as presented in equation below (Grawira Ganjur Giwangkara1, 2020).

$$\tau = c + (\sigma \,.\, \text{Tan}\, \varphi) \qquad 2.1$$

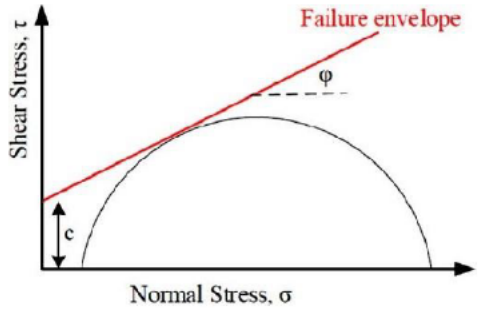

Figure 1: Mohr-Coulomb Chart on Shear Strength (Grawira Ganjur Giwangkara1, 2020)

2.3 Factors Controlling the Shear Behaviour of Rock Joints

According to (Thirukumaran, 2014) there are many factors that control the shear response to precisely predict the shear behaviour of the rock joints but are often challenging to measure and are often correlated. In this section the selected parameters are elaborated which affects the shear behaviour and are as follows:

- Boundary Conditions
- Joint Surface Roughness
- Joint Surface Strength
- Initial Normal Stress
- Presence of infill material (gouge)
- Shearing rate
- Scale Effect
- Degree of Matching
- Normal Stress History
- Presence of Water
- Joint Surface Roughness Characterisation
- Joint Surface Roughness/Characterisation

These parameters are discussed briefly in the following subsections.

2.3.1 Boundary Conditions

For rock joints, as stated in (Thirukumaran, 2014), the boundary conditions vary based on the deformability of the adjacent rock. And as the adjacent rock deforms sufficiently which allows the joints to dilate devoid of constraint, shearing occurs under zero normal stiffness. Thus, this boundary condition is referred to as Constant Normal Stress (CNL), where the boundary normal stiffness $K_n = 0$. Figure 2, illustrates the CNL conditions.

(i). Constant Normal Load (CNL condition) (ii). Rock Slope (non-reinforcement)

Figure 2: Represents the Constant Normal Load Condition (Y. Tasaku, Y. Jiang, Y. Tanahashi & B. Li, 2008)

(Thirukumaran, 2014) expressed that in most field situations, like underground excavations, joint dilation becomes constrained by the adjacent rock mass, leading to rise in normal stress exerted on the joint interface. Hence this condition is characterized as Constant Normal Stiffness (CNS) where, K_n is equal to a constant. Figure 3 below shows the joint behaviour of the rock in the roof and wall of an underground excavation (Indraratna S. T., 2015).

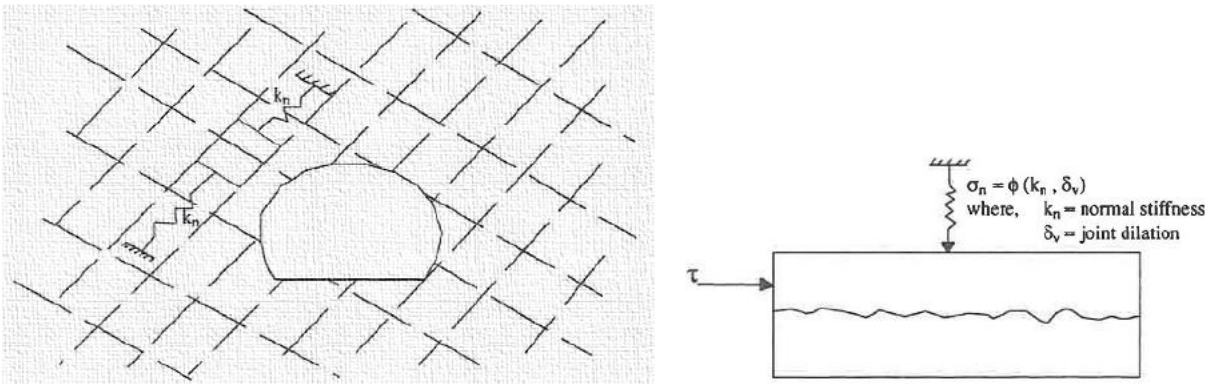

(i). Underground excavation in jointed rock (Indraratna S. T., 2015)

(ii). Representation of equivalent 2D model for jointed rock on the top of roof (Indraratna S. T., 2015)

Figure 3: Represents the Joint behaviour of the walls and roof in an underground excavation (Indraratna S. T., 2015)

Since the normal stiffness boundary (K_n) can fluctuate linearly or non-linearly from zero (referring to CNL) to the maximum value of the corresponding stiffness of the intact or the solid rock (Thirukumaran, 2014).

Therefore, (Skinas, 1990) recommended that for maximum boundary normal stiffness ($K_{n,max}$) can be expressed as the following formula:

$$K_{a.max} = \frac{E_r}{2c(1 - v^2)} \quad 2.2$$

where the parameters are as:

E_r - Young's Modulus of rock mass

L - Length of a rectangular jointed block

c - constant and

v - Poission's ratio

(Thirukumaran, 2014) reported that, over the last 3 decades there has been several research carried out on the effect of boundary normal stiffness on shear behaviour, and it was concluded that:

- shear strength increases due to an increase in the normal stiffness (K_n)
- joint dilation reduces due to the increasing of normal stiffness (K_n)

2.3.2 Joint Surface Roughness

(Nick Barton, 2023) reported that surface roughness plays an important role in estimating the shear strength of the rock joint, especially relating to undisplaced and interlocked features of unfilled joints. This is due to absence of the following:

- planarity means of dilation
- elevated local stresses and
- heightened permeability

(Thirukumaran, 2014), presented that the roughness of rock joints has substantial effect on the characteristics of jointed rock masses in relation to hydraulic and shear strength. Furthermore, it was reported that in earlier research, roughness of the joints were quantified as an effective dilation parameter (the mean inclination angle of asperity).

(Thirukumaran, 2014) further highlighted that, joint roughness becomes very intricate because of the unpredictable uneven shapes of the asperities. This complication may or can reduce the shear displacement to increase which leads to a gradually asperity damage. Hence, the shear displacement increases due to the declining of the inclination angle of asperity.

To address these challenges (Barton, N & V. Choubey, 1977) established a joint roughness coefficient (JRC), which is a numerical index ranging from 0 (smooth) to 20 (very rough). Since then, numerous studies have been carried out to refine the JRC concept or even creating new techniques in quantifying to calculate the roughness of the joints surface. Figure 4 presents the JRC index as mentioned in (Barton, N & V. Choubey, 1977).

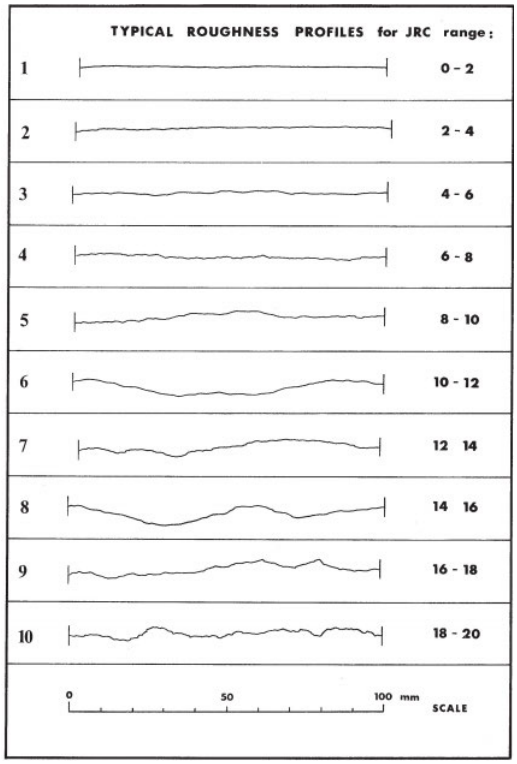

Figure 4: Joint Roughness Coefficient (JRC) 2-D Profile (Barton, N & V. Choubey, 1977)

(Thirukumaran, 2014), concluded that joints with reasonably larger roughness demonstrated increased shear strength and dilated farther compared to the lower roughness joints, regardless of the boundary normal stiffness.

2.3.3 Joint Surface Strength

(Thirukumaran, 2014) reported, that surface degradation of a Joint surface may take place during the shearing contingently upon the following factors:

- the strength
- the size
- the shapes of the asperities and
- the applied stresses

(Barton, N & V. Choubey, 1977), noted that the joint surface compressive strength (JCS) works as the main parameter that dominates the shear behaviour of joints, surpassing the significance of the tensile strength. He proposed that the JCS could be approximated as the compressive strength of intact rock for new joint surface (where no weathering occurs). Hence, for a weathered joint surface, the JCS should be assessed through the Schmidt Hammer Index Test.

(Barton, N & V. Choubey, 1977) concluded from their extensive test findings that, they inferred a joint surface built by a weaker roughness (low JCS to high JRC) is more prone to damage during shearing compared to a more robust smooth surface. Conversely both type of surfaces shows minimum dilation, in relation to surfaces with higher JCS and higher JRC dilates effectively upon reaching the peak strength.

2.3.4 Initial Normal Stress

(Thirukumaran, 2014), noted that the magnitude of initial applied normal stress relies mainly on the asperity damage. Therefore, most researchers use the ratio of the initial normal stress as the compressive strength of joint wall to study joint surface degradation, which is expressed as:

$$\sigma_{n0}/\sigma_c \quad (2.3)$$

where σ_{n0} – is the initial normal stress

σ_c – is the compressive strength of joint surface/intact rock

(Thirukumaran, 2014), noted that numerous researchers have concentrated on the impact of initial normal stress on the shear behaviour of joints subjected to CNS boundary conditions.

These research findings indicated that, under lower initial normal stress, the joint dilation was more definite (greater), as noted by (Thirukumaran, 2014), at the higher initial normal stress stage the asperities experience substantial damage, resulting in reduction of joint dilation. Hence, there was an increase in the peak shear strength as the initial normal stress increased.

2.3.5 Presence of Infill Material (Gouge)

(Thirukumaran, 2014) stated that in numerous natural joint, surfaces are divided by materials that could have either originated from the joint surface itself due to sequential tectonic activities or weathering, or they might have been carried by water flow. He further mentioned that the presence of Infill material within the joint surface generally decreases the shear strength of the joint due to the low frictional properties of the infill material.

Many scholars have examined that the shear behaviour of infilled joints is primarily influenced by factors such as:

- types of infill
- thickness of infill
- degree of saturation
- infill overconsolidation, and
- strength and roughness of the joint surface

(Thirukumaran, 2014), stated that, for infilled joints where the thicknesses of the fill exceeded a critical ratio of 1.5 (i.e.);

$$\text{ratio} = t/a \quad (2.4)$$

Where

- t - thickness of infill, and
- a – is the mean asperity height

The effect of the asperities is underlying, and the shear behaviour is manipulated by the infill.

(B Indraratna, 2008), concluded from has extensive investigation which concentrated on the influence of the infill overconsolidation affected on shear strength of infilled joints in which he stated that as the infill becomes overconsolidated (i.e. the overconsolidation ratio OCR), the peak shear strength of the infilled joint rose, while the critical t /a value decreased. Further in his studies (Indraratna B. , 2013) demonstrated that the shear strength of infilled joints increases as the degree of saturation in the infill decreased.

2.3.6 Shearing Rate

(A.M. Crawford & J.H. Curran, 1981) carried out a series of direct shear tests on dry joint specimens using CNL across various normal loads, with shearing rates ranging from 0.05 - 50 mm/sec. Their research indicated that the impact of shearing rate varies depending on the type of rock and the magnitude of applied normal stress.

They concluded that for hard rocks, shear resistance typically decreases with higher shearing rates, while for soft rocks increased, shear resistance increased up to a critical shearing rate, beyond which it stabilises.

(Haque, A & Indraratna, B , 2000), investigated the shearing rate under CNS boundary conditions through a series of tests on saw tooth model joints, spanning shearing rates from 0.35 to 1.67 mm/min, all under the identical initial normal stress of 0.56 MPa. They concluded that the peak shear strength of soft rock joints is affected by the shearing rate. After their study, they selected a shearing rate of 0.5 mm/min as the preferred value for their testing program.

2.3.7 Scale Effects

(Thirukumaran, 2014), reported that several researchers have experimentally examined the changes in the shear behaviour of joints with increasing scale and they have supported how the peak shear strength decreases with larger joint size due to a decrease in the effective (actual) contact area.

(Bandis. S, Lumsden. A C & Barton, N R, 1981), noted that a decrease in peak shear strength, peak dilation and shear stiffness as joint size increased in a comprehensive series of tests involving the replica rock joints.

They concluded that while the peak shear displacement increased as the joint scale increased, they mentioned that the scale effects were more evident in rough undulating joints but stayed minimum for planar joints.

2.3.8 Degree of Matching

(Thirukumaran, 2014), highlighted that the level of joint surface matching was directly related to the mechanical and hydraulic properties of a joint. The findings from (Zhao J, 1997a) and (Zhao J, 1997b) indicated that the tests on various granite joints demonstrated that the peak shear strength of unmatched joint was significantly lower than a matched joint with the same roughness.

Hence, the shear behaviour of a minimally rough joint remains unaffected by the degree of matching. To address this effect, (Zhao J, 1997a) introduced a numerical index termed the “joint matching coefficient” (JMC) to quantify the level of joint surface matching.

For instance,

- a joint with JMC = 1 denotes perfect matching.

where;

- a joint with JMC ≈ 0 indicates complete mismatch.

This joint matching coefficient (JMC) was subsequently integrated into Barton’s peak shear strength criteria (Zhao J, 1997b).

Furthermore (Thirukumaran, 2014), stated that (Zhao J, 1997a) observed that the asperities of a rough joint with mismatched surface are not as tightly interlocked as those of matched joint, resulting in relatively lower shear stiffness compared to matched rough joint.

As indicated in (Thirukumaran, 2014), (Zhao J, 1997a) stated that the surfaces of a natural joint frequently lack close matching due to the diverse geological processes like:

- weathering
- shearing and
- other forms of hydro-thermo-mechanical alterations

In contrast, a recently formed tensile fracture may exhibit closely matched surfaces.

2.3.9 Normal Stress History

(Barton, N, 1973), stated that majority of the natural joints surfaces do not completely close, and their level of closure varies based on the normal stress acting on them. As a result of fluctuations in the normal stress experiences at the joint interface over time, rough joints, especially those under tension, may experience mechanical over-closed.

(Barton, N, 1973), investigated how the normal stress influences the shear behaviour of the rock joints, introducing the notion of an overconsolidation ratio (OCR),

Represented as:

$$OCR = \sigma_{n0}/\sigma_{n1} \quad (2.5)$$

Where;

- σ_{n0} - normal stress acting on the joint plane before
- σ_{n1} - after disturbance (construction)

(Barton, N, 1973), carried a series of direct shear tests on the tension joints that were overconsolidated distinctly showed that as the OCR increased, the peak shear strength of the joint also increased. (Babanouri, 2011), in a more recent study emphasised the significance of the overconsolidation ratio on rock joints.

Both of their findings indicated that as the overconsolidation ratio rose, shear parameters such as, the peak shear strength, dilation, shear stiffness and degree of asperity damage increased.

Hence, the extent of overconsolidation would vary depending on:

- the engineering scenario
- the orientation of the critical joints set, and
- the magnitude of the horizontal stress

2.3.10 Presence of Water

(Barton, N, 1973), extensively studied the influence of water on rock joints, in which he determined that polished joint surfaces generally remained unaffected or exhibited increased shear strength when it was slightly wet.

He concluded that, presence of water generally reduces the strength of most rough joints. As this phenomenon could be related to the adverse effect that moisture has on the compressive strength of the brittle material, that governs the shear strength of rough joints.

2.4 Joint Surface Roughness Characterisation

For a considerable time, it has been acknowledged that the roughness of joints plays a crucial role on the mechanical and hydraulic behaviour of jointed rock masses (Thirukumaran, 2014). He stated that numerous have tried to develop a reliable and precise method for characterising the roughness of rock joint surfaces.

The primary aim of this subsection is to evaluate the current techniques for surface measurement and the methodologies employed in quantifying joint roughness that is utilised for characterising the roughness of joint surfaces.

2.4.1 Assessment/Measurement of the Joint Characteristics

(Patton F.D. , 1966) stated that, the significance of the surface features of joints in determining their shear strength. He acknowledged that the shear resistance arising from roughness on the joint surfaces needed to be surpassed during deformation, either through sliding or shearing.

Figure 5 shows the primary features of the joint which include:

i. joint surface smoothness,

ii. joint wall waviness or planarity,

iii. joint size or length,

iv. joint persistence and termination,

v. joint filling or coating, and

vi. synthesised in joint alteration

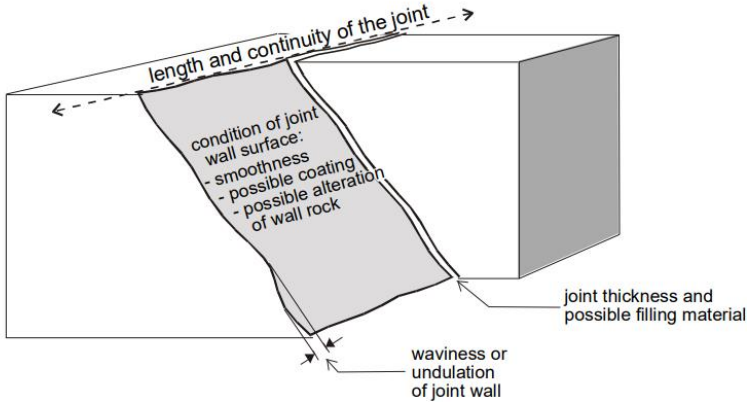

Figure 5: Shows the main joint characteristics, (Palmström A., 2001)

(Palmström A., 2001) stated, that the Q system incorporates joint roughness as a parameter. Initially, this system for assessing joint roughness was formulated in South Africa (Piteau, 1970, 1973) before being adopted in the United States by Cecil (1971).

The Rock Mass Rating (RMR) classification system considers the state of discontinuities, which encompass the following:

i. joint length and persistence,

ii. joint separation,

iii. joint roughness,

iv. in addition to infilling (gouge), and

v. weathering

2.4.2 Joint Roughness

(Patton F.D. , 1966) stated Joint roughness encompasses the state of the joint wall surface, whether filled or unfilled (clean) joints. A quantitative representation known as the joint roughness factor includes the macroscopic undulations of the joint wall, the waviness or planarity of the joint, and the microscopic smoothness of the joint surface, as shown in Figure 6. It has been estimated to split the roughness into these two distinct features since it is often simpler to assess them individually during the joint survey.

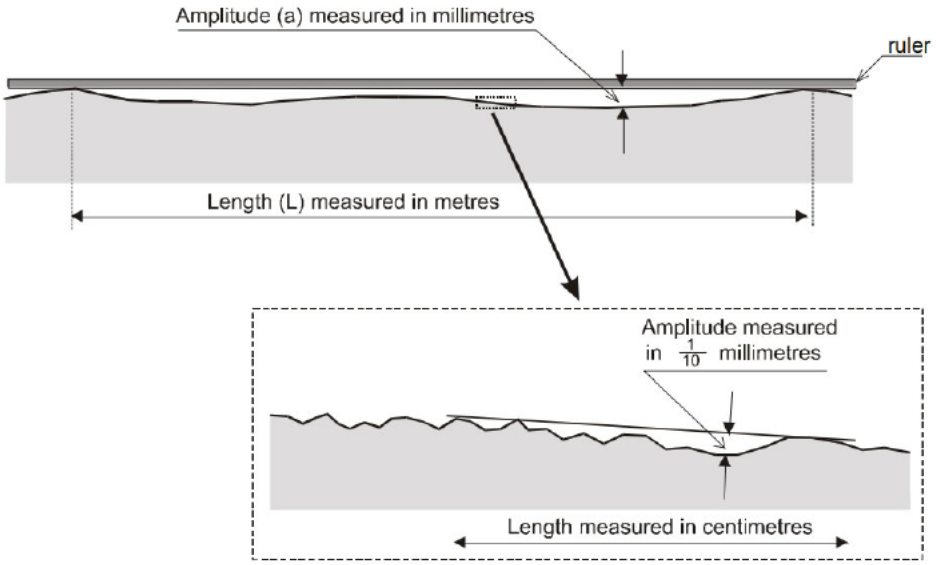

Figure 6: Shows the Macroscopic undulations or waviness of the joint plane (Top) and microscopic smoothness of the joint surface (Bottom) main joint characteristics, (Palmström A., 2001)

2.4.3 Joint Planarity or Waviness

The waviness of the joint wall establishes as deviations from planarity. It is described by the following expression.

$$U = \frac{\text{max. amplitude } (a_{max}) \text{ from planarity}}{\text{length of joint } (L_j)} \qquad 2.6$$

Whereas:

- a_{max} - the maximum amplitude or offset, can be determined by placing a straight edge on the joint surface.
- L_j - the length of the edge should match that of the joint, (this may not always be feasible).

Since observing or measuring the exact length of the joint is often impractical, simplifications are commonly made in determining **(U)**. A method outlined by Piteau (1970) suggests using a standard 0.9 m long edge, as illustrated in Figure 7. For smaller joints, even shorter lengths may suffice. The simplified waviness or undulation is then determined by the following equation, (Palmström A., 2001):

$$u = \frac{\text{measured max. amplitude (a)}}{\text{measured length along joint (L)}} \qquad 2.7$$

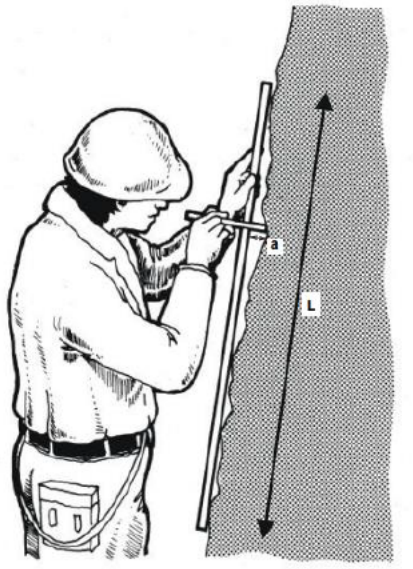

Figure 7: Shows the most precise and feasible assessment of joint wall waviness or undulation (according to Milne et al., 1992)

Following some familiarization with measurements, as illustrated in Figure 7, the joint waviness can be approximately evaluated through straightforward observations. In situations requiring numerous joint assessments, waviness is often determined through visual observation due to the time-consuming nature of the measurement, (Palmström A., 2001).

Table 1: Document Content Map

Term	Undulation (u = a/L)	Waviness Factor (jw)
Interlocking (large scale)		3
Stepped		2.5
Large undulation	u > 3%	2
Large undulation	u = 0.3 - 3%	1.5
Planar	u < 3%	1

2.4.4 Joint Smoothness

(Palmström A., 2001) mentioned that, surface smoothness or roughness refers to the texture of the asperities on the joint surface, discernible by touch. This characteristic significantly influences the state of joints. Clean and closed asperities on matching joint surfaces interlock, hindering shear movement along the joint surfaces.

Asperities typically exhibit a wavelength and amplitude measured in tenths of millimetres, as depicted in Figure 6, and are easily observable on a core-sized exposure of a discontinuity. The descriptive terms applicable to them are outlined in Table 2, (Palmström A., 2001).

Commonly, smoothness is assessed by physically examining the joint surface, utilising the descriptions provided in Table 2 to assign a rating for js. A more precise technique, particularly for determining the joint roughness coefficient **(JRC)** as defined by, (Barton N. R, 1976) is illustrated in Figure 8, also referenced in Figure 10, (Palmström A., 2001).

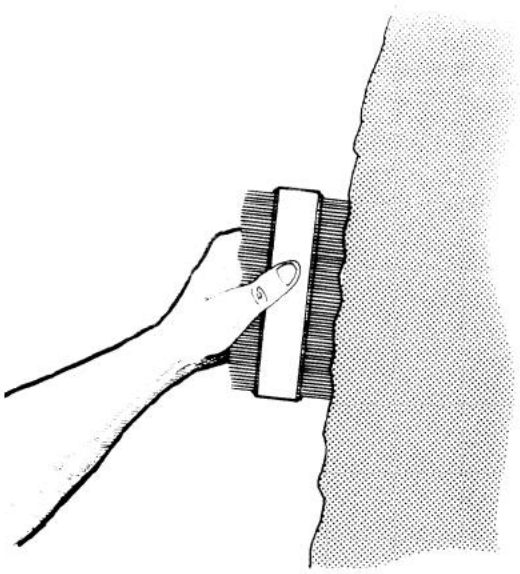

Figure 8: Shows the hands-on assessment of joint surface smoothness (according to Milne et al., 1992)

Table 2: The definition of the smoothness factor (js) as proposed by (Palmström, 1995)

Term	Description	Smoothness Factor, (js)
Very rough	Near vertical steps and ridges occur with interlocking effect on the joint surface.	3
Rough	Some ridge and side-angle steps are evident; asperities are clearly visible; discontinuity surface feels very abrasive. (like sandpaper grade approx.< 30)	2
Sightly rough	Asperities on the discontinuity surfaces are distinguishable and can be felt. (like sandpaper grade approx. 30 - 300).	1.5
Smooth	Surface appear smooth and feels so to the touch. (smoother than sandpaper grade approx. 300).	1
Polished	Visual evidence of polishing exists, or very smooth surface as is often seen in coatings of chlorite and specially talc.	0.75
Slickensided	Polished and often striated surface that results from friction along a fault surface or other movement surface.	0.6 – 1.5

Due to the limited visibility of the joint in drill cores, they offer only a restricted insight into the joint attributes, primarily providing indications of their smoothness, as show in Figure 9.

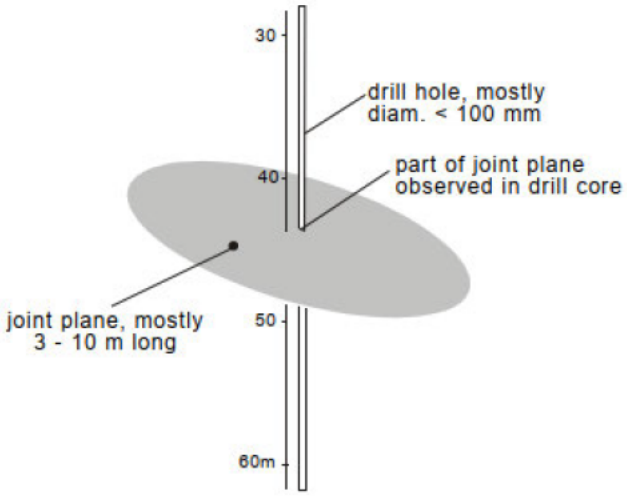

Figure 9: Shows very small portion of the joint observed in drill core, (Palmström A., 2001)

(Palmström A., 2001) suggested that, the joint roughness factor (jR) is calculated as the following expression;

$$jR = js * jw \quad (2.8)$$

or this can be obtained directly from Table 3.

Notably, the ratings for these parameters align with those used for Jr in the Q system. In instances where joint filling is sufficiently thick to prevent contact between the two joint walls, any shear movement will be confined to the filling, rendering the joint roughness of minimal or no significance.

In such scenarios, measuring the smoothness and sometimes even the waviness can be challenging or unfeasible. Consequently, the roughness factor is assigned a unit value.

Table 3: Combination of the joint waviness and joint smoothness factor into the joint roughness factor (jR), which is similar to (Jr) in the Q-system, (Palmström A., 2001)

(The ratings marked with *bold italics* are employed for Jr in the Q system)		**Large Scale Waviness of Joint Plane**				
		Planar	Slightly Undulating	Undulating	Strongly Undulating	Stepped or Interlocking
Small scale smoothness of joint surface	Very rough	2	3	4	6	6
	Rough	***1.5***	2	***3***	4.5	6
	Smooth	***1***	1.5	***2***	3	4
	Polished or slickensided*	***0.5***	1	***1.5***	2	3
	For filled joints jR = 1, For irregular joints a rating of jR = 6 is suggested					
* for slickensided surfaces the ratings apply to possible movement along the lineations						

In realistic application, smoothness is assessed by running the hand along the joint surface, while waviness is determined through simple observation after some training.

(Barton N. R, 1976) introduced the joint roughness coefficient (JRC), as show in Figures 10a and 10b, which provides an indication of the smoothness and waviness (planarity) along a 0.1m length of the joint.

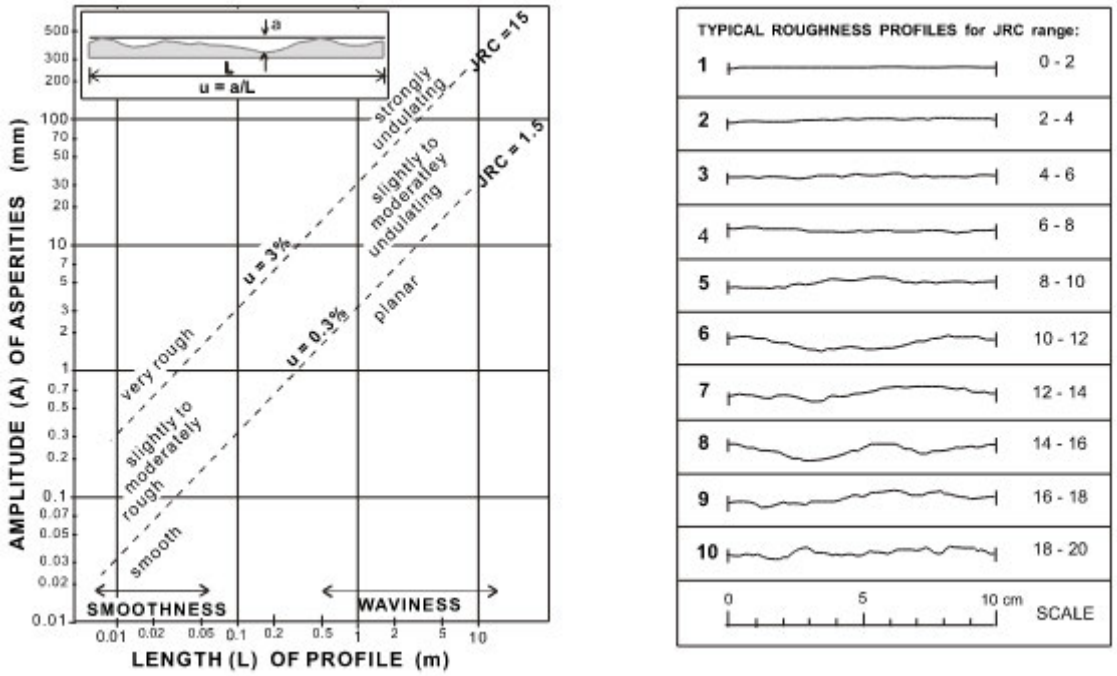

(a) Joint Roughness Coefficient (b) Joint waviness and smoothness

Figure 10: Shows the JRC introduced by, (Barton N. R, 1976)

2.5 Direct Shear and Multi-Stage Testing History

As far back as 1776 (Lambe T.W, Whitman, R.V, 1969), Coulomb employed direct shear testing as a laboratory method to ascertain soil material properties. Even today, direct shear testing remains a prevalent practice for assessing both soil and rock discontinuities.

(Nicholas R. MacDonald, Timothy R. M. Packulak and Jennifer J. Day, 2023) stated that, the concept of multi-stage testing traces back to 1950 when it was initially applied in triaxial testing to evaluate soil strength properties.

(De Beer, 1950) conducted the original test stating, "by incrementally increasing the axial load and determining the corresponding minimum lateral principal stress for each step, a set of ultimate principal stress combinations is obtained. Mohr circles corresponding to these combinations can be constructed, and the envelope of these circles can be determined."

The literature indicates that (Taylor D.W, 1951), (Davis H.E, Holtz W.G & Housel W.S, 1951) and (Kovari K & Tisa A, 1975) adopted the multi-stage testing in both triaxial and direct shear testing of rock and soil has been evident since some of the earliest studies on direct shear testing.

While (Ripley C.F & Lee K.L, 1961) in early studies suggested that its implementation influences the strength outcomes of subsequent stages. The broader adoption was considered by (Kim M.M & Ko H-Y, 1979), (Kovari K & Tisa A, 1975) and (Taylor D.W, 1951) of a multi-stage technique was seen as a beneficial approach to gather additional data from a specimen, requiring only one sample for testing instead of multiple samples.

(Muralha J, 2007), also echoed this sentiment, asserting that employing a joint sample for a single shearing under a constant normal stress is impractical. Instead, multiple shearing under varying normal stresses are conducted on the same joint, facilitating the evaluation of its failure envelope.

In the initial proposed approach (Franklin J.A, Kanji M.A, Herget G, Ladanyi B, Drozd K, Dvorak A, Egger P, Kutter H, & Rummel F; et al., 1974 – 2006) for laboratory determination of direct shear strength, the direct shear test was described as a means of determining peak and residual shear strengths for a test horizon.

It was further stated by (Franklin J.A, Kanji M.A, Herget G, Ladanyi B, Drozd K, Dvorak A, Egger P, Kutter H, & Rummel F; et al., 1974 – 2006) that the proposed method, the utilisation of a multi-stage procedure was exclusively outlined and recommended for establishing extra residual strength values, without any reference to its application in determining additional peak shear strengths.

Following the attainment of peak strength, the original ISRM guideline states, "having established a residual strength, the normal stress may be increased or reduced, and shearing continued to obtain additional residual strength values."

2.6 Modern Practice for Laboratory Direct Shear Testing of Rock Joints and Fractures

(Nicholas R. MacDonald, Timothy R. M. Packulak and Jennifer J. Day, 2023) highlighted that, Laboratory direct shear testing of rock specimens entails applying a consistent shear displacement rate to a sample while maintaining an applied normal load, which is sustained under one of three boundary conditions:

- constant normal load (CNL),
- constant normal stress (CNL*), or
- constant normal stiffness (CNS)

The choice of a suitable boundary condition relies on the practical application of the test outcomes, as elaborated in Section 2.61. It's important to highlight that regardless of the boundary condition or

staging method employed in a test, all direct shear testing apparatuses consist of several components such as:

- a robust testing frame
- specimen holder
- devices for applying normal and shear loads
- instrumentation for monitoring load and displacement
- pressure maintenance mechanisms, and
- equipment for data acquisition

Additionally, these machines can be servo-controlled, allowing for user-defined computer programming to manage the testing process.

The programming of the servo-controlled component might differ based on the specific testing protocol. A depiction of a standard direct shear testing setup is provided in Figure 11.

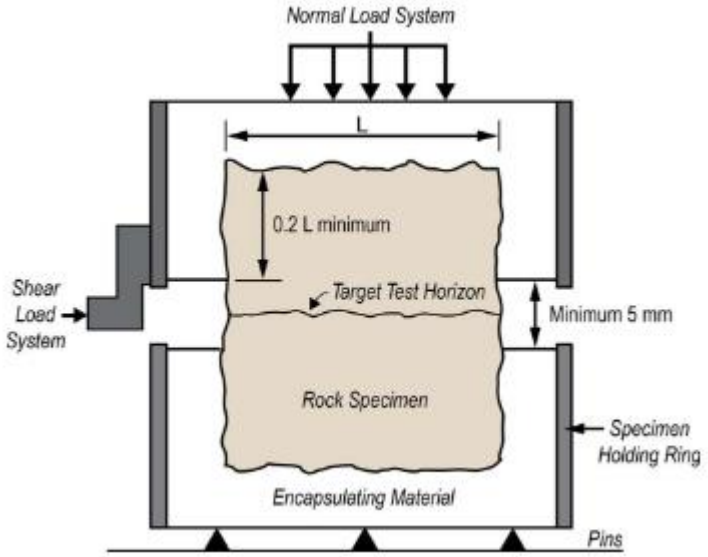

Figure 11: Shows the general test setup of a direct shear box with an encapsulated rock fracture specimen, (Nicholas R. MacDonald, Timothy R. M. Packulak and Jennifer J. Day, 2023)

In general, the initiation of all three boundary conditions involves imposing a specific target normal load or stress onto the test specimen. This is followed by applying a shear force at a consistent rate of displacement until reaching the yield, peak, and subsequently residual shear strengths.

Occasionally, two distinct peak shear strengths may manifest. Figure 12 and Figure 13, illustrates examples of these shear strength parameters derived from direct shear test data.

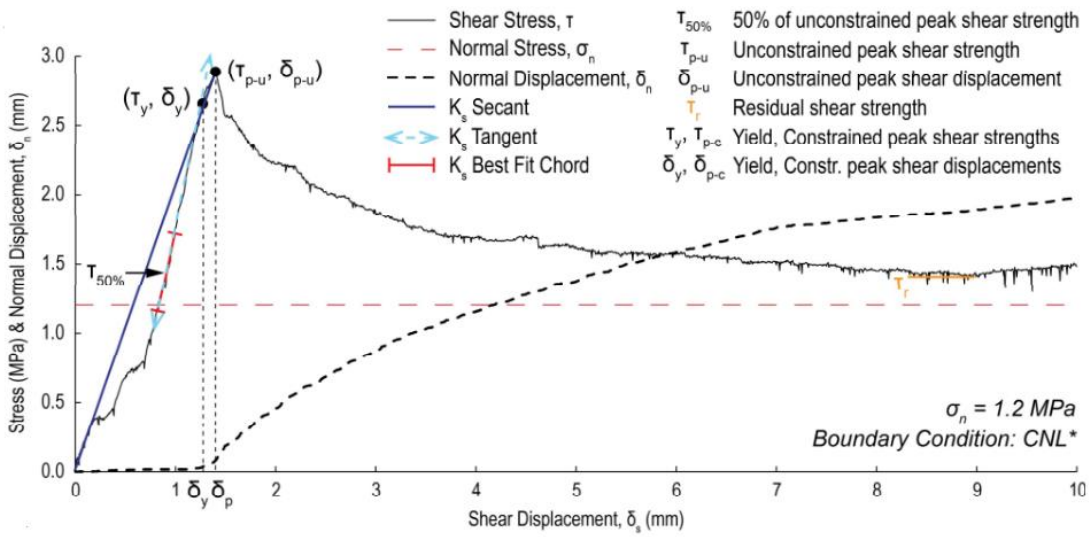

Figure 12: Shows the depicts shear stress versus shear displacement direct shear test data, along with standard linear shear stiffness measurements and shear strength parameters for a rough, clean limestone joint subjected to a constant normal stress (CNL*) boundary condition, (Nicholas R. MacDonald, Timothy R. M. Packulak and Jennifer J. Day, 2023)

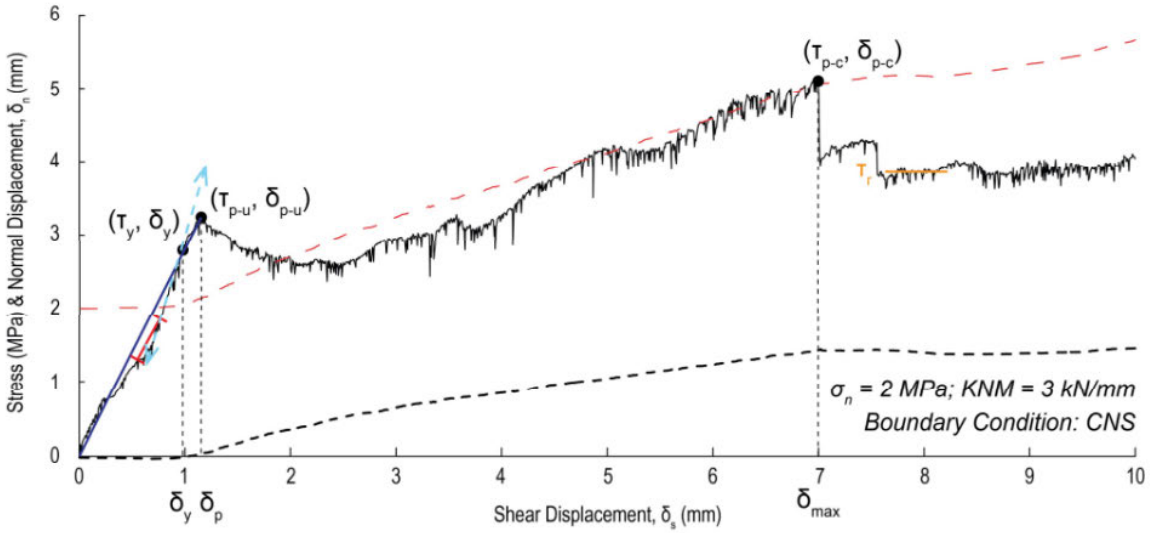

Figure 13: Shows the depicts shear stress versus shear displacement direct shear test data, along with standard linear shear stiffness measurements and shear strength parameters for a rough, clean granitic crystalline joint under a constant normal stiffness (CNS) boundary condition, (Nicholas R. MacDonald, Timothy R. M. Packulak and Jennifer J. Day, 2023)

2.6.1 Direct Shear Test Boundary Conditions

(Packulak T.R.M, 2018) and (Goodman R.E, 1976) stated the in laboratory direct shear testing, defining the boundary condition for sample testing is essential. Varying these conditions helps replicate real-world stress scenarios. Generally, this simplifies into two external conditions:

i. maintaining a relatively constant normal stress during shearing, achieved with CNL or CNL* boundary conditions, and

ii. allowing the normal stress to vary during shearing, achieved with a CNS boundary condition. Each boundary condition represents distinct scenarios encountered in rock engineering designs.

(Goodman R.E, 1976) mentioned that, employing CNL or CNL* boundary conditions reflects fracture behaviour in slopes and similar near-surface gravity-driven settings, where the applied normal load or stress remains consistent as shown in Figure 14.

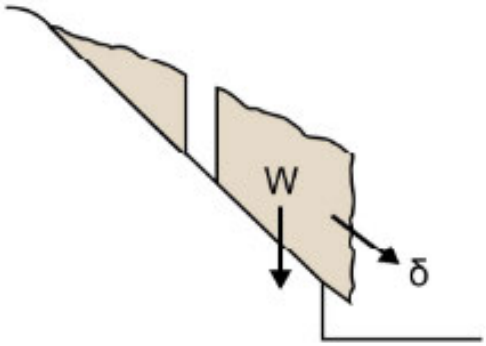

Figure 14: Shows the Sliding block along a slope (represented in laboratory tests by CNL/CNL* boundary conditions), (Goodman R.E, 1976)

Conversely, a CNS boundary condition typifies rock fractures near underground excavations like tunnels, mines, and nuclear waste repositories. In these settings, sliding blocks are constrained between parallel dilatant joints, where minimal to no normal displacement occurs, or there is a controlled stiffness response as depicted in Figure 15.

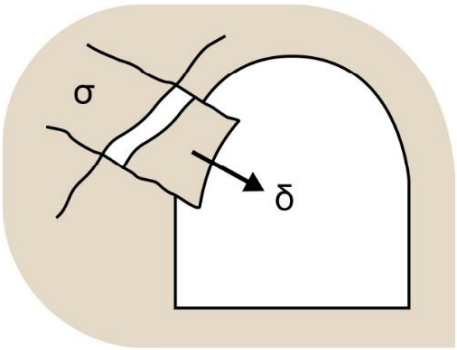

Figure 15: Shows the sliding block in an underground excavation (represented in laboratory tests by CNS boundary conditions), (Goodman R.E, 1976)

2.6.2 Constant Normal Load (CNL) and Constant Normal Stress (CNL*)

The traditional and original boundary condition utilized in laboratory direct shear testing is the Constant Normal Load (CNL), (Goodman R.E, 1976). CNL testing involves applying a consistent normal load to the specimen, accomplished through either weights or hydraulic pressure. This load remains constant throughout the duration of the direct shear test.

(Goodman R.E, 1976) further stated that, in recent years, advancements in servo-controlled laboratory direct shear machines have enabled the execution of direct shear tests under CNL* boundary conditions.

(Younkin G.W, 2003) mentioned that, a servo-controlled apparatus is an automated system that utilises a negative feedback loop from the system to regulate internal mechanisms, reducing the error between the machine input and the desired output.

In the case of CNL and CNL* testing, if the measured normal stress is lower than the input, the machine will adjust by increasing the normal load until the desired normal stress is reached during shear displacement. Utilising an input geometry that represents the cross-sectional target shear area of the specimen, the servo-controlled direct shear machine can compute and revise the contact surface area.

At every instance of shear displacement, the servo-controlled machine can determine the alteration in surface area and the speed at which shear displacement is happening. This capability enables the machine to continually compute and adjust the necessary applied normal load throughout the duration of a shear test.

Such ongoing feedback ensures that the applied normal load adapts appropriately, thus sustaining a consistent normal stress. An illustration of the evolving contact surface area of a specimen during CNL or CNL* testing process is demonstrated in Figure 16 and Figure 17 below.

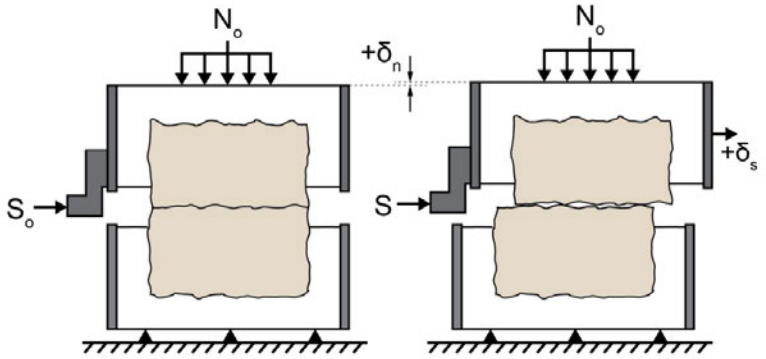

Figure 16: Shows the progressively changing specimen contact surface area during a laboratory direct shear test for a vertical section perpendicular to shear direction, (Younkin G.W, 2003)

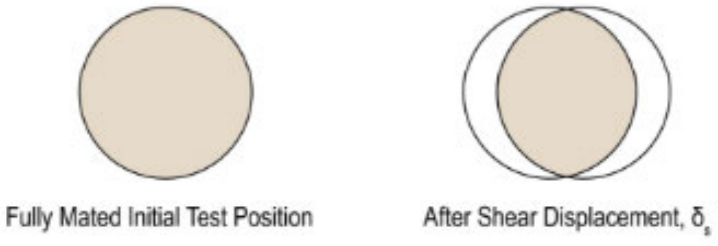

Figure 17: Shows the progressively changing specimen contact surface area during a laboratory direct shear test for the plan views of contact area within target shear surface horizons, (Younkin G.W, 2003)

2.6.3 Constant Normal Stiffness (CNS)

(Obert L, Brady B.T, & Schmechel F.W, 1976) confirmed in their study that, the CNL and CNL* boundary conditions accurately depict scenarios in near-surface projects where fractures are free to dilate, they are deemed inappropriate for projects at depth. In deeper projects, the dilation of fractures is constrained by the surrounding rock mass. They further, concluded that for jointed rock masses where dilation is restricted and a strengthening effect is observed due to the normal stiffness of the rock mass, a CNS boundary condition should be utilised.

In further research, (Johnston I.W, Lam T.S.K, & Williams A.F. Sr. , 1987) investigated the interface between cast-in-place concrete piles and a sandstone rock mass. Their findings suggested that employing a CNS boundary condition better reflects the shear behaviour of rough rock joints when dilation is restricted. This highlights the applicability of a CNS boundary condition in such scenarios.

(Obert L, Brady B.T, & Schmechel F.W, 1976) and (Indraratna B, Haque A & Aziz N, 1999) stated that, a CNS boundary condition entails limiting a fracture's dilation capacity, leading to a rise in the applied normal stress. Consequently, this elevation in normal stress enhances the measured shear strength of the fracture.

The alteration in the applied normal load **(ΔF_n)** to the test specimen is contingent upon the change in normal displacement **($\Delta\delta_n$)** of the specimen and the normal stiffness of the machine **(KNM)**, as expressed in equation 2.6, (Obert L, Brady B.T, & Schmechel F.W, 1976).

$$N = N_0 + \Delta F_n = N_0 + KNM(\Delta\delta_n) \quad 2.9$$

Where

- KNM - represents the machine's normal stiffness
- N - denotes the applied normal stress, and
- N_0 - represents the initial applied normal stress

The implementation of the CNS boundary condition can be achieved through two machine types, which are as, (Saeb S & Amadei B, 1992):

i. a CNL machine equipped with known stiffness springs, or

ii. a servo-controlled direct shear machine

In a spring-outfitted CNL machine, the lower half of the specimen box is restricted to horizontal movements, while the upper half is firmly constrained to vertical motion only. Additionally, to replicate CNS conditions, the constrained upper half of the box can solely move against a spring.

(Johnston I.W, Lam T.S.K, & Williams A.F. Sr. , 1987), stated that a steel shaft transfers the normal force through a load cell and a screw jack to a suspended spring system situated at the frame's top as illustrated in Figure 18a and Figure 18b.

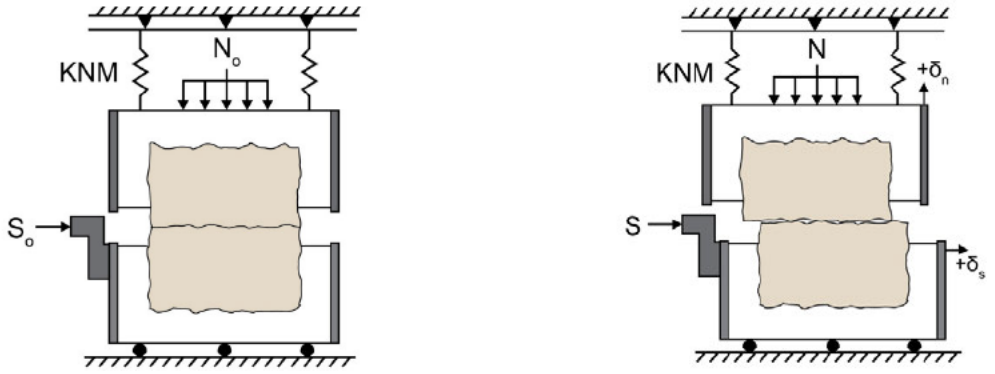

Figure 18:Depicts the vertical cross-sections perpendicular to the shear direction of constant normal stiffness (CNS) direct shear tests, illustrating (a, b)

In the case of a servo-controlled machine, a negative feedback loop is employed to meet a user-defined constant machine normal stiffness, as shown in Figure 19a and Figure 19b.

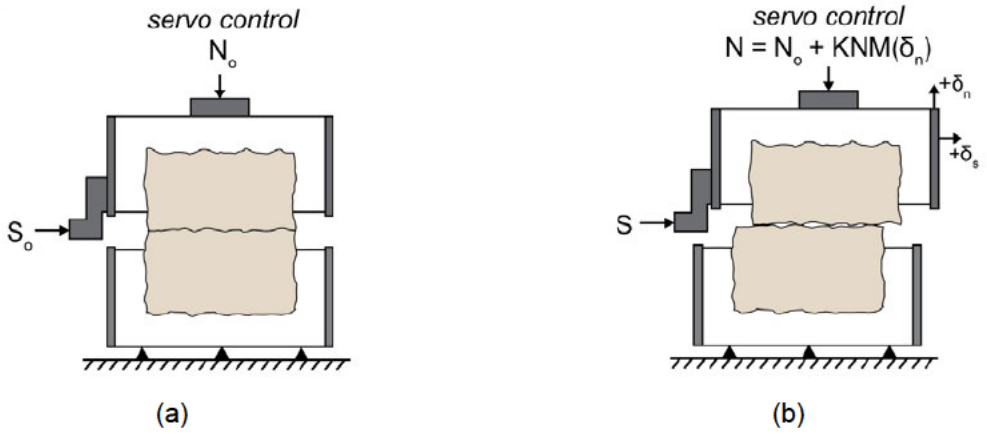

Figure 19:Depicts the vertical cross-sections perpendicular to the shear direction of constant normal stiffness (CNS) direct shear tests with physical springs with known stiffness (KNM) illustrating (a, b)

The servo control of KNM, shown on Figure 18a and Figure 19a, initial conditions and Figure 18b and Figure 19b shown the post-shear displacements.

(Packulak T.R.M, & Day J.J, 2022) mentioned in the underground tunnelling scenarios, the machine's normal stiffness (KNM) can be determined using the elastic properties of a rock block (Young's modulus **(E)**, and Poisson's ratio **(v)**, the spacing between joints in the rock mass **(L)**, and the fracture surface area of the test **(A)**. This calculation can be performed using the equation below.

$$KNM = \frac{E}{2L(1 - v^2)}A \qquad 2.10$$

2.6.4 Single and Multi-Stage Direct Shear Testing

(ISRM & Franklin J.A, 1974 - 2007) stated that, the typical method for conducting direct shear testing involves a one-stage process. It requires testing at least three to five specimens of similar characteristics sourced from the same discontinuity or sampling horizon.

Each specimen undergoes testing at varying normal stresses, and the outcomes are utilised to establish a shear strength envelope for the discontinuity. Once the residual shear stress of the tested specimen is determined, a one-stage test is considered complete.

Figures 20, [21], [22] and [23] below depicts the theoretical outcomes of four standard single-stage direct shear tests conducted at various normal loads, under CNL/CNL* boundary conditions, along with their respective failure envelopes.

Direct shear test data, representing various test methods under CNL/CNL* boundary conditions, including results from the legend:

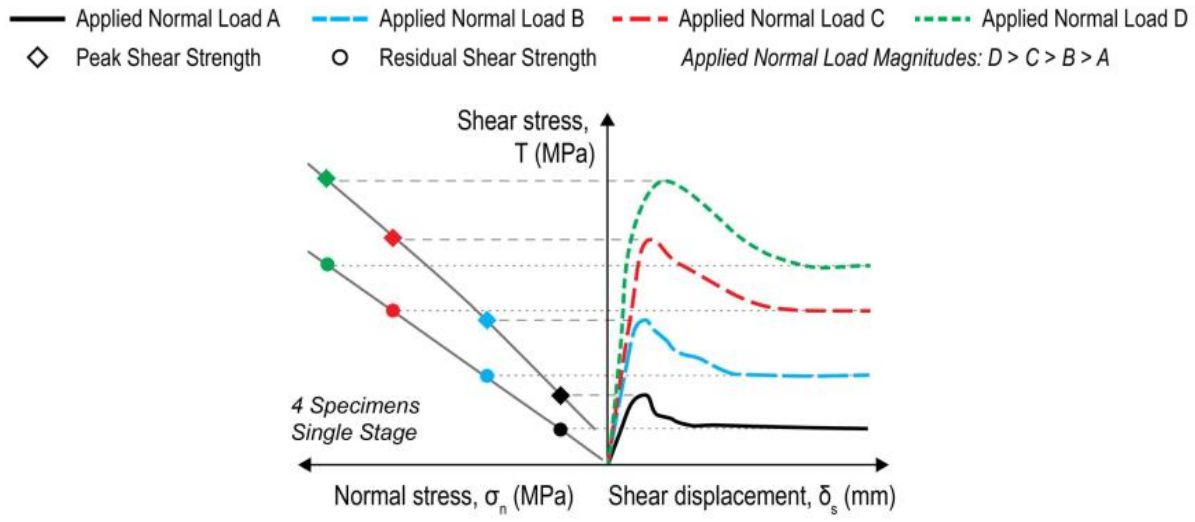

Figure 20: Shows a single stage comprising four specimens and their corresponding failure envelopes, (Nicholas R. MacDonald, Timothy R. M. Packulak and Jennifer J. Day, 2023)

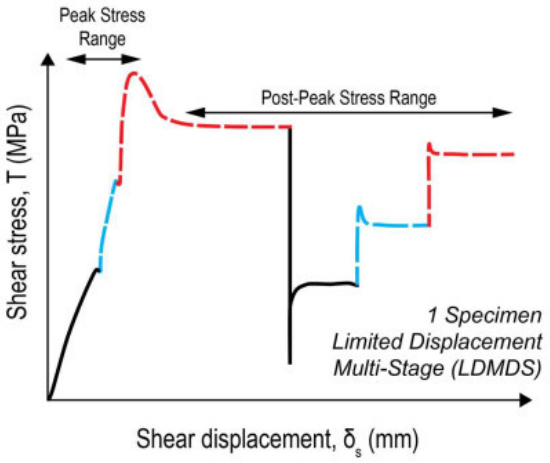

Figure 21: Shows multi-stage without repositioning from 1 specimen, (Nicholas R. MacDonald, Timothy R. M. Packulak and Jennifer J. Day, 2023)

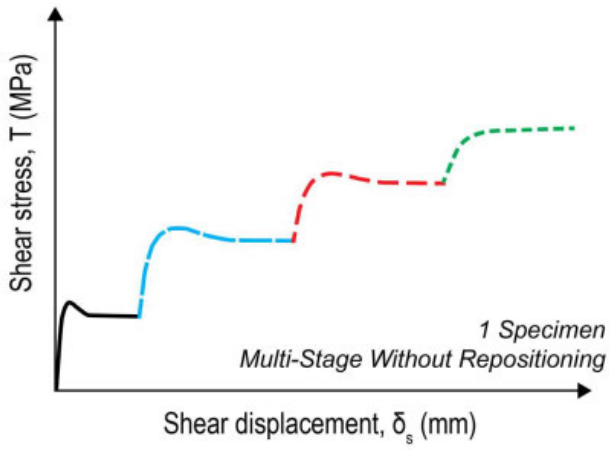

Figure 22: Shows limited displacement multi-stage from 1 specimen, (Nicholas R. MacDonald, Timothy R. M. Packulak and Jennifer J. Day, 2023)

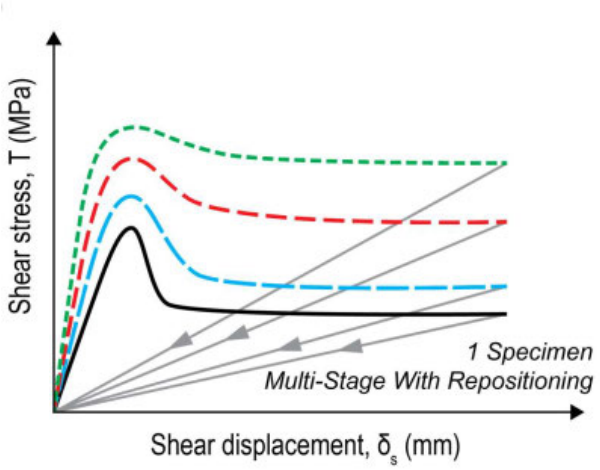

Figure 23: Shows multi-stage with repositioning from 1 specimen, (Nicholas R. MacDonald, Timothy R. M. Packulak and Jennifer J. Day, 2023)

2.6.5 Conventional Multi-Stage Direct Shear Testing

(Muralha J, Grasselli G, Tatone B, Blümel M, Chryssanthakis P & Yujing J, 2014) stated that, in practical terms, acquiring multiple specimens from the same discontinuity or set of discontinuities that share similar characteristics for conducting multiple single-stage tests can be challenging and costly. Consequently, it has become customary to conduct repeated tests on the same specimen under various increasing normal stresses to establish a failure envelope.

Comparable to the single-stage approach, establishing the failure envelope necessitates a minimum of three to five normal stresses. Unlike a single-stage test, the attainment of residual shear stress for a specimen denotes the conclusion of stage 1.

After stage 1, an additional two to four stages must be carried out on the same specimen. In a multi-stage testing protocol, two methods can be employed for the subsequent stages as follows:

i. multi-stage without repositioning, Figure 22

ii. multi-stage with repositioning, Figure 23

As per (ASTM, 2016), the repositioning entails resetting the specimen to zero shear displacement between each stage before incrementing the normal load. Alternatively, for subsequent stages, the specimen can initiate from the final position of the preceding shear stage.

Regarding the normal load applied in each stage, ASTM D5607-16 suggests that successive stages should use incrementally higher normal loads, starting from the minimum required. This approach helps minimize the impact of specimen degradation and wear. It's important to note that as per the current ASTM standard, establishing residual strength is necessary before increasing the normal load for each subsequent stage.

It is important to note a significant distinction between the ISRM publications from 1974 and 2014. Unlike the original 1974 ISRM Suggested Method, the revised 2014 version has withdrawn its recommendation to utilize multi-stage testing for obtaining additional residual strength values. Instead, it now advises to "evaluate the peak and ultimate or residual shear stress for each sample of the same rock joint or test horizon in the case of single-stage tests, or for all stages of multi-stage tests of the same rock sample" using data records and shear stress versus shear displacement graphs (ASTM, 2016).

(ASTM, 2016) also stated that, for a similar guideline apply for determining peak and/or residual dilation angles. While multi-stage results are taken into account for these parameters, it's important to acknowledge the limitations of multi-stage testing. The ISRM Suggested Method includes a cautionary note stating, "In the case of multi-stage tests, the apparent cohesion can be exaggerated due to accumulation of damage with successive shearing of the same joint specimen".

2.7 Numerical Methods

In this research, numerical models are developed utilising version 7.0 of the Universal Distinct Element Code (UDEC) software. This software (UDEC) is employing the distinct element code for discontinuum modelling in two-dimension (2D).

(Itasca, 2019), states that UDEC simulates the behaviour of the disjointed material (such as a jointed rock mass) under static or dynamic loading. The fractured material is depicted as a collection of discrete blocks.

(Poeck, 2016), stated the discontinuities are considered as the boundary (interface) conditions between blocks allowing significant displacements along them and rotations of the blocks. Each block can exhibit the characteristics of the rigid or deformable material.

Deformable blocks are divided into a mesh comprising finite-difference elements, with each element reacting based on a predetermined linear or nonlinear stress-strain relationship. The movement of the discontinuities is also controlled by linear or nonlinear force-displacement relationship for both the normal and shear directions.

UDEC includes various predefined material behaviour models for both the intact blocks and the discontinuities, enabling simulation that reflects the response typical of discontinuous geological or analogous materials.

(Itasca, 2019), uses UDEC as a Lagrangian based calculation approach, ideally for capturing the extensive moments and deformations within the blocky system. UDEC incorporates the robust built-in programming language called “FISH”. This feature allows users to write customised functions, enhancing the versatility of UDEC. This feature also provides the users with a distinctive ability to modify analyses to meet the specific requirements.

I have chosen UDEC because of its capability to simulate the softening characteristics observed in blocks and discontinuities which is a crucial aspect for investigating unstable failure. Furthermore, UDEC includes an energy calculation algorithm that consider the transfer and release energy when simulating variations in loading conditions or excavation geometry are simulated.

2.7.1 Model Construction

(Poeck, 2016), mentioned that UDEC operates through commands which requires the users to input commands directly into the command prompt or import them from an external data file for model construction and execution.

The Graphical Interface for UDEC, Itasca Codes (GIIC) aids users in constructing models through a menu-driven mode, the program’s operational principles remain consistent. Commands utilised in creating a model via the menu-driven mode are internally stored.

The menu-driven interface is generally not suitable for simulating complex underground infrastructure (road, rail tunnels and shafts) and mining projects. Such simulations often demand numerous:

- sequenced commands
- custom FISH functions for data management, and
- extended computation period of time between stages necessitating inputs.

(Itasca, 2019), states that UDEC defines a model by delineating the necessary 2D space for analysis and forming a single block covering the entire area. Subsequently, the block can be divided into smaller segments or shaped into various forms using joint commands and by eliminating undesired blocks. Joints can function as deformable geological discontinuities with appropriate constitutive laws and properties, or they can be employed to defined geometric boundaries before being eliminated.

2.7.2 Boundary Conditions

In (Itasca, 2019) manual it is mentioned that boundary conditions are essential for anchoring a model in space or constraining displacement along specific directions. For example, when gravity is applied to a model, it's necessary to limit the vertical motion at one or more boundaries to prevent infinite displacement during cycling.

Boundaries constrained solely in the direction perpendicular to their surface are termed as roller boundaries, whereas those constrained in both orthogonal directions are known as fixed boundaries. Open boundaries, such as the ground surface or the sides of an unconfined compression test specimen, are permissible, (Itasca, 2019).

Boundary conditions can additionally be employed to define a loading condition and will entail either stress or velocity designation. A stress boundary condition imposes constant forces to all of the grid points within a designated range. The magnitude of force applied to a grid point is determined by the desired stress level (value) and the spacing between adjacent grid points.

Further in (Itasca, 2019) manual, a velocity boundary condition imposes a consistent (constant) displacement to the grid points within a specified range. The incremental displacement incremented at each calculation step, or cycle, is calculated by multiplying the specified velocity by the mechanical time step.

UDEC employs a mechanical time step of 0.001 seconds for cycling the model and a velocity boundary condition of 0.5 meters per second is set at the boundary, the displacement of grid points will increase by 0.0005 meters at the start of each cycle. Consequently, the boundary displacement will accumulate to 1.0 meters after 2000 calculation steps, (Itasca, 2019).

A stress boundary signifies an exceptionally yielding (soft) loading condition, allowing displacements in the direction of the applied load to occur unrestrictedly and swiftly in the absence of the opposing forces, (Itasca, 2019).

This scenario would occur, if a stress condition of a suitable magnitude were imposed on an unconfined compression test specimen. On the other hand, the velocity boundary condition, when utilised with sufficiently small values, represents an exceedingly rigid loading condition. The failure of a compression test specimen can be meticulously managed through incremental displacements of small magnitudes, (Itasca, 2019).

2.7.3 Mesh Generation

In (Itasca, 2019) manual it is stated that, in order for blocks to become deformable, they need to be segmented into finite difference zones. Within UDEC, quad zoning creates square or rectangular zones comprising four internal triangular elements, touted as offering the most precise solution for plasticity issues.

On the other hand, edge zoning creates individual triangular zones with irregular edge lengths, suitable for filling irregularly shaped blocks and is suggested for scenarios where quad zones are impractical. Figure 24 illustrates the examples of quad and edge zoning.

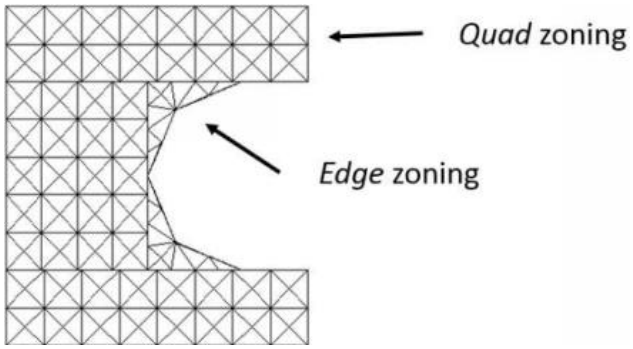

Figure 24: Example of Quad and Edge zoning in UDEC, (Poeck, 2016)

In this research the models developed, zones are created to predominantly from equilateral right triangles wherever feasible. This approach is taken to avoid zones with a high aspect ratio, nearing 10:1, as such ratio could potentially compromise solution accuracy.

2.8 Block Constitutive Models

(Poeck, 2016) states that, blocks that are rendered deformable necessitate allocation of a constitutive law along with material properties. The study employs three distinct constitutive laws which includes:

- an Elastic block model
- Mohr-Coulomb model, and
- Mohr-Coulomb strain softening model

Elastic blocks demonstrate a gradual linear increase in strain proportional to the applied load without any limit to its strength. Mohr Coulomb elements, on the other hand, shows a linear increase in strain with applied load until reaching peak strength, beyond which they undergo further deformation at a constant stress level, (Poeck, 2016).

This relation is alternatively known as nonlinear or exhibiting elastic-plastic behaviour. The strain softening version of the Mohr-Coulomb constitutive model, also termed as elastic-brittle-plastic, demonstrates a decrease in load-bearing capability once peak strength is attained, diminishing to a residual strength value with ongoing deformation. The simplified stress versus strain characteristics of each block constitutive model is illustrated in Figure 25, (Poeck, 2016).

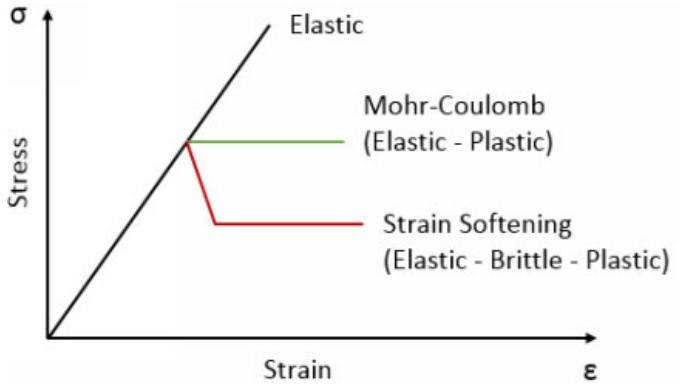

Figure 25: Generalized Stress-Strain Behaviour of Different Material Constitutive Models (Poeck, 2016)

The depicted shapes of the Mohr-Coulomb and strain softening curves in the figure depict the idealised response of a singular finite difference zone, but they may differ with the dimensions and configuration of a larger failing medium, (Poeck, 2016).

For example, board pillars housing numerous Mohr-Coulomb zones might not display a strictly elastic-plastic reaction, as the pillar's failure unfolds progressively when individual zones attain their peak strength across its expanse, (Poeck, 2016).

2.8.1 Elastic Blocks

(Itasca, 2019), Elastic blocks serve as valuable tools in evaluating stress distributions around excavations assumed to be in equilibrium and in estimating deformations resulting solely from elastic strain. With their infinite strength, elastic elements are not employed in materials anticipated to fail. Elastic elements find widespread application, notably in extending the far field region of the model to counter symmetry effects at the boundary or to act as inert mass in the overburden.

To incorporate elastic blocks into a model, only three material properties are used. Density is specified using the keyword **"dens"** and is quantified in terms of the mass per volume unit. In International Standard (SI) units, mass is measured in kilograms (Kg), whereas in empirical units, it is measured in slugs, (Itasca, 2019).

In UDEC, the stiffness of a block is determined by specifying a bulk modulus, denoted by **"bulk"** or **"K"**, and shear modulus is denoted as **"Shear"** or **"G"**, both measured in units of force per unit area. Bulk and Shear Modulus can be computed using Young's modulus **(E)** and Poisson's ratio **(v)** as expressed in the following equations, (Itasca, 2019):

$$K = \frac{\mathrm{E}}{3(1-2v)} \qquad 2.11$$

and

$$G = \frac{\mathrm{E}}{2(1+v)} \qquad 2.12$$

In UDEC, Young's modulus **(E)** or Poisson's ratio **(v)** cannot be directly inputted, nor will the software automatically derive the equivalent bulk and shear moduli. However, the built-in programming language **"FISH"**, within UDEC can be utilised to compute the bulk and shear moduli if necessary, (Itasca, 2019).

2.8.2 Mohr-Coulomb Blocks

(Poeck, 2016) states that, the Mohr-Coulomb strength criterion delineates the development of a failure plane due to normal and shear loading, derived from internal strength characteristics that can be assessed via compressive laboratory experiments. Integrated into numerical modelling codes, this criterion finds extensive application in geotechnical and is widely used in the following engineering analysis, (Itasca, 2019):

- Geotechnical,
- Structural, and
- Mechanical

This modelling helps in to ascertain the strength of intricate 2D and 3D structures subjected to diverse loading conditions.

When subjected to biaxial, compressive loading, an idealized material specimen, develops a shear plane labelled as **"ab"** upon reaching failure, as presented in Figure 26, (Itasca, 2019).

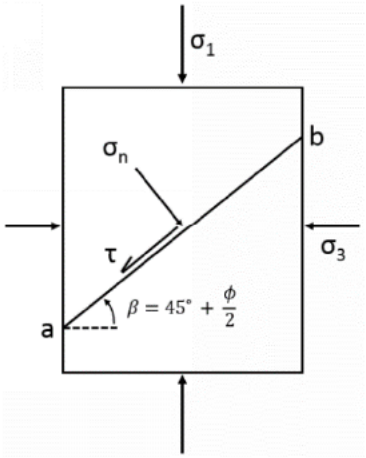

Figure 26: Biaxial, Compressive Loading of an Idealized Specimen, (Poeck, 2016)

The stress tangent to the failure plane is denoted by **τ,** while the angle of the plane's orientation relative to the horizontal axis within the specimen is represented by **β**.

Figure 27 shows Mohr's circle representing biaxial loading conditions. This demonstrates that, at a constant maximum principle stress **(σ_1)**, there exist a linear envelope where a specific value of the minor principle stress **(σ_3)**, leads to shear failure. Failure occurs at the point where Mohr's circle intersects this linear envelope. The Y coordinate of this intersection point indicates the shear stress acting on the fracture plane, (Poeck, 2016).

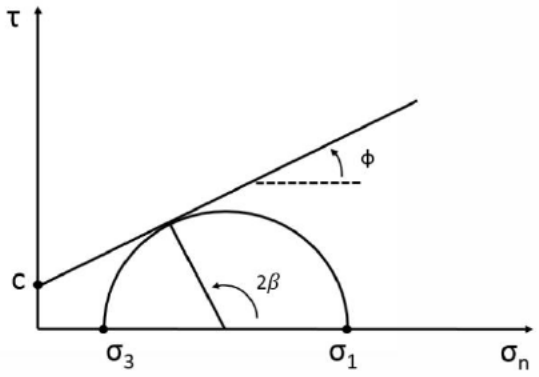

Figure 27: Diagram of Mohr's Circle for Biaxial Loading Conditions, (Poeck, 2016)

The linear envelope is determined by the internal friction angle **(φ)**, and the cohesion **(c)**, of the block material. Equation 2.11 encapsulates the Mohr-Coulomb criterion, expressing the shear stress developed along a failure plane as a function of the resultant normal stress on the plane **(σ_n)**, the friction angle **(Φ)**, and the cohesion **(c)**. Further, derivations can establish connections between the principle stresses to the shear stress or normal stress at the point of failure, (Poeck, 2016).

$$K = \mathrm{c} + \sigma\mathrm{n}(\tan \Phi) \qquad 2.13$$

(Itasca, 2019), within UDEC, both the density and elastic properties of Mohr-Coulomb blocks are defined with parameters identical to those used for elastic blocks. Strength characteristics of the blocks are determined through the utilization of specific keywords (codes) such as:

- ***fric*** - friction angle in units of degrees, and
- ***coh*** - cohesion value in units of force per unit of area

Optionally, users can also specify tensile strength and a dilation angle.

2.8.3 Mohr-Coulomb Strain-Softening Blocks

(Poeck, 2016) states that, in the Mohr-Coulomb strain softening constitutive model, the parameters including cohesion, friction angle, dilation angle, and tensile strength are subjected to modification post the initiation of plastic yielding. In contrast, the conventional Mohr-Coulomb model, these properties remain constant.

The distinction in stress-strain characteristics between these two constitutive laws is illustrated in Figure 25. This adjustment of strength parameters aims to emulate the typical behaviour of rocks under compressive loading, where the material's load-bearing capacity diminishes after failure, (Poeck, 2016).

A simple method of achieve strength reduction involves decreasing cohesion once a specific plastic strain threshold is reached. Desired cohesion values are stored in a table within UDEC, alongside the corresponding plastic strain levels at which these values are to be applied, (Poeck, 2016).

UDEC computes the strain on each zone in the model at every calculation step and interpolates the appropriate cohesion value from the softening table. Figure 28, shows a simple set of cohesion softening parameters, plotting cohesion values against corresponding strain values, (Poeck, 2016)

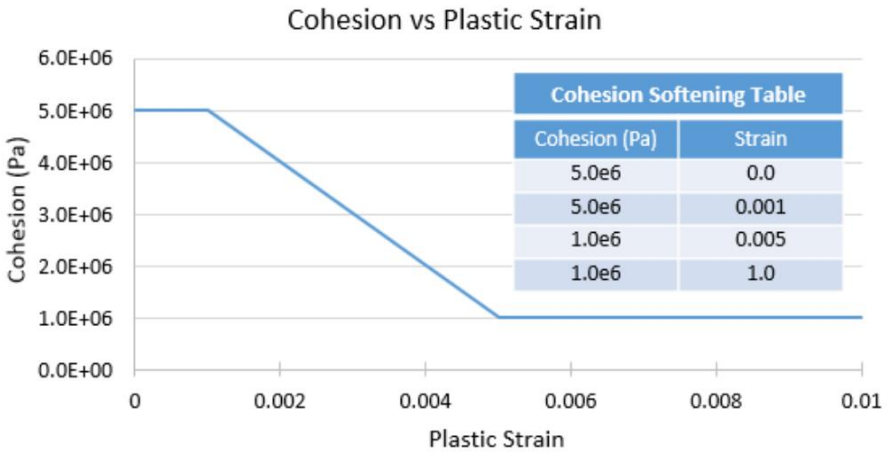

Figure 28: Simplified Cohesion Softening Parameters, (Poeck, 2016)

In most recent and advanced calibration methods (Tanimoto C, 1996) and (Edelbro, 2009), adjustments to the friction angle and dilation angle can be made to replicate behaviours observed in laboratory tests or specific site conditions.

Irrespective of the parameters used, the careful selection of an appropriate zone size is crucial when modelling materials exhibiting strain softening. To realistically simulate failure modes in a medium, it's essential to intersect the smallest dimension with numerous strain softening zones, (Poeck, 2016).

This approach ensures accuracy without excessively prolonging computation times. Once softening properties are calibrated for a specific zone size, they should be uniformly applied across the entire material model, (Poeck, 2016).

The decrease in strength observed in strain softening materials is crucial for studying and comprehending unstable failure phenomena. Under appropriate loading conditions, the failure of such materials allows for sudden displacements, representing the release of kinetic energy, (Poeck, 2016).

2.9 Joint Constitutive Models

(Cundall, 1990) studies, three distinct joint constitutive models were employed, these are as:

- the Shear slip along a fracture is regulated by either a fixed condition,
- the Coulomb Slip (CS) criteria, and
- a Continuously Yielding (CY) displacement-softening law

In a fixed condition, shear slip is completely constrained, and any deformation across the joint arises solely from elastic strain. A Coulomb slip model demonstrates elastic-plastic characteristics under shear loading, maintaining a constant shear stress post-failure, (Poeck, 2016).

The Continuously-Yielding joint model, designed for UDEC, demonstrates a decrease in shear strength after reaching the peak with ongoing deformation. The idealized shear stress versus shear strain behaviour for each of the three joint models is shown in Figure 29, (Poeck, 2016).

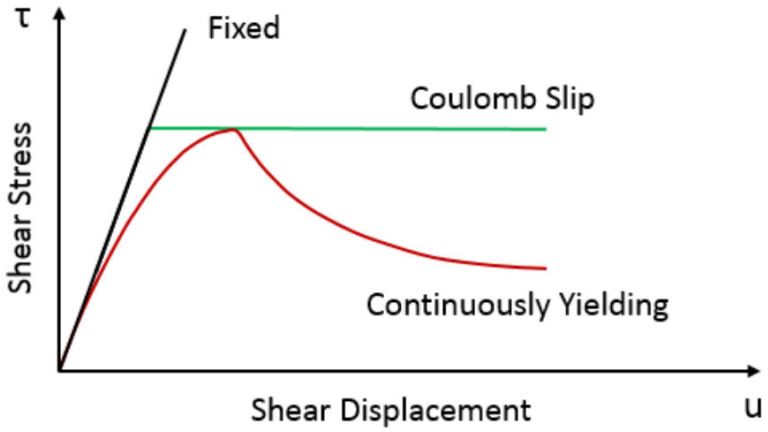

Figure 29: Generalized Shear Stress-Displacement Behaviour of Joint Constitutive Models, (Poeck, 2016)

Input parameters for normal and shear stiffness are necessary for each of the joint constitutive models. The shear stiffness dictates the extent of elastic deformation before the contact reaches its maximum strength, (Poeck, 2016).

The normal stiffness parameter regulates the degree of overlap between grid points on either side of the contact. Insufficient normal stiffness may result in numerical errors, while excessively high stiffness can prolong computation time, (Poeck, 2016).

2.9.1 Fixed Joints

The (Itasca, 2019) manual stated that, there are two methods to establish fixed joint conditions in UDEC. The first one can utilise the ***join_contact*** command for individual joints or set of joints in the model. Alternatively, applying a Coulomb slip constitutive model at specific joint locations and allocates artificially elevated or high strength properties.

Connected contacts are inherently secured against shear or tension failure and are endowed with a normal stiffness, denoted as ***(jkn)***, which is 100 times the average block stiffness in the model. The shear stiffness, designated as ***(jks)***, is established as a set of half the value of the computed normal stiffness, (Itasca, 2019).

On the other hand, employing a Coulomb slip constitutive model with an exceptionally high failure envelope ensures the prevention of shear and tensile failure, allowing for evaluation of the impact of different joint stiffness values on the modelling results, when necessary, (Itasca, 2019).

2.9.2 Coulomb Slip Joints

A Coulomb slip joint mirror a failure plane created within a Mohr-Coulomb block but is treated as a pre-existing contact between two separate blocks. The stiffness of a **CS** joint is controlled by the identical normal and shear parameters outlined for fixed joints, (Itasca, 2019).

Strength is regulated by the following factors:

- friction angle **(jfric)**, measured in degrees
- cohesion value **(jcoh)**, in units of force per unit area

Tensile strength **(jtens)**, in the normal direction can be specified in units of force per unit of area or kept at a default at a default value of zero. If desired, Joint dilation can be assigned in units of degrees, (Itasca, 2019).

2.9.3 Continuously-Yielding Joint

(Cundall, 1990), mentioned that, the CY model aims to replicate the phenomena witnessed in shear experiments involving rock joints, including post-peak softening and dilation.

As outlined in (Itasca, 2019), the theory and Background section of the UDEC manual. The Continuously-Yielding model is regarded as more “realistic” compared to the standard Mohr-Coulomb joint model because it endeavours to incorporates certain nonlinear behaviour observed physical tests, such as:

- joint shearing damage,
- normal stiffness dependence on normal stress, and
- decrease in dilation angle with plastic shear displacement

The key characteristics as per the (Itasca, 2019) manual, the Continuously-Yielding model encompass the following aspects:

i. The shear stress/shear displacement curve consistently converges towards a predetermined “target” shear strength for the joint, meaning that the instantaneous slope of the curve directly correlates with the disparity between strength and stress.

ii. The designated shear strength steadily decreases with the accumulation of plastic displacement (a measure of damage).

iii. The dilation angle is calculated as the variance between the apparent friction angle (established by the present shear stress and normal stress) and the residual friction angle.

As a result of these assumptions, the model demonstrates the typical peak/residual behaviour observed in rock joints automatically. Additionally, hysteresis is evident during unloading and reloading cycles across all levels of strain, regardless of their magnitude, (Itasca, 2019).

The initial stiffness of a CY joint is determined by the identical normal and shear parameters as the rest of the joint models. Figure 29 demonstrates the effective stiffness of the CY joint diminishes gradually as shear strain develops during loading. The peak shear strength is defined by three parameters which includes, (Itasca, 2019):

- an initial friction angle ***(jifric)***, measured in units of degrees,
- an intrinsic friction angle ***(jfric)***, measured in degrees, and
- a joint roughness value ***(jrough)***, with units in meters

Similar to other constitutive laws governing shear failure, the peak shear strength of a CY joint influenced by the magnitude of normal force. In UDEC, the tensile strength of a CY joint is consistently assumed to be zero, (Itasca, 2019).

The behaviour of a CY joint resembles that of a discontinuity with asperities, which must be surpassed or damaged for shear displacement to transpire. Initially, sliding on a CY joint is governed by the joint roughness and the frictional characteristics between asperities, as illustrated in Figure 30, (Itasca, 2019).

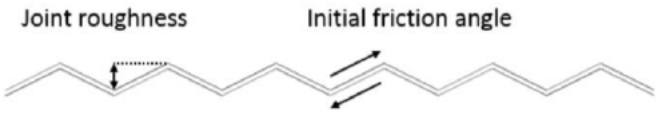

Figure 30: Conceptual Diagram of a Rock Discontinuity with Asperities. Initial Strength is Controlled by Asperities

With an increase in loading along the shear direction, the asperities undergo damage, and the residual strength of the joint is dictated by the intrinsic friction angle value. The residual condition of the joint is theorized in Figure 31, (Itasca, 2019).

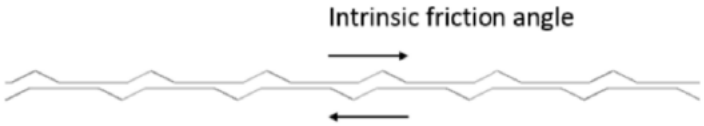

Figure 31: Conceptual Diagram of a Rock Discontinuity with Asperities. Initial Strength is Controlled by residual strength is reduced as asperities are damaged

CY joint suggests the capability to simulate unstable slip provided that the surrounding rock or loading system meets the requisite conditions for instability. In such instances, the post-peak reduction in shear strength exhibited by the CY joint allows the loading system to undergo sudden displacements which result in the release of kinetic energy, (Itasca, 2019).

(Cundall, 1990) stated the CY joint model allows the capability to simulate unstable slip that the surrounding rock or loading system meets the requisite conditions for instability. In such scenarios, the post-peak decline in shear strength demonstrated by the CY joint enables sudden displacements within the loading system, leading to the release of kinetic energy.

The CY model differs from the Mohr-Coulomb plasticity model by incorporating joint shear and normal stiffness dependencies on normal stress. Additionally, it considers non-linear hardening and softening behaviour in the post-peak stage, consistent with typical observations in physical discontinuity shear tests, (Itasca, 2019).

In a CY joint model, the curve depicting discontinuity shear stress versus displacement consistently converges towards a designated shear strength **(τ_m)**, by adjusting the instantaneous gradient of the curve according to the disparity between strength and stress as presented in Figure 32. The dilation angle is defined as the variance between the apparent and the residual friction angles, (Itasca, 2019).

The designated shear strength **(τ_m)**, is determined by both the normal stress and the accumulated plastic shear displacement of the simulated discontinuity, as defined Equation 2.14.

$$\tau_m = \sigma_n \, tan\phi_m sgn(\Delta u_s) \qquad 2.14$$

Parameter **(ϕ_m)** can be interpreted as the friction angle that would applicable if the joint were to undergo maximum dilation. As damage accumulates, this angle progressively decreases as per equation 2.12, (Itasca, 2019).

$$\Delta\phi_m = -1/R(\phi_m - \phi)\left(\Delta u_s^P\right) \quad 2.15$$

Hence plastic displacement increment is expressed as in equation 2.16.

$$\Delta u_s^P = (1- F)\,\Delta u_s \quad 2.16$$

ϕ represents the fundamental or inherent (intrinsic) friction angle (residual friction angle) of the rock surface. While R is a material parameter denoting the joint roughness, expressed in length, (Itasca, 2019).

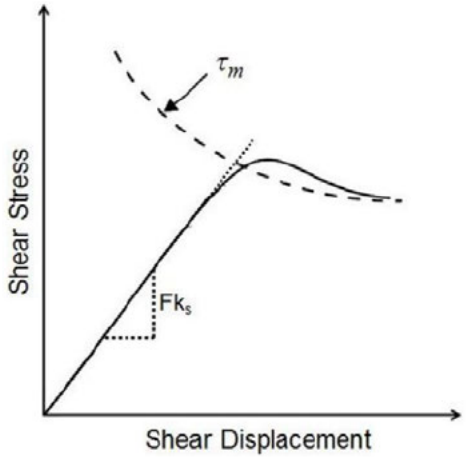

Figure 32: Schematic of Typical Shear Stress vs Displacement Curve and the Target Shear Strength (τ_m) of the CY Joint Model (after Itasca 2010)

With rising normal stress, the designated shear strength increases, consequently bolstering the shear strength of the simulated discontinuity. Conversely, as the accumulated plastic shear displacement increases, the designated shear strength gradually diminishes. This leads to the softening trend in the post-peak segment of the discontinuity shear stress-displacement curve, (Itasca, 2019).

The occurrence of post-peak softening is pivotal for analysing unstable shear failures. This research highlights the shear stiffness of a discontinuity is characterised as the quotient of applied shear stress to shear displacement within a linear elastic range, expressed in unit of Pa/m, (Itasca, 2019).

In the CY joint model, the shear stiffness is regulated by the parameter shear stiffness **(k_s)**, determining how stiff the joint behaves under shear stress. Normal stiffness of a dis-continuity is calculated as the ratio of applied normal stress to normal displacement and shares the same unit as shear stiffness (Pa/m), (Itasca, 2019).

2.10 Barton Model

In (Barton, N, 1973), the Barton-Bandis model was developed with the aim of considering how joint surface roughness influences both joint deformation and strength. The criterion for nonlinear joint strength is as follows:

$$\tau = \sigma_n tan\left[\phi_r + JRC\ log\left(\frac{JCS}{\sigma_n}\right)\right] \quad 2.14$$

where,

- JRC - is joint roughness coefficient,
- JRC - is joint wall compressive strength, and
- ϕ_r - is residual joint friction angle

As per (Barton, N & V. Choubey, 1977), unweathered rock joints, the residual friction angle (ϕ_r) matches the basic friction angle (ϕ_b). To estimate the residual friction angle of the weathered rock joints, Schmidt rebound on dry unweathered sawn surface (R) and the wet surface (r) can be used and expressed as:

$$\phi_r = (\phi_b - 20^o) + 20(\frac{r}{R}) \quad 2.15$$

(Barton, 1971) stated that, the Joint Compressive Strength (JCS) of an unweathered joint is equivalent to the uniaxial compressive strength of the intact rock. However, for a weathered joint, it may decrease to one-fourth of this value.

The Schmidt hammer, employing the Miller method (1965), can be used to measure the JCS of a weathered joint as expressed in the following equation.

$$log_{10}JCS = 0.00088_{\gamma} + 1.01 \quad 2.16$$

where,

- γ - is the density of rock (kN/m³)
- R – is the rebound number on dry joint surface

The JRC value starting from 0 for exceptionally smooth surfaces to a maximum of 20 for the rough surfaces. Determining JRC involves conducting a tilt test, where the joint set is gradually titled until the upper joint block slip under its own weight. The angle of tilt is then noted and JRC can be calculated as follows, (Barton, 1971).

$$JRC = \frac{\alpha - \phi_r}{\log(\frac{JCS}{\sigma_{n0}})} \quad 2.17$$

Where;

σ_n – represents the effective normal stress induced by the gravitational force exerted by the upper block with a certain thickness, expressed as:

$$\sigma_{n0} = \gamma h cos\alpha \quad 2.18$$

Where ***"h"*** represents the upper block thickness.

(Barton, N & V. Choubey, 1977) stated that, conducting the tilt test to determine JRC values exceeding 10 is typically impractical, primarily because of the risk of toppling prior to sliding and the

cohesion intercept. Moreover, throughout the tilt test the distribution of applied normal stress across the joint surface is non-uniform (Manuel J.A. Leal Gomes, 2009).

(Barton, N & V. Choubey, 1977) mentioned that, JRC can be retroactively determined from the outcomes of push or pull tests, however due to the influence of cohesion on joints with highly pronounced steps, a JRC value of approximately 12 is typically the upper limit for satisfactory testing. Additionally, JRC can be derived from the findings of direct shear tests conducted on rock joints.

In order to enhance the predictive accuracy of the shear criterion (Barton, N & V. Choubey, 1977), devised a set of typical joint profiles to estimate the JRC value through visual comparison with the joint surfaces, as shown in Figure 33.

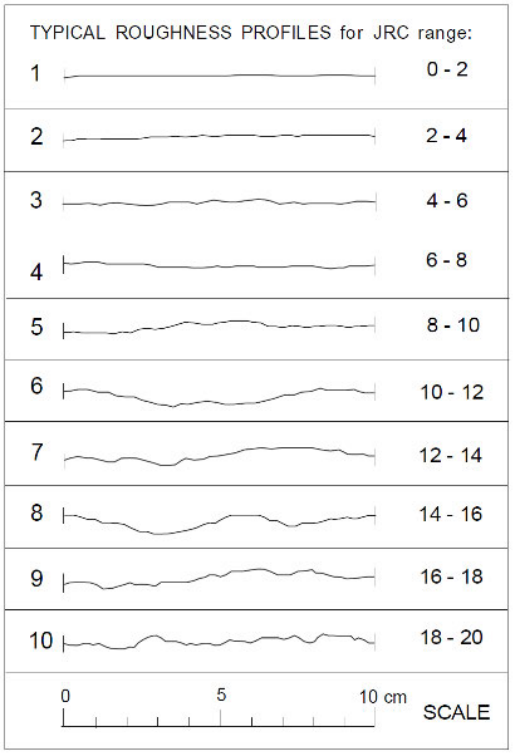

Figure 33: Estimation of JRC from joint profiles for laboratory scale by visual comparison to standard JRC profiles (Barton, N & V. Choubey, 1977)

(N. Barton & S. Bandis, 1982) mentioned that in practical field conditions, the extent of the joint surface can span several meters or even tens of meters necessitating the estimation of the JRC value on a full scale, devising a method to estimate JRC by utilising the maximum asperity amplitude, as illustrated in Figure 34.

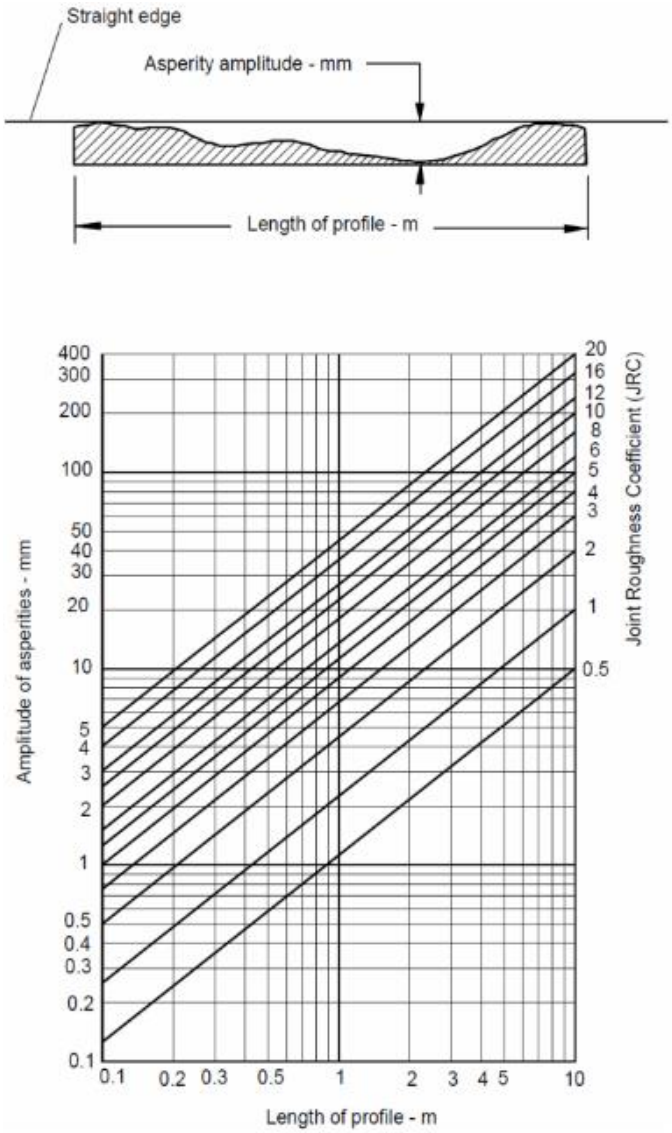

Figure 34: Estimation of JRC from joint profiles for large scale by measurement of the asperity amplitude (N. Barton & S. Bandis, 1982)

Figure 35, illustrates a typical outcome of a direct shear test. The peak shear displacement denoted as "σ_{peak}" represents the necessary shear displacement to attain the peak shear strength.

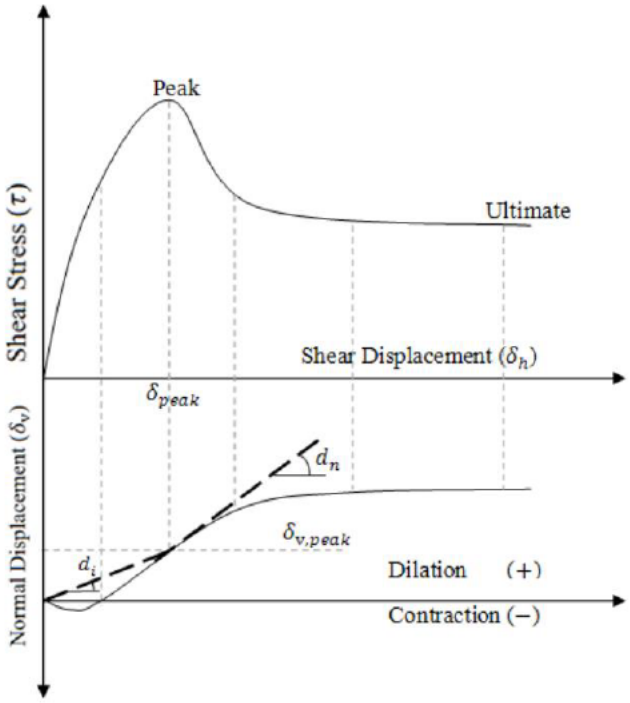

Figure 35: A typical result of direct shear test for rough rock joint, (B Indraratna, 2008)

The initial dilation angle **"d_i"**, and the peak dilation angle **"d_n"** are defined as follows expression:

$$d_i = \arctan\left(\frac{\sigma_{v.peak}}{\sigma_{peak}}\right) \quad 2.19$$

And

$$d_n = \left(\frac{\partial \delta_{v.peak}}{\partial \delta_{peak}}\right)_{at\ \delta_h = \delta_{peak}} \quad 2.20$$

(Barton, N & V. Choubey, 1977), conducted direct shear tests on 136 samples and determined that the average initial dilation angle is approximately one third of the peak dilation angle. They also observed that both initial and peak dilation angles can occasionally be negative or zero. Consequently, they suggested the following equations to estimate these parameters:

$$d_i = \frac{1}{3} JRC\ log\left(\frac{JCS}{\sigma_n}\right) \quad 2.21$$

And

$$d_i = \frac{1}{M} JRC\ log\left(\frac{JCS}{\sigma_n}\right) \quad 2.22$$

As per (N. Barton, 1982), many numerical methods employed to simulate the **"full"** stress-displacement characteristics tend to exhibit an overly cautious, sudden decline towards residual strength. Figure 36 presents a viable model that integrates suitable values of (JRC_{mob}/JRC_{peak}) and (δ/δ_{peak}) for a comprehensive representation of rock joint behaviour, aligning with observations from shear tests. The figure below shows the modelling of strength-deformation-dilation trends, noting that ***"i"*** changes with the normal stress.

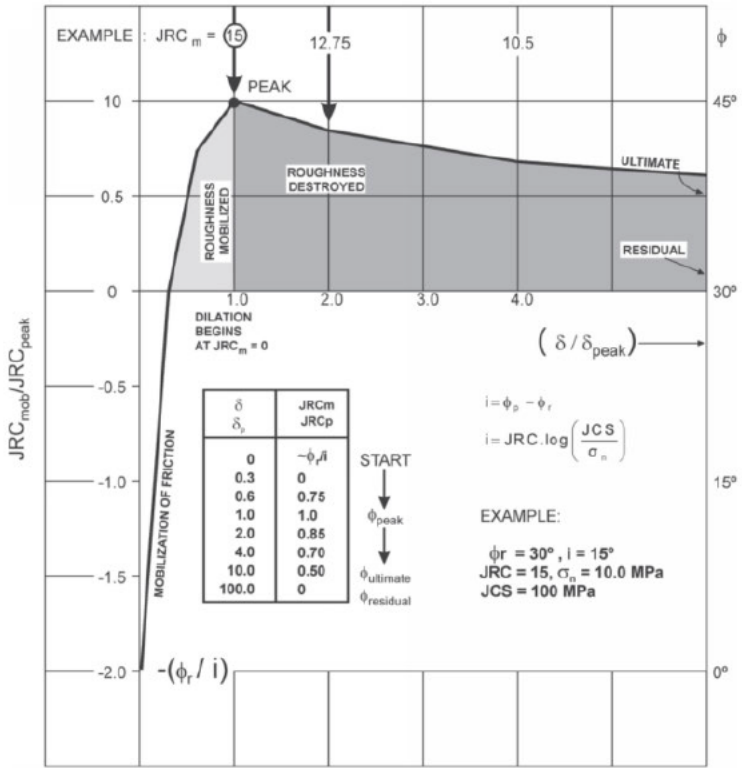

Figure 36: Presents the $JRC_{mobilized}$ concept developed by (N. Barton & S. Bandis, 1982)

In cases of shearing under low or high normal stress, the damage coefficient M, as proposed by (N Barton & R Olsson , 2001), assumes values of 1 or 2, respectively. Alternatively, (Barton, N & V. Choubey, 1977), provided an approximation for this parameter through the following relationship:

$$M = \left(\frac{JCS}{12log\left(\frac{JCS}{\sigma_n}\right)} \right) + 0.70 \qquad 2.23$$

Barton's initial experiments were conducted under extremely low normal stress conditions, making his model most suitable for stresses within the range of, (N. Barton, 1982):

$$0.01 < \frac{\sigma_n}{JCS} < 0.3$$

However, as the normal stress approaches zero, the logarithmic component of the equation tends toward infinity, rendering the equation invalid. Consequently, Barton proposed that the maximum value of the tangential term as, (N. Barton, 1982):

$[\phi_r + JRC \log\left(\frac{JCS}{\sigma_n}\right)]$, which should be 70°

2.11 Localization and Path Dependence

(Poeck, 2016), mentioned that the finite difference method utilized in UDEC adopts explicit time-stepping to solve the equations of motion for a grid-based system, subject to designated loading and boundary conditions. The ultimate outcome for a UDEC-modelled system could vary based on the initial conditions set in the simulation.

This occurrence, termed bifurcation, is frequently observed in the outcomes of basic compressive tests conducted on Mohr-Coulomb materials (Itasca, 2019). Instead of displaying even stress and deformation distributions, the sample might undergo shear strains within a localized band of zones, mirroring the behaviour seen in geological materials subjected to similar loading conditions.

Nevertheless, (Itasca, 2019) stated that, slight adjustments to modelling parameters can influence the specific failure trajectory observed in a simulation. This insight is derived from the section of the UDEC software User's Guide entitled **"Problem Solving with UDEC"**.

(Poeck, 2016) stated, that in the majority of nonlinear, inelastic systems, there exists an infinite array of solutions that meet the criteria of equilibrium, compatibility, and constitutive relations. Without a specified path, there is no definitive "correct" solution to the physical problem.

When the path isn't designated, all feasible solutions are considered valid. This scenario can lead to ongoing debates among modelers and users, especially if a seemingly insignificant parameter in the solution process, such as damping, influences the ultimate outcome. Numerically, all solutions hold validity (Poeck, 2016).

For instance, a mining excavation simulation conducted with low damping might exhibit significant overshooting, resulting in larger final displacements, whereas high damping would mitigate the overshooting, resulting in smaller final displacements.

As per (Itasca, 2019), materials susceptible to strain softening are particularly prone to experiencing localization effects. The load-displacement characteristics of these materials will be influenced by the zone size utilized in the model, determining the thickness of the shear band that emerges.

In strain softening materials with adequately small zone sizes, the failure path may exhibit random orientations, contingent upon the geometry of the model and the intricacy of the loading conditions (Itasca, 2019).

2.12 Use of Rock Bolts in Construction Support Systems

As stated in (Yu Chen & Haodong Xiao , 2024), rock bolts are an important element in geotechnical engineering which are broadly used to improve the stability of tunnels and slopes. With anchorage into the rock mass, the rock bolts provide support and prevent the movement of rock blocks which mitigates the risk of collapse and ensures the structural integrity.

The application of the rock bolts is essential in ground conditions where the is high ground stress, such as deep tunnels and steep slopes which helps to control deformation and maintain long-term stability, (Yu Chen & Haodong Xiao , 2024).

In experiments, direct shear tests are usually used to estimate the shear strength and deformation properties of rock discontinuities. The Universal Distinct Element Code (UDEC) is a numerical modelling tool that simulates the mechanical behaviour of jointed rock masses under constant normal load (CNL) conditions, (Yu Chen & Haodong Xiao , 2024).

2.12.1 Assumptions of Rock Bolt Support

As mentioned in (Kelleg, 2024), rock bolt support involves well installation of a specific types and numbers of rock bolts in rock or soil slopes. These bolts are deeply embedded and tensioned to counteract groundwater pressure and the slope's weight, (Kelleg, 2024).

By controlling displacement through bending strength and friction, stability is achieved under constant pressure. This method effectively utilises the fundamental strength of the rock and soil which reduces the deformation and internal forces, hence it enhances the safety of the project. With increasing soil depth, the advantages of rock bolt support become more obvious which makes it more economical and efficient of its use, (Kelleg, 2024).

2.12.2 Stability of Rock Mass using Rock Bolts

In infrastructure construction and mining sectors, rock bolting is highly valued by designers and engineers for its efficacy and cost-efficiency. In both surface and underground tunnelling and mining operations use rock bolts as a reliable means of reinforcement, (Spang, K & Egger, P, 1990).

These support system such as the bolts, or cable bolts, are installed in boreholes drilled into the surrounding on slopes or underground mining structure. The primary function is to improve the shear resistance of rock joints and extend the normal stress acting on these joints, (Richard E. Goodman, 1991). This self-supporting mechanism substantially improves the integrity of jointed rock masses allowing for efficient bending and suspension of unstable rock blocks while keeping key blocks connected without collapsing, (Mahdi Saadat , 2019).

As (Mahdi Saadat , 2019) stated that when the unstable blocks move towards the tunnel face or the rock bolt elongation occurs, the tension forces are transferred to the adjoining rock mass as compression. Hence, the tension forces and shearing occur along the joint surface, which is a major component causing to the failure of bolted rock joints, (Mahdi Saadat , 2019).

From, (Mahdi Saadat , 2019) undertakings, it is concluded that, in the broader field examinations and recent experimental investigations have emphasised on the importance of shear loading in analysing rock bolt performance. Overlooking shear forces can increase the uncertainty of reinforcement design in areas with sliding potential.

2.12.3 Field Observations

In underground structures rock bolts are used to stabilise unstable blocks developed around excavations. These unstable blocks result from rock excavation through a network of discontinuities, (Richard E. Goodman, 1991). When the sliding direction of a rock block is parallel to the rock bolt

axis, only a pull-out force is induced. But, if the displacement direction forms an angle with the bolt axis, the system experiences both pull and shear loads. Therefore, the total sliding displacement (δtot) is divided into axial (δp) and shear (δs) displacements, (Chen W & Li L, 2015). The axial displacement produces tensile force along the rock bolt, while the shear displacement applies a shear force on the system. Figure 37 illustrates an example of an unstable block reinforced using rock bolt.

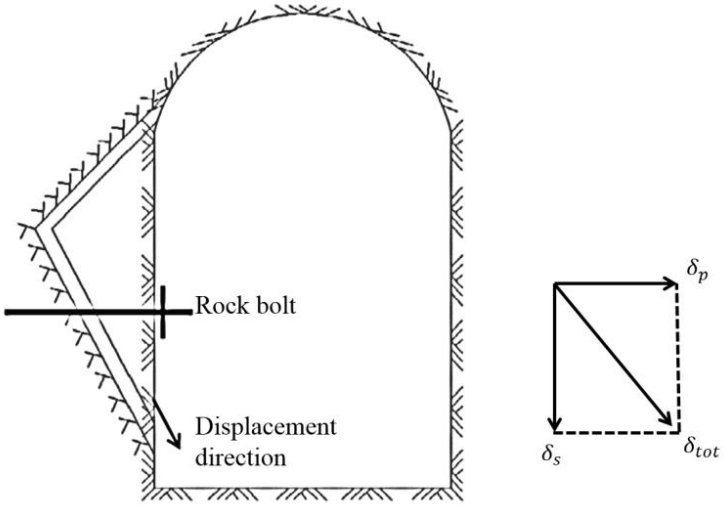

Figure 37: Presents the loading behaviour of rock bolt due to rock joint displacement modified by, (Chen W & Li L, 2015)

The performance of fully grouted rock bolts is affected by rock mass quality, the in-situ stress conditions and excavation geometry, (Charlie Li, 2017). Near the ground surface of the rock joints can create unstable blocks around underground openings which can collapse under low-stress conditions due to gravity, (Charlie Li, 2017). In such cases rock bolts are necessary for stabilising these blocks and avoiding probable damage and catastrophes.

Furthermore, deep underground excavation or mining can experience high-stress conditions that improve rock mass quality by reducing geological defects or keeping rock joints closed, (Li, C. C, 2010). In this case roof collapse is primarily caused by high in-situ stress rather than rock falls. Hence, at greater depths rock bolts are essential for maintaining the reliability of the rock mass and avoiding collapses, (Charlie Li, 2017).

2.12.4 Local Reinforcement at Joints

The local reinforcement formulation focuses solely on the local effects of reinforcement as it intersects existing discontinuities. This approach is based on laboratory observations of fully grouted, untensioned reinforcement in high-quality rocks with a single discontinuity, which show that strains in the reinforcement are concentrated at the discontinuity, (S. Bjurstroem, 1974) and (Pells, P. J. N, 1974).

2.12.5 Axial Behaviour

Generally, the axial testing of rock reinforcement has primarily focused on pull-out tests due to, (Itasca, 2024).

- The ease of experimentation and analysis of results.
- The condition of axial restraint which is the main function of reinforcement in established conceptual models.

Figure 38 represents a good understanding of axial force-displacement relations, (Itasca, 2024).

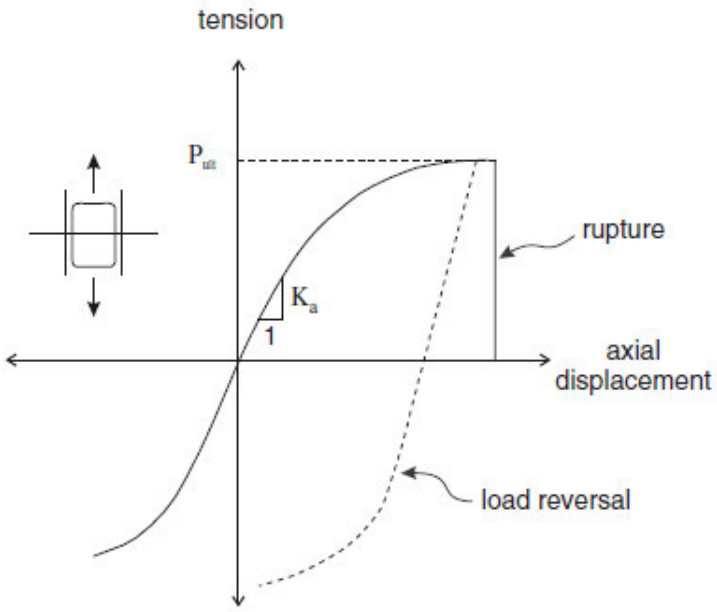

Figure 38: Presents the Axial behaviour of local reinforcement systems, (Itasca, 2024).

Figure 38 shows that the response in tension and compression is identical, even though this may not apply to all reinforcing systems. If the results of the pull-test are not available, the theoretical expression provided by, (Gerdeen J. C, Weaver T. A., & Heasley K. A, 1977) can be used to estimate the axial stiffness for fully bonded solid reinforcing elements, (Itasca, 2024).

2.12.6 Shear Behaviour

Differentiation in the reinforcement, modifies the shear stiffness and strength of discontinuities has been computed by laboratory shear testing of reinforced discontinuities. Experimental results and theoretical investigations prove that shearing along a discontinuity, causes bending stresses in the reinforcement, which deteriorates rapidly with distance into the rock from the shear surface. These bending stresses become irrelevant within one to two reinforcing element diameters, (Itasca, 2024).

The shear force against the displacement relationship used to represent shear behaviour is illustrated in Figure 39. This figure indicates the responses for reinforcement at various locations relative to the traversed discontinuity and the direction of shear, (Itasca, 2024).

If the results of the shear stiffness are not available, the theoretical expression provided by, (Gerdeen J. C, Weaver T. A., & Heasley K. A, 1977) can be adopted, (Itasca, 2024).

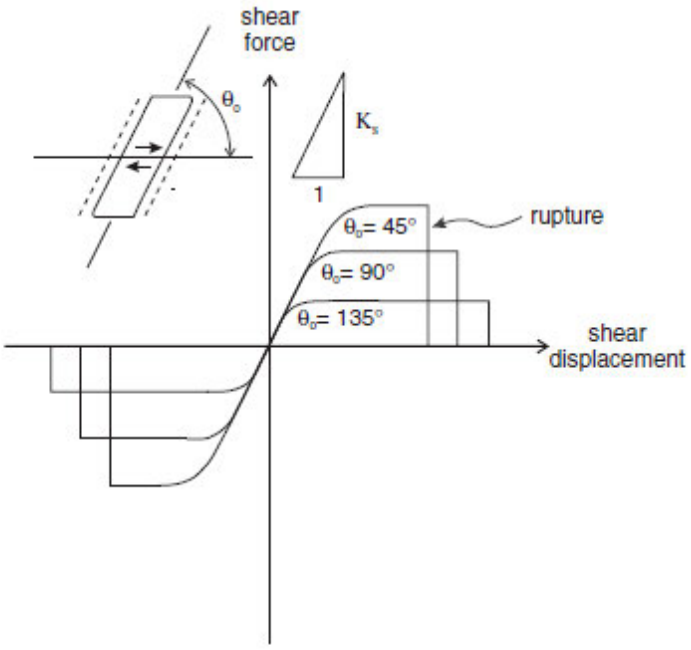

Figure 39: Shear behaviour of reinforcement system, (Itasca, 2024).

Empirical relations can estimate the maximum shear force for a reinforcement element at different orientations relative to a discontinuity and the direction of shear and the expression for maximum shear force can be found at, (Gerdeen J. C, Weaver T. A., & Heasley K. A, 1977). Also, for the derivation of the expression from shear tests on ungrouted reinforcement perpendicular to a discontinuity in granite can be found at, (Gerdeen J. C, Weaver T. A., & Heasley K. A, 1977).

In an assessment of maximum shear resistance, (St. John, C. M., & Van Dillen, D. E., 1983) developed the findings of, (Azuar J. J, Dardaine M, & Pellet F, 1979). They discovered that the maximum shear force for reinforcement perpendicular to a discontinuity was about half the product of the reinforcement's uniaxial tensile strength and its cross-sectional area, (Itasca, 2024).

This force enhanced to 80-90% of that product when the reinforcement was tilted in the direction of shear. Shear displacements leading to rupture occurred after approximately two reinforcement diameters for the perpendicular case and one diameter for the inclined case, (Itasca, 2024).

(St. John, C. M., & Van Dillen, D. E., 1983), give explanation of the changes in strength and displacement before rupture by seeing the extent of rock crushing around the reinforcement. They recorded the amount of displacement before rupture varied differing on the orientation of the reinforcement relation to the shear direction as more substantial crushing appearing in the inclined case, (Itasca, 2024).

2.12.7 Numerical Formulation

From the 3DEC model it is assumed that during the shear displacement along a discontinuity, the reinforcement deforms as illustrated in Figure 40. The segment of reinforcement that spans the discontinuity and changes orientation during shear displacement is known as the active length, (Itasca, 2024).

These geometric changes were initially proposed by (Haas C. J, 1976) for conventional point-anchored reinforcement and later adopted by (Fuller P. G & Cox W. R, 1978) for fully grouted reinforcement, (Itasca, 2024).

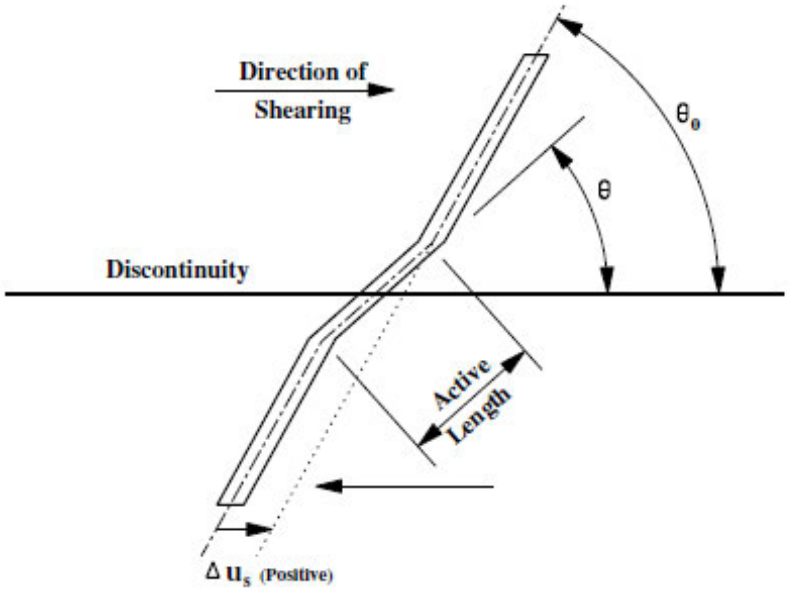

Figure 40: Assumed reinforcement geometry after shear displacement, Δus, (Itasca, 2024).

In an assumption, the active length varies orientation solely due to the geometric effects of shear and normal displacements at the discontinuity, (Itasca, 2024).

The model can be envisioned as consisting of two springs at the discontinuity interface aligning parallel and perpendicular to the reinforcement axis as illustrated in Figure 41. After shear displacement the axial spring line up with the active length whereas the shear spring remains perpendicular to the original orientation. Hence, similar geometric changes occur with displacements normal to the discontinuity, (Itasca, 2024).

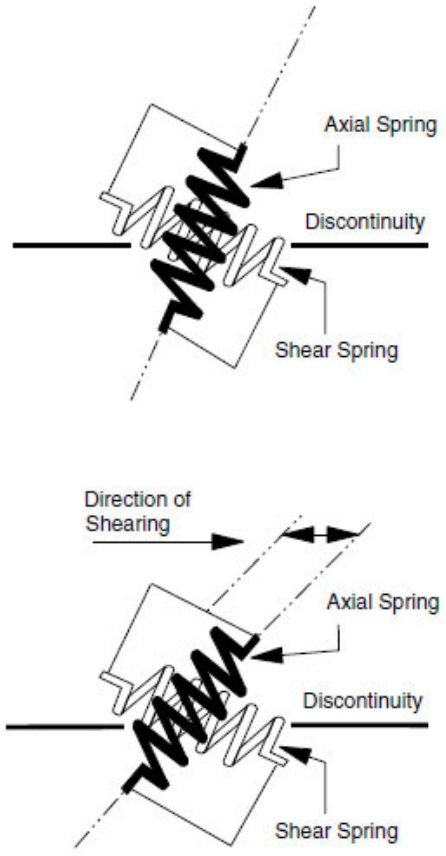

Figure 41: Orientation of shear and axial springs representing reinforcement prior to and after shear displacement, (Itasca, 2024).

From the force vs displacement models in 3DEC demonstrating axial and shear behaviour, it uses continuous linear algorithms based on stiffness (axial or shear) and ultimate load capacity. The local reinforcement formulation in 3DEC is a basic version, for more comprehensive formulation use UDEC (Itasca 2011), (Itasca, 2024).

Rupture limit can be set for the shear force and if the relative shear strain in the reinforcement element goes beyond a specified strain limit, the shear force will be reduced to zero, (Itasca, 2024).

The force vs displacement relationships depicted earlier are used to estimate the forces in the springs resulting from incremental displacements at the endpoints of the active length. The resulting shear and axial forces are then solved into components parallel and perpendicular to the discontinuity, as illustrated in Figure 42. These forces are subsequently applied to the adjacent blocks, (Itasca, 2024).

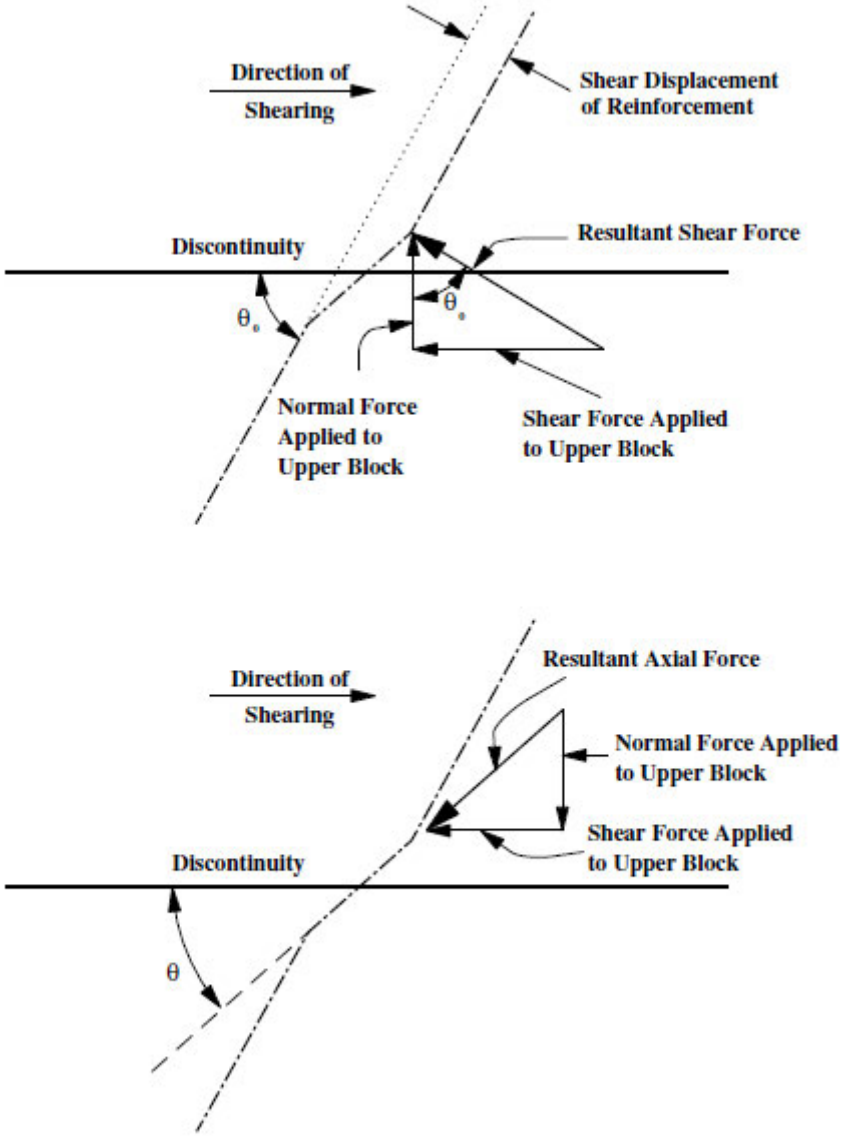

Figure 42: Resolution of reinforcement shear and axial forces into components parallel and perpendicular to discontinuity, (Itasca, 2024).

2.12.8 Approximation of Active Length

Assumption for the local deformation is shown in Figure 40, if an estimate of the active length is necessary. As demonstrated the active length extends approximately one to two reinforcing element diameters on either side of the discontinuity. If the experimental data is not available a theoretical analysis can be used to determine the active length and when defining the elastic shear stiffness (Gerdeen, J.C., et al, 1977) can be adopted, (Itasca, 2024).

This method was originally developed for reinforcement positioned perpendicular to the shear plane. (Dight P. M, 1982) provided a theoretical assessment to verify the distance from the shear plane to the point of maximum moment corresponding to the location of the plastic hinge in the reinforcement element, (Itasca, 2024).

This method does not impose any constraints on the orientation of the reinforcement relation to the shear plane. A key finding from this examination is that the distance of the plastic hinge from the shear plane remains relatively constant with shear displacement for displacements greater than 10 mm in the reinforcing systems, (Itasca, 2024).

2.13 Summary and Conclusion

In the summary of this literature review, this section has examined the current approaches used to assess the mechanical characteristics of rock joints and jointed rock formations. The following paragraphs discuss the specific coverage in this regard:

In overall this study provides an overview of the prevailing empirical and analytical techniques utilized to assess the impact of joint roughness on the shear behaviour of rock joints. Additionally, it presents the limitations associated with these methods. Furthermore, the discussion highlights the necessity for further investigation into the shearing mechanisms of rock joints, including the involvement of various order asperities in the shearing process, (Poeck, 2016).

Various researchers have investigated the impact of scale on joint roughness and the shear behaviour of rock joints, yielding conflicting findings. While some studies indicate a negative scale effect, others suggest positive outcomes or no discernible scale effect at all. Consequently, the precise nature of the scale effect remains uncertain, (Poeck, 2016).

The existing methods in estimation of the mechanical properties of rock mass can be classified into six groups of:

i. Empirical
ii. Analytical
iii. in-situ Test
iv. Laboratory Experiments
v. Back Analysis, and
vi. Numerical Modelling

Numerical modelling provides the greatest potential for understanding the complex behaviour of jointed rock masses, (Poeck, 2016).

When conducting numerical simulations of the direct shear test, continuum models face limitations in accurately representing the shear behaviour of intricate geometries and the degradation of asperities throughout the shearing process. However, software's like UDEC, FLAC and PFC have demonstrated proficiency in simulating complex joint geometries and the degradation of asperities, (Poeck, 2016).

In general, UDEC has commonly utilized the bond removal method to model joints, but this approach is limited by the inherent micro-scale roughness of the joint surface. To address this limitation, the smooth joint model was introduced. However, despite its potential advantages, the suitability and effectiveness of this method have not been thoroughly investigated in existing literature, (Poeck, 2016).

3 Methodology

3.1 Numerical Modelling of Rock Joints Shear Behaviour Under Contant Normal Loading Conditions (CNL)

3.1.1 UDEC Software and Numerical Modelling Background

(Itasca, 2019) stated that, the Universal Distinct Element Code (UDEC) is a software designed for 2-Dimensional numerical modelling, employed to replicate the behaviour of fragmented materials under either static or dynamic loads. Primarily utilised in rock engineering, UDEC facilitates the examination of rock slope failures and the assessment of how rock fractures impact underground constructions and foundation stability.

As (Abdullah R. A, Fowell R. J & Murphy W, 2010) mentioned that, belonging to the Discrete Element Method category of numerical modelling tools, UDEC enables the movement, rotation, and separation of individual rigid or deformable blocks. These blocks are interconnected through interfaces, representing discontinuities, which are handled as boundary conditions with predefined joint characteristics. UDEC offers various joint behaviour models, with the ones utilised in this study being the Coulomb Slip (Area-Contact), Continuously Yielding and Barton-Bandis joint constitutive models.

As mentioned in (Itasca, 2019), The Coulomb Slip (Area) joint constitutive model is widely recognized as a conventional approach for depicting shear failure in rock material. This model computes incremental normal and shear displacements across the joint surface area. However, it does not incorporate considerations for joint surface roughness or the accumulation of damage or weakening along the joint surface.

(Barton, N & V. Choubey, 1977) developed the Barton-Bandis joint constitutive model to characterize the impact of surface roughness on the strength and deformation of discontinuities, employing a set of empirical relationships. This model computes the shear resistance of a discontinuity by utilizing the Joint Roughness Coefficient (JRC).

As stated in (Itasca, 2019), UDEC, JRC is understood as a function dependent on:

- discontinuity length
- normal stress
- present shear displacement, and
- the history of shear displacement

Moreover, this joint model integrates the impact of damage incurred by the joint surface asperities due to shear displacement. This phenomenon is simulated by introducing a damage factor that adjusts the assigned JRC value, becoming notable when the maximum peak shear stress is attained.

In this study, UDEC models were constructed employing the mentioned types of joint constitutive models to simulate laboratory direct shear test results documented in previous research papers. Subsequently, the peak shear strengths computed by these models were compared against the peak shear strength values observed in undamaged single-stage laboratory tests. This comparison aimed to assess whether these values were reasonable and reflective of the specimens under consideration.

While the joint models can replicate pre-peak (undamaged) behaviour, only the Barton-Bandis model can simulate strength degradation with displacement observed in the post-peak range. Although post-peak strength is not the primary focus of this research, the experimental data gathered from previous studies presented an excellent opportunity to validate the Barton-Bandis model.

3.1.2 Direct Shear Tests

To strengthen the credibility of the past laboratory test findings, direct shear models were generated utilizing 2-D Universal Distinct Element Code (UDEC) version 7.0. The objective of the UDEC modelling was to construct straightforward numerical representations representing the physical direct shear tests conducted in the laboratory and then place alongside the physical and model outcomes.

Specifically, the peak shear stresses observed in the numerical models would be contrasted with those exhibited by each specimen in single-stage undamaged laboratory tests to assess the reasonableness of the laboratory values. Alternatively, the experimental data can serve to validate that the numerical models yield realistic outcomes.

3.2 Model Descriptions and Numerical Modelling

3.2.1 Model Description and Set-up

At first, a initial model was developed to be adaptable for different normal stress values and joint constitutive models. This model comprised two rectangular blocks stacked vertically, separated by a single discontinuity feature, representing the top and bottom of the physical joint specimen divided by the discontinuity.

The upper block measured 200mm in width, while the lower block was 300mm wide, with both blocks having a height of 100mm. The lower block was made slightly longer than the upper block to ensure a constant joint length between them during displacement, as required by the Barton-Bandis joint model, which specifies a joint length of 200mm.

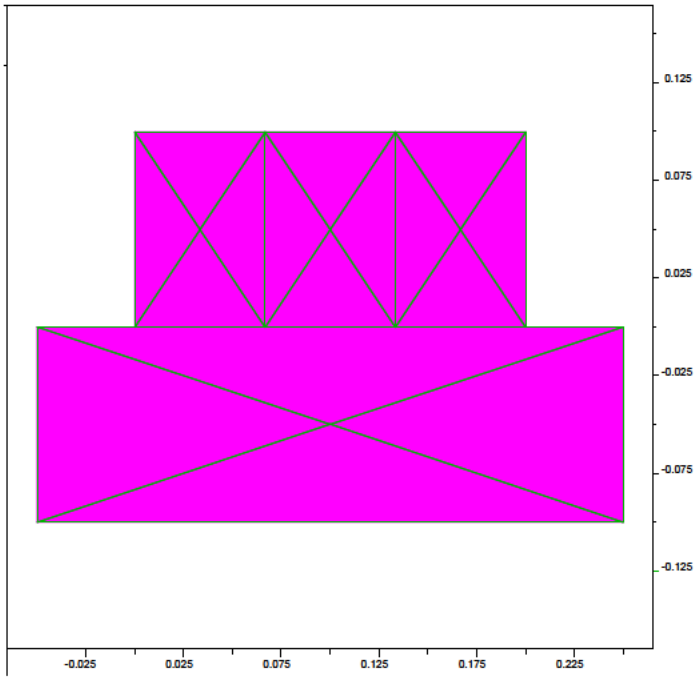

Figure 43: Represents the block

The block rounding and edge length parameters were kept at their default auto-set values of $1.25x10^{-3}$ and $2.5x10^{-3}$, respectively. While increasing the rounding and edge radius can mitigate boundary overlap issues, it also reduces data resolution. The default auto-set values were sufficient for all models.

To model the blocks as deformable materials, they were segmented using a block zone scale of 0.025. While a smaller block zone scale could provide a more detailed resolution of shear stress

values along the discontinuity, it would also increase computing time. On the other hand, a larger block edge length ratio would reduce computing time but decrease model resolution. The selected block zone scale of 0.025 was considered to offer an optimal balance between resolution and computing efficiency, (Poeck, 2016).

The properties of the model block material were taken for the UDEC 7.0 manual. The blocks were modelled as elastic because the shear stresses under the assigned normal stresses were low enough compared to the material's strength, ensuring no failure within the intact block material. The block material density was set at 2400 kg/m³. The bulk and shear moduli were set to (1.667 times) Pa and (1.25 times) Pa, respectively, and a Poisson's ratio of 0.2. Boundary conditions were applied to the blocks to replicate the conditions of the laboratory direct shear test, (Poeck, 2016).

The base and sides of the lower block were fixed in the x and y-directions, simulating the encapsulated bottom portion of the joint specimen as it was secured in the testing apparatus.

Table 3-1: Summary of UDEC Model Block Material Parameters

Model Parameter	Value
Mass-Density (kg/m³)	2400
Bulk Modulus (Pa)	4000
Shear Modulus (Pa)	3000
Elastic Modulus (Pa)	2.5E8
Poisson Ratio	0.2
Gravity (m/s²)	9.81

A normal stress of 10MPa was applied to the top of the upper block, simulating the stress exerted by the actuator in the laboratory testing apparatus into UDEC software. Additionally, gravity was applied to the model at 9.81 m/s² in the negative y-direction. The boundary and stress conditions applied to the model are also illustrated in figure 44.

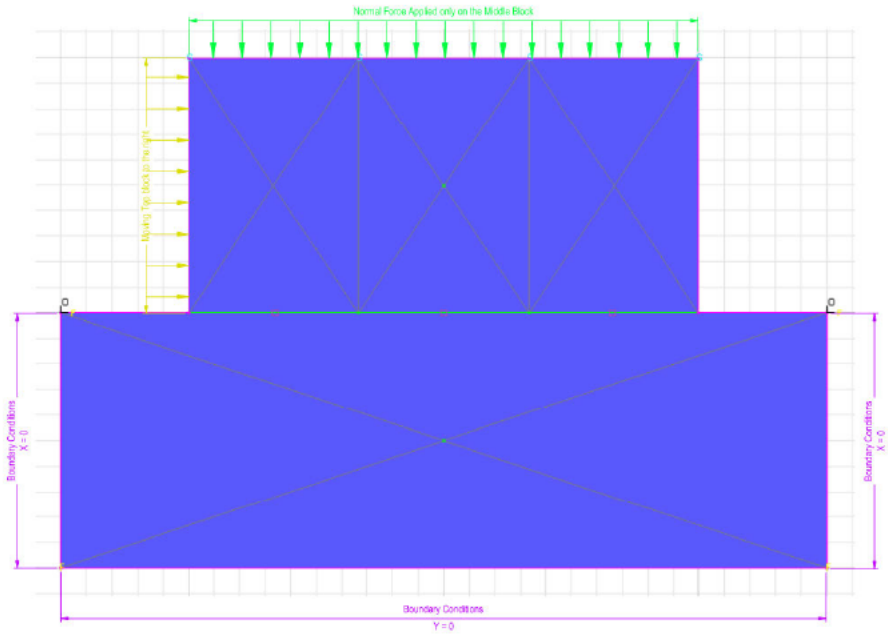

Figure 44: Represents the block Model

After achieving static equilibrium under gravity, the obtained laboratory direct shear test was simulated by subjecting the top block to a prescribe horizontal (x-direction) velocity. The x-velocity applied was equivalent to the laboratory shear rate of 0.002 m/min and all simulations were run until peak shear stress was achieved. Shear stress and displacement were calculated using a FISH function derived from an example in the UDEC user's manual.

FISH is a programming language embedded within all Itasca programs that enables the user to define new variables and functions. This FISH function uses a programming loop to determine shear stress with each step-in shear displacement. Shear stress and shear displacement data were recorded as the model was run and cycled.

These data were then exported and plotted in Microsoft Excel to obtain shear displacement vs. shear stress graphs similar to the plot as output by UDEC.

3.3 Numerical Results and Analysis for Barton-Bandis Joint Model for CNL Conditions

Comparative model for Barton-Bandis (B-B) was created as described in section 2.7 with model details and results summarised in the following section. To evaluate the B-B model's capability in replicating the shear behaviour of joints, a direct shear test was simulated on a planar joint. The planar joint plane was integrated into the Joint model, and a constant normal stress of 10 MPa initially was applied to the upper block.

3.3.1 Effect of Joint Roughness on Shear Stress of Rock Joints

The results shown in Figure 45, represents the relationship between shear stress against the horizontal displacement for joints with different roughness coefficients (jrco).

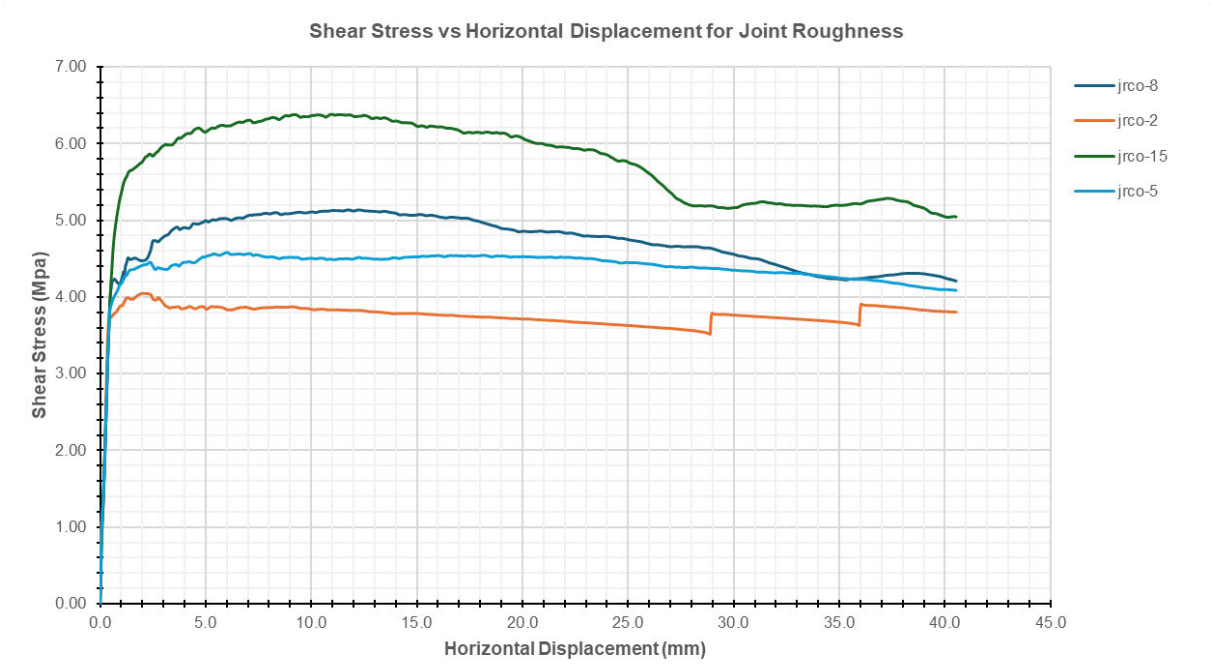

Figure 45: Presents the graph of Shear Stress vs the Horizontal Displacement for varies Joint Roughness

Initially, Shear Stress increases across all the curves, which is known as the elastic zone. Shear Stress rises rapidly as horizontal displacement begins, indicating an increase in resistance.

The Peak Shear Stress hits at different displacements on each curve as:

- **jrco-15:** Peaks at about 6.5 MPa with the displacement around 10 mm.
- **jrco-8:** Peaks at about 5.2 MPa with the displacement around 11mm.
- **jrco-5:** Peaks at about 4.5 MPa with the displacement around 6 mm.
- **jrco-2:** Peaks at about 4 MPa with the displacement around 2.5 mm.

The post peak shear stress starts to decrease after reaching the peak as:

- **jrco-15**: decreases steadily, staying above 5MPa at 40mm
- **jrco-8**: decreases steadily, staying above 4MPa at 40mm
- **jrco-5:** decreases steadily, staying above 4MPa at 40mm
- **jrco-2:** decreases more sharply, fluctuating around 3.5

Theoretical Explanation

This graphical representation demonstrates the joint roughness substantially influences the shear stress against horizontal displacement of rock joints. This is due to the higher joint roughness coefficients (JRC) resulting in the greater shear strength increasing the interlocking of joint surfaces which leads to the higher resistance against sliding (Solak, K.C., Tuncay, E, 2023).

When the horizontal displacement increases, the shear stress at the start rises sharply due to this interlocking of the joint, but ultimately reaches a peak and stabilises, reflecting the residual friction angle (Solak, K.C., Tuncay, E, 2023).

3.3.2 Effect of Joint Roughness on Normal Stress of Rock Joints

The results shown in figure 46 shows the relationship between Normal Stress against the Horizontal Stress for Barton-Bandis rock joint with different roughness coefficients (jrco).

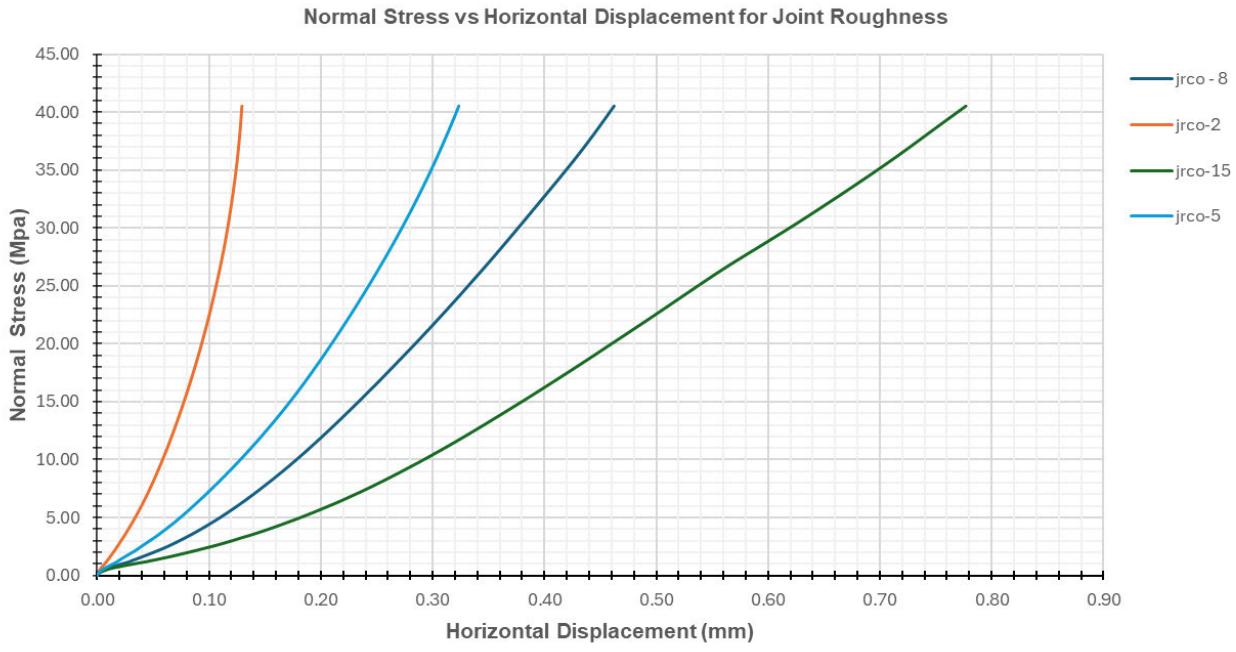

Figure 46: Presents the graph of Normal Stress vs the Horizontal Displacement for varies Joint Roughness

The general trend for all curves, shows that normal stress increases with the horizontal displacement. This indicates that as the rock joints are displaced horizontally, the normal stress acting on them increases.

The effect of joint roughness coefficient (jrco) is as:

- **jrco-2:** This graph shows the steepest increase in normal stress with horizontal displacement. The graph rises sharply, indicating that for a low roughness coefficient, even a small horizontal displacement results in a significant increase in normal stress.

- **jrco-5:** This graph is less steep compared to jrco-2, indicating a more gradual increase in normal stress with horizontal displacement.

- **jrco-8:** This graph shows an even more gradual increase in normal stress with horizontal displacement compared to jrco-5.

- **jrco-15:** This graph shows the most gradual increase in normal stress with horizontal displacement, indicating that for a high roughness coefficient, a larger horizontal displacement is required to achieve the same increase in normal stress as compared to lower roughness coefficients.

Theoretical Explanation

This graphical representation demonstrates that the joint roughness has a significant affect the normal stress of rock joints due to the higher joint roughness coefficients (JRC) which leads to the increased normal stiffness. This means that the rougher joints require greater force to reach the same amount of closure compared to smoother joints (Barton N. , 2018).

This relationship is fundamental for precisely calculating the mechanical behaviour of rock joints under variable normal loads, as it influences the peak and residual normal stress values (Barton N. , 2018).

3.3.3 Effects of Compressive Strength on Shear Stress of Rock Joints

The results shown in figure 47 shows the relationship between Shear Stress against the Horizontal Stress for Barton-Bandis rock joint with different Compressive Strength (jcso).

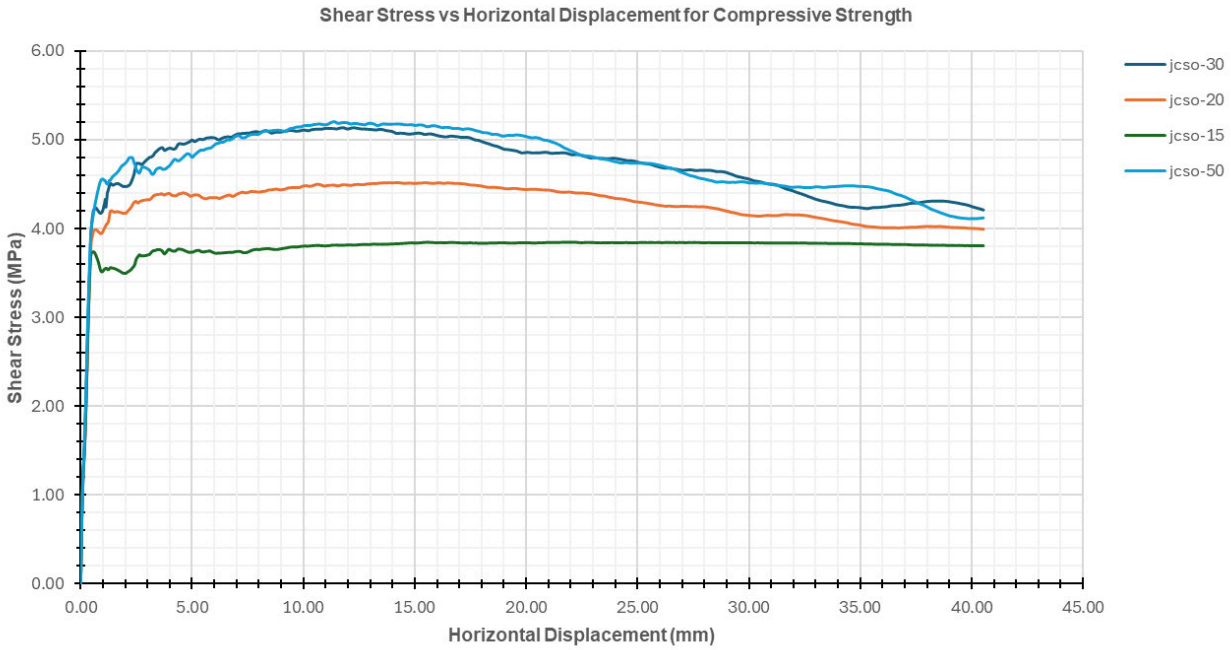

Figure 47: Presents the graph of Shear Stress vs the Horizontal Displacement for varies Compressive Strength

The general trend for all graphs, shows that shear stress increases for all the different values of the compressive strength, which is known as the elastic zone. Shear stress rises rapidly as horizontal displacement begins, indicating an increase in resistance.

The effect of compressive strength (jcso) is as:

- **jcso-50:** Initially there is an increase in the shear stress. It the roses rapidly peaks at around 5.2 MPa at about 12 mm displacement. It then gradually decreases, varies slightly, and stabilises around 4.1 MPa by 45 mm.

- **jcso-30:** Shear stress rises rapidly, peaks at about 5.1 MPa around 5 mm of displacement. It then gradually decreases, changes slightly, and stabilises around 4.5 MPa by 45 mm.

- **jcso-20:** There is a quick rise in the shear stress and peaks at 4.5 MPa at about 5 mm displacement. It then gradually decreases and stabilising around 4 MPa by 45 mm.

- **jcso-15:** Initially there is an increase in the shear stress and peaks at around 3.9 MPa at about 10 mm displacement. It then remains relatively constant with a slight decrease, stabilising around 3.8 MPa by 45 mm.

The differences among the graphs likely reflect varying conditions of the rock joints (like different levels of compressive strength or joint conditions). The jcso-30 and jcso-50 conditions result in higher peak shear stress compared to jcso-20 and jcso-15, indicating better shear strength under these conditions.

Theoretical Explanation

This graphical representation demonstrates that the compressive strength (Joint Wall Compressive Strength, JCS) performs an essential role in the determination of the shear stress against horizontal displacement of rock joints. The higher JCS values results in the greater shear strength, this is due to the joint walls can withstand higher compressive forces before weakening (Hempen, 2018).

Thus, this increase in the strength leads to a higher peak shear stress and a more evident shear strength envelope. As the horizontal displacement increases, the shear stress increases sharply due to the interlocking of rough joint surfaces, before it reaches the peak and stabilises which reflects on the residual friction angle (Hempen, 2018).

3.3.4 Effects of Compressive Strength on Normal Stress of Rock Joints

The results shown in figure 48 shows the relationship between Normal Stress against the Horizontal Stress for Barton-Bandis rock joint with different Compressive Strength (jcso).

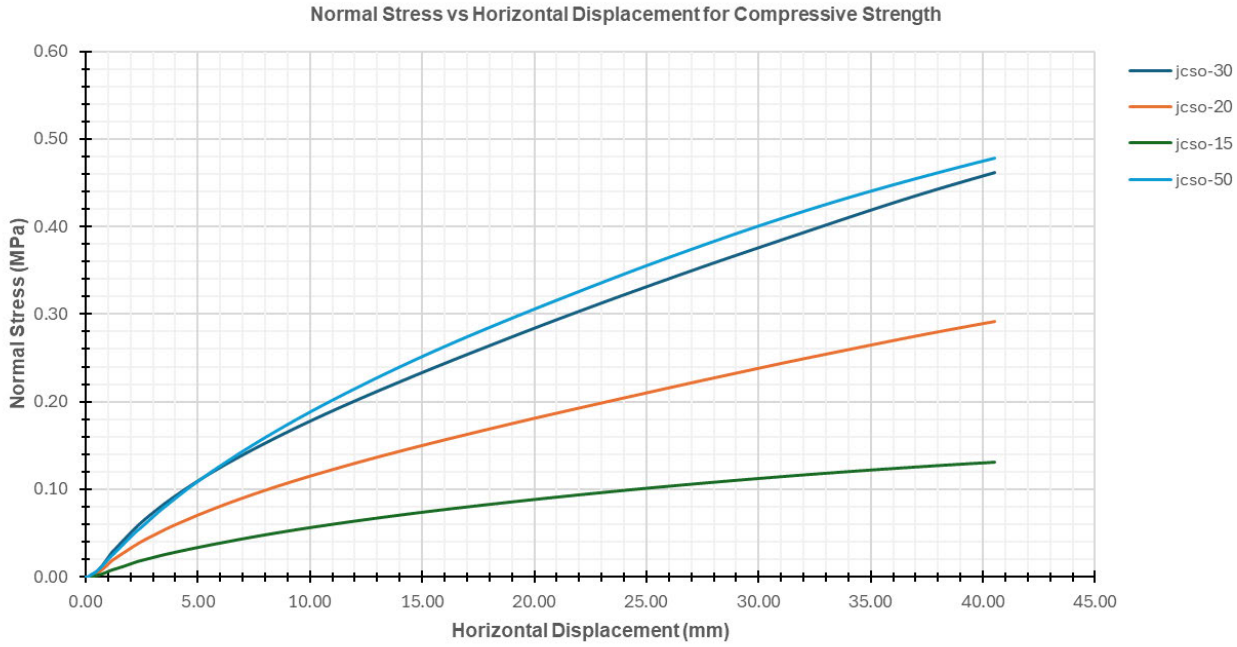

Figure 48: Presents the graph of Normal Stress vs the Horizontal Displacement for varies Compressive Strength

The general trend for all graphs shows that normal stress increases with the horizontal displacement. This indicates that as the rock joints are displaced horizontally as the normal stress acting on them increases.

The effect of compressive strength (jcso) is as:

- **jcso-50:** Initially there is a rapid increase in normal stress with horizontal displacement, the normal stress reaches at approximately 0.48 MPa at 45 mm displacement.
- **jcso-30:** There is a steady increase in normal stress as horizontal displacement rises. The normal stress reaches about 0.46 MPa at 45 mm displacement.
- **jcso-20:** Shows an increase in normal stress but at a slower rate compared to jcso-30. The normal stress reaches around 0.29 MPa at 45 mm displacement.
- **jcso-15:** This graph has the slowest increase in normal stress, relatively flat as the normal stress reaches about 0.13 MPa at 45 mm displacement.

This graphical representation generally shows how the normal stress builds up with horizontal displacement which is influenced by compressive strength joint properties.

Theoretical Explanation

This graphical representation demonstrates that the compressive strength of rock joints extensively effects the normal stress and horizontal displacement relationship. As the compressive strength increases the joint is resistance to shear displacement which results in higher normal stress required to achieve the same horizontal displacement compared to joints with lower compressive strength (Nicholas R. MacDonald,Timothy R. M. Packulak & Jennifer J. Day, 2023)

This effect is anticipated to the increased interlocking of rough joint surfaces which increases the shear strength and stiffness of the joint adopting the stress-displacement behaviour observed in the UDEC simulation (Barton N. , 2018).

3.3.5 Effects of UCS on Shear Stress of Rock Joints

The results shown in figure 49 shows the relationship between Shear Stress against the Horizontal Stress for Barton-Bandis rock joint with different UCS.

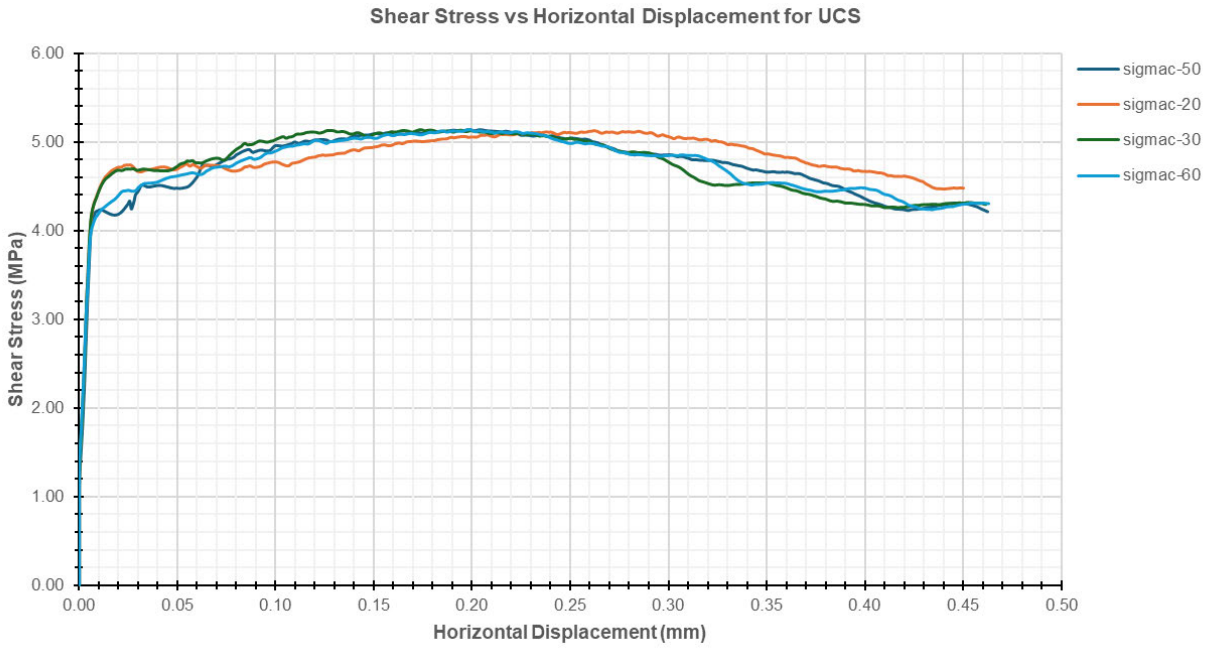

Figure 49: Presents the graph of Shear Stress vs the Horizontal Displacement for varies UCS

The general trend for all graphs shows that there is initial increase which is rapidly, this is known as the elastic zone. Shear stress rises rapidly as horizontal displacement begins, indicating that initially the rock joints are strongly resisting shear deformation.

Each graph reaches a peak shear stress at different displacements and the effect of Uniaxial Compressive Strength (UCS) is as:

- **Peak Shear Stress**
  - **sigmac-60:** Peaks, around 5.0 MPa at 0.2 mm, indicating strong resistance.
  - **sigmac-50:** Similarly, this peaks at around 5.0 MPa at 0.2 mm.
  - **sigmac-30:** Peaks at about 4.5 MPa at 5 mm.
  - **sigmac-20:** Peaks lower at around 5.1 MPa at 0.25 mm.

- **Post-Peak Behaviour**

  After the peak, the shear stress decreases gradually with further horizontal displacement, showing a reduction in the rock joint's ability to resist shear. This is likely due to damage or failure mechanisms within the joint.

Theoretical Explanation

This graphical representation demonstrates that the Uniaxial Compressive Strength (UCS) of rock joint plays a key role in influencing the shear stress against horizontal displacement. The higher UCS values improves the joint shear strength which leads to the increase in the shear stress required to attain a given horizontal displacement (Yong-Ki Lee, Jung-Wook Park & Jae-Joon Song, 2013).

This is due to the higher UCS signifies a stronger joint material which can better stand shear forces and results in a steeper shear stress-displacement graph. Thus, the joint shear strength and stiffness are directly affected by the UCS which influencing the overall stress-displacement behaviour in the UDEC simulation (Yong-Ki Lee, Jung-Wook Park & Jae-Joon Song, 2013).

3.3.6 Effects of UCS on Normal Stress of Rock Joints

The results shown in figure 50 shows the relationship between Normal Stress against the Horizontal Stress for Barton-Bandis rock joint with different Uniaxial Compressive Strength (UCS).

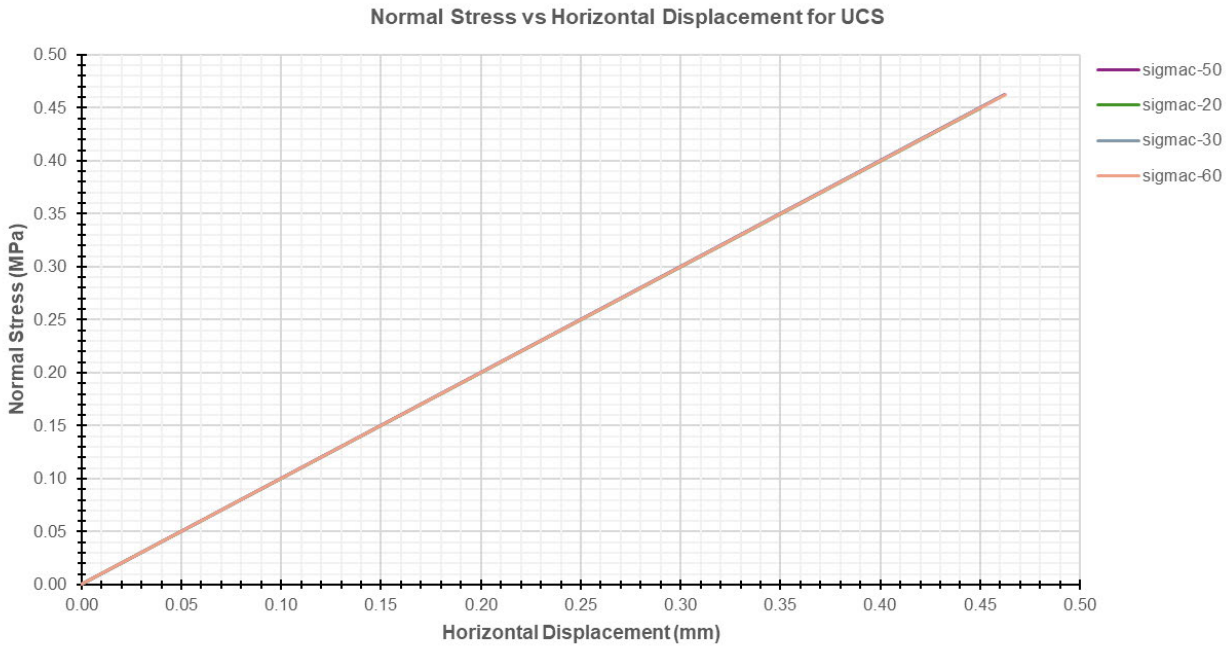

Figure 50: Presents the graph of Normal Stress vs the Horizontal Displacement for varies UCS

The general trend for all graph shows that normal stress increases with the horizontal displacement. The indication of all the 4 graphs overlapping each other shows that normal stress increases proportionally with horizontal displacement, typical for small displacements.

This shows that there is a linear relationship between normal stress and horizontal displacement. As the horizontal displacement increases, normal stress increases proportionally, indicating consistent behaviour across different conditions.

The overlapping of the lines in the graph for sigmac-50, sigmac-20, sigmac-30, and sigmac-60, suggesting the behaviour is not significantly different across these conditions.

Theoretical Explanation

This graphical representation demonstrates that the Uniaxial Compressive Strength (UCS) of rock joints affects the normal stress versus horizontal displacement relationship. When UCS increases the joint is resistant to deformation under normal stress as this also increases (Mahmoud B, Behzad N, Javad T. & Mohsen S B., 2020).

This is due to the higher normal stresses needed to attain the same horizontal displacement compared to joints with lower UCS. This higher UCS implies that the rock material is stronger and more capable of resisting the applied forces without substantial deformation, hence this assuming the normal stress-displacement behaviour increases (Mahmoud B, Behzad N, Javad T. & Mohsen S B., 2020).

3.3.7 Effects of Normal Load on Shear Strength of Rock Joints

The results shown in figure 51 shows Shear Stress (in MPa) against Horizontal Displacement (in mm) for Varies Normal Loads, 5 MPa, 8 MPa, and 10 MPa.

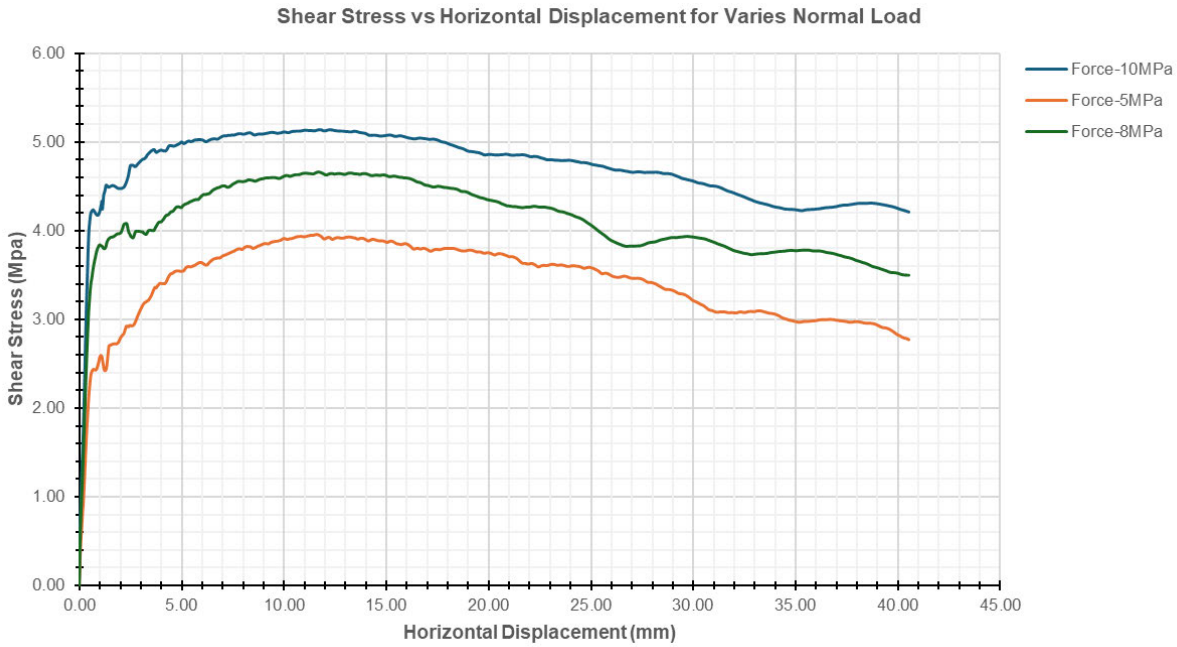

Figure 51: Presents the graph of Shear Stress vs the Horizontal Displacement for varies Normal Load

Initially, for all the three normal loads, the shear stress increases rapidly with a small increase in horizontal displacement. This initial rise is steepest for the 10 MPa load, followed by the 8 MPa and 5 MPa loads.

Each graph reaches a peak shear stress value. The peak shear stress is highest for the 10 MPa load, followed by the 8 MPa and 5 MPa loads. The peaks occur at different horizontal displacements, with the 10 MPa load peaking earlier than the others.

After reaching the peak, shear stress decreases gradually with further horizontal displacement. The rate of decrease is more pronounced for the 5 MPa load compared to the 8 MPa and 10 MPa loads.

Theoretical Explanation

This graphical representation demonstrates that the normal load substantially influences the shear strength against horizontal displacement of rock joints. When the normal load increases, the interlocking and frictional resistance between the joint surfaces increases which leads to higher shear strength to be required to attain a given horizontal displacement (Sui-Min H, Amitava G, Asadul H. C. & Mikko P. A, 1993).

This is due to a steeper shear strength-displacement graph as normal load increases. Hence, greater the normal load, the more the joint surfaces withstand the shear displacement which influences the

overall shear strength-displacement behaviour as seen in the UDEC simulation (Sui-Min H, Amitava G, Asadul H. C. & Mikko P. A, 1993).

3.3.8 Effects of Normal Load on Normal Stress of Rock Joints

The results shown in figure 52 shows Normal Stress against the Horizontal Displacement for Varies normal load outlines how normal stress varies with horizontal displacement for rock joints under different normal loads using the Barton-Bandis model

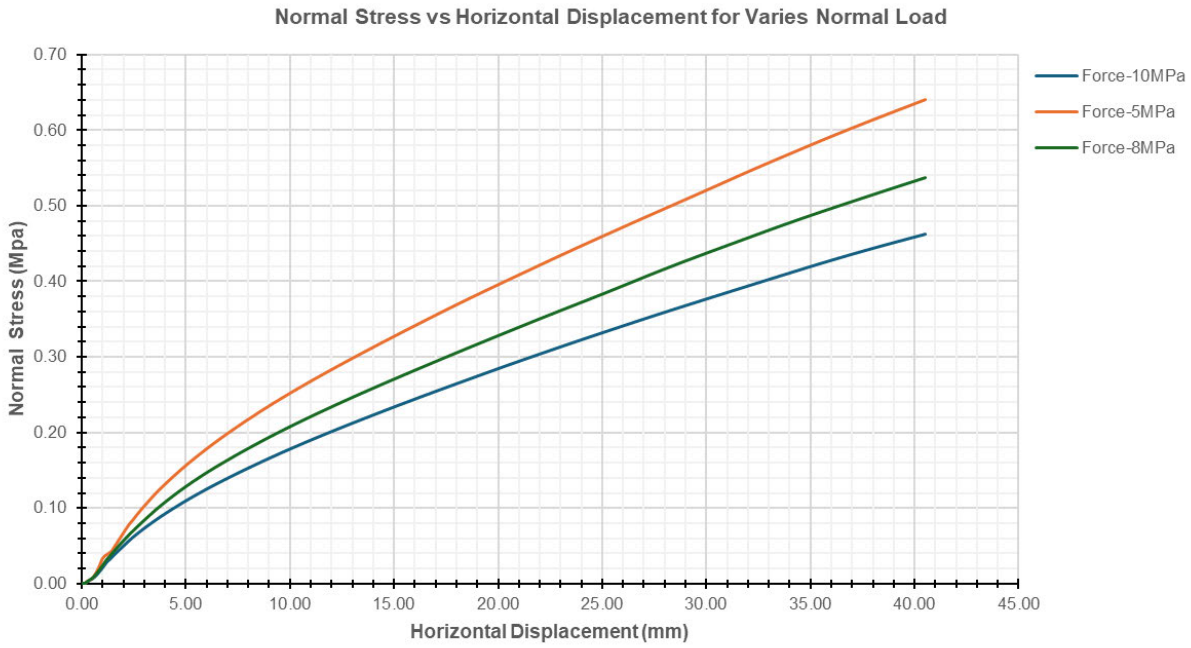

Figure 52: Presents the graph of Normal Stress vs the Horizontal Displacement for varies Normal Load

The general trend for all graphs shows that normal stress increases with the horizontal displacement. The graphs show the positive correlation, meaning normal stress increases with horizontal displacement.

As for the individual graphs:

- **5 MPa:** this is the highest increase in normal stress with horizontal displacement, indicating a steep rise.
- **8 MPa:** this is the moderate increase, sitting between the graph for 5 MPa and 10 MPa.
- **10 MPa:** this is the lowest increase, showing the most gradual rise in normal stress for the same horizontal displacement.

Theoretical Explanation

This graphical representation demonstrates that the normal load directly impacts the normal stress against the horizontal displacement relationship of rock joints. As there is an increase in normal load, it worsens the frictional resistance and interlocking effect between the joint surfaces which increases the normal strength of the joint, (Sui-Min H, Amitava G, Asadul H. C. & Mikko P. A, 1993).

Hence, this results in greater normal stress needed to attain a definite horizontal displacement which leads to a steeper normal stress-displacement graph. Fundamentally, the higher normal loads

increases the joint to resist and deform, which affects the overall stress-displacement behaviour as seen in the UDEC simulation, (Sui-Min H, Amitava G, Asadul H. C. & Mikko P. A, 1993).

3.4 Numerical Results and Analysis for Mohor Coulomb Joint Model for CNL Conditions

Comparative model for Mohor Coulomb was created as described in section 2.7 with model details and results summarised in the following section. To evaluate the MC model 's capability in replicating the shear behaviour of joints, a direct shear test was simulated on a planar joint. The planar joint plane was integrated into the Joint model, and a constant normal stress of 10 MPa initially was applied to the upper block.

3.4.1 Effects of Joint Friction on the Shear Stress of Rock Joints

The results shown in figure 53, shows the graph of Shear Stress against the Horizontal Displacement for varies Joint Friction illustrates how shear stress changes with horizontal displacement for rock joints with different friction values.

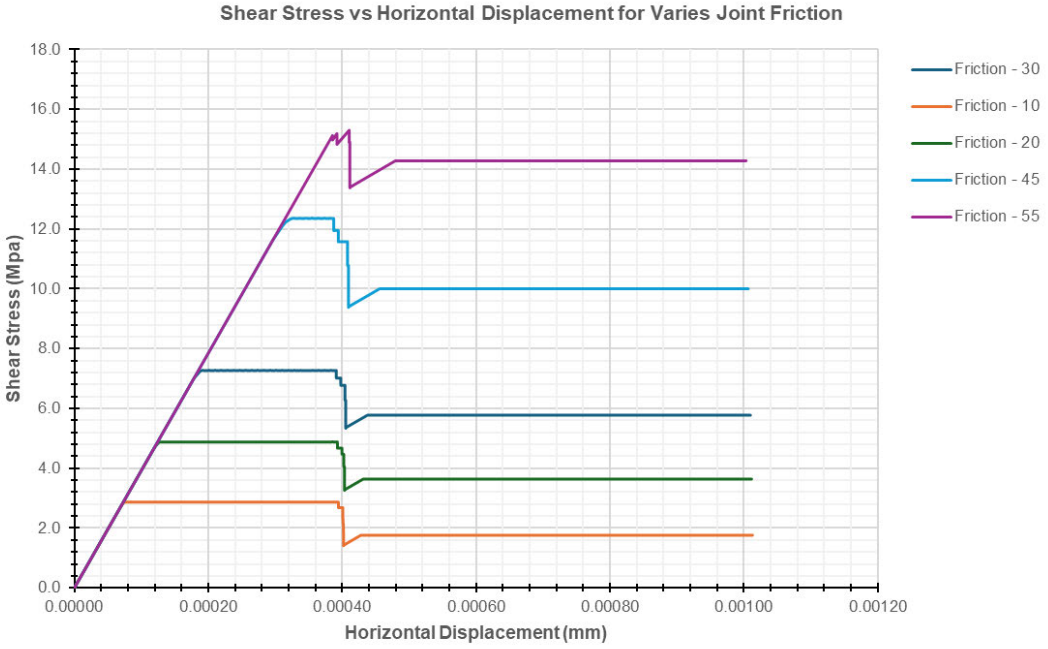

Figure 53: Presents the graph of Shear Stress vs the Horizontal Displacement for varies joint friction

Initially, all graphs show a linear increase in shear stress with horizontal displacement. This elastic behaviour indicates that the rock joints deform proportionally to the applied shear stress.

Each graphs reaches a peak shear stress at specific horizontal displacements, with the fiction as:

- **Peak Shear Stress**

  - **friction 10:** Peaks around 3 MPa
  - **friction 20:** Peaks around 5 MPa
  - **friction 30:** Peaks around 7 MPa
  - **friction 45:** Peaks around 12.5 MPa
  - **friction 55:** Peaks around 15 MPa

The higher friction values result in higher peak shear stress, reflecting increased resistance to shear deformation.

- **Post-Peak Behaviour**
  After the peak, shear stress drops sharply and stabilises at a lower value. The drop is more pronounced for higher friction values.

- **Residual Shear Stress**
  Shear stress stabilises at a residual value after the peak:

  - Higher friction values maintain higher residual shear stress.
  - Reflects the remaining shear resistance after significant deformation.

Theoretical Explanation

This graphical representation demonstrates that the joint friction substantially influences the shear stress against horizontal displacement of rock joints. As the joint friction increases, the shear strength needing greater shear stress to attain a given horizontal displacement, (ITASCA, Version 9.1.13, 2024).

This is due to frictional resistance between joint surfaces opposing the shear movement which results in a steeper shear stress-displacement graph. Hence, the joint shear strength and stiffness are directly influenced by the frictional properties and affects the general stress-displacement behaviour, as seen in the UDEC simulation, (ITASCA, Version 9.1.13, 2024).

3.4.2 Effects of Joint Friction on the Normal Stress of Rock Joints

The results shown in figure 54, shows the graph of Normal Stress against the Horizontal Displacement for varies Joint Friction illustrates how shear stress changes with horizontal displacement for rock joints with different friction values.

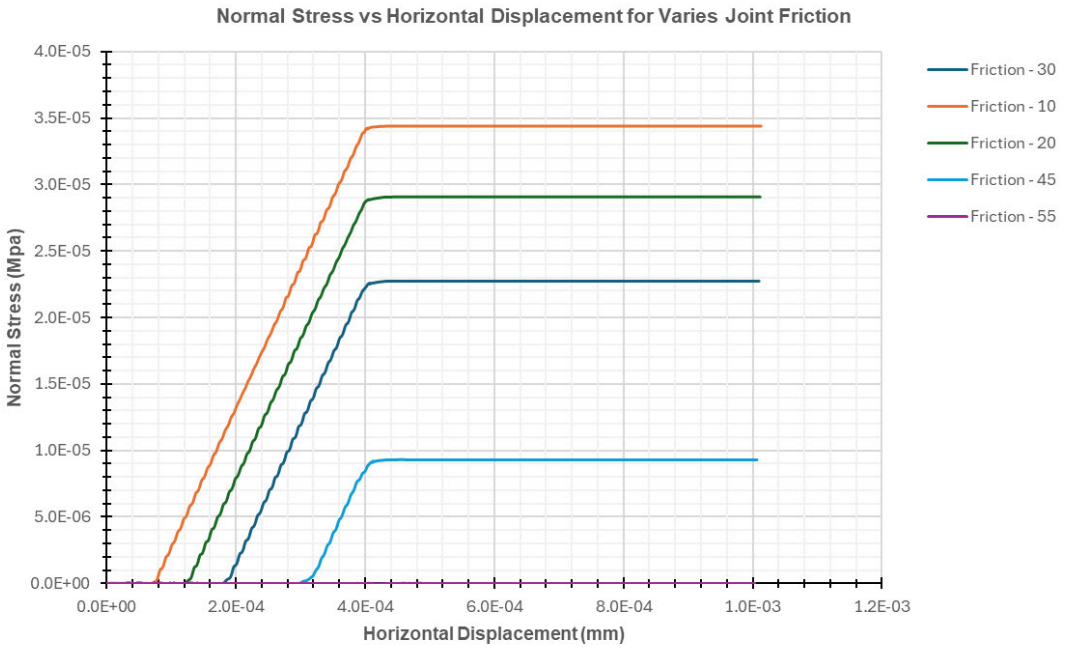

Figure 54: Presents the graph of Normal Stress vs the Horizontal Displacement for varies joint friction

Initially for all the friction values normal stress increases rapidly with a small increase in horizontal displacement. The initial slope is steep, indicating a significant rise in normal stress with even minimal displacement.

After reaching the peak the graphs finally reach the residual strength, where the normal stress remains relatively constant despite further increases in horizontal displacement. This residual strength indicates that the normal stress has reached a maximum value for the given friction and does not increase further with additional displacement.

Theoretical Explanation

This graphical representation demonstrates that the joint friction substantially influences the normal stress against horizontal relationship of rock joints. Due to the higher joint friction, it increases the normal stress needed to achieve a given horizontal displacement, which enhances the frictional resistance between joint surfaces, (ITASCA, Version 9.1.13, 2024).

This outcome is due to a steeper normal stress-displacement graph, which indicates a greater resistance to deformation. Hence, the frictional properties of the joint surfaces directly affect the normal stress-displacement behaviour as seen in the UDEC simulation, (ITASCA, Version 9.1.13, 2024).

3.4.3 Effects of Joint Dilation on Shear Stress of Rock Joints

The results shown in figure 55, shows the graph of Shear Stress against the Horizontal Displacement for varies dilation shows how shear stress changes with horizontal displacement for rock joints with different dilation values.

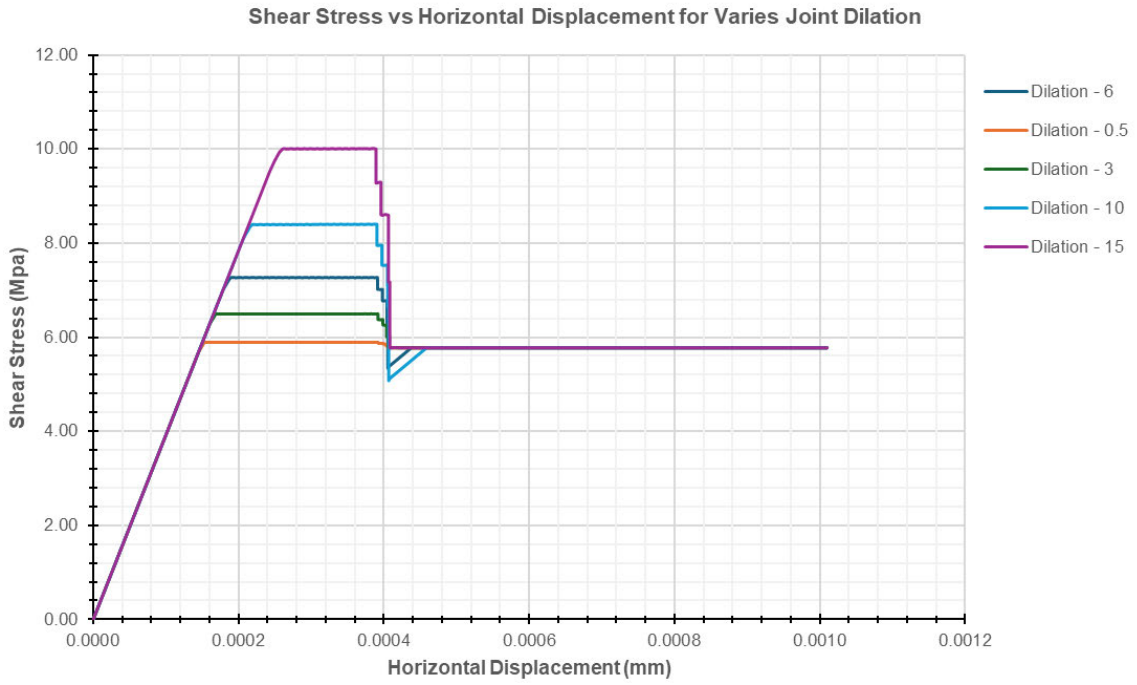

Figure 55: Presents the graph of Shear Stress vs the Horizontal Displacement for varies joint Dilation

Initially there is a linear increase for all dilation values as the shear stress increases with horizontal displacement. This indicates elastic behaviour, where the rock joints deform proportionally to the applied shear stress.

The peak shear stress varies with different dilation values as:

- **Dilation 0.5:** Peaks at a lower shear stress of 0.5 MPa with the displacement of 0.00007 mm.

- **Dilation 3:** This peaks around 6.3 MPa with the displacement of 0.00008 mm.
- **Dilation 6:** This peaks around 7.2 MPa with the displacement of 0.00009 mm.
- **Dilation 10:** This peaks around 8.4 MPa with the displacement of 0.00023 mm.
- **Dilation 15:** This peaks around 10 MPa with the displacement of 0.00026 mm.

After the peak, the shear stress decreases for all dilation values reaching the post-peak behaviour. The drop is sharper for lower dilation values (Dilation 0.5, Dilation 3) and more gradual for higher values (Dilation 10, Dilation 15).

Residual Shear Stress for Dilation 15 shows almost constant shear stress after the peak, while others stabilize at lower values.

Theoretical Explanation

This graphical representation demonstrates that the joint dilation affects the shear stress against horizontal displacement of rock joints. When the joint dilates (opens) during shearing, the normal stress decreases which reduces the frictional resistance and therefore lowering the shear stress required for a given horizontal displacement, (ITASCA, Version 9.1.13, 2024).

This behaviour is due to a less steep shear stress-displacement graph which indicates that dilation reduces the joint's shear strength. Hence, the dilation properties of rock joints directly influences the shear stress-displacement relationship as seen in the UDEC simulation, (ITASCA, Version 9.1.13, 2024).

3.4.4 Effects of Joint Dilation on the Normal Stress of Rock Joints

The results shown in figure 56, shows the graph of Normal Stress against the Horizontal Displacement for varies Joint Dilation illustrates how normal stress changes with horizontal displacement for rock joints with different dilation values.

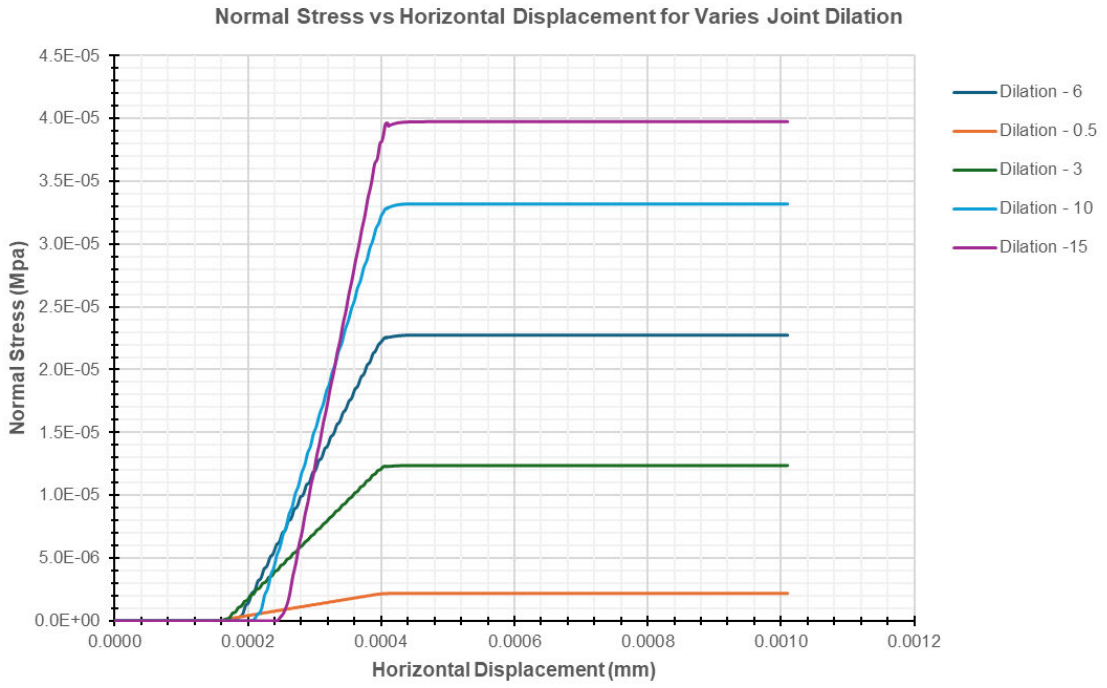

Figure 56: Presents the graph of Normal Stress vs the Horizontal Displacement for varies joint Dilation

Initially for all the dilation values normal stress increases rapidly with a small increase in horizontal displacement. The initial slope is steep, indicating that the rock joints are more resistant to deform.

As for the individual graphs:

- **Dilation 0.5:** The normal stress increases very slightly with horizontal displacement and then residual strength reaches quickly at a low value (~5E-06 MPa).
- **Dilation 3:** The normal stress increases more steeply compared to dilation 0.5 and residual strength reaches at a higher value (~1.5E-05 MPa).
- **Dilation 6:** The normal stress increases even more steeply, and residual strength reaches at an even higher value (~2.5E-05 MPa).
- **Dilation 10:** The normal stress increases sharply, and residual strength reaches at a higher value (~3.5E-05 MPa).
- **Dilation 15:** The normal stress increases very sharply, and residual strength reaches at the highest value (~4.0E-05 MPa).

Theoretical Explanation

This graphical representation demonstrates that the joint dilation affects the normal stress against the horizontal displacement relationship of rock joints. As the joint dilation happens during shearing, the separation between the joint surfaces increases which leads to a reduction in normal stress, (ITASCA, Version 9.1.13, 2024).

This reduction this due to the normal stress subsequently lowers the frictional resistance which results in a less steep normal stress-displacement graph. Hence, the dilation properties directly affect the joint's normal stress-displacement behaviour as seen in the UDEC simulations, (ITASCA, Version 9.1.13, 2024).

3.4.5 Effects of Normal Load on the Shear Stress of Rock Joints

The results shown in figure 57, shows the graph of Shear Stress against the Horizontal Displacement for rock joint subjected to varies Normal Load which shows how shear stress changes with horizontal displacement for rock joints with different applied normal load values.

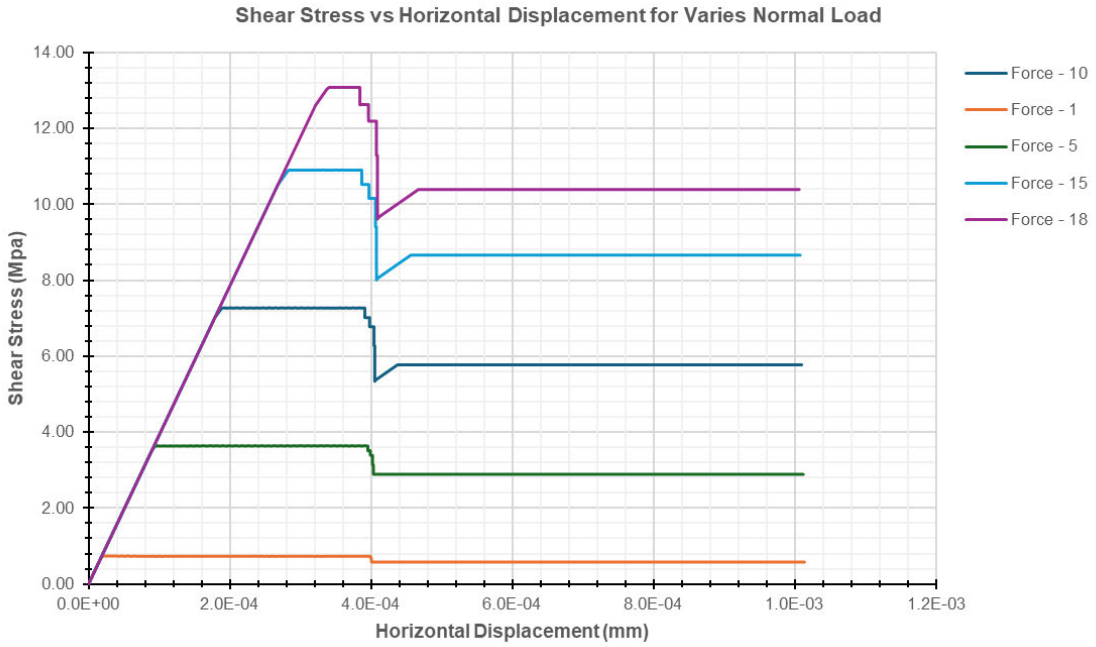

Figure 57: Presents the graph of Shear Stress vs the Horizontal Displacement for varies Normal Load

Initially there is linear increase in the shear stress as shown by each graph as the horizontal displacement increases, indicating elastic behaviour. The slope of the initial rise varies slightly with different normal loads, reflecting their respective stiffness.

For Peak Shear Stress the results are as:

- Each graph reaches a peak, representing the maximum shear stress the rock joint can withstand before failing.
- The peaks differ as:
  - Normal Load -1: Peaks at about 1 MPa.
  - Normal Load -5: Peaks around 3.8 MPa.
  - Normal Load -10: Peaks at approximately 7.5 MPa.
  - Normal Load -15: Peaks around 11 MPa.
  - Normal Load -18: Peaks at about 13 MPa.

- For the Post-Peak Behaviour:
  - After reaching the peak, the shear stress drops, indicating failure.
  - For lower normal loads (e.g., Normal Load-1 and 5), the drop is sharp.
  - For higher normal loads (e.g., Normal Load-10, 15 and 18), the decrease is more gradual, and the shear stress stabilises at higher values.

Theoretical Explanation

This graphical representation demonstrates that the normal load substantially affects the shear stress against the horizontal displacement relationship of rock joints. As the normal load is increased, it enhances the frictional resistance between joint surfaces which results in higher shear stress needed to attain a given horizontal displacement, (ITASCA, Version 9.1.13, 2024).

Therefore, this leads to a steeper shear stress-displacement graph which indicates that it requires greater resistance to shear deformation. Hence, the normal load directly affects the shear stress-displacement behaviour as seen in the UDEC simulation, (ITASCA, Version 9.1.13, 2024).

3.4.6 Effects of Normal Load on the Normal Stress of Rock Joints

The results shown in figure 58, shows the graph of Normal Stress against the Horizontal Displacement for varies applied normal load illustrates how normal stress changes with horizontal displacement for rock joints with different applied normal loads values.

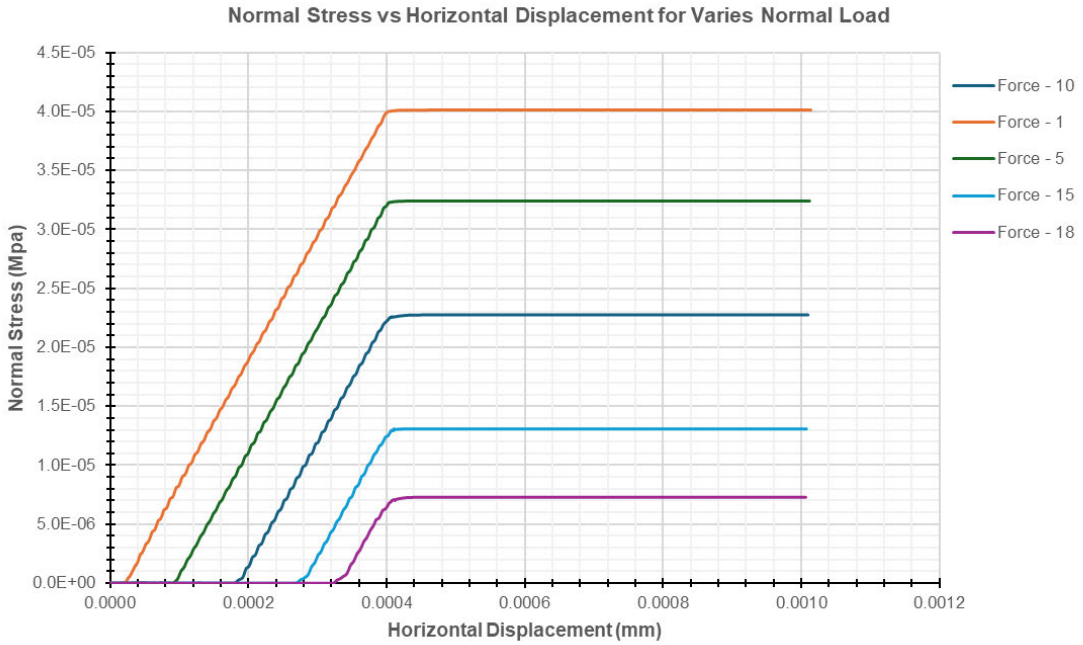

Figure 58: Presents the graph of Normal Stress vs the Horizontal Displacement for varies Normal Load

Initially for all the Normal Load values normal stress increases rapidly with a small increase in horizontal displacement. The initial slope is steep, indicating that the rock joints are more resistant to deform.

As for the individual graphs:

- **Normal Load – 1 MPa:** The normal stress increases linearly with horizontal displacement up to approximately 0.0004 mm. It reaches a maximum stress of around 4.0E-05 MPa, after which it remains constant.
- **Normal Load – 5 MPa:** The normal stress increases linearly with horizontal displacement up to approximately 0.0005 mm. It reaches a maximum stress of around 3.25E-05 MPa, then stabilises.
- **Normal Load – 10 MPa:** The normal stress increases linearly with horizontal displacement up to approximately 0.0006 mm. It reaches a maximum stress of around 2.25E-05 MPa and levels off.
- **Normal Load – 15 MPa:** The normal stress increases linearly with horizontal displacement up to approximately 0.0007 mm. It reaches a maximum stress of around 1.25E-05 MPa, then stabilises.
- **Normal Load – 18 MPa:** The normal stress increases linearly with horizontal displacement up to approximately 0.0008 mm. It reaches a maximum stress of around 5.0E-06 MPa, then stabilises.

Theoretical Explanation

This graphical representation demonstrates that the normal load substantially effects the normal stress against the horizontal displacement relationship of rock joints. As the normal load is increased, the contact forces between the joint surfaces intensifies which leads to a greater normal stress required to attain the same horizontal displacement, (ITASCA, Version 9.1.13, 2024).

This is due to a steeper normal stress-displacement graph which indicates the joints is resistance to deformation. Hence, the normal load completely affects the normal stress-displacement behaviour as seen in the UDEC simulation, (ITASCA, Version 9.1.13, 2024).

3.4.7 Effects of Velocity on the Shear Stress of Rock Joints

The results shown in figure 59, shows the graph of Shear Stress against the Horizontal Displacement for varies Velocity. This shows the relationship between shear stress (MPa) and horizontal displacement (mm) for different applied velocities to move a block, using the Mohr-Coulomb failure criterion.

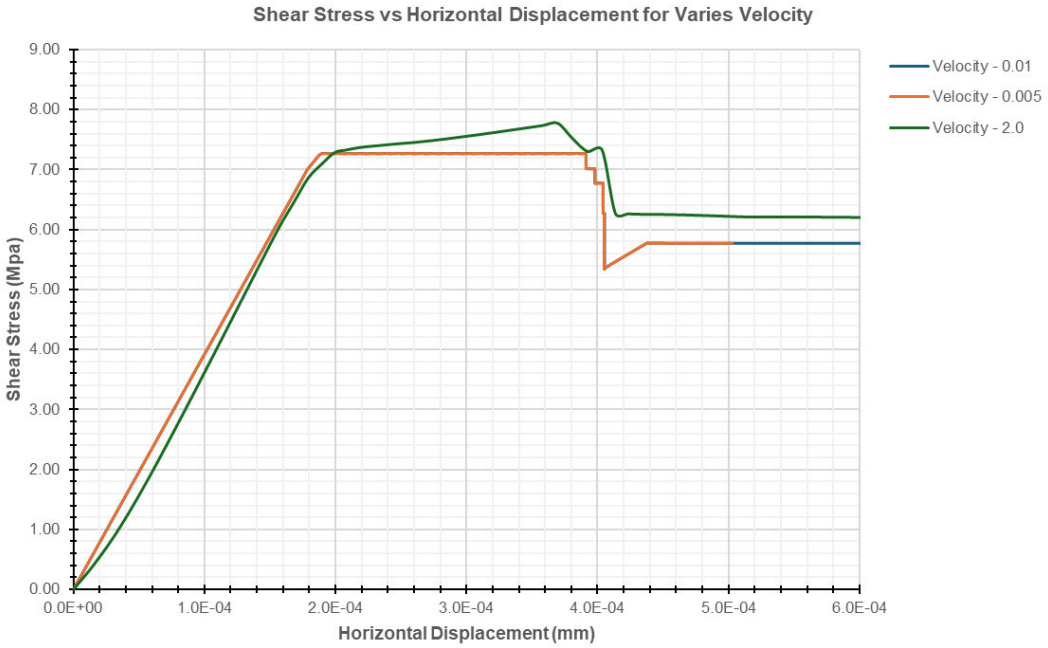

Figure 59: Presents the graph of Shear Stress vs the Horizontal Displacement for varies velocities

Initially there is a rapid increase in shear stress as horizontal displacement begins. As the block starts to move, the shear stress rises quickly.

After the initial increase, all graphs reach residual stage, where the shear stress remains relatively constant despite further displacement. This stage represents the peak shear strength of the rock joint.

At post-peak, there is a noticeable drop in shear stress for all velocities. The magnitude of the drop varies, with the velocity 2.0 m/s^2 showing the most significant drop.

After the drop, the shear stress stabilises at a lower value, thus the shear stress remains constant with further horizontal displacement.

Theoretical Explanation

This graphical representation demonstrates that the velocity of shearing, substantially affects the shear stress against horizontal displacement of rock joints. With higher shearing velocities, this can

reduce the shear strength, friction angle, and shear stiffness of the joint which results in the lower shear stress needed for a given horizontal displacement, (ITASCA, Version 9.1.13, 2024).

This behaviour is due to the rapid shearing, which might not accept adequate time for stress redistribution and frictional resistance to fully develop and leads to a less steep shear stress-displacement graph, (ITASCA, Version 9.1.13, 2024).

3.4.8 Effects of Velocity on the Normal Stress of Rock Joints

The results shown in figure 60, shows the graph of Normal Stress against the Horizontal Displacement for varies velocities load. This illustrates how normal stress changes with horizontal displacement for rock joints with different applied velocities to move a block, using the Mohr-Coulomb failure criterion values.

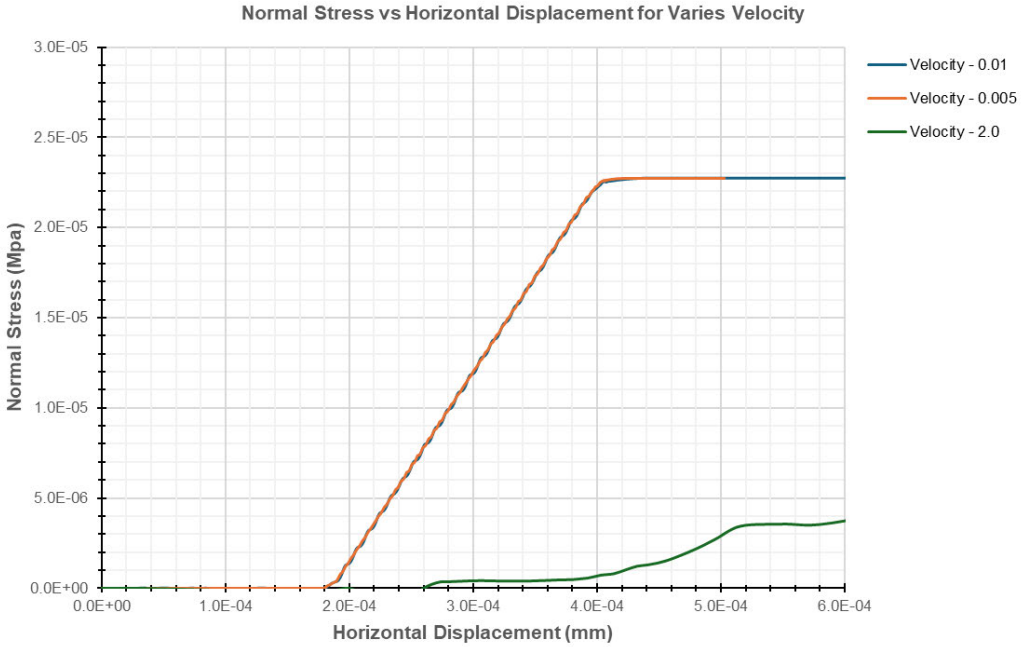

Figure 60: Presents the graph of Normal Stress vs the Horizontal Displacement for varies velocities

The normal stress increases rapidly with a small increase in horizontal displacement for velocities 0.01 m/s^2 and 0.005 m/s^2, while for velocity 2.0 m/s^2, the normal stress increases gradually.

As for the individual graphs for the normal stress are as:

- **Velocity - 0.01:** Increases rapidly in normal stress as horizontal displacement increases up to approximately 4.0E-04 mm. After which it stabilises, indicating that normal stress remains constant despite further increases in horizontal displacement.
- **Velocity - 0.005:** Similar trend as for velocity 0.01 m/s^2, with a rapid increase in normal stress up to approximately 4.0E-04 mm. It then stabilises, indicating the normal stress has reached the residual stage despite further displacement.
- **Velocity - 2.0:** This graph shows a slower increase in normal stress compared to the other two velocities. It continues to rise gradually beyond 4.0E-04 mm of horizontal displacement, indicating that normal stress keeps increasing with further displacement.

Theoretical Explanation

This graphical representation demonstrates that the velocity of shearing affects the normal stress against the horizontal displacement relationship of rock joints. With higher shearing velocities, this can reduce the normal stress necessary for a given horizontal displacement, (ITASCA, Version 9.1.13, 2024).

This is due to the rapid shearing reduces the full advancement of frictional resistance and stress redistribution which leads to a less steep normal stress-displacement graph. Hence, greater shearing velocity reduces the joint's resistance to deformation, (ITASCA, Version 9.1.13, 2024).

3.5 Numerical Results and Analysis for Continuously Yeilding Joint Model for CNL Conditions

Comparative model for Continuously Yielding was created as described in section 2.7 with model details and results summarised in the following section. To evaluate the CY model ’s capability in replicating the shear behaviour of joints, a direct shear test was simulated on a planar joint. The planar joint plane was integrated into the Joint model, and a constant normal stress of 10 MPa initially was applied to the upper block.

3.5.1 Effects of Joint Roughness on the Shear Stress of Rock Joints

The results shown in figure 61, shows the graphs of Shear Stress against the Horizontal Displacement for varies Joint Roughness. It shows how shear stress (MPa) changes with horizontal displacement (mm) for different joint roughness in rock joints, based on the Continuously Yielding model.

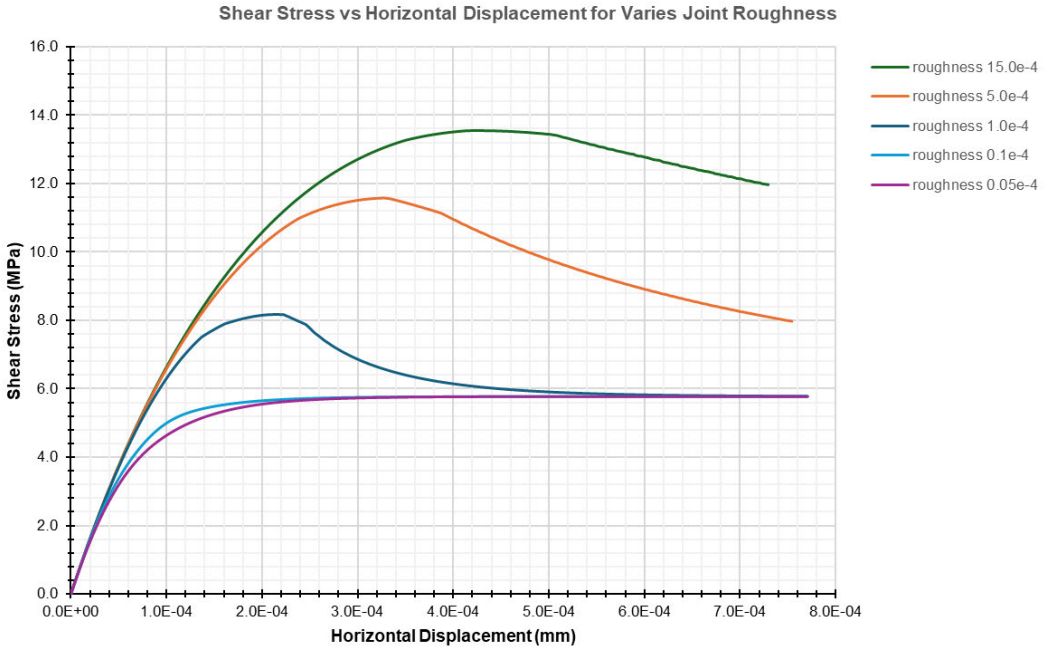

Figure 61: Presents the graph of Shear Stress vs the Horizontal Displacement for varies Joint Roughness

In the initial stage, the graphs show a rise in shear stress with horizontal displacement. This indicates the resistance existing by the joint roughness as the block starts to move.

At the peak shear stress stage, each graph peaks at a certain displacement as follows:

- **Roughness 15.0e-4:** Peak at 13.8 MPa with the displacement of 4.0e-4 mm.
- **Roughness 5.0e-4:** Peak at 11.8 MPa with the displacement around 3.0e-4 mm.
- **Roughness 1.0e-4:** Peak at 8.2 MPa with the displacement around 2.0e-4 mm.
- **Roughness 0.1e-4:** Lower peak at 5.8 MPa with the displacement around 2.0e-4 mm.
- **Roughness 0.05e-4:** Lowest peak at 5.8 MPa with the displacement around 2.0e-4 mm.

Therefore, higher roughness values result in higher peak shear stress.

As the graphs reaches the post-peak the shear stress decreases for higher roughness values (15.0e-4 and 5.0e-4). This decrease is more pronounced for higher roughness values due to breakdown of interlocking asperities.

Lower roughness values for the rest of the graph tend to reach the residual stage, indicating stable shear stress after the initial peak.

Theoretical Explanation

This graphical representation demonstrates that the joint roughness has a substantially impact on the shear stress against horizontal displacement of rock joints. With higher joint roughness coefficients (JRC), improves the interlocking of joint surfaces which results in increase in shear strength and higher peak shear stress, (ITASCA, 2024).

As the horizontal displacement continues, the shear stress rises rapidly due to this interlocking effect. After a certain time, it finally reaches a peak and stabilises which indicates the residual friction angle. This behaviour underlines the critical role of joint roughness in decisive the shear reaction of rock joints under continuous yielding conditions, (ITASCA, 2024).

3.5.2 Effects of Joint Roughness on the Normal Stress of Rock Joints

The results shown in figure 62, shows the graphs shows the graphs of Normal Stress against the Horizontal Displacement for varies Joint Roughness. It shows how normal stress (MPa) changes with horizontal displacement (mm) for different joint roughness in rock joints, based on the Continuously Yielding model.

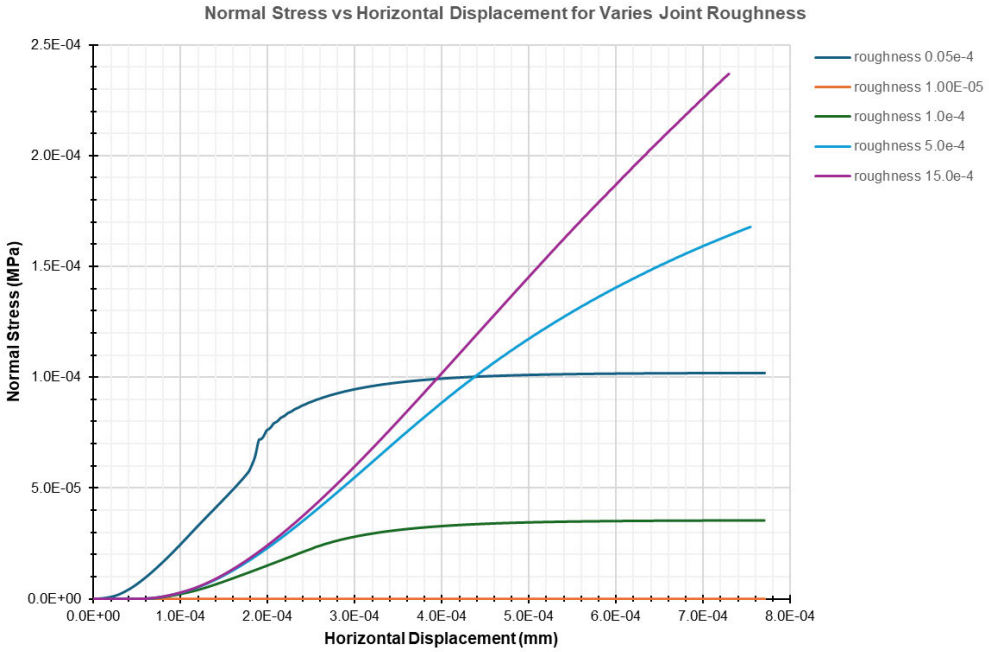

Figure 62: Presents the graph of Normal Stress vs the Horizontal Displacement for varies Joint Roughness

The normal stress increases gradually with a small increase in horizontal displacement for different joint roughness.

As for the individual graphs for the normal stress are as:

- **Roughness 0.05e-4:** Rapid initial increase in normal stress with horizontal displacement. Residual stage reaches quickly, indicating that normal stress remains constant after initial displacement.
- **Roughness 1.00e-05**: Slight increase in normal stress, nearly flat. This Indicates minimal increase in normal stress regardless of horizontal displacement.
- **Roughness 1.0e-4**: Initial increase in normal stress, similar to the roughness 0.05e-4 but at a lower level. It stabilises after initial rise.
- **Roughness 5.0e-4**: Steady linear increase in normal stress with horizontal displacement. This indicates continuous relationship between normal stress and displacement.
- **Roughness 15.0e-4**: Steep increase in normal stress and continues to rise without stabilising off, indicating a strong dependence on displacement for high roughness values.

Theoretical Explanation

This graphical representation demonstrates that the joint roughness extensively effects the normal stress against horizontal displacement of rock joints. As the Joint Roughness Coefficients (JRC) increases, it leads to increase in normal stiffness. This means that for the rougher joints, it will take a greater force to attain the same amount of closure compared to smoother joints, (Jie Liu, Jiahong Wu, Xiaoshuang Li, He Zhang & Yanbin Song, 2022).

Hence, this relationship is fundamental for accurately predicting the mechanical behaviour of rock joints under varying normal loads, as it changes both the peak and residual normal stress values, (Jie Liu, Jiahong Wu, Xiaoshuang Li, He Zhang & Yanbin Song, 2022)

3.5.3 Effects of Velocity on the Shear Stress of Rock Joints

The results shown in figure 63, shows the graphs of shear stress against the Horizontal Displacement for different velocities. It shows how shear stress (MPa) changes with horizontal displacement (mm) at different velocities to move the rock joints, based on the Continuously Yielding model.

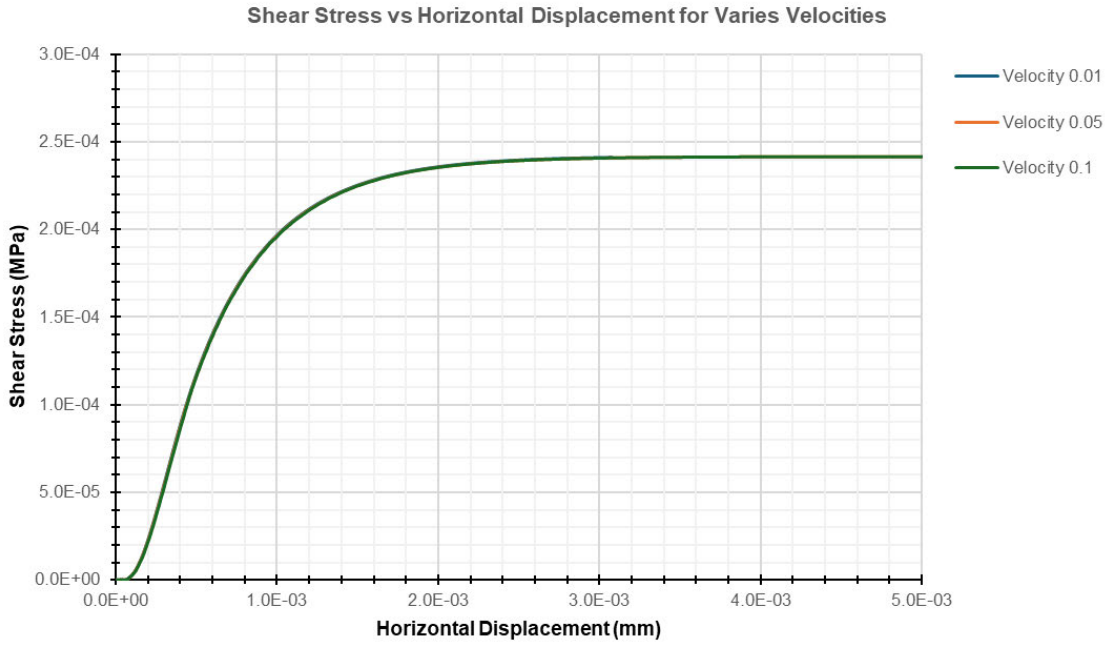

Figure 63: Presents the graph of Shear Stress vs the Horizontal Displacement for varies Velocities

There is rapidly rise in shear stress with a small increase in the horizontal displacement for all the three velocities as indicated in the graph, showing a steep initial slope. This reflects the resistance provided by the rock joints as the block starts to move.

After the initial rapid rise, the shear stress reaches the residual stage, meaning it stays relatively constant with further increases in horizontal displacement. The stage indicates the peak shear strength of the rock joints.

Since all three graph overlaps, the velocity comparison indicates that, similar shear stress behaviour across these velocities. The yielding model suggests that the velocity does not significantly affect the shear stress in this range.

Theoretical Explanation

This graphical representation demonstrates that the shear velocity affects the shear stress against horizontal displacement of rock joints. As the shear velocities is increased, it leads to an increase in the shear stress due to the dynamic effects and inertia which can cause the joint surfaces to cooperate more vigorously, (N. Barton & S. Bandis, 1982).

This behaviour is due to a higher peak shear stress and theoretically a changed shear strength envelope compared to constant conditions. Hence, the residual shear stress may not be substantially affected as it is more related on the joint roughness and material properties, (N. Barton & S. Bandis, 1982).

3.5.4 Effects of Velocity on the Normal Stress of Rock Joints

The results shown in figure 64, shows the graphs shows the graphs of Normal Stress against the Horizontal Displacement for varies velocities. It shows how normal stress (MPa) changes with horizontal displacement (mm) at different velocities to move the rock joints, based on the Continuously Yielding model.

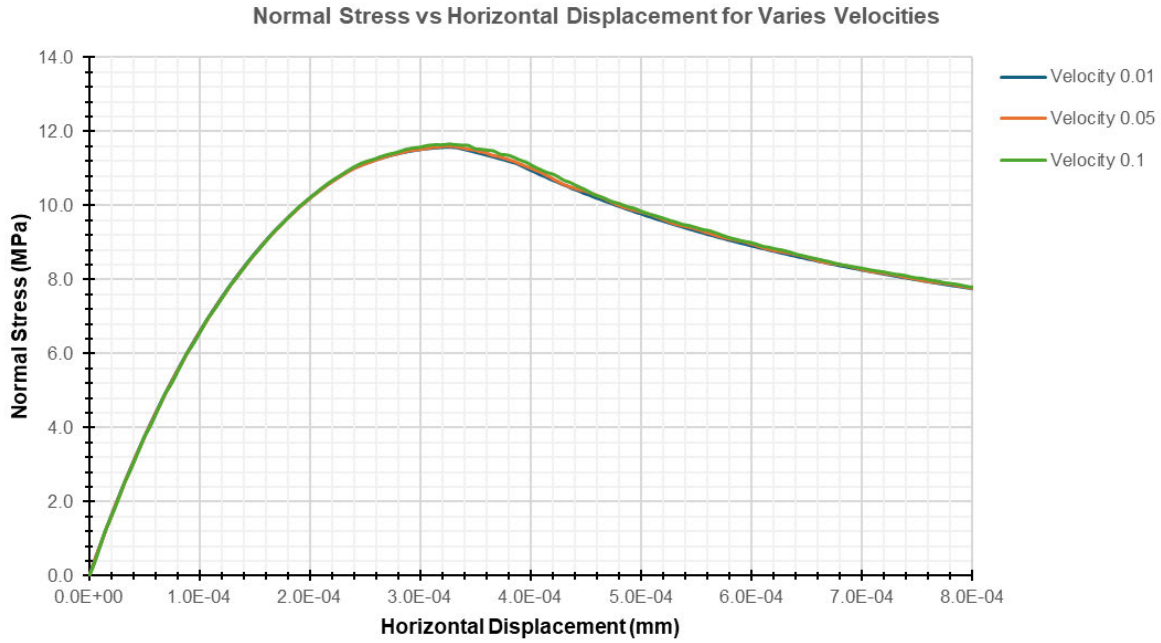

Figure 64: Presents the graph of Normal Stress vs the Horizontal Displacement for varies Velocities

All the three graphs show an initial increase in normal stress as horizontal displacement increases. This rise indicates that the rock joint initially resists the movement of the block.

As the graph reaches a peak normal stress value at a certain horizontal displacement, around 11.5 MPa for all three velocities. This peak represents the maximum normal stress the joint can withstand before yielding.

After reaching the peak, the normal stress decreases gradually with further horizontal displacement (this stage is Post-Peak Decline). This gradual decline indicates a reduction in resistance as the joint continues to yield.

Theoretical Explanation

This graphical representation demonstrates that the shear velocity affects the normal stress against horizontal displacement of rock joints. As the shear velocities are increase, it leads to an active influence, triggering variations in normal stress due to inertia and rapid changes in joint closure, (N. Barton & S. Bandis, 1982).

This results in differences in the normal stress distribution, which potentially affects the overall mechanical behaviour of the rock joints, (N. Barton & S. Bandis, 1982).

3.5.5 Effects of Joint Friction on the Shear Stress of Rock Joints

The results shown in figure 65, shows the graphs of Shear Stress against the Horizontal Displacement for varies joint frictions. It shows how shear stress (MPa) changes with horizontal displacement (mm) at different values of the joint friction to move the rock joints, based on the Continuously Yielding model.

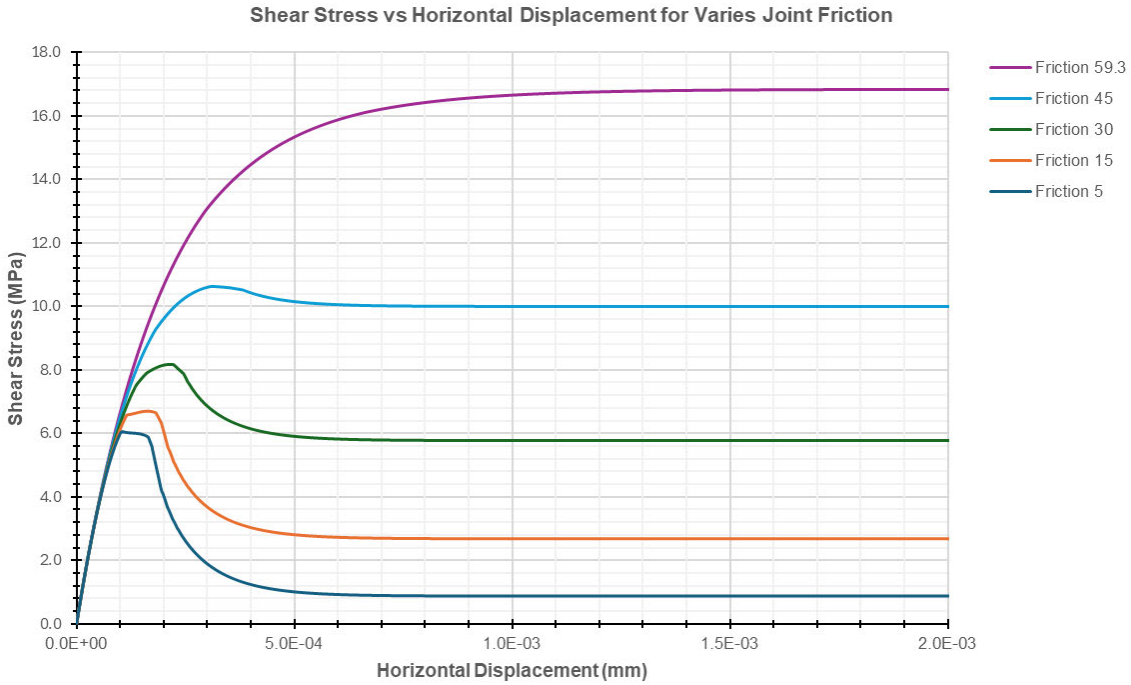

Figure 65: Presents the graph of Shear Stress vs the Horizontal Displacement for varies Joint Friction

There is a rapid increase in the shear stress for all friction values with a small increase in horizontal displacement. This indicates that as the block begins to move, there's a significant increase in resistance (shear stress).

As for the peak shear stress each graph reaches the peak stage at a certain horizontal displacement as:

- **Friction – 5:** Peaks around 6 MPa.

- **Friction – 15:** Peaks around 7 MPa.
- **Friction - 30:** Peaks around 8.1 MPa.
- **Friction – 45:** Peaks around 10.3 MPa.
- **Friction - 59.3:** Peaks around 17 MPa.

Thus, higher friction values result in higher peak shear stress due to increased resistance.

After peaking, shear stress decreases and then stabilises, this is known as the Post-Peak Behaviour. As the higher friction values decrease more gradually and stabilise at higher values, while lower friction values decrease sharply and stabilise at lower values.

Eventually, shear stress stabilises for all friction values, indicating the block has reached a steady state of movement.

Theoretical Explanation

This graphical representation demonstrates that the joint friction substantially affects the shear stress against horizontal displacement of rock joints. As the friction coefficients gets higher, there is a greater shear strength as a result due to the frictional resistance along the joint surfaces, (N. Barton & S. Bandis, 1982).

This results in a higher peak shear stress and a more defined shear strength envelope. As horizontal displacement continues, the shear stress rises rapidly due to the frictional resistance, but finally reaches a peak and stabilises, as a result of achieving the residual friction angle, (N. Barton & S. Bandis, 1982).

3.5.6 Effects of Joint Friction on the Normal Stress of Rock Joints

The results shown in figure 66, shows the graphs shows the graphs of Normal Stress against the Horizontal Displacement for varies joint frictions. It shows how normal stress (MPa) changes with horizontal displacement (mm) at different friction values to move the rock joints, based on the Continuously Yielding model.

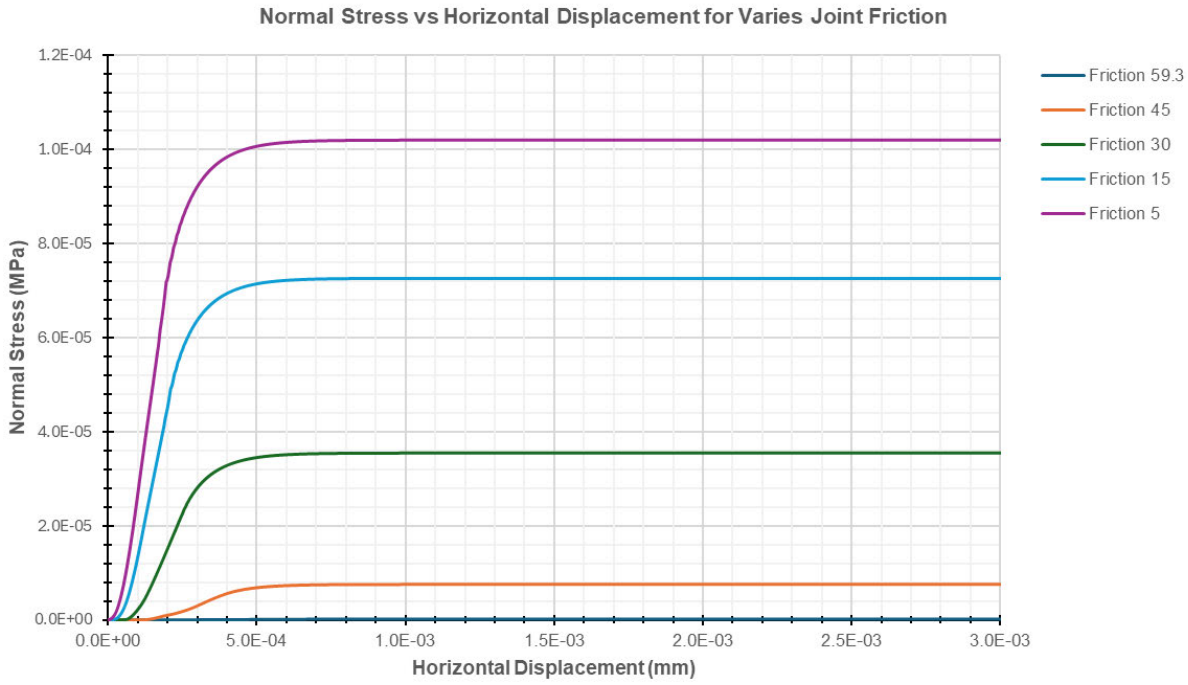

Figure 66: Presents the graph of Normal Stress vs the Horizontal Displacement for varies Joint Friction

There is a rapid increase in the normal stress for all friction values with a small increase in horizontal displacement.

Explanation for the individual friction values is as:

- **Friction – 59.3:** Shows the slowest increase in normal stress with horizontal displacement. Peaks early and stabilizes quickly at a lower normal stress, indicating minimal resistance and easy movement.
- **Friction – 45:** Increases more steeply than friction 59.3. It reaches a higher stabilisation, indicating greater resistance to movement.
- **Friction – 30:** Exhibits a steeper increase in normal stress and reaches an even higher residual stage compared to the previous two.
- **Friction - 15:** Steeper rise and reaches the higher stability than friction 30, indicating significant resistance to horizontal displacement.
- **Friction - 5:** Displays the steepest increase in normal stress. It reaches the highest peak, suggesting very high resistance and minimal displacement with the highest friction.

Theoretical Explanation

This graphical representation demonstrates that the joint friction substantially affects the normal stress against horizontal displacement of rock joints. As the friction coefficients get higher, this results in the greater normal stress due to increased resistance to sliding along the joint surfaces, (N. Barton & S. Bandis, 1982).

Hence, this correlation is fundamental for precisely predicting the mechanical behaviour of rock joints under variable normal loads which affects both the peak and residual normal stress values, (N. Barton & S. Bandis, 1982).

3.5.7 Effects of Normal Load on the Shear Stress of Rock Joints

The results shown in figure 67, shows the graphs of Shear Stress against the Horizontal Displacement for varies applied Normal Load. It shows how shear stress (MPa) changes with horizontal displacement (mm) at different values of the normal load to move the rock joints, based on the Continuously Yielding model.

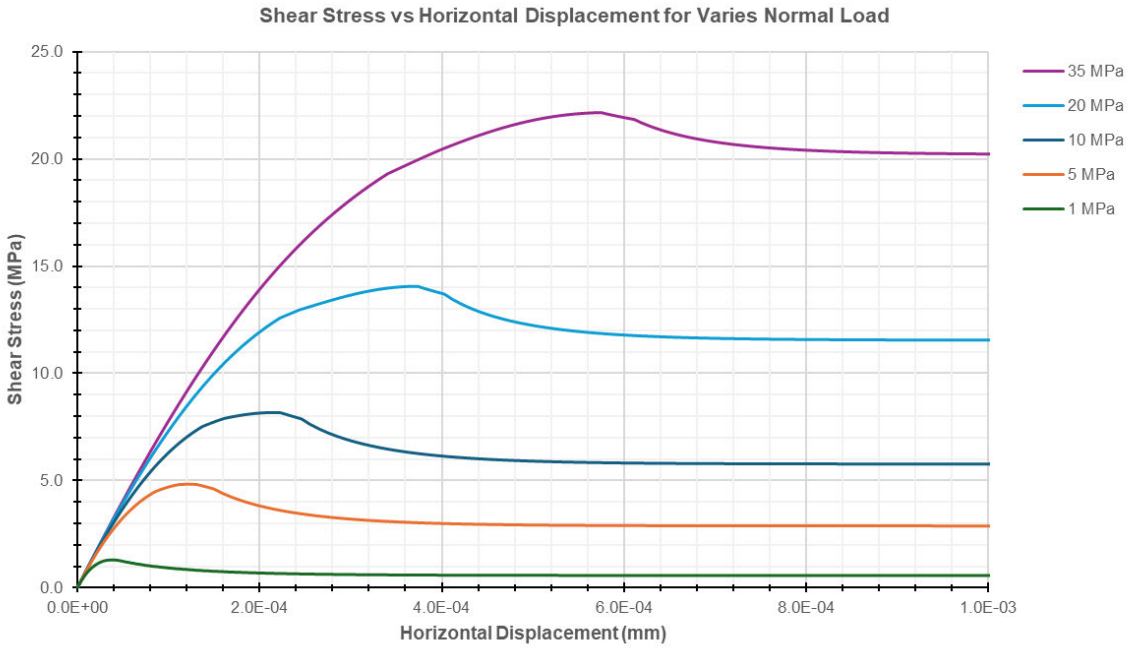

Figure 67: Presents the graph of Shear Stress vs the Horizontal Displacement for varies Normal Load

Initially the shear stress increases rapidly with the horizontal displacement for all normal loads. The increase is steepest for higher normal loads.

Peak Shear Stress for each graph reaches a peak shear stress at varying horizontal displacements as:

- **35 MPa:** Peaks around 23 MPa with the displacement of about 6.0e-04 mm.
- **20 MPa:** Peaks around 14 MPa with the displacement of about 4.0e-04 mm.
- **10 MPa:** Peaks around 8 MPa with the displacement of about 2.0e-04 mm.
- **5 MPa:** Peaks around 4.5 MPa with the displacement of about 1.0e-04 mm.
- **1 MPa:** Peaks around 1 MPa with the displacement of about 0.15e-04 mm.

Thus, higher normal loads result in higher peak shear stresses.

After peaking, shear stress decreases and then stabilises, this is known as the Post-Peak Behaviour. The decrease is more gradual for higher normal loads, with shear stress stabilising at higher values.

Eventually, shear stress stabilises, representing the residual shear strength of the rock joint. Higher normal loads have higher residual shear strengths.

Theoretical Explanation

This graphical representation demonstrates that the varying Normal Load substantially affects the shear stress against horizontal displacement of rock joints. As the applied normal load gets higher, it increases the normal stress on the joint surfaces which enhances the frictional resistance and increases the shear strength, (N. Barton & S. Bandis, 1982).

This is due to a higher peak shear stress and a more defined shear strength envelope. As horizontal displacement proceeds, the shear stress rises rapidly due to the increasing normal load, after which it reaches a peak and stabilises, (N. Barton & S. Bandis, 1982).

3.5.8 Effects of Normal Load on the Normal Stress of Rock Joints

The results shown in figure 68, shows the graphs of Normal Stress against the Horizontal Displacement for varies normal load. It shows how normal stress (MPa) changes with horizontal displacement (mm) at different values of normal load to move the rock joints, based on the Continuously Yielding model.

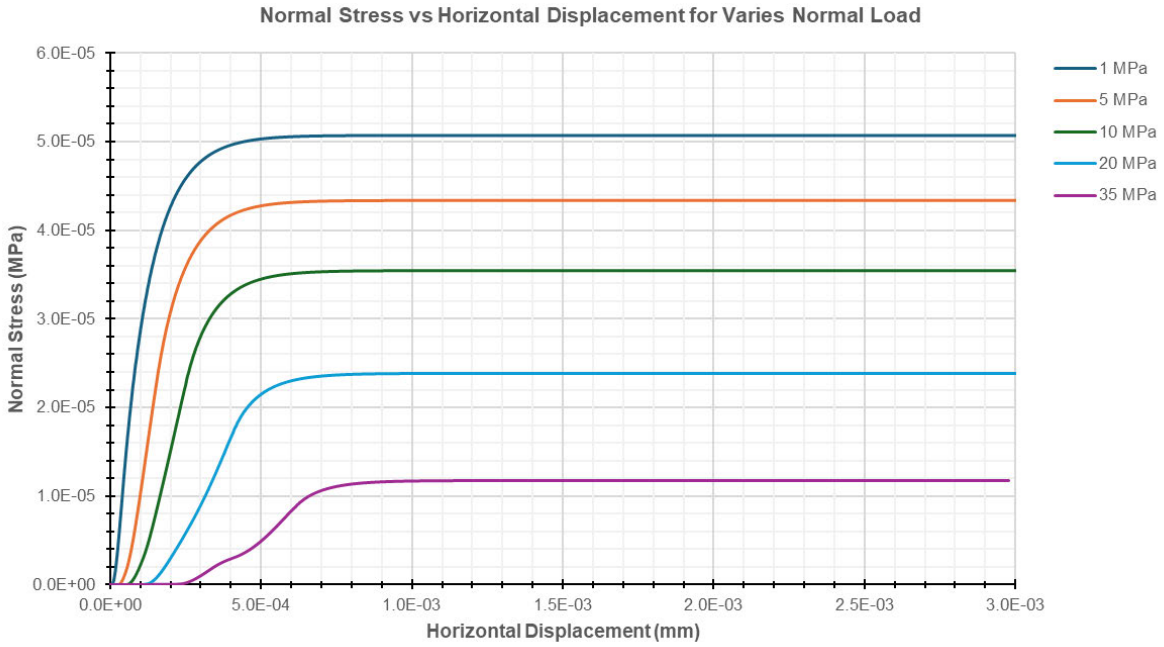

Figure 68: Presents the graph of Normal Stress vs the Horizontal Displacement for varies Normal Load

There is an increase for all graphs, which demonstrate a rapid rise in normal stress with a small increase in horizontal displacement. This indicates a stiff initial response of the rock joint, resisting the initial movement.

Each graph eventually reaches a residual stage, where the normal stress remains relatively constant despite further horizontal displacement. This residual stage signifies that the rock joint has yielded and is now deforming plastically.

As for the higher applied normal loads (20 MPa, 35 MPa) reach higher residual stage compared to lower loads (1 MPa, 5 MPa, 10 MPa). The rock joints under higher loads can sustain more stress before yielding.

Theoretical Explanation

This graphical representation demonstrates that the varying Normal Load substantially affects the normal stress against horizontal displacement of rock joints. As the applied normal load is increased,

the normal stress on the joint surfaces increases which enhances the frictional resistance and increases the shear strength, (N. Barton & S. Bandis, 1982).

Is results in a higher peak shear stress and a more defined shear strength envelope. Hence. as the horizontal displacement increases the shear stress rises more rapidly, which is due to the increased normal load, which finally reaches a peak and stabilises, (N. Barton & S. Bandis, 1982).

3.6 Summary of Findings

From the findings of this study, we have investigated the shear behaviour of rock joints under the Barton-Bandis, Mohr-Coulomb, and Continuously Yielding joint models using UDEC under constant normal load (CNL) conditions.

The analysis investigates essential parameters such as joint roughness, joint friction, dilation, shear and normal stiffness, velocity, UCS, compressive strength and normal load, revealing significant insights into the mechanical response of rock joints under various loading conditions.

Each model offers exclusive depths on the interfaces between shear and normal displacements, contributing to an inclusive understanding of rock joint behaviour in different stress conditions. The subsections below describe the findings of each models used.

3.6.1 Barton-Bandis Joint Model

From the findings of this joint model, it can be concluded that, the impact of various parameters such as joint roughness, friction, uniaxial compressive strength (UCS), compressive strength, shear velocity, and normal load plays an important role. This model provides a complete insight of how these factors affect shear and normal stresses against the horizontal displacement under constant normal load (CNL) conditions.

As for the shear stress against the horizontal displacement the shear stress increases with the roughness of the joint surface and the normal load applied, whereas the horizontal displacement increases with shear stress, but the rate of increase can differ based on joint roughness and normal load, (Barton N. R, 1976).

For normal stress against the horizontal displacement, the normal stress affects the horizontal displacement with higher normal stresses in general leading to smaller horizontal displacements due to increased friction, whereas for the horizontal displacement joints are free to dilate, resulting in larger horizontal displacements, (Barton, N & V. Choubey, 1977).

A brief explanation of the findings for the individual parameters for Barton-Bandis joint model are as:

- Higher joint roughness coefficients lead to increased shear strength and reduction in horizontal displacement.
- Due to the frictional properties of the joint surface, extensively influence the shear strength and deformation behaviour of the rock joint.
- The UCS values generally correlate with higher shear strength of the joint.
- Higher compressive strength causes to greater shear strength.
- The velocity (shear rate) can affect the dynamic friction coefficient, with higher velocities typically reducing the friction coefficient.
- Higher normal loads increase the shear strength and reduce the horizontal displacement.

3.6.2 Mohor Coulomb Joint Model

Under this joint model the key parameters investigated includes the joint friction, dilation, shear and normal stiffness, velocity, and normal load. The outcomes of these relationships between these parameters and the shear and normal displacement behaviours of the joints emphasises on the important understanding of the mechanical response of rock joints under varying loading conditions, (P. Barsanescu, 2015).

A brief explanation of the findings for the individual parameters for Mohor Coulomb joint model are as:

- **Shear Stress against the Horizontal Displacement**

  The joint friction increases with the roughness of the joint surface. Dilation (joint opening) of the joint occurs initially but may reduce with continued shearing. The shear stiffness of the joint decreases as the displacement increases. Higher shear velocities can lead to a reduction in post-peak shear strength. The shear strength increases with an increase in normal load, but the rate of increase reduces at higher loads.

- **Normal Stress against the Horizontal Displacement**

  The normal stiffness of the joint reduces as the joint opens. The normal stress is restricted by the tensile strength of the joint. Dilation is affected by the normal stress and the shear displacement. As the critical shear displacement is reached the dilation stops and the normal stress does not increase further.

3.6.3 Continuously Yielding Joint Model

This assessment reflects on the shear behaviour of rock joints under Constant Normal Load (CNL) conditions using the Continuously Yielding Joint Model in UDEC. The key parameters used in these simulations were joint friction, dilation, shear and normal stiffness, velocity, roughness, and normal loads. From the findings it was concluded that relationships between shear and normal displacements, were critical and stated how rock joints respond mechanically under various loading conditions, (Thirukumaran, 2014).

A brief explanation of the findings for the individual parameters for Continuously Yielding Joint model are as:

- **Shear Stress against the Horizontal Displacement**

  The joint friction friction decreases with increasing shear displacement due to progressive damage. Dilation initially increases but decreases as the joint undergoes further shearing. Shear stiffness reduces as the joint experiences more displacement. Higher shear velocities can lead to a reduction in shear strength. Joint roughness affects the initial shear strength and the rate of strength reduction. The shear strength increases with normal load but at a diminishing rate.

- **Normal Stress against the Horizontal Displacement**

  Normal stiffness decreases as the joint opens. Normal stress is limited by the tensile strength of the joint. Dilation is influenced by normal stress and shear displacement. As the critical shear displacement is reached the dilation stops, and normal stress does not increase further.

3.7 Numerical Results and Analysis for Mohor Coulomb Joint Model for CNL Conditions with Rock Bolt

This model is the same as the model used in section 3.2 of this report, but with the introduction of the rock bolt through the block. As the initial model was developed to be adaptable for different normal stress values and joint constitutive models. This model comprised two rectangular blocks stacked vertically, separated by a single discontinuity feature, representing the top and bottom of the physical joint specimen divided by the discontinuity.

To evaluate the Mohor Coulomb model's capability in replicating the shear behaviour of joints, a direct shear test was simulated on a planar joint. The planar joint plane was integrated into the Joint model, and a constant normal stress of 10 MPa initially was applied to the upper block.

The properties of the Rock Bolt material were taken for the UDEC 7.0 manual. Table 3-2 shows the assigned values of the rock bolt.

Table 3-2: Summary of Rock Bolt Parameters

Model Parameter			Value
Elastic		Young's Modulus (Pa)	2e11
		Density (Kg/m^3)	1e-3
Geometric		Cross Sectional Area (m^2)	5e-4
		Moment of Inertia (Kg.m^2)	2e-8
Element Yield		Tensile Yield Strength (Pa)	2.25e5
		Compress Yield Strength (Pa)	2.23e5
		Tensile Failure Strain	0.2
Coupling Spring Constant	**Normal**	Stiffness (Pa)	2e7
		Cohesive Strength (Pa)	1e5
		Friction Angle	45
	Shear	Stiffness (Pa)	2e7
		Cohesive Strength (Pa)	1e5
		Friction Angle	45
		Perimeter (m)	8e-2

Figure 69 shows the block model similar to the model used in section 3.2 of this report, but with the introduction of the rock bolt through the block.

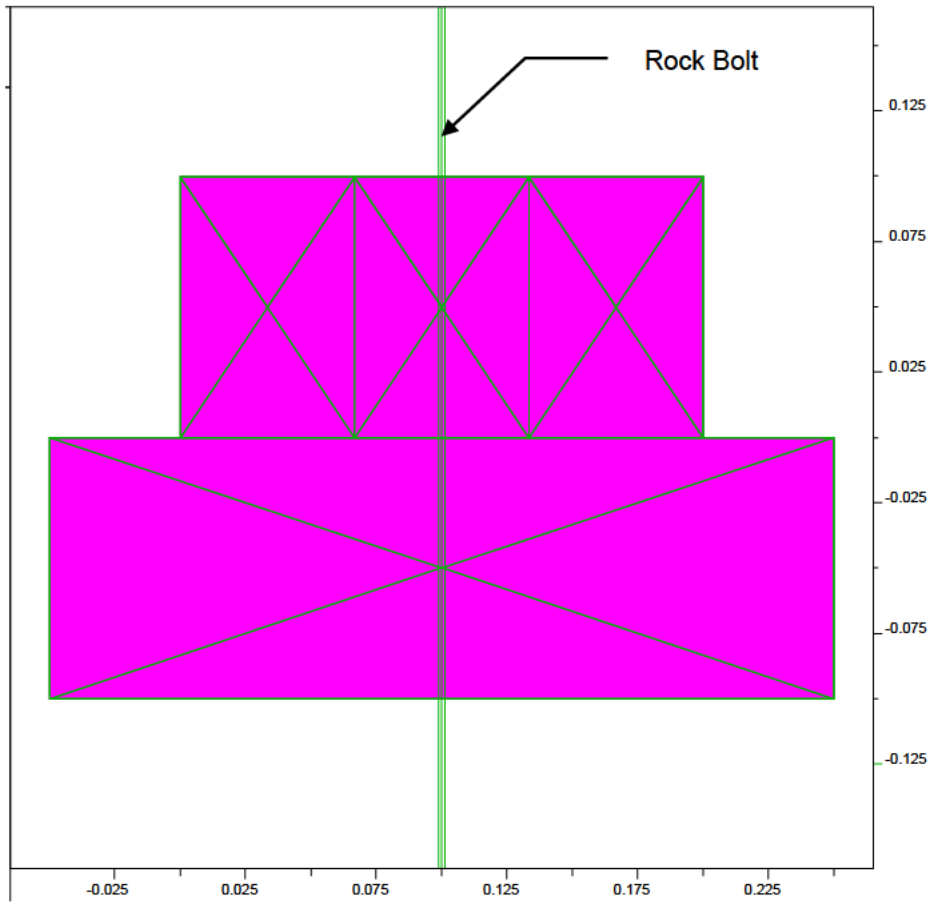

Figure 69: Represents the block Model with rock blot

This block model has been used for all UDEC simulation for Barton-Bandis, Mohor Coulomb and Continuously Yielding joint models. The boundary conditions remains the same excepts the varying normal loads and shearing rate (velocity) as described in each models.

3.7.1 Effects of Joint Friction on the Shear Stress of Rock Joints with Rock Bolt

The results shown in figure 70, shows the graph of Shear Stress against the Horizontal Displacement for varies Joint Friction with introduction of rock bolt into the joint model simulation in UDEC. This illustrates how shear stress changes with horizontal displacement for rock joints with different friction values.

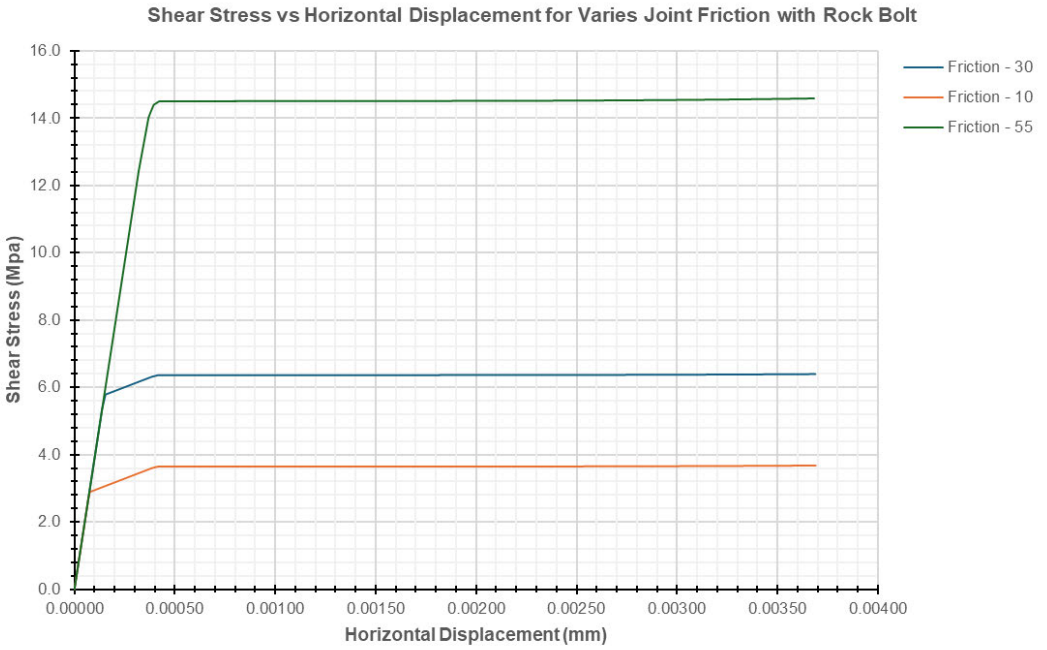

Figure 70: Presents the graph of Shear Stress vs the Horizontal Displacement for varies Joint Friction

Initially, all curves show a linear increase in shear stress with horizontal displacement. This elastic behaviour indicates that the rock joints and the bolt system deform proportionally to the applied shear stress.

Each graph description is as:

- **Friction - 10**
  Shear stress increases rapidly with the initial horizontal displacement, showing elastic behaviour. Residual stage has been reached around 4 MPa, indicating the joint has reached its shear strength.
- **Friction - 30**
  Rapid increase in shear stress, higher than the Friction-10 graph. Residual stage has reached around 6.2 MPa, showing higher resistance due to increased friction.
- **Friction – 55**
  There is a sharp increase in shear stress, higher than both previous graphs. Residual stage has been reached around 14.2 MPa, indicating the highest resistance among the three due to maximum friction.

Theoretical Explanation

This graphical representation demonstrates that the varying joint friction substantially affects the shear stress against horizontal displacement of rock joints. As the Rock bolt substantially enhances the shear stress capacity of rock joints under horizontal displacement in the UDEC simulation when joint friction varies, (Jun Wang, Derek B. Apel, Huawei Xu & Chong Wei , 2022).

When normal force increases the joint movement is limited, thus the rock bolts improve the shear strength and energy absorption capacity of the joint and successfully mitigates the shear displacement, (Jun Wang, Derek B. Apel, Huawei Xu & Chong Wei , 2022).

3.7.2 Effects of Joint Friction on the Normal Stress of Rock Joints with Rock Bolt

The results shown in figure 71, shows the graph of Normal Stress against the Horizontal Displacement for varies Joint friction with introduction of rock bolt into the joint model simulation in UDEC. This illustrates how normal stress changes with horizontal displacement for rock joints with different friction values.

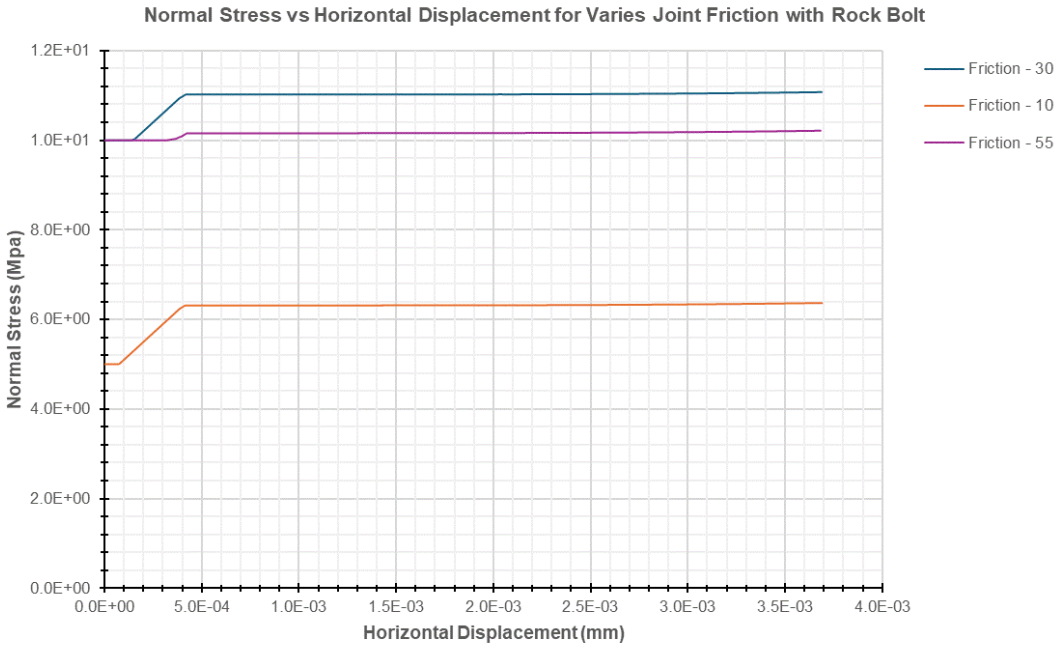

Figure 71: Presents the graph of Normal Stress vs the Horizontal Displacement for varies Joint Friction

Initially for all the joint friction values, normal stress increases gradually with a small increase in horizontal displacement. The initial slope is flat and rise significantly, indicating that the rock joints are more resistant to deform.

As for the individual graphs:

- **Friction 55:** Starts at approximately 10 MPa then slightly increase in normal stress, stabilising around 11 MPa with horizontal displacement.
- **Friction 30:** Starts at approximately 10 MPa, slight increase in normal stress as horizontal displacement increases. It reaches the residual stage around 10.1 MPa, indicating that the normal stress stabilises despite further displacement.
- **Friction 10:** Starts at approximately 5 MPa, then a sharp increase in normal stress up to around 6.2 MPa with a small horizontal displacement. It reaches residual stage quickly after the initial rise.

Theoretical Explanation

This graphical representation demonstrates that the varying joint friction substantially affects the normal stress against horizontal displacement of rock joints. The Rock bolts extensively influence the

normal stress distribution against horizontal displacement in the UDEC simulation, especially under varying joint friction conditions, (Jun Wang, Derek B. Apel, Huawei Xu & Chong Wei , 2022).

When increasing the normal force and restricting joint movement the rock bolts enhance the normal stress capacity of rock joints, thus it improves the overall stability of the rock mass, (Malavika Varma, V. B. Maji & A. Boominathan , 2024).

3.7.3 Effects of Joint Dilation on the Shear Stress of Rock Joints with Rock Bolt

The results shown in figure 72, shows the graph of Normal Stress against the Horizontal Displacement for varies Joint Dilation with introduction of rock bolt into the joint model simulation in UDEC. this illustrates how normal stress changes with horizontal displacement for rock joints with different dilation values.

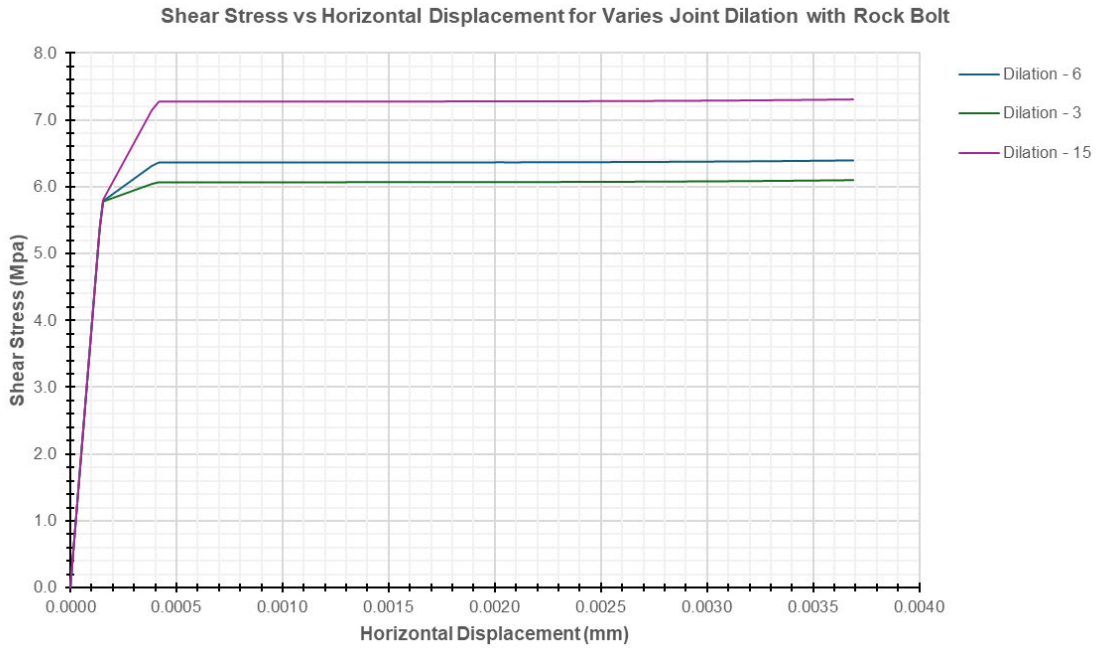

Figure 72: Presents the graph of Shear Stress vs the Horizontal Displacement for varies Joint Dilation

Initially for all the dilation values normal stress increases rapidly with a minimal horizontal displacement. This reflects the initial resistance provided by the joint and rock bolt system.

The peak shear stress varies with different dilation values as:

- **Dilation 3:** peaks around 6.0 MPa.
- **Dilation 6:** peaks around 6.5 MPa.
- **Dilation 15:** Highest peak, indicating strong resistance to shear at around 7.3 MPa.

Higher dilation values result in higher residual shear stresses, indicating stronger resistance.

Theoretical Explanation

This graphical representation demonstrates that the varying joint dilation substantially affects the shear stress against horizontal displacement of rock joints. As the Rock bolt substantially enhances the shear stress capacity of rock joints under horizontal displacement in the UDEC simulation when joint dilation varies, (Jun Wang, Derek B. Apel, Huawei Xu & Chong Wei , 2022).

When normal force increases the joint movement is limited, thus the rock bolts improve the shear strength and energy absorption capacity of the joint and successfully mitigates the shear displacement, (Jun Wang, Derek B. Apel, Huawei Xu & Chong Wei , 2022).

3.7.4 Effects of Joint Dilation on the Normal Stress of Rock Joints with Rock Bolt

The results shown in figure 73, shows the graph of Normal Stress against the Horizontal Displacement for varies Joint dilation with introduction of rock bolt into the joint model simulation in UDEC. This illustrates how normal stress changes with horizontal displacement for rock joints with different dilation values.

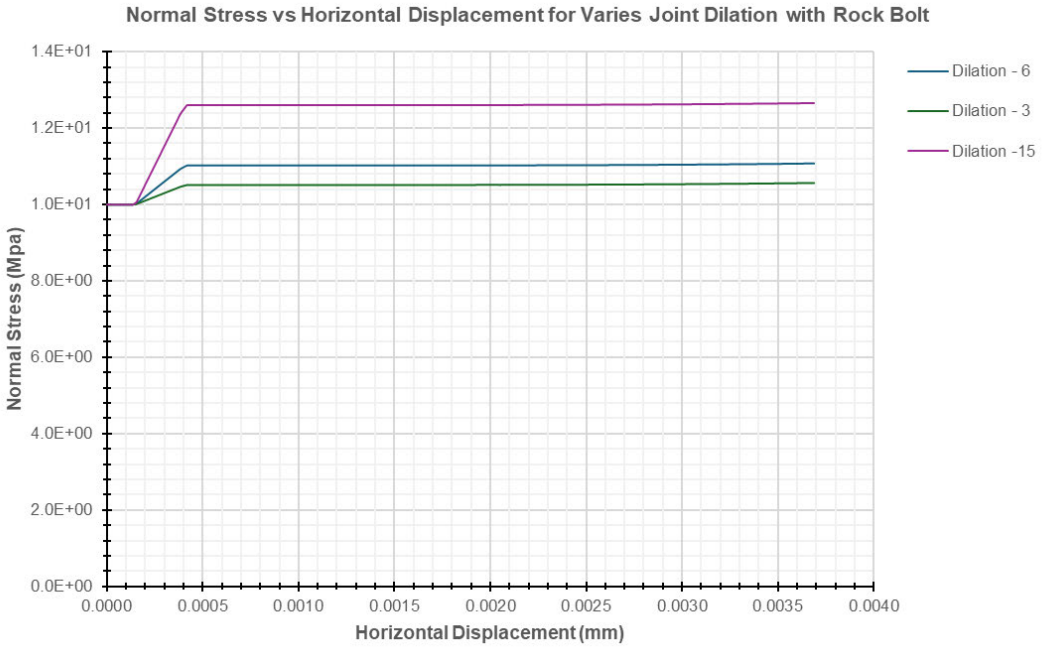

Figure 73: Presents the graph of Normal hear Stress vs the Horizontal Displacement for varies Joint Dilation

Initially for all the joint friction values, normal stress increases gradually with a small increase in horizontal displacement. The initial slope is flat and rise significantly, indicating that the rock joints are more resistant to deform.

As for the individual graphs:

- **Dilation 3:** Sharp increase initially, then levels of around 10.2 MPa. It is lower than the other graphs, indicates minimal dilation effect.
- **Dilation 6:** There is a sharp initial rise, then reaches the residual stage. It peaks around 10.4 MPa (Mid-range), indicating moderate dilation effect.
- **Dilation 15:** There steep increase, reaching the peak around 12.3 MPa. This indicating significant dilation effect.

Theoretical Explanation

This graphical representation demonstrates that the varying joint dilation substantially affects the normal stress against horizontal displacement of rock joints. The use of Rock bolts drastically influences the normal stress against horizontal displacement by enhancing the normal stiffness and limiting joint dilation, (Yu Chen & Haodong Xiao , 2024).

As a result, it increases the resistance to shear displacement and improves the stability of the rock mass. This outcome is more defined when joint dilation is limited which leads to higher peak shear strength and reduced deformation, (Jung-Wook Park, Yong-Ki Lee, Jae-Joon Song & Byung-Hee Choi , 2013).

3.7.5 Effects of Normal Load on the Shear Stress of Rock Joints with Rock Bolt

The results shown in figure 74, shows the graph of Normal Stress against the Horizontal Displacement for varies Normal Load with introduction of rock bolt into the joint model simulation in UDEC. This illustrates how normal stress changes with horizontal displacement for rock joints with different normal load values.

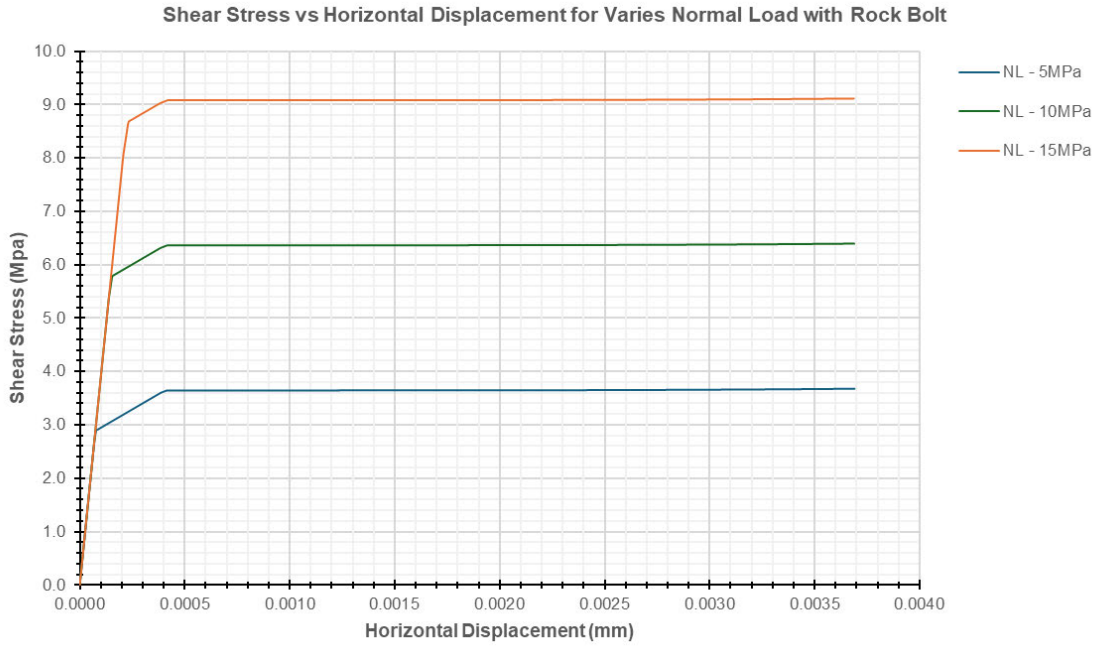

Figure 74: Presents the graph of Shear Stress vs the Horizontal Displacement for varies Normal Load

Initially there is linear increase in the shear stress as shown by each graph as the horizontal displacement increases, indicating elastic behaviour. This reflects the initial resistance provided by the joint and rock bolt system.

The stress varies with different normal load values as:

- **Normal Load – 15 MPa:** The shear stress rises rapidly from 0 to about 9 MPa as horizontal displacement goes from 0 to around 0.0005 mm. After the initial spike, shear stress stabilizes at around 9 MPa, staying constant as displacement increases to 0.004 mm.

- **Normal Load – 10 MPa:** Initially shear stress quickly rises from 0 to about 6.4 MPa with initial horizontal displacement up to 0.0005 mm. It then stabilizes at around 6.4 MPa, maintaining this level despite further displacement.

- **Normal Load – 5 MPa:** Initially shear stress jumps from 0 to around 3 MPa for the same initial displacement, it then reaches residual stage of at 3 MPa, holding steady as displacement continues.

Theoretical Explanation

This graphical representation demonstrates that the applied normal load substantially affects the shear stress against horizontal displacement of rock joints. As the Rock bolt substantially enhances the shear stress capacity of rock joints under horizontal displacement in the UDEC simulation when normal load varies, (Jun Wang, Derek B. Apel, Huawei Xu & Chong Wei , 2022).

When normal force increases the joint movement is limited, thus the rock bolts improve the shear strength and energy absorption capacity of the joint and successfully mitigates the shear displacement, (Jun Wang, Derek B. Apel, Huawei Xu & Chong Wei , 2022).

3.7.6 Effects of Normal Load on the Normal Stress of Rock Joints with Rock Bolt

The results shown in figure 75, shows the graph of Normal Stress against the Horizontal Displacement for varies Normal Load with introduction of rock bolt into the joint model simulation in UDEC. This illustrates how normal stress changes with horizontal displacement for rock joints with different normal load values.

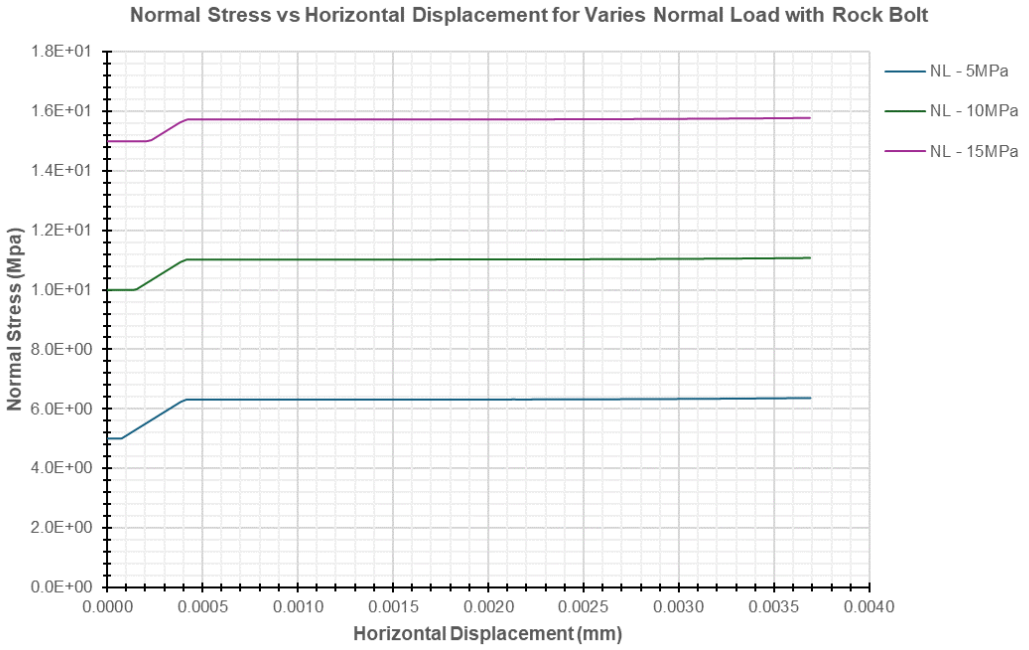

Figure 75: Presents the graph of Normal Stress vs the Horizontal Displacement for varies Normal Load

Initially for all the normal load values, normal stress increases rapidly with a sharp increase before moving. The normal stress levels of slightly then rises significantly before reaches residual stage. This flatting and rising, indicating that the rock joints are more resistant to deform.

As for the individual graphs:

- **Normal Load – 5 MPa:** The normal stress starts around 5 MPa. The horizontal displacement increases from 0 to 0.0005 mm, normal stress increases slightly. It then remains constant around 6.2 MPa despite further displacement.

- **Normal Load – 10 MPa:** The normal stress starts around 10 MPa then shows a small increase in normal stress with initial displacement. It then remains constant at approximately 11 MPa with further displacement.

- **Normal Load – 15 MPa:** The normal stress starts around 15 MPa, then there is a slight increase in normal stress as displacement increases. It then remains constant around 15.8 MPa for additional horizontal displacement.

Theoretical Explanation

This graphical representation demonstrates that the varying applied normal loads substantially affects the normal stress against horizontal displacement of rock joints. The Rock bolts extensively influence the normal stress distribution against horizontal displacement in the UDEC simulation, especially under varying normal load conditions, (Jun Wang, Derek B. Apel, Huawei Xu & Chong Wei , 2022).

When increasing the normal force and restricting joint movement the rock bolts enhance the normal stress capacity of rock joints, thus it improves the overall stability of the rock mass, (Malavika Varma, V. B. Maji & A. Boominathan , 2024).

3.7.7 Effects of Velocity on the Shear Stress of Rock Joints with Rock Bolt

The results shown in figure 76, shows the graph of Normal Stress against the Horizontal Displacement for varies applied velocities with introduction of rock bolt into the joint model simulation in UDEC. This illustrates how normal stress changes with horizontal displacement for rock joints with different velocity values.

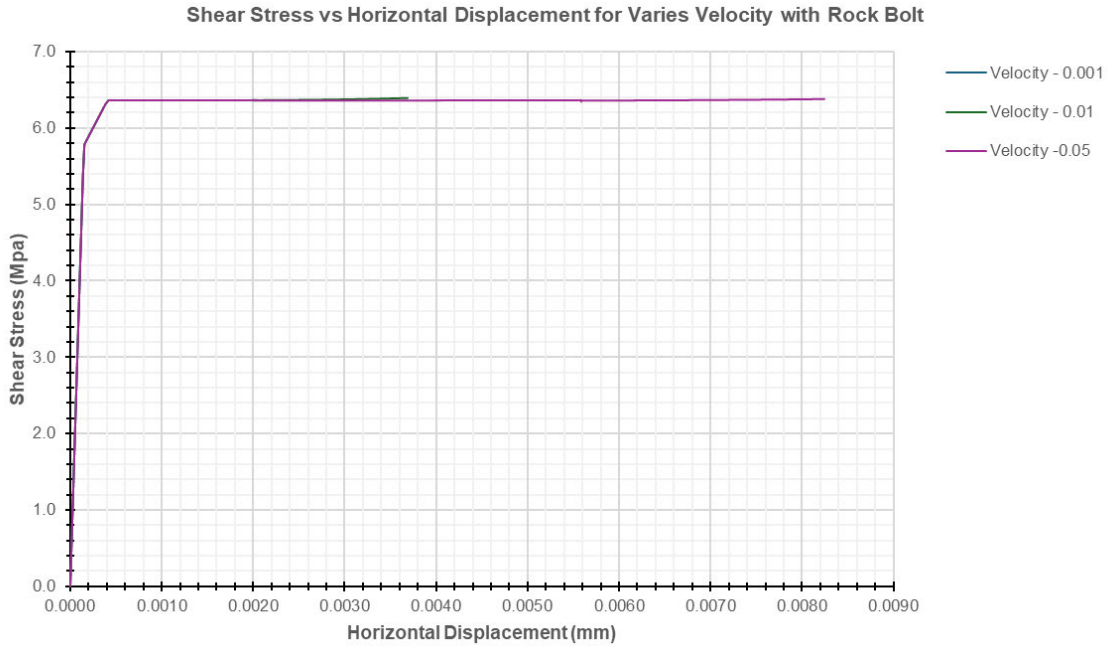

Figure 76: Presents the graph of Shear Stress vs the Horizontal Displacement for varies Velocity

Initially for all three velocities (0.001, 0.01, and 0.05), normal stress increases quickly as horizontal displacement begins. This steep rise shows the rock joint and rock bolt's initial resistance.

After the initial rapid rise, the shear stress reaches residual stage around 6.5 MPa, regardless of the velocity. This residual stage suggests that once the initial shearing force is overcome, the rock joint maintains a consistent resistance with continuous displacement.

Theoretical Explanation

This graphical representation demonstrates that the applied shear velocity substantially affects the shear stress against horizontal displacement of rock joints. With the bolts, it increases the peak shear

stress and limit horizontal displacement, When increasing the normal force and restricting joint movement, (Sunhao Zhang, Yujing Jiang, Hengjie Luan, Bo Li, Jianrong Liu & Changsheng Wang , 2024).

Therefore, the shear stress against the shear displacement correlation shows better resistance and delayed failure which indicates that there is an improved stability of the rock mass, (Sunhao Zhang, Yujing Jiang, Hengjie Luan, Bo Li, Jianrong Liu & Changsheng Wang , 2024)

3.7.8 Effects of Velocity on the Normal Stress of Rock Joints with Rock Bolt

The results shown in figure 77, shows the graph of Normal Stress against the Horizontal Displacement for varies velocities with introduction of rock bolt into the joint model simulation in UDEC. This illustrates how normal stress changes with horizontal displacement for rock joints with different velocity values.

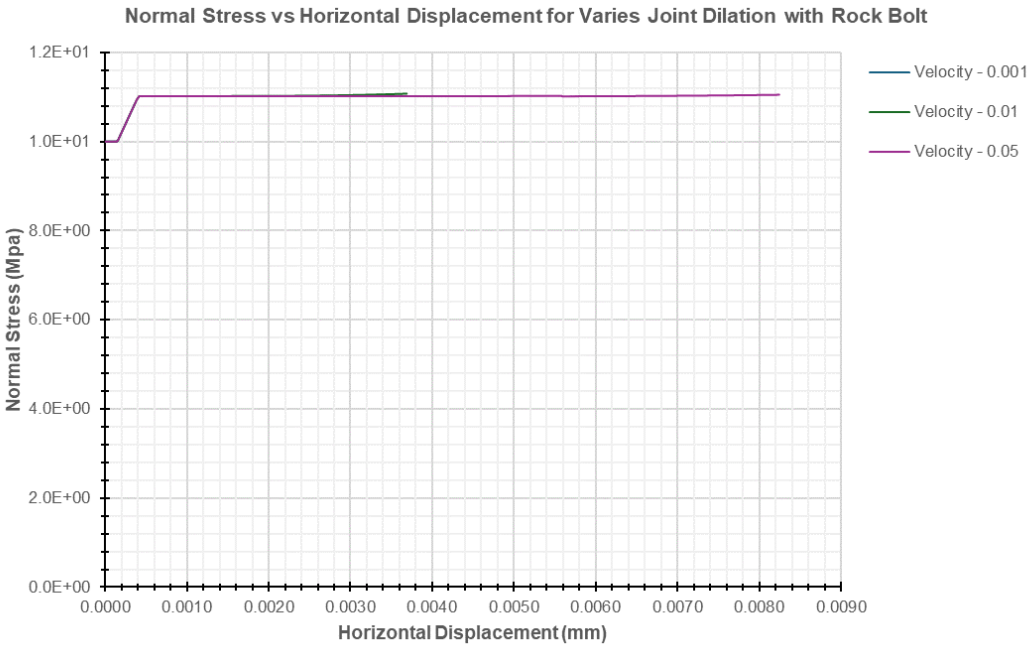

Figure 77: Presents the graph of Normal Stress vs the Horizontal Displacement for varies Velocity

For all three velocities, the normal stress starts at 10 MPa initially. It the increases sharply with the peak at 10.5 MPa and then remains constant with the same value of 10.5 MPa for all velocities.

The horizontal displacement remains very small, within the range of 0.0000 to 0.0090 mm.

The graph demonstrates that for rock joints reinforced with rock bolts, the normal stress quickly reaches stabilization at around 10.5 MPa regardless of the shearing rate applied. This suggests that the reinforcement provided by the rock bolts effectively maintains the stability of the rock joint under varying shearing conditions.

Theoretical Explanation

This graphical representation demonstrates that the applied shear velocity substantially effects on the normal stress against horizontal displacement of rock joints. As the Rock bolt enhances the normal stress resistance of rock joints under varying shear, it increases the peak normal stress and limit horizontal displacement, providing greater stability of the rock mass (Sunhao Zhang, Yujing Jiang, Hengjie Luan, Bo Li, Jianrong Liu & Changsheng Wang , 2024).

This is due to a more robust stress vs displacement relationship which indicates an improved performance and prolonged failure of the rock joints, (Sunhao Zhang, Yujing Jiang, Hengjie Luan, Bo Li, Jianrong Liu & Changsheng Wang , 2024).

3.8 Numerical Results and Analysis for Continuously Yeilding Joint Model for CNL Conditions with Rock Bolt

This model is the same as the model used in section 3.7 of this report, as the initial model was developed to be adaptable for different normal stress values and joint constitutive models. This model comprised two rectangular blocks stacked vertically, separated by a single discontinuity feature, representing the top and bottom of the physical joint specimen divided by the discontinuity.

3.8.1 Effects of Joint Roughness on Shear Stress of Rock Joints with Rock Bolt

The results shown in figure 78, shows the graph of Shear Stress against the Horizontal Displacement for varies Joint Roughness with introduction of rock bolt into the joint model simulation in UDEC. This illustrates how shear stress changes with horizontal displacement for rock joints with different joint roughness values.

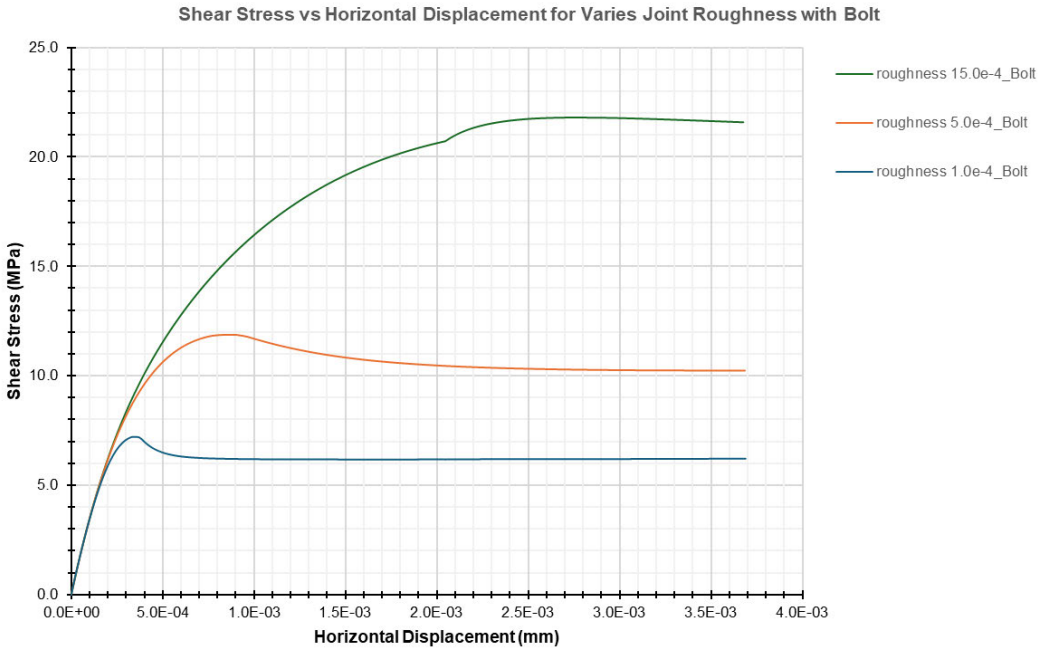

Figure 78: Presents the graph of Shear Stress vs the Horizontal Displacement for varies Joint Roughness

In the initial stage, the graphs show a rapid rise in shear stress with horizontal displacement. This indicates the resistance offered by the joint roughness as the block starts to move.

At the Peak Shear Stress stage, each graph peaks at a certain displacement as follows:

- **Roughness 15.0e-4:** Rapid rise in shear stress around 21.5 MPa before reaching the residual stage.
- **Roughness 5.0e-4:** Slower rise compared to green graph with the maximum stress recorded around 12 MPa, then slight decrease in shear stress before reaching the stabilising stage.

- **Roughness 1.0e-4:** slowest rise in the shear stress and peaks around 7 MPa with the displacement of 3.5e-4 mm and the slightly decrease in shear stress before reaching the residual stage.

Therefore, higher roughness values result in higher peak shear stress. With higher roughness (15.0e-4) results in higher peak shear stress due to greater interlocking and resistance, whereas for lower roughness (1.0e-4) results in lower peak shear stress due to less interlocking.

Theoretical Explanation

This graphical representation demonstrates that the joint roughness has substantially effects on the shear stress against horizontal displacement of rock joints. It is believed that the rock bolts can be assumed through the contact between the joint surface asperities and the reinforcing elements. Joint roughness is computed by the Joint Roughness Coefficient (JRC) which improves the shear strength due to mechanical interlocking, (Yinge Zhu, Gang Wang, Anqi Li, Huiyuan Chen, Tingfang Liu & Hui Guan , 2022).

In the UDEC simulation the shear stress against the displacement graph typically shows an initial elastic stage then a peak shear stress and a residual stage. This model captures the gradual degradation of asperities and reflects on the real behaviour under constant loading. Rock bolts further provides stability of the joint which reduces the asperity degradation and maintaining higher shear strength, (Yinge Zhu, Gang Wang, Anqi Li, Huiyuan Chen, Tingfang Liu & Hui Guan , 2022).

3.8.2 Effects of Joint Roughness on Normal Stress of Rock Joints with Rock Bolt

The results shown in figure 79, shows the graph of Normal Stress against the Horizontal Displacement for varies Joint Roughness with introduction of rock bolt into the joint model simulation in UDEC. This illustrates how normal stress changes with horizontal displacement for rock joints with different joint roughness values.

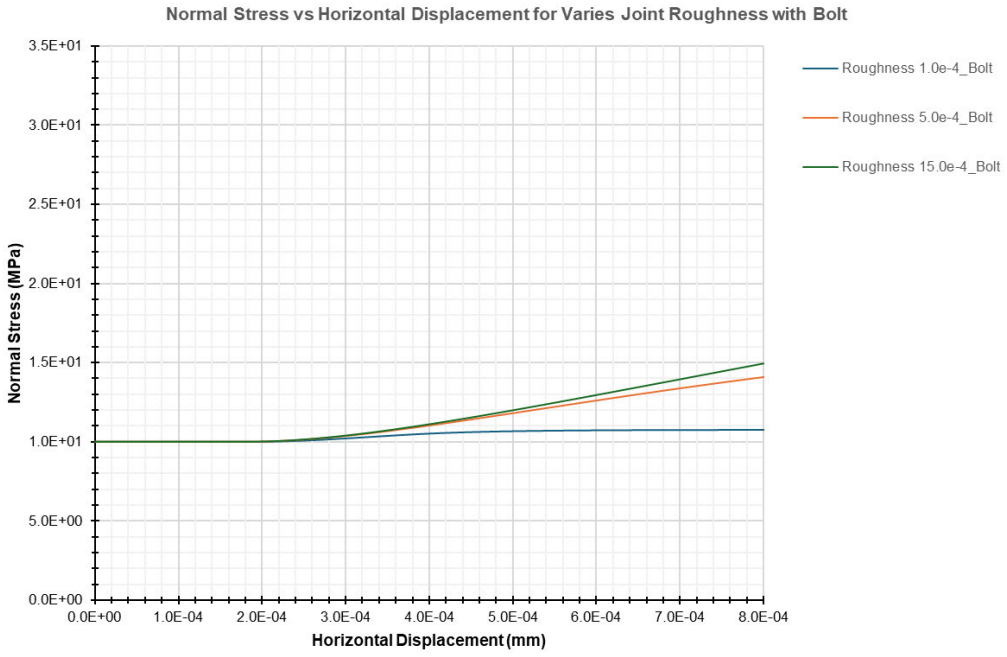

Figure 79: Presents the graph of Normal Stress vs the Horizontal Displacement for varies Joint Roughness

In the initial stage, the normal stress increased to 1.0e+01 MPa and remained for the displacement of around 2.0e-04 mm before the shear stress increased further.

At the Peak normal stress stage, each graph peaks at a certain displacement as follows:

- **Roughness 15.0e-4:** Maintained upward trend with the normal stress increases significantly with horizontal displacement. This is due to the very rough joint surface causing substantial resistance to movement.
- **Roughness 5.0e-4:** This graph trend was slight upward slope. The normal stress progressively increases with horizontal displacement which indicated that the moderate joint roughness causing some resistance to movement.
- **Roughness 1.0e-4:** This graphs trend was fairly flat, as the normal stress remains almost constant with increasing horizontal displacement. This trend is due to smooth joint surface with the rock bolt effectively restricting movement.

Theoretical Explanation

This graphical representation demonstrates that the joint roughness has substantially effects on the normal stress against horizontal displacement of rock joints. It can be described that the interaction between the joint surface asperities, applied normal load and Joint roughness measures through the Joint Roughness Coefficient (JRC) which has an effect on the normal stress distribution along the joint surface, (Liu He, Zhiming Zhao, Jiayi Chen & Diyi Liu , 2020).

The normal stress against the displacement relationship in general shows an increase in normal stress due to asperity interlocking which is followed by a peak and then a decrease as asperities degrades. The rock bolts help uphold joint integrity, reducing asperity degradation and stabilising normal stress, (Liu He, Zhiming Zhao, Jiayi Chen & Diyi Liu , 2020).

3.8.3 Effects of Joint Friction on Shear Stress of Rock Joints with Rock Bolt

The results shown in figure 80, shows the graph of Shear Stress against the Horizontal Displacement for varies Joint Friction with introduction of rock bolt into the joint model simulation in UDEC. This illustrates how shear stress changes with horizontal displacement for rock joints with different joint friction values.

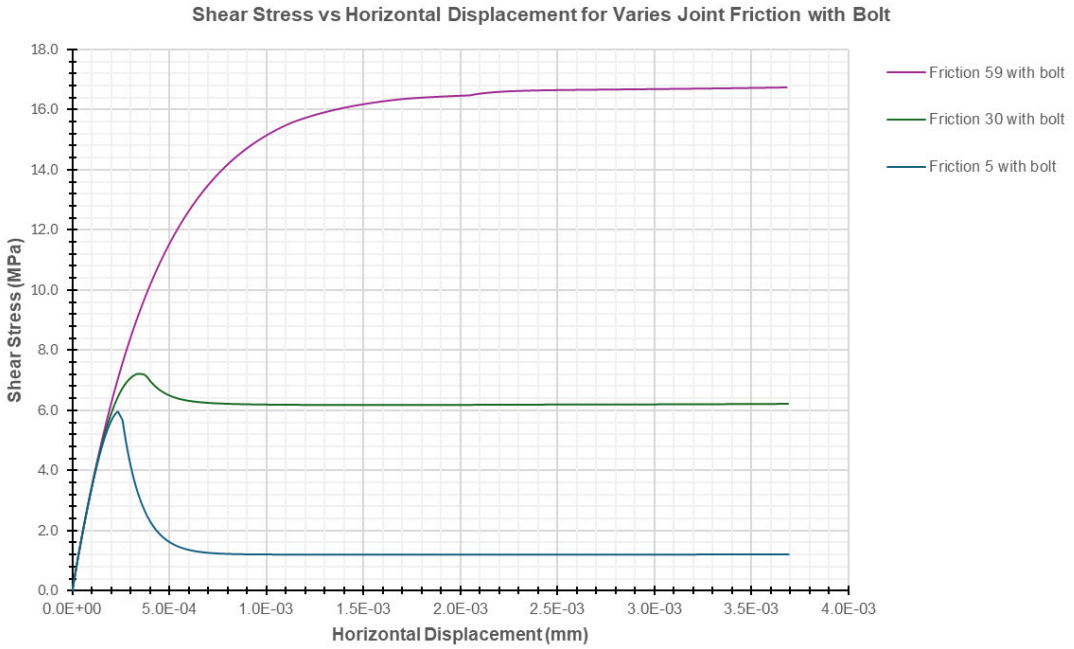

Figure 80: Presents the graph of Shear Stress vs the Horizontal Displacement for varies Joint Friction

In the initial stage, the graphs show a fast rise in shear stress with horizontal displacement. This indicates the resistance offered by the joint friction as the block starts to move.

At the Peak Shear Stress stage, each graph peaks at a certain displacement as follows:

- **Friction 59:** Initially the shear stress spikes rapidly, reaching around 16.5 MPa at a horizontal displacement of about 0.0005 mm. After peaking, shear stress stabilizes at approximately 16.5 MPa as displacement continues.
- **Friction 30:** There is an initial Increase in the shear stress which rises quickly, peaking roughly around 7.0 MPa at about 0.00035 mm displacement. After the post-peak, the shear stress drops slightly and then stabilizes around 6 MPa.
- **Friction 5:** There is an increase in the shear stress initially, after reaching around 6.0 MPa at 0.00025 mm displacement. As the post-peak is reached, the shear stress falls sharply and stabilises around 1.5 MPa.

Hence, increased friction leads to higher peak shear stress. This is due to the greater friction meaning more resistance against shear displacement. As the peak is reached the shear stress tends to stabilize at a higher level. Therefore, the increased resistance helps maintain a higher residual shear stress, providing better stability even after yielding.

Theoretical Explanation

This graphical representation demonstrates that the joint friction has substantially effects on the shear stress against horizontal displacement of rock joints with rock bolts. It is assumed that the contact between the joint surface asperities, applied shear force, joint friction is influenced by the Joint

Roughness Coefficient (JRC) and the friction angle which enhances shear strength due to mechanical interlocking and frictional resistance, (Liu He, Zhiming Zhao, Jiayi Chen & Diyi Liu , 2020).

The shear stress against the displacement graph shows an initial elastic stage followed by a peak shear stress and finally a residual stage. This UDEC simulation reviles that the advancing degradation of asperities and reflects on the real behaviour under maintained loading. Moreover, the rock bolts help sustain the joint reliability, decreasing asperity degradation and stabilising shear stress, (Liu He, Zhiming Zhao, Jiayi Chen & Diyi Liu , 2020).

3.8.4 Effects of Joint Friction on Normal Stress of Rock Joints with Rock Bolt

The results shown in figure 81, shows the graph of Normal Stress against the Horizontal Displacement for varies Joint Friction with introduction of rock bolt into the joint model simulation in UDEC. This illustrates how normal stress changes with horizontal displacement for rock joints with different joint friction values.

Figure 81: Presents the graph of Normal Stress vs the Horizontal Displacement for varies Joint Friction

- **Friction 59:** At the starts the shear stress is approximately 10 MPa and remains constant as horizontal displacement increases. This is due to a high-friction joint where normal stress is not significantly affected by displacement due to strong resistance provided by the friction and rock bolt.
- **Friction 30:** This graph also starts at around 10 MPa and remains constant with increasing displacement, as this shows the similar behaviour to Friction 59, where the joint maintains stability and normal stress does not change much due to effective frictional resistance and bolt reinforcement.
- **Friction 5:** The graph starts at about 10 MPa but increases rapidly to around 13.9 MPa with a small displacement (~0.0005 mm), then reaches the residual stage. As for the lower friction values, the joint initially yields, causing an increase in normal stress until it reaches stability. This shows that the lower friction joint deforms more easily under applied stress, requiring the rock bolt to provide additional resistance to stabilize the normal stress.

Theoretical Explanation

This graphical representation demonstrates that the joint roughness has substantially effects on the normal stress against horizontal displacement of rock joints. It can be described that the interaction between the joint surface asperities and the applied normal loads affected by the joint friction, joint roughness coefficient (JRC) and the friction angle which affects the normal stress distribution along the joint surface, (Liu He, Zhiming Zhao, Jiayi Chen & Diyi Liu , 2020).

The normal stress against the displacement relationship shows an increase in normal stress due to asperity interlocking which is followed by a peak and then a decrease as asperities degrades. This UDEC simulation reviles that there is a continuing degradation which reflects the real behaviour under sustained loading. Furthermore, the rock bolts help maintain joint integrity which reduces the asperity degradation and stabilising normal stress, (Liu He, Zhiming Zhao, Jiayi Chen & Diyi Liu , 2020).

3.8.5 Effects of Normal Load on Shear Stress of Rock Joints with Rock Bolt

The results shown in figure 82, shows the graph of Shear Stress against the Horizontal Displacement for varies applied Normal Load with introduction of rock bolt into the joint model simulation in UDEC. This illustrates how shear stress changes with horizontal displacement for rock joints with different normal load values.

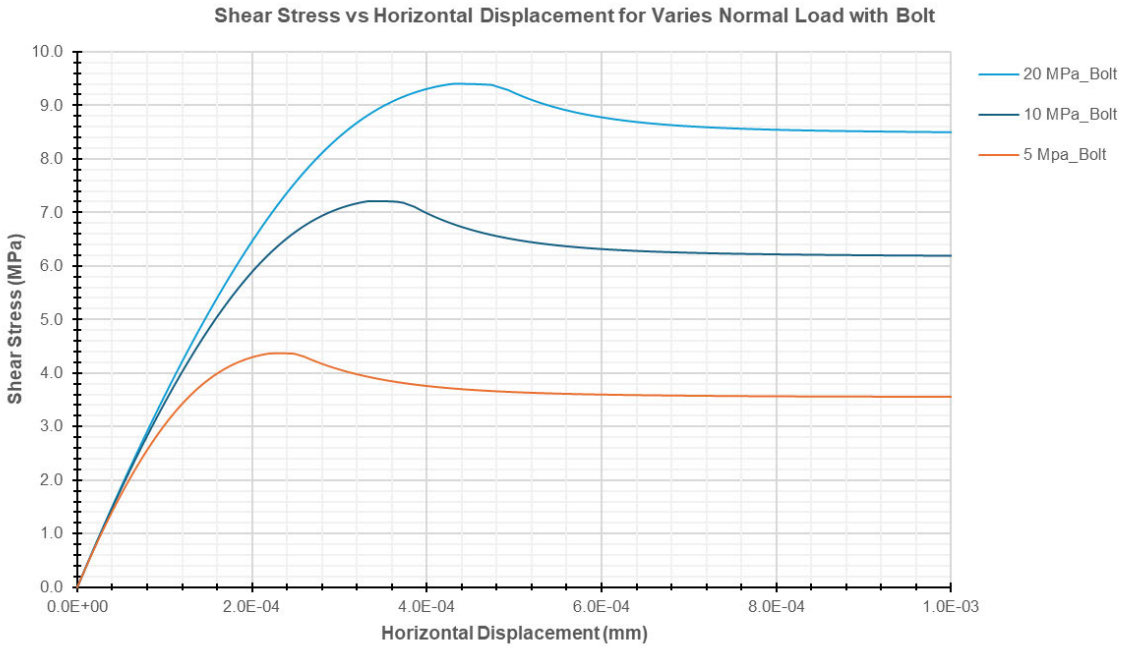

Figure 82: Presents the graph of Shear Stress vs the Horizontal Displacement for varies Normal Load

Initially there is an increase for all three normal loads graphs, as the shear stress increases rapidly with a small initial horizontal displacement. The steepest rise is for the highest normal load (20 MPa), followed by 10 MPa and then 5 MPa.

After the peak stage, each graph reaches the shear stress as follows:

- **20 MPa:** Peaks around 14 MPa, with the displacement of 4.5e-04 mm.
- **10 MPa:** Peaks around 7.2 MPa with the displacement of 3.5e-04 mm.
- **5 MPa:** Peaks around 4.4 MPa with the displacement of 2.5e-04 mm.

This indicates that higher normal loads result in higher peak shear stress due to greater resistance.

After reaching the post-peak Behaviour the shear stress gradually decreases with further horizontal displacement. This decrease is more pronounced for the 20 MPa and 10 MPa loads, while the 5 MPa load shows a relatively stable shear stress after the peak.

Theoretical Explanation

This graphical representation demonstrates that the applied normal load has substantially effects on the shear stress against horizontal displacement of rock joints with rock bolts. It is assumed that the interaction between the joint surface asperities and the applied higher normal loads increase the contact area and frictional resistance between joint surfaces which enhances the shear strength, (Liu He, Zhiming Zhao, Jiayi Chen & Diyi Liu , 2020).

The shear stress against the displacement graph shows a primary elastic stage followed by a peak shear stress and finally a residual stage. This UDEC simulation reviles the advancing degradation of asperities which reflects the real behaviour of the joints under maintained loading. Hence, the rock bolts help sustain joint integrity which reduces asperity degradation and stabilising shear stress, (Liu He, Zhiming Zhao, Jiayi Chen & Diyi Liu , 2020).

3.8.6 Effects of Normal Load on Normal Stress of Rock Joints with Rock Bolt

The results shown in figure 83, shows the graph of Normal Stress against the Horizontal Displacement for varies applied Normal Load with introduction of rock bolt into the joint model simulation in UDEC. This illustrates how normal stress changes with horizontal displacement for rock joints with different normal load values.

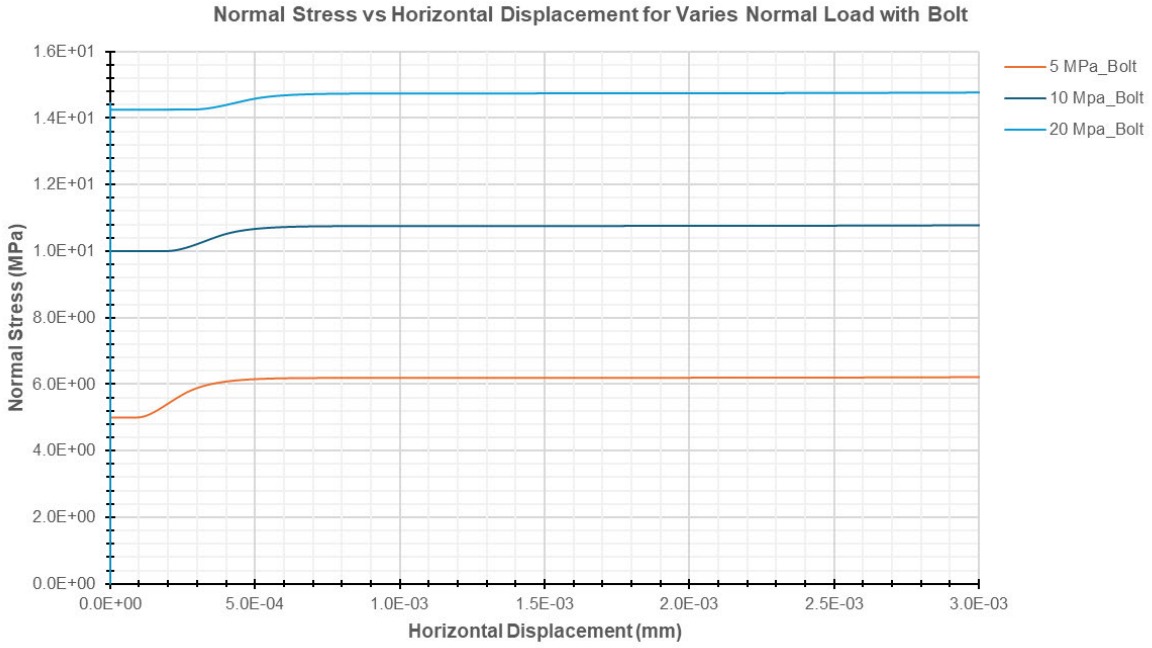

Figure 83: Presents the graph of Normal Stress vs the Horizontal Displacement for varies Normal Load

In the initial stage, the normal stress increased very sharply maintaining 0 mm displacement for all the applied normal loads. Then we have some movement which are described as follows:

- **5 MPa:** The graph rises at approximately 4.5 MPa and gradually increases to about 6.1 MPa. This shows that there is a slight initial increase, then it reaches the stability. This indicates that some yielding and resistance provided by the rock joint and bolt combination.

- **10 MPa:** The movement begins around 10 MPa and remains relatively constant for 0.0002 mm and then rises gradually reaching the peak of 11.4 MPa. This indicates that the normal stress does not significantly change with displacement. The joint and bolt system effectively sustains the applied normal load, showing minimal additional deformation.
- **20 MPa:** The graph rises very sharply at about 14 MPa and stays relatively constant with displacement with the displacement of 0.0003 mm, then rise gradually to stabilises at around 14.5 MPa. This shows stable normal stress, indicating strong resistance and minimal additional yielding despite the higher load.

Theoretical Explanation

This graphical representation demonstrates that the applied normal load has substantially effects on the normal stress against horizontal displacement of rock joints with rock bolts. It can be described that the interaction between the joint surface asperities and the applied higher normal load increase the contact area and frictional resistance between joint surfaces which enhances the normal stress, (Mohammad Reza Shahverdiloo & Shokrollah Zare, 2021).

The normal stress against the displacement relationship shows that there is an increase in normal stress due to asperity interlocking which is followed by a peak and finally decreases as asperities degrade. The UDEC simulations reviles that this gradual degradation reflects the real behaviour of the joints under constant loading. Moreover, the rock bolts help sustain joint integrity which reduces the asperity degradation and stabilising normal stress, (Mohammad Reza Shahverdiloo & Shokrollah Zare, 2021).

3.9 Numerical Results and Analysis for Barton-Bandis Joint Model for CNL Conditions with Rock Bolt

This model is the same as the model used in section 3.7 of this report, as the initial model was developed to be adaptable for different normal stress values and joint constitutive models. This model comprised two rectangular blocks stacked vertically, separated by a single discontinuity feature, representing the top and bottom of the physical joint specimen divided by the discontinuity.

3.9.1 Effects of Joint Roughness on Shear Stress of Rock Joints with Rock Bolt

The results shown in figure 84, shows the graph of Shear Stress against the Horizontal Displacement for varies Joint Roughness with introduction of rock bolt into the joint model simulation in UDEC. This illustrates how shear stress changes with horizontal displacement for rock joints with different joint roughness values.

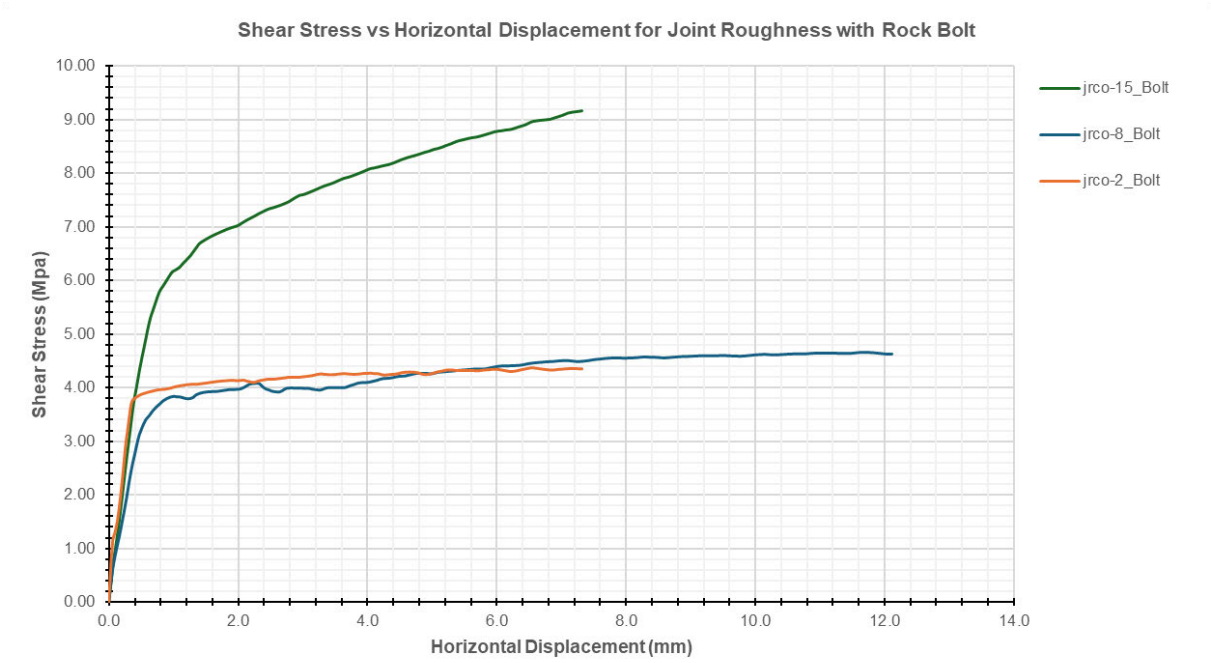

Figure 84: Presents the graph of Shear Stress vs the Horizontal Displacement for varies Joint Roughness

In the initial stage, the shear stress increased rapidly with significant displacements for all the joint roughness.

After the peak stage, each graph reaches the shear stress as follows:

- **Jrco-15:** Initially the shear stress rises rapidly with small horizontal displacement, it continues to rise steadily, peaking around 9.2 MPa at approximately 8.0 mm displacement. As a result, the higher shear stress and greater resistance to displacement.
- **jrco-8:** There is a rapid rise in shear stress initially. The shear stress peaks of around 4 MPa and remains relatively constant. This is the result of moderate shear stress and resistance.
- **jrco-2:** There is a rapid rise in shear stress. It then peaks around 3.9 MPa and stays constant. This is due to lower shear stress and resistance.

Theoretical Explanation

This graphical representation demonstrates that the joint roughness has substantially effects on the shear stress against horizontal displacement of rock joints with rock bolts. It is assumed that the contact between the joint surface asperities, applied shear force, joint friction is influenced by the Joint Roughness Coefficient (JRC) and the friction angle which enhances shear strength due to mechanical interlocking and frictional resistance, (Yinge Zhu, Gang Wang, Anqi Li, Huiyuan Chen, Tingfang Liu & Hui Guan , 2022).

The shear stress against the displacement graph shows an initial elastic stage followed by a peak shear stress and finally a residual stage. This UDEC simulation reviles that the advancing degradation of asperities and reflects on the real behaviour under maintained loading. Moreover, the rock bolts help sustain the joint reliability, decreasing asperity degradation and stabilising shear stress, (Yinge Zhu, Gang Wang, Anqi Li, Huiyuan Chen, Tingfang Liu & Hui Guan , 2022).

3.9.2 Effects of Joint Roughness on Normal Stress of Rock Joints with Rock Bolt

The results shown in figure 85, shows the graph of Normal Stress against the Horizontal Displacement for varies Joint Roughness with introduction of rock bolt into the joint model simulation in UDEC. This illustrates how normal stress changes with horizontal displacement for rock joints with different joint roughness values.

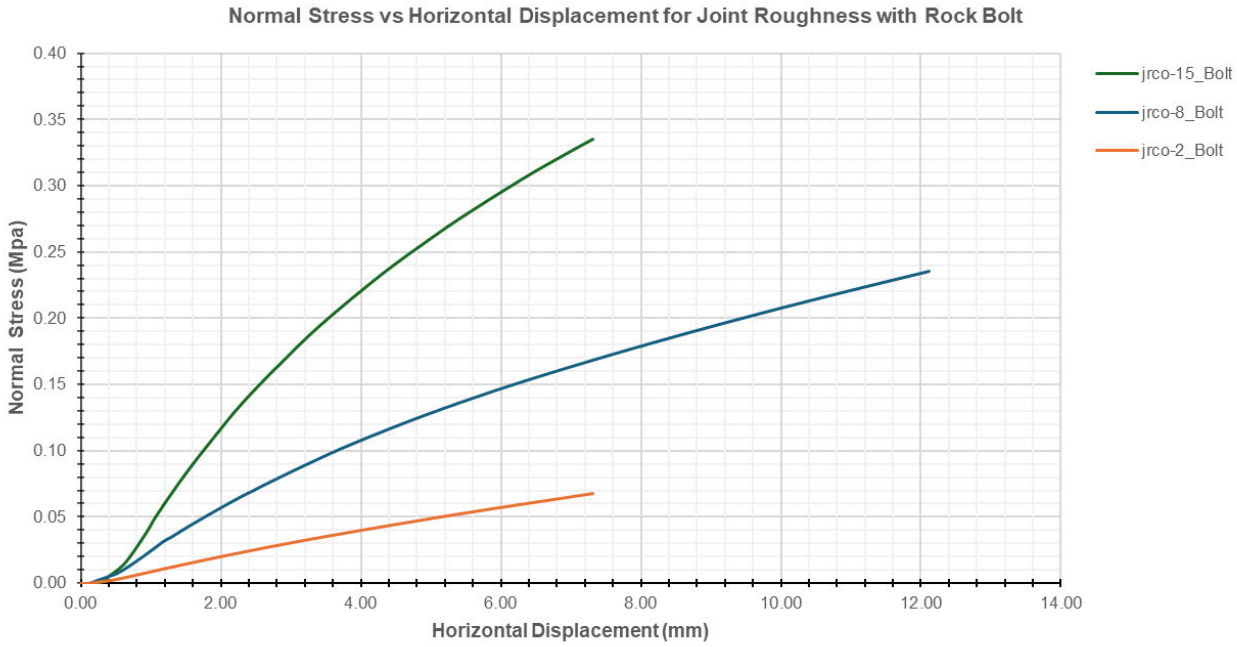

Figure 85: Presents the graph of Normal Stress vs the Horizontal Displacement for varies Joint Roughness

The graphs illustrate that higher joint roughness (jrco) leads to higher normal stress for a given horizontal displacement in rock joints reinforced with rock bolts under CNL conditions. For the individual graphs the descriptions are as:

- **Jrco-15:** The graph starts steeply from the origin, indicating a rapid rise in normal stress with horizontal displacement. It continues to rise non-linearly, showing higher normal stress values as the horizontal displacement increases.

- **Jrco-8:** Initially the normal stress increases at a moderate rate, then it steepens indicating a gradual rise in normal stress with increasing horizontal displacement.
- **Jrc-2:** There is a very gradual rise in the normal stress initially, then it continues to rise at a steady rate, indicating the slowest increase in normal stress with horizontal displacement.

Theoretical Explanation

This graphical representation demonstrates that the joint roughness has substantially effects on the normal stress against horizontal displacement of rock joints. It can be described that the interaction between the joint surface asperities, applied normal load and Joint roughness measures through the Joint Roughness Coefficient (JRC) has an effect on the normal stress distribution along the joint surface, (Yinge Zhu, Gang Wang, Anqi Li, Huiyuan Chen, Tingfang Liu & Hui Guan , 2022).

The normal stress against the displacement relationship in general shows an increase in normal stress due to asperity interlocking which is followed by a peak and then a decrease as asperities degrades. The rock bolts help uphold joint integrity, reducing asperity degradation and stabilising normal stress, (Yinge Zhu, Gang Wang, Anqi Li, Huiyuan Chen, Tingfang Liu & Hui Guan , 2022).

3.9.3 Effects of Compressive Strength on Shear Stress of Rock Joints with Rock Bolt

The results shown in figure 86, shows the graph of Shear Stress against the Horizontal Displacement for varies Joint Compressive Strength with introduction of rock bolt into the joint model simulation in UDEC. This illustrates how shear stress changes with horizontal displacement for rock joints with different joint compressive strength values.

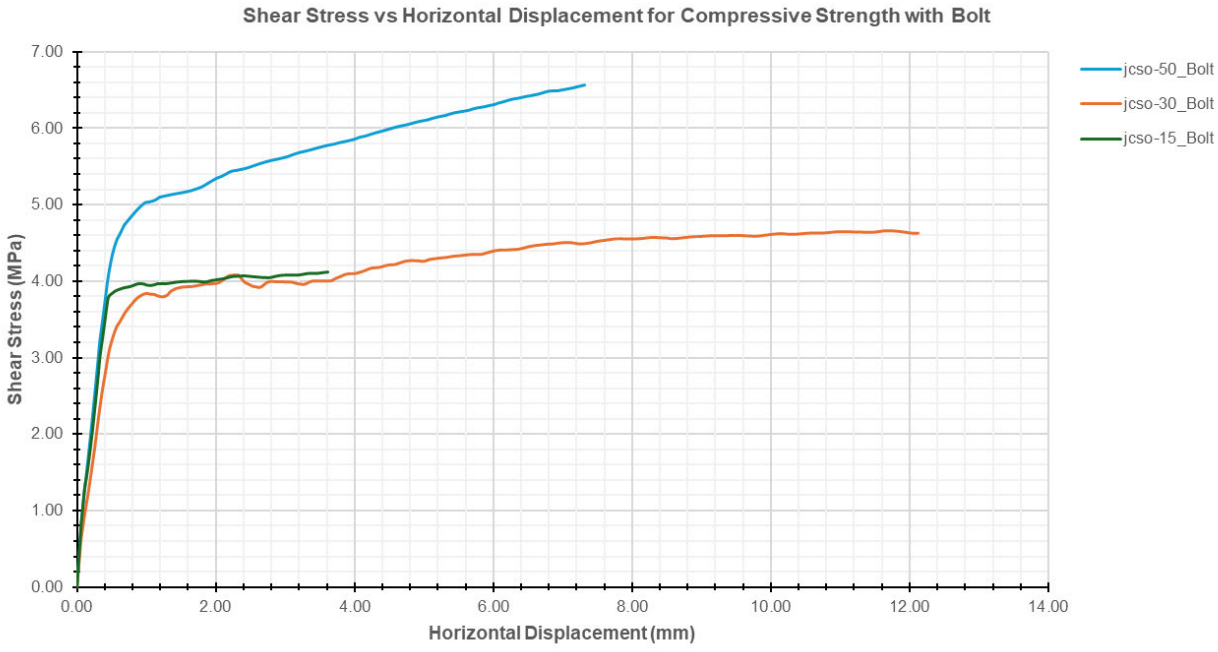

Figure 86: Presents the graph of Shear Stress vs the Horizontal Displacement for varies Compressive Strength

The graphs illustrate the elastic behaviour, where the shear stress increases rapidly with a small displacement. The maximum resistance the joint can sustain before yielding. Thus, as for higher compressive strength joints (jcso-50) provides greater resistance, resulting in higher peak shear stress.

For the individual graphs the descriptions are as:

- **jcso-50:** Initially the graph rises steeply, indicating a rapid increase in shear stress with small horizontal displacement. It peaks around 6.5 MPa at 7 mm displacement, and then stabilises.
- **jcso-30:** Also shows similar rapid rise but less steep than jcso-50. It peaks and stabilises 4 MPa with increasing displacement up to 13 mm.
- **jcso-15:** this graph quickly rises reaching lower maximum shear stress. It the stabilises around 4 MPa, sustains the least shear stress before displacement.

Theoretical Explanation

This graphical representation demonstrates that the compressive strength has substantially effects on the shear stress against horizontal displacement of rock joints with rock bolts. It is assumed that the contact between the joint surface asperities, applied shear force and Joint compressive strength (JCS) influences the shear strength by determining the resistance of the joint walls to crushing and deformation. Which means that higher JCS values lead to increased shear strength due to greater resistance to asperity degradation, (Liu He, Zhiming Zhao, Jiayi Chen & Diyi Liu , 2020).

The shear stress against the displacement graph shows firstly an elastic stage followed by a peak shear stress and finally the residual stage. UDEC simulation reviles that the advancing degradation of asperities reflects the real behaviour under maintained loading. Also the rock bolts help sustain joint integrity, reducing asperity degradation and stabilising shear stress, (Liu He, Zhiming Zhao, Jiayi Chen & Diyi Liu , 2020).

3.9.4 Effects of Compressive Strength on Normal Stress of Rock Joints with Rock Bolt

The results shown in figure 87, shows the graph of Normal Stress against the Horizontal Displacement for varies Joint Compressive Strength with introduction of rock bolt into the joint model simulation in UDEC. This illustrates how normal stress changes with horizontal displacement for rock joints with different joint compressive strength values.

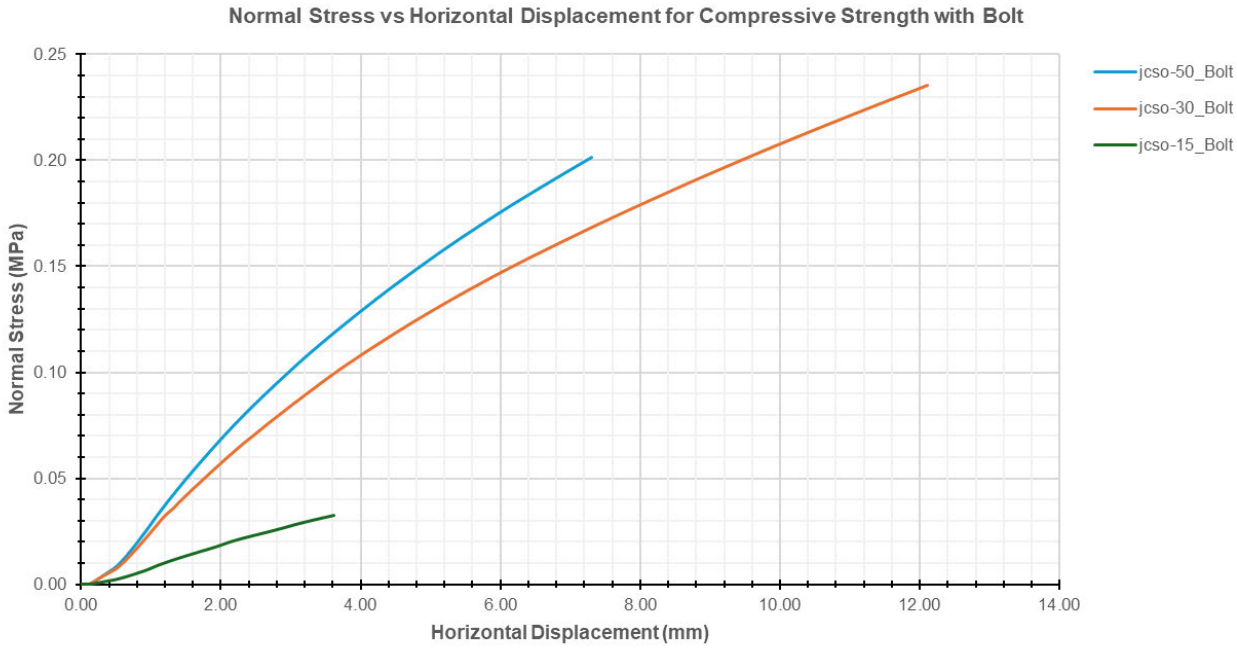

Figure 87: Presents the graph of Normal Stress vs the Horizontal Displacement for varies Compressive Strength

Higher compressive strength (jcso-50) joints are more robust and exhibit greater resistance to shear forces, reflected by higher normal stress values as horizontal displacement increases.

For the individual graphs the descriptions are as:

- **jcso-50:** The graph starts steeply indicating a rapid rise in normal stress with horizontal displacement. The graph continues to rise, reaching approximately 0.20 MPa at around 7 mm displacement. This indicates the highest normal stress values, which leads to strong resistance to shear due to the highest compressive strength of the joint.
- **jcso-30:** Initially the graph rises gradually, but at a slower rate compared to jcso-50 graph. It reaches normal stress around 0.28 MPa at approximately 12 mm displacement. This indicates the moderate resistance to shear.
- **jcso-15:** The graph rises gradually, indicating a slower increase in normal stress with displacement. It reaches approximately 0.025 MPa at around 3.9 mm displacement, then flattens out. This shows that the lowest normal stress values, indicating the least resistance to shear.

Theoretical Explanation

This graphical representation demonstrates that the compressive strength has substantially effects on the normal stress against horizontal displacement of rock joints with rock bolts which is subjected to the interaction between the joint surface asperities and the applied normal load. The higher JCS values, there is more enhancement for the normal stress capacity of the joint by increasing the

resistance of the joint walls to crushing and deformation, (Liu He, Zhiming Zhao, Jiayi Chen & Diyi Liu , 2020).

The normal stress against the displacement relationship, shows an increase in normal stress due to asperity interlocking then followed by a peak and finally a decrease as asperities degrade, (Liu He, Zhiming Zhao, Jiayi Chen & Diyi Liu , 2020).

3.9.5 Effects of UCS on Shear Stress of Rock Joints with Rock Bolt

The results shown in figure 88, shows the graph of Shear Stress against the Horizontal Displacement for varies UCS of the block with introduction of rock bolt into the joint model simulation in UDEC. This illustrates how shear stress changes with horizontal displacement for rock joints with different UCS values.

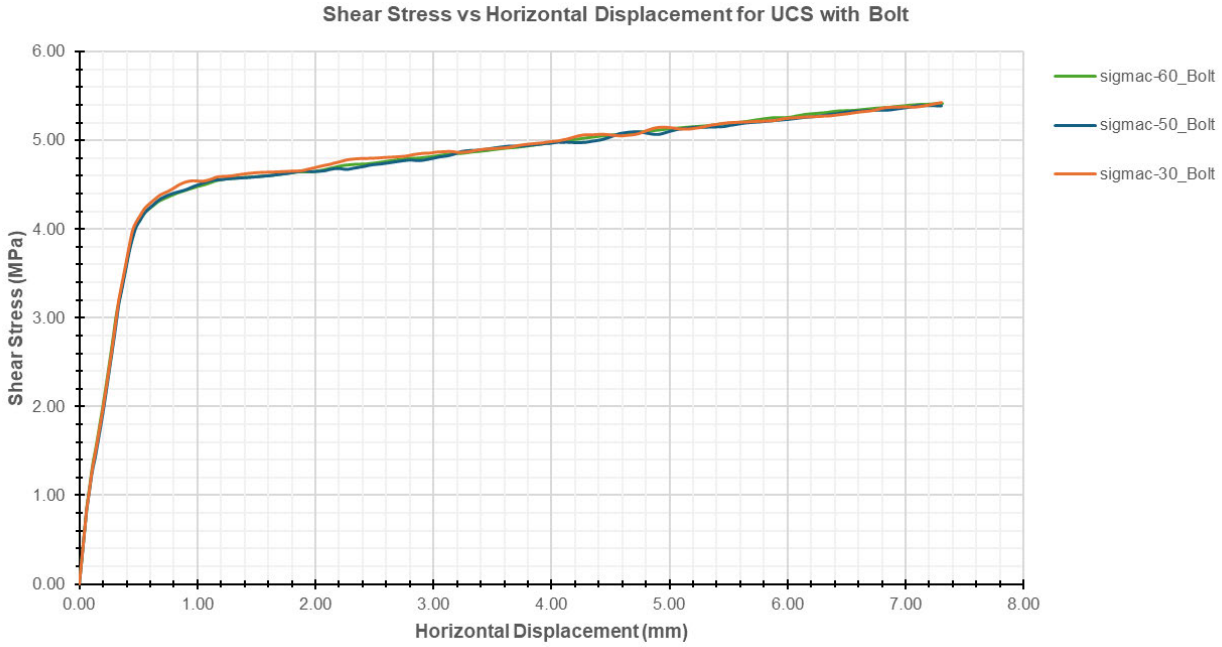

Figure 88: Presents the graph of Shear Stress vs the Horizontal Displacement for varies UCS

As we can see the trend for the graphs above, higher UCS values lead to higher shear stress and greater resistance to displacement in rock joints with rock bolts under CNL conditions.

For the individual graphs the descriptions are as:

- **sigmac-60:** Initially the graph rises sharply indicating the increase in shear stress at small displacements. It then peaks around 4.5 MPa at 1.5 mm displacement, then stabilises. It then gradually increases beyond the peak and steady rise in shear stress up to approximately 5.5 MPa.
- **sigmac-50:** There is a rapid increase in shear stress, before it reaches the peak around 4.5 MPa. It then gradually increases and continues rising slowly.
- **sigmac-30:** Initial Increase: Quick rise in shear stress but slower than green and blue curves. Plateau: Peaks around 4.5 MPa at 1.5 mm displacement. Gradual Increase: Steady rise up to around 7 MPa.

Theoretical Explanation

This graphical representation demonstrates that the UCS has substantially effects on the shear stress against horizontal displacement of rock joints with rock bolts. It is assumed that the contact between

the joint surface asperities, applied shear force and UCS influences the shear strength by determining the resistance of the joint walls to crushing and deformation. Which means that higher UCS values lead to increased shear strength due to greater resistance to asperity degradation, (Liu He, Zhiming Zhao, Jiayi Chen & Diyi Liu , 2020).

The shear stress against the displacement graph shows firstly an elastic stage followed by a peak shear stress and finally the residual stage. UDEC simulation reviles that the advancing degradation of asperities reflects the real behaviour under maintained loading. Also the rock bolts help sustain joint integrity, reducing asperity degradation and stabilising shear stress, (Liu He, Zhiming Zhao, Jiayi Chen & Diyi Liu , 2020).

3.9.6 Effects of UCS on Normal Stress of Rock Joints with Rock Bolt

The results shown in figure 89, shows the graph of Normal Stress against the Horizontal Displacement for varies UCS of the block with introduction of rock bolt into the joint model simulation in UDEC. This illustrates how shear stress changes with horizontal displacement for rock joints with different UCS values.

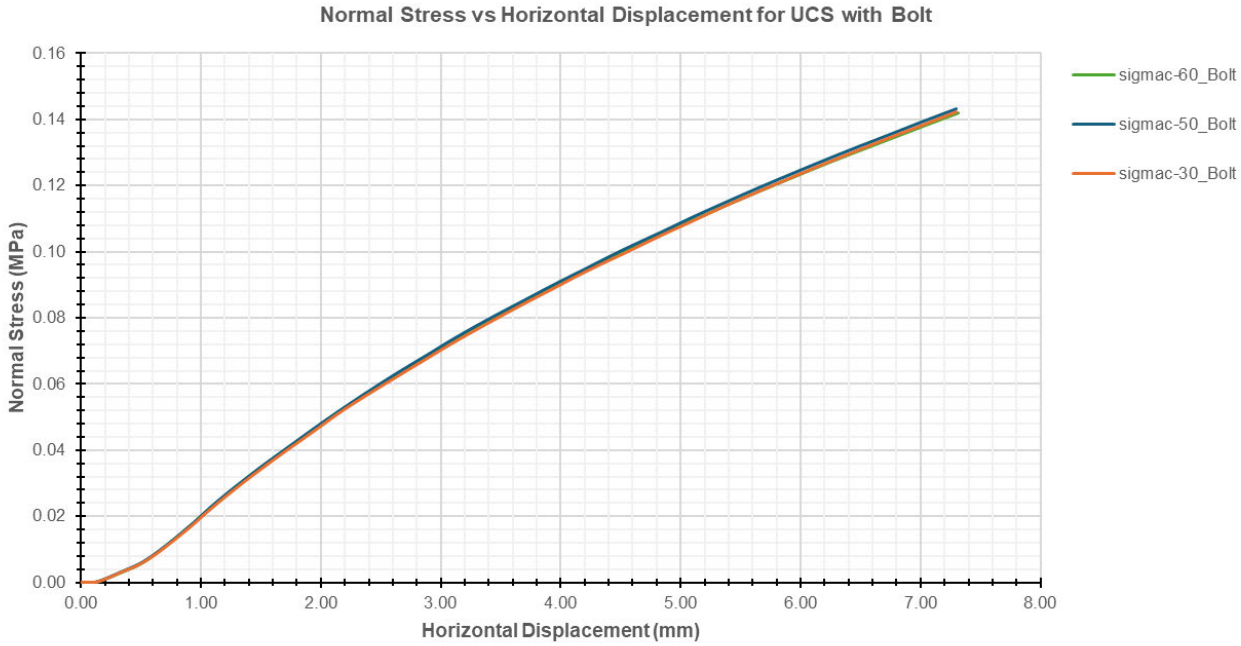

Figure 89: Presents the graph of Normal Stress vs the Horizontal Displacement for varies UCS

As presented in the figure above all the graph shows an increase in normal stress as horizontal displacement increases. The normal stress gradually rises initially and increases more rapid with increasing displacement.

The graph for sigmac-60 and sigmac-50 overlap, indicating similar behaviour. The graph for sigmac-30 is lower, showing slightly less normal stress for the same displacement.

Theoretical Explanation

This graphical representation demonstrates that the UCS has substantially effects on the normal stress against horizontal displacement of rock joints with rock bolts which is subjected to the interaction between the joint surface asperities and the applied normal load. The higher UCS values, there is more enhancement for the normal stress capacity of the joint by increasing the resistance of the joint walls to crushing and deformation, (Liu He, Zhiming Zhao, Jiayi Chen & Diyi Liu , 2020).

The normal stress against the displacement relationship, shows an increase in normal stress due to asperity interlocking then followed by a peak and finally a decrease as asperities degrade. The UDEC simulation describes this advanced degradation which reflects the real behaviour under constant loading. Moreover, rock bolts help sustain joint integrity, reducing asperity degradation and stabilising normal stress, (Liu He, Zhiming Zhao, Jiayi Chen & Diyi Liu , 2020).

3.9.7 Effects of Normal Loads on Shear Stress of Rock Joints with Rock Bolt

The results shown in figure 90, shows the graph of Shear Stress against the Horizontal Displacement for varies applied Normal Loads to the block with introduction of rock bolt into the joint model simulation in UDEC. This illustrates how shear stress changes with horizontal displacement for rock joints with different normal load values.

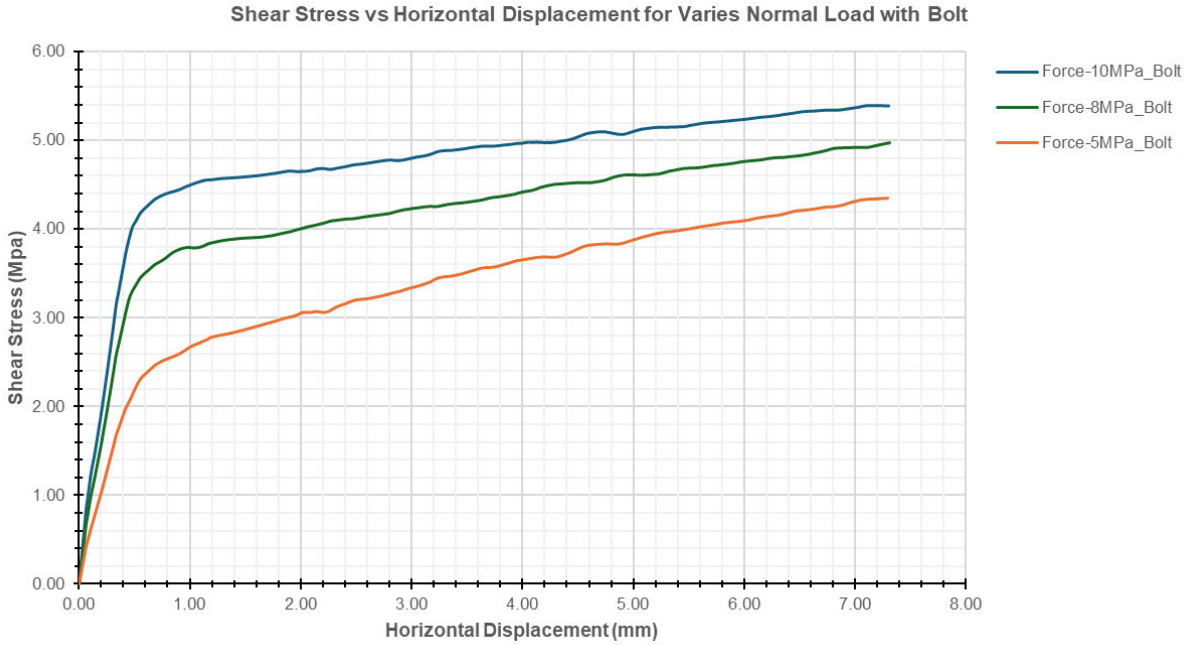

Figure 90: Presents the graph of Shear Stress vs the Horizontal Displacement for varies Normal Loads

As presented in the figure above we can see the trends of the graphs have higher shear stress which have the greater resistance to displacement in rock joints with rock bolts under CNL conditions for the applied normal loads.

For the individual graphs the descriptions are as:

- **10 MPa:** Initially the graph shows a rapid increase in shear stress as horizontal displacement begins. It peaks at around 4.5 MPa and stabilises as displacement continues. Due to the higher normal load the joint has higher initial resistance and sustained shear stress.
- **8 MPa:** This follows the similar trend as 10 MPa graph as it rises rapidly but less steep. It peaks around 3.8 MPa and then stabilises. This shows that the moderate initial resistance and sustained shear stress indicating the medium normal load.
- **5 MPa:** Initially there is a rapid rise of the graph but is the least steep compared to the other graph. It peaks around 2.5 MPa and stabilises. This indicates that the lowest initial resistance and sustained shear stress due to the lowest normal load.

Theoretical Explanation

This graphical representation demonstrates that the applied normal load has substantially effects on the shear stress against horizontal displacement of rock joints with rock bolts due to the interaction between the joint surface asperities and the applied normal loads. It is anticipated that higher normal load increases the contact area and frictional resistance between joint surfaces and improves the shear strength, (Liu He, Zhiming Zhao, Jiayi Chen & Diyi Liu , 2020).

The shear stress against the displacement graph, shows firstly with the elastic stage followed by the peak shear stress and finally reaches the residual stage. The UDEC simulation confirms the gradual degradation of asperities which reflects on the real behaviour under constant loading. Whereas the rock bolts help sustain joint integrity which reduces the asperity degradation and stabilising shear stress, (Liu He, Zhiming Zhao, Jiayi Chen & Diyi Liu , 2020).

3.9.8 Effects of Normal Loads on Normal Stress of Rock Joints with Rock Bolt

The results shown in figure 91, shows the graph of Normal Stress against the Horizontal Displacement for varies applied Normal Loads to the block with introduction of rock bolt into the joint model simulation in UDEC. This illustrates how shear stress changes with horizontal displacement for rock joints with different normal load values.

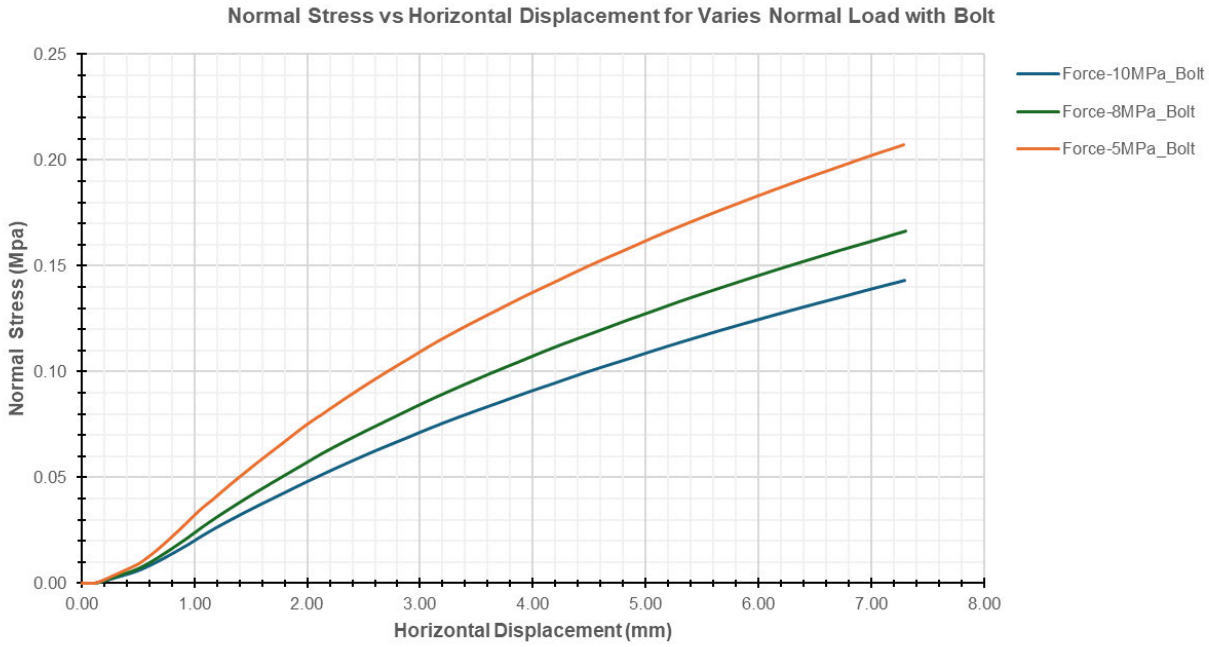

Figure 91: Presents the graph of Normal Stress vs the Horizontal Displacement for varies Normal Loads

As presented in the figure above, the graphs show that the joints with higher applied normal loads experience a more gradual increase in normal stress with horizontal displacement which shows that the joints have greater resistance and stability. Moreover, the joint with lower normal loads demonstrates a more rapid increase in normal stress, indicating less resistance.

For the individual graphs the descriptions are as:

- **5 MPa:** Initially there is a steady increase in normal stress with horizontal displacement. The normal stress rises more rapidly as displacement increases. After peaking the highest normal stress at around 0.20 MPa at the maximum displacement of 7.3 mm.

- **8 MPa:** The graph shows that there is an increase in the normal stress steadily. The normal stress rises and it less steep compared to 5 MPa graph. It then continuous to increase and at approximately 0.14 MPa at the maximum displacement of 7.3 mm.
- **10 MPa:** The graph starts with a gradual increase in normal stress. It then forms a least steep increase in normal stress compared to other two graphs. It the continues to increase with the normal stress around 0.12 MPa at the maximum displacement of 7.3 mm.

Theoretical Explanation

This graphical representation demonstrates that the varying applied normal load has substantially effects on the normal stress against horizontal displacement of rock joints with rock bolts which is subjected to the interaction between the joint surface asperities and the applied normal load. With higher normal loads values, it increases the contact area and frictional resistance between joint surfaces hence it enhances the normal stress, (Mohammad Reza Shahverdiloo & Shokrollah Zare , 2021).

As for the normal stress against the displacement relationship, it shows that for a identify increase in normal stress is due to asperity interlocking which is then followed by a peak and finally it decreases as asperities degrade. Hence, the rock bolts help sustain joint integrity which reduces the asperity degradation and stabilising normal stress, (Mohammad Reza Shahverdiloo & Shokrollah Zare , 2021).

3.10 Summary of Findings

From the findings of this study, we have investigated the shear behaviour of rock joints under the Barton-Bandis, Mohr-Coulomb, and Continuously Yielding joint models using UDEC under constant normal load (CNL) conditions with direct shear tests and rock bolts which shows the behaviour of the discrete mechanical responses and strengths of the rock joints.

These models emphasise the major role of joint roughness, strength parameters, and bolt reinforcement in improving the shear resistance and stability of rock mass structures. The subsections below describe the findings of each models used.

3.10.1 Barton-Bandis Joint Model with Rock Bolt

From the findings of this joint model, it can be concluded that, the impact of various parameters such as joint roughness, friction, uniaxial compressive strength (UCS), compressive strength, shear velocity, and normal load with rock bolt support system plays an important role. This model provides a complete insight of how these factors and support system affect shear and normal stresses against the horizontal displacement under constant normal load (CNL) conditions of the direct shear test simulation, (Bandis. S, Lumsden. A C & Barton, N R, 1981).

A brief explanation of the findings for the individual parameters are as:

- **Shear Stress against the Horizontal Displacement**

  The peak shear and normal stresses increase with the joint roughness coefficient. The horizontal displacement increases as the joint experience's dilation, which is more obvious at higher joint roughness coefficient values. After the peak, the shear stress decreases and reaches stability at a residual value, which is influenced by the joint-wall compressive strength and residual friction angle, (Barton, 1971).

- **Normal Stress against the Horizontal Displacement**

  As the Normal Stress increases, the horizontal displacement increases as well. This is due to the dilation of the joint. The decrease of the joint aperture is affected by the normal load and the roughness of the joint surfaces, (Barton, 1971).

- **Rock Bolt Influence**

  The presence of a rock bolt through the rock joint helps to stabilise the joint which reduces the peak shear displacement and increasing the overall shear strength of the joint. As well as the rock bolts transfer load from the joint to the adjacent rock mass, improving the rock joint shear resistance, (Mahdi Saadat , 2019)

3.10.2 Mohor Coulomb Joint Model with Rock Bolt

Under this joint model the key parameters investigated includes the joint friction, dilation, shear and normal stiffness, velocity, and normal load. The outcomes of these correlations provide important understandings through UDEC simulations under Constant Normal Load (CNL) conditions with direct shear tests and support system of the rock bolts. These simulations underline the key roles of joint roughness and friction in describing the shear stress response for which the shear and normal stiffness parameters affect the deformation characteristics. The inclusion of rock bolts significantly improves joint stability and shear resistance of the rock joint, (P. Barsanescu, 2015).

A brief explanation of the findings for the individual parameters are as:

- **Shear Stress against the Horizontal Displacement**

  Peak shear stress is reached when the shear strength of the joint is exceeded. As the peak shear stress is reached, the shear stress declines to a residual value, which is lower than the peak value. Hence the shear stress decreases with increasing horizontal displacement due to the degradation of asperities on the joint surface (P. Barsanescu, 2015).

- **Normal Stress against the Horizontal Displacement**

  The Normal Stress Behaviour under CNL conditions remains constant during the shearing process. As the joint experiences shearing process the joint dilates due to the movement of asperities. This dilation process is restricted by the stiffness of the surrounding rock mass. Hence the tensile strength of the joint has exceeded, the normal stress reaches the stability at a residual value (P. Barsanescu, 2015).

- **Rock Bolt Influence**

  The rock bolt system helps to stabilise the joint by providing additional normal force. This increases shear strength and reduces the displacement. Thus, the existence of rock bolt constraint the dilation of the rock joint and leads to a more stable shear behaviour.

3.10.3 Continuously Yielding Joint Model with Rock Bolt

This assessment reflects on the shear behaviour of rock joints under Constant Normal Load (CNL) for the rock joints using the Continuously Yielding Joint Model with UDEC. The integration of a rock bolt system substantially influences the results. The findings focus that rock bolts enhance joint stability by improving normal stiffness, providing greater resistance to shear displacement, and improving overall joint performance. This examination examines the critical parameters such as shear and normal stiffness, friction, and roughness, and presents an understanding of the behaviour of shear and normal stresses against the horizontal displacement, (Goodman, 1993).

A brief explanation of the findings for the individual parameters for Continuously Yielding Joint model are as:

- **Shear Stress against the Horizontal Displacement**

  Initially there is an increase in the shear stress with horizontal displacement as it reaching the peak value, after the peak shear stress decreases reaching a residual strength due to the damage and wear of the joint surfaces, (Goodman, 1993).

- **Normal Stress against the Horizontal Displacement:**

  The Normal stress increases with horizontal displacement due to the dilation of the joint. This relationship confirms that the higher normal stress leads to the greater resistance to shear displacement, (Goodman, 1993).

- **Rock Bolt Influence**

  This joint model provides a more accurate illustration of rock joint behaviour compared to the Mohr-Coulomb model, as it interprets the nonlinearities and advancing damage. Use of rock bolt improve the stability of the joint by increasing the normal stiffness and providing additional support against shear displacement, (Chen W & Li L, 2015).

4 Conclusion

From the findings of this study, we can conclude that UDEC simulation of the direct shear test under constant normal load conditions effectively validates the characteristic shear and normal stress responses to horizontal displacement which highlights the critical role of joint roughness and material properties in determining shear strength.

As indicated from the simulation, the results states that as the horizontal displacement increases both shear and normal stresses demonstrate individual relationships. Initially as the shearing process begins, the shear stress increases rapidly reaching a peak before gradually decreasing which associates with the usual behaviour examined in the direct shear tests, (Thomas Frühwirt, Daniel Pötschke & Heinz Konietzky , 2021).

On the other hand, normal stress remains relatively constant due to the CNL condition which confirms that the normal load applied to the joint does not vary substantially during the shearing process, (Zhezhe Zhang, Baohua Guo, Shengjin Cheng, Pengbo Zhong & Chuangwei Zhu, 2024).

Moreover, UDEC simulation focusses on the importance of joint roughness and material properties in affecting shear strength and displacement behaviour. The roughness of the joint surfaces contributes to the initial increase in shear stress while the material properties determine the residual strength post-peak shear stress, (Shrivastava, A.K & Rao, K.S, 2010).

These findings are fundamental for identifying the mechanical behaviour of rock joints in geotechnical engineering applications, supporting a consistent method for foreseeing joint behaviour under varying load conditions, (Haque, A & Indraratna, B , 2000).

When incorporating rock bolts into the UDEC simulation under constant normal load (CNL) conditions, the results show a remarkable improvement in the stability and shear strength of the rock joint. The existence of rock bolts helps to disperse the shear stress more uniformly across the joint which leads to a higher peak shear stress and a steadier decrease of the post-peak before stabilising, (Thomas Frühwirt, Daniel Pötschke & Heinz Konietzky , 2021).

The rock bolt reinforcing also influences in the reduction of horizontal displacement for a known shear stress which indicates the better resistance to shearing. Whereas the normal stress remains relatively constant due to the CNL condition. Generally, the displacement behaviour is substantially influenced by the added support of the rock bolts which successfully restrain the joint movement and improves the mechanical interlock between the rock surfaces, (Zhezhe Zhang, Baohua Guo, Shengjin Cheng, Pengbo Zhong & Chuangwei Zhu, 2024).

4.1 Summary for Barton-Bandis UDEC Joint Model for Contant Normal Loading Conditions (CNL)

4.1.1 B-B UDEC Simulation for Unbolted Model

Barton-Bandis UDEC joint model under CNL conditions provides a full outline of the understanding of the shear behaviour of rock joints. The key parameters used in this study were as joint roughness coefficient (JRC), joint friction, compressive strength, uniaxial compressive strength (UCS), friction angle, shear velocity, and applied normal force which played a significant role in defining the shear and normal stress responses against horizontal displacement, (Barton N. , 2018).

As presented in the results of section 3.3 of this report, the model illustrations, that with a higher joint roughness and friction angles values, there is an increase in peak shear strength whereas the compressive strength and UCS effects the overall stability and deformation characteristics of the joint. The applied normal force maintains a constant normal stress which ensures variations in shear stress are mainly due to the joint properties and shear displacement, (Barton N. , 2018).

As seen from the simulations, Barton-Bandis joint model realistically describes the non-linear relationship between shear stress and horizontal displacement and highlights the importance of joint roughness and material strength. When the horizontal displacement increases the shear stress from the start rises to a peak before decreasing which reflects the mobilisation of the joint system and following degradation of joint roughness, (L. Jing, O. Stephansson & E. Nordlund , 1993).

On the other hand, the normal stress remains reasonably stable due to the CNL condition except the interaction between shear and normal stresses is obvious in the displacement behaviour, (L. Jing, O. Stephansson & E. Nordlund , 1993).

4.1.2 B-B UDEC Simulation for Bolted Model

The Barton-Bandis UDEC joint model under CNL conditions for a bolted model and the simulation presented in section 3.3 of this report explains that there an enhanced stability and shear strength of rock joints in relation to the key parameters mentioned in section 4.1.1 has a suggestively impact on the shear and normal stress outcome against horizontal displacement, (Barton N. , 2018).

The presence of rock bolts helps to distribute (or redistribute) the shear stress more uniformly which results in higher peak shear strength and decreased horizontal displacement for a known shear stress. This support system maintains relatively constant normal stress appropriately to the CNL condition, hence maintaining the restrict joint movement and improving the mechanical interlock between rock surfaces, (Barton N. , 2018).

4.2 Summary for Mohor Coulomb UDEC Joint Model for Contant Normal Loading Conditions (CNL)

4.2.1 M-C UDEC Simulation for Unbolted Model

Mohr Coulomb UDEC joint model under the CNL conditions for an unbolted model provides worthy understanding of the shear and normal stress behaviour against horizontal displacement. The key parameters used in the simulation are as joint friction, friction angle, dilation, shear velocity, and applied normal force substantially effect the model's response.

As presented in the results of section 3.4 of this report, the model illustrates that as the horizontal displacement increases, shear stress starts to rise rapidly to a peak value before decreasing which reflects a typical behaviour of rock joints under shear loading.

Friction angle and joint friction are important in determining the peak shear strength as dilation is affected by the volumetric changes during shearing process. Hence, the applied normal force makes certain that normal stress remains constant and allows for a clear analysis of shear stress differences, (Itasca, 2024).

For this UDEC modelling simulation, the dilation angle plays a fundamental role in the joint's behaviour, as it controls the boundary of volumetric extension during shear displacement. For higher values of dilation angles it increases the normal stress and as a result the joints shear strength increases, (Jan Nemcik, Ali Mirzaghorbanali & Naj Aziz , 2013).

Shear velocity influences the rate of which shear displacement occurs and thus it changes the stress distribution along the joint. In general Mohr Coulomb model efficiently confines the complex contacts between shear and normal stresses, providing a better outline for predicting the mechanical behaviour of unbolted rock joints under varying load conditions, (Jan Nemcik, Ali Mirzaghorbanali & Naj Aziz , 2013).

4.2.2 M-C UDEC Simulation for Bolted Model

The Mohr Coulomb UDEC joint model under CNL conditions for the bolted blocks and the simulation presented in section 3.4 of this report explains that there is a substantial improvement in joint stability and shear strength of rock joints in relation to the key parameters mentioned in section 4.2.1 are vital for defining the shear and normal stress responses against horizontal displacement.

The presence of rock bolts improves the distribution (or redistribution) of shear stress which results in higher peak shear strength and decrease in the horizontal displacement for a known value of the shear stress. The dilation angle affects the volumetric changes during shearing process when the applied normal force maintains constant normal stress which ensures an actual control of joint movement and adjusted mechanical interlocking between rock surfaces, (Itasca, 2024).

4.3 Summary for Continuously Yielding Joint Model for Contant Normal Loading Conditions (CNL)

4.3.1 C-Y UDEC Simulation for Unbolted Model

Continuously yielding UDEC joint model under CNL conditions for an unbolted block provides a full outline of the understanding of shear and normal stress behaviour against horizontal displacement. The key parameters used in the simulation are as joint friction, joint roughness, shear velocity, and applied normal force which extensively influences the model's response.

As presented in the results of section 3.5 of this report, the model illustrates that horizontal displacement increases as the shear stress starts to rise to a peak before progressively reducing which reflects the progressive damage and weakening of the joint. The joint roughness and friction are vital in deciding the peak shear strength whereas the applied normal force confirms that normal stress remains reasonably constant for a strong assessment of shear stress changes. Hence, the shear velocity influences the rate of displacement of the stress distribution along the joint, (Itasca, 2024).

The CY model efficiently illustrates the non-linear behaviour of rock joints which includes the effects of joint roughness and assumes the plastic displacement on shear strength. As the joint experiences shear displacement, the UDEC model experiences reduction in dilation angle and continues to damage the joint surfaces which leads to a reduction in shear strength, (Itasca, 2024).

4.3.2 C-Y UDEC Simulation for Bolted Model

The CY UDEC joint model under CNL conditions for a bolted blocks and the simulation presented in section 3.5 of this report explains that there is a substantial improvement in the mechanical behaviour of rock joints in relation to the key parameters mentioned in section 4.3.1 are vital for defining the shear and normal stress responses against horizontal displacement, (Itasca, 2024).

The presence of rock bolts improves the distribution (or redistribution) of shear stress which leads to higher peak shear strength and reduced horizontal displacement for a known value of the shear stress. This strengthening system helps to maintain a constant normal stress due to the CNL condition. Hence it restricts the joint movement and develops the mechanical interlocking between rock surfaces, (Itasca, 2024).

4.4 Comparison of UDEC Joint Models for Contant Normal Loading Conditions (CNL)

4.4.1 Comparison between Barton-Bandis (B-B) and Mohor Coulomb (M-C) Joint Models Simulation for Unbolted Model

Barton-Bandis (B-B) and Mohr-Coulomb (M-C) models are commonly used for numerically simulating the shear strength of rock joints under constant normal load (CNL) conditions. The B-B model interprets for the joint roughness and basic friction angle which is exceptionally effective in attaining the non-linear behaviour of rock joints. Whereas the M-C model uses the linear failure principle to predict the shear behaviour, which is easy, but it can't accurately represent the complex interfaces between the joint, (R. A. Abdullah, R. J. Fowell & W. Murphy, 2010).

When comparing the unbolted models, the B-B model typically shows higher shear strength at lower normal stresses due to its consideration of joint roughness, while the M-C model may underestimate shear strength in these conditions, (Mahmoud Behnia, Behzad Nateghpour, Javad Tavakoli & Mohsen Sharifi Broujerdi , 2020).

Comparison between B-B and M-C can be challenging due to their fundamental difference approaches to model the joint behaviour such as model complexity, shear strength representation and displacement behaviour. From the UDCE simulation we can just compare the varying normal load and see the behaviour of the stress against the displacement in the following graphs.

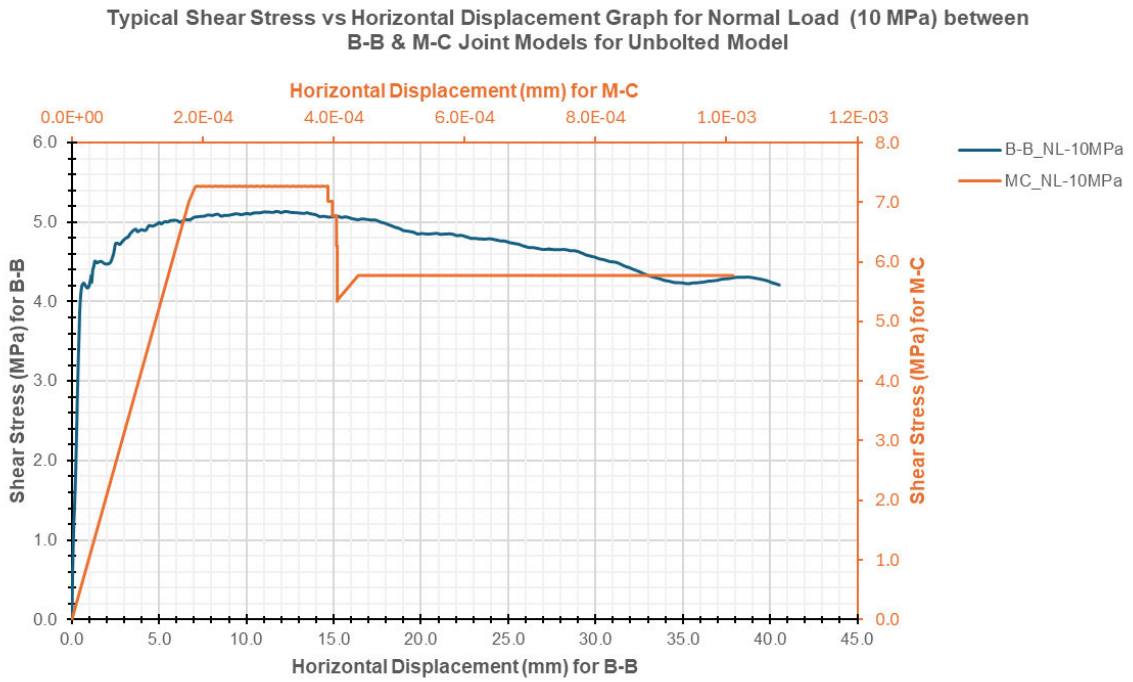

Figure 92: Presents the graph of Shear Stress vs the Horizontal Displacement for Normal Load of 10 MPa for unbolted model

From Figure 92, M-C overestimates the shear stress, as the shear stress rises rapidly, then fails and stabilises soon after. Whereas B-B model performs the simulation in a nonlinear and complex interactions at the joint interface.

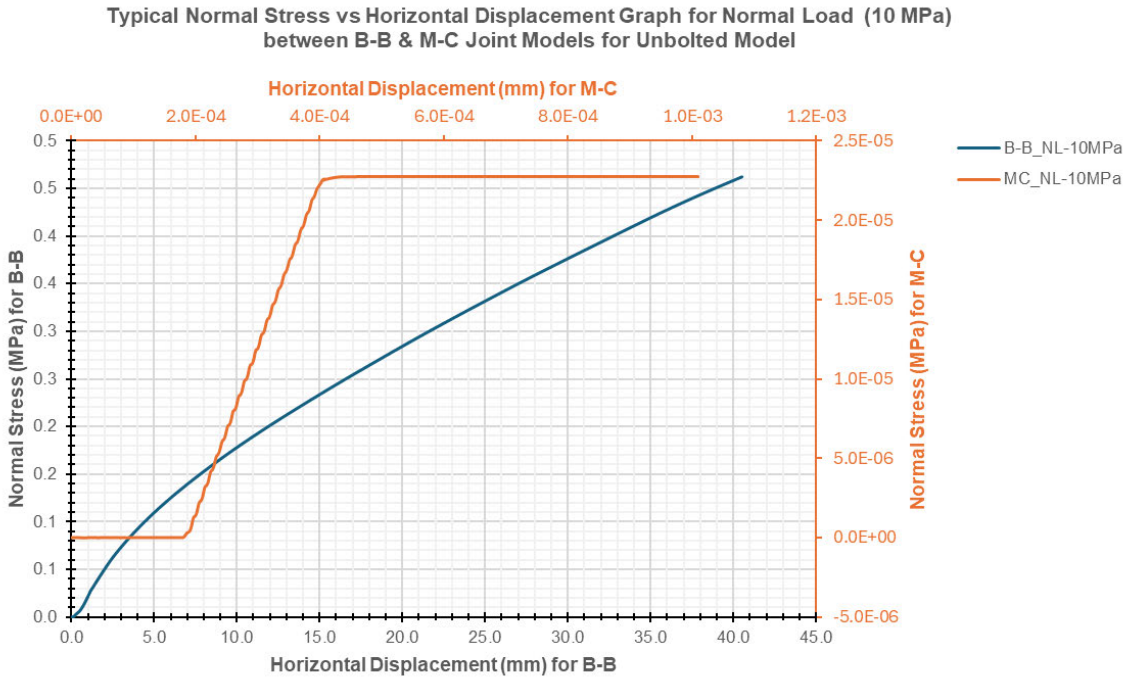

Figure 93: Presents the graph of Normal Stress vs the Horizontal Displacement for Normal Load of 10 MPa for unbolted model

From Figure 93, M-C model has a linear approach to the simulation and may not indicated the increased shear strength due to roughness rather at higher normal stresses. This inconsistency makes the comparisons difficult, as the M-C model might have overestimated the shear strength with difference in varying normal loads.

Whereas the B-B model's capability to represent shear strength as a function of normal stress and roughness which can be more accurately calculated for the behaviour of rough joints under varying conditions.

4.4.2 Comparison between Barton-Bandis and Mohor Coulomb UDEC Joint Models Simulation for Bolted Model

The B-B and M-C criteria, for bolted models both can be utilised to simulate the reinforcing effects of rock bolts. Bolting usually increases the normal stress within the joint which enhances the shear resistance. The B-B model has detailed parameters and can more precisely predict the increased shear strength due to bolting specifically in rough joints, (Daniil Iakovlev, 2015).

Whereas the M-C model possibly will not entirely acquire the increased shear strength provided by the bolts mainly in highly irregular joints. In contrast to the graphical comparisons it is often illustrated that the B-B model predicts higher shear strength and greater displacement before failure, compared to the M-C model which reflects on the model's ability to the non-linear behaviour of bolted joints more efficiently, (Daniil Iakovlev, 2015).

As illustrated in Figure 94, the B-B model includes joint roughness and non-linear shear strength parameters, hence it is expected that the shear stress will continue to a higher peak of around 6 MPa with a greater displacement before failure compared to the M-C model.

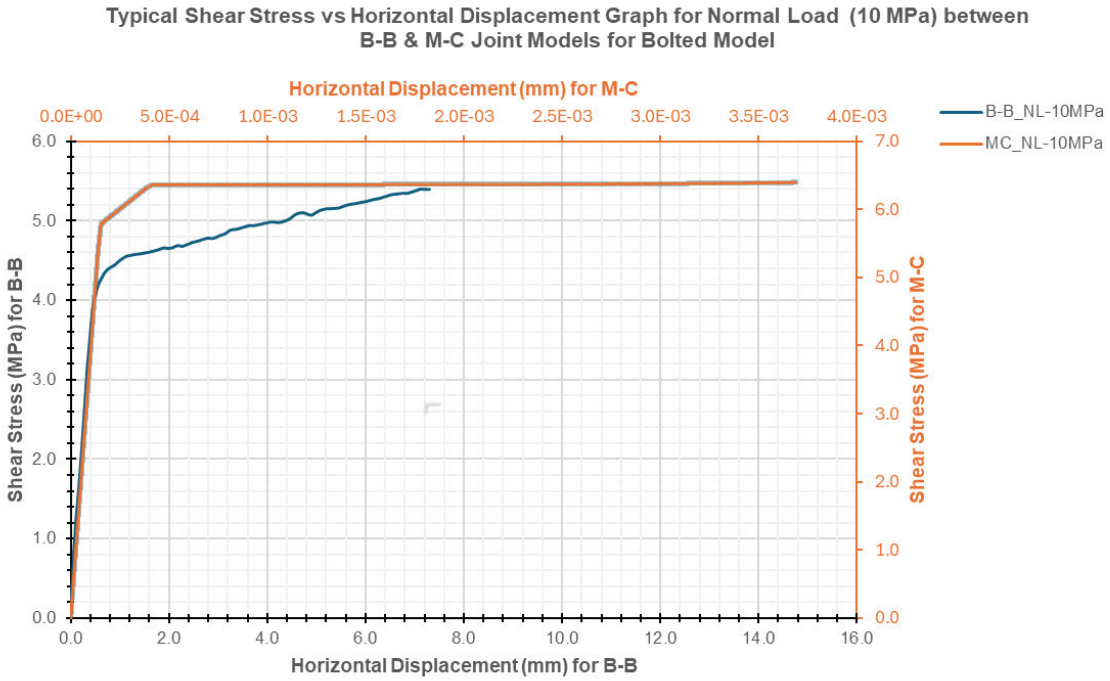

Figure 94: Presents the graph of Shear Stress vs the Horizontal Displacement for Normal Load of 10 MPa for bolted model

From Figure 94, M-C overestimates the shear stress, as the shear stress rises rapidly, then fails and stabilises soon after. Whereas B-B model performs the simulation in a nonlinear and complex interactions at the joint interface more accurately.

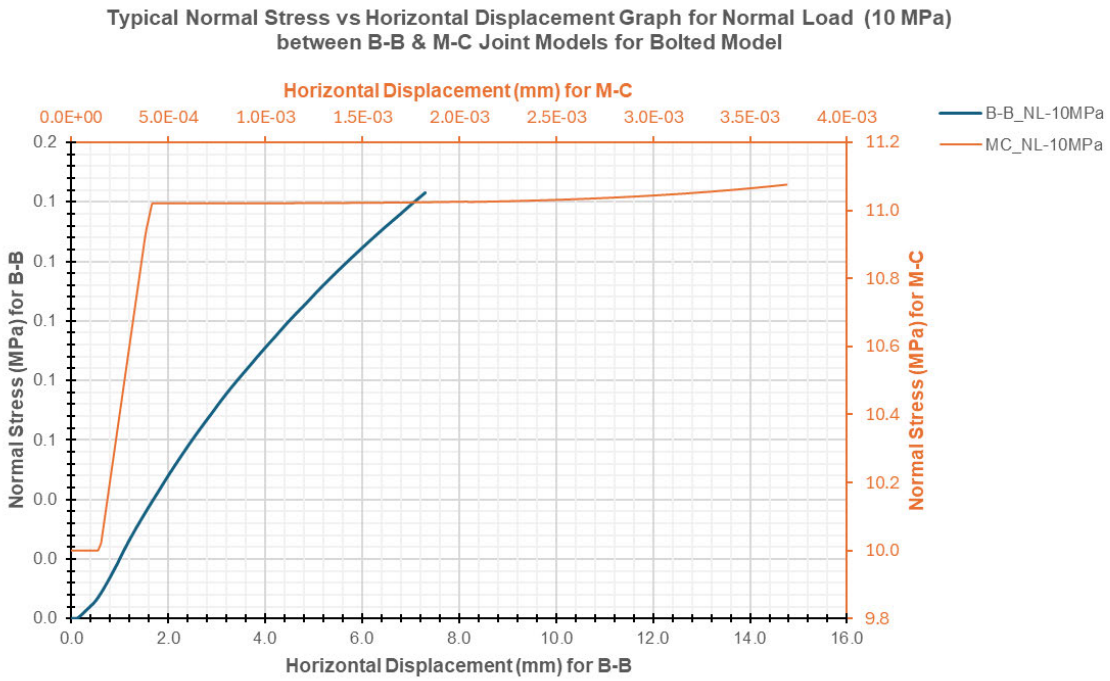

Figure 95: Presents the graph of Normal Stress vs the Horizontal Displacement for Normal Load of 10 MPa for bolted model

From the illustration of Figure 95 it can be explained that B-B model supports more closely with experimental data which reflects the improved shear resistance due to bolting compared to the M-C model of its linear failure approach. This may have been due to the undervalue of the shear strength and displacement which leads to more conservative stability assessments.

4.4.3 Summary of Comparison between B-B and M-C

From the simulations carried out using the Universal Distinct Element Code (UDEC), the B-B model in general predicts larger deformations and more accurate failure approaches in both unbolted and bolted conditions. Hence, it can be stated that due to its capability to interpret for the non-linear increase in shear strength with normal stress and joint roughness, (Mahmoud Behnia, Behzad Nateghpour, Javad Tavakoli & Mohsen Sharifi Broujerdi , 2020).

Whereas the M-C model is easier to implement, and this model not usually captures these conditions which leads to an overestimation of joint stability. From the graphs obtained in this study, it can be compared that the shear and normal stress against horizontal displacement shows, the B-B model stipulates a closer match to experimental data with higher displacements and better outcome in simulating joint behaviour under varying conditions, (Daniil Iakovlev, 2015).

4.4.4 Comparison between Barton-Bandis (B-B) and Continuously Yielding (C-Y) Joint Models Simulation for Unbolted Model

The UDEC simulations for unbolted models using constant normal load (CNL) conditions for Barton-Bandis (B-B) and Continuously Yielding (C-Y) joint models demonstrate discrete behaviours. The B-B model incorporates joint roughness and non-linear shear strength parameters and predicts higher shear strength and more accurate deformation relationships due to its comprehensive understanding of joint surface characteristics. Hence, this model is specifically valuable in describing the non-linear increase in shear strength with normal stress and the effects of joint roughness, (Gregory L. Hempen, 2018).

On the other hand, the C-Y model is designed to simulate the steady yielding of joints under stress which provides a more continuous and smooth transition from elastic to plastic behaviour. This model is suitable for representing the progressive failure and yielding of joints under varying stress situations, (Sui-Min H, Amitava G, Asadul H. C & Mikko P. A, 1993).

As illustrated in Figure 96, the B-B model associates more closely with experimental data for rough joints whereas the C-Y model extends a more general approach appropriate for a wide range of joint conditions.

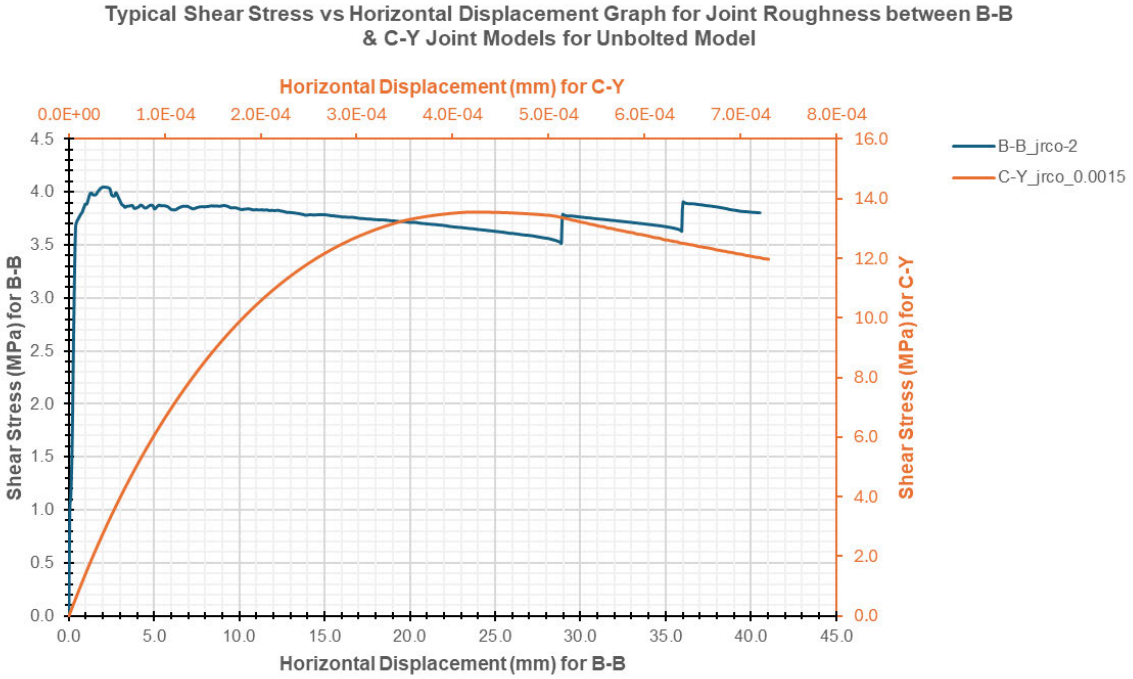

Figure 96: Presents the graph of Shear Stress vs the Horizontal Displacement for Joint Roughness for unbolted model

As seen in figure 90, the horizontal displacement increases as the shear stress starts to rise to a peak before decreasing which reflects the mobilisation of the joint system and following degradation of joint roughness afterwards.

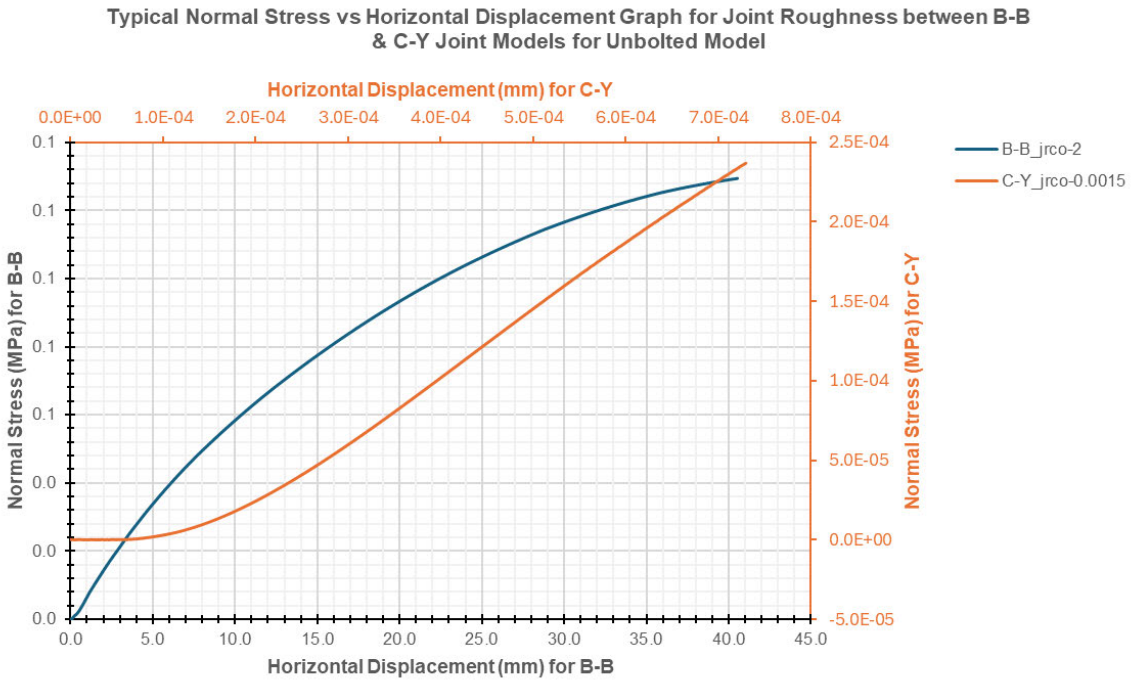

Figure 97: Presents the graph of Normal Stress vs the Horizontal Displacement for Joint Roughness for unbolted model

As illustrated in figure 97, the normal stress increases for both the B-B and C-Y models against horizontal displacement due to the applied load causing the joint surfaces to come into closer contact and improving the frictional resistance. Hence, there is an increase in the contact area and friction which results in higher normal stress as the displacement continues.

4.4.5 Comparison between Barton-Bandis (B-B) and Continuously Yielding (C-Y) Joint Models Simulation for Bolted Model

As for the bolted models of B-B and C-Y, UDEC has a comprehensive approach to simulate the reinforcement effects of rock bolts under CNL conditions. The B-B model includes the designated parameters which has more precisely calculations that supports the improved shear strength due to bolting in rough joints. The model generally illustrates a higher normal and shear stress values with greater displacement before failing which reflects the capability to model the non-linear behaviour of bolted joints more realistically, (Barton N. , 2018).

On the other hand, the C-Y model not entirely portrays the increase in shear strength provided by the bolts in highly irregular joints. As seen in figure 92 the B-B model predicts higher shear strength and greater displacement before failure compared to the C-Y model which reflects its strength in simulating joint behaviour under varying conditions, (Sui-Min H, Amitava G, Asadul H. C & Mikko P. A, 1993).

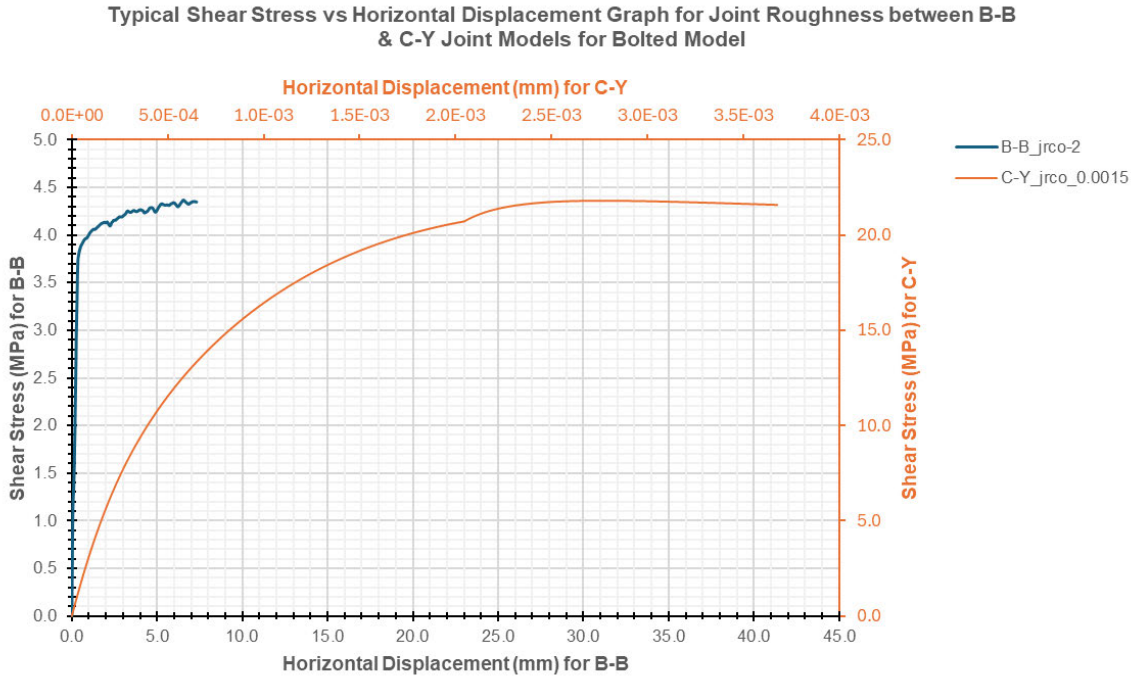

Figure 98: Presents the graph of Shear Stress vs the Horizontal Displacement for Joint Roughness for bolted model

As illustrated in figure 98, the shear stress increases for both the B-B and C-Y models against horizontal displacement due to the applied shear force initiating the joint surfaces to interlock and mobilise its roughness which improves the frictional resistance. Therefore, this interlocking and increased friction develops in higher shear stress as displacement continues.

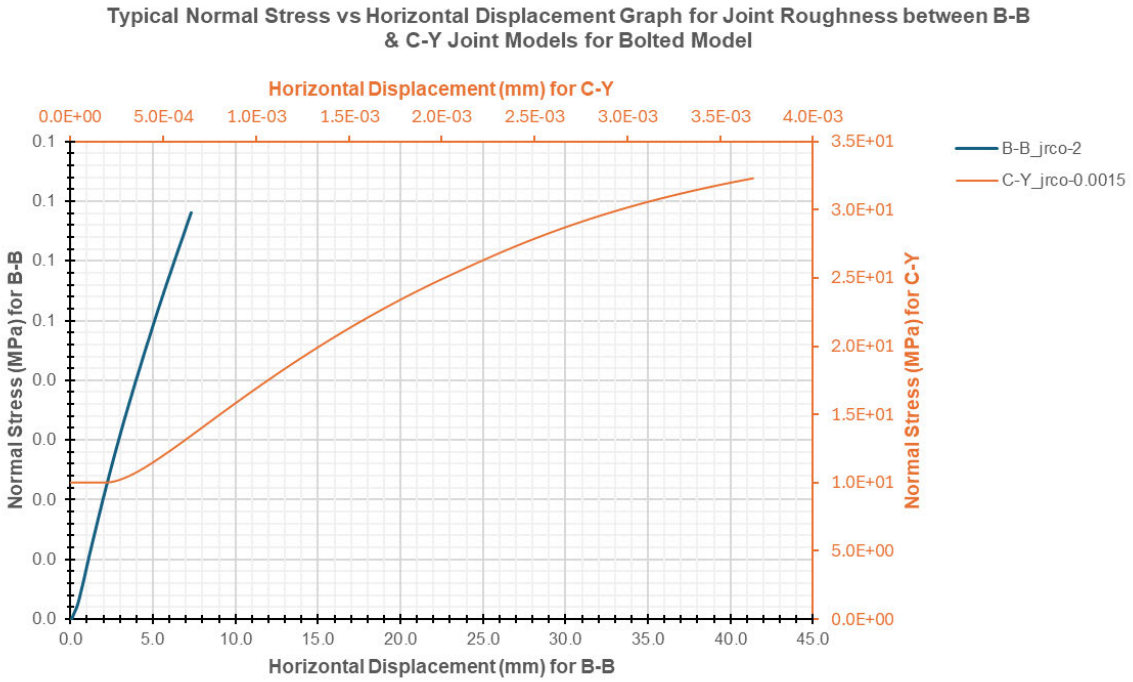

Figure 99: Presents the graph of Normal Stress vs the Horizontal Displacement for Joint Roughness for bolted model

As presented in figure 99 the normal stress increases with horizontal displacement for both the B-B and C-Y models due to the bolt's enhancement and restraint of the joint surfaces which increases the

frictional resistance. Therefore, this increased restriction leads to higher normal stress as the joint surfaces are forced closer together during displacement.

4.4.6 Summary of Comparison between B-B and C-Y

In general, the B-B model generally results in larger deformations and more realistic failure modes under both unbolted and bolted conditions due to its ability to account for the non-linear increase in shear strength with normal stress and joint roughness, (Barton N. , 2018).

Whereas the C-Y model is easier to implement which specifies a smoother alteration from elastic to plastic behaviour and is useful for a wide range of joint conditions. Comparing with the results obtained for this study the shear and normal stress against horizontal displacement typically shows that the B-B model provides a closer match to experimental data of past studies mainly at higher displacements and weights on the strength of simulating joint behaviour of changing conditions, (Sui-Min H, Amitava G, Asadul H. C & Mikko P. A, 1993).

4.4.7 Comparison between Mohor Coulomb (M-C) and Continuously Yielding (C-Y) Joint Models Simulation for Unbolted Model

The M-C and C-Y joint models displays different behaviour of UDEC simulations for unbolted models for CNL conditions. M-C joint model is a linear failure criterion that delivers a basic method to estimate the shear and normal stress which usually simplify the complex interactions at the joint interface. It regularly underestimates shear strength and displacement which leads to moderate stability estimates of the joints, (P. Barsanescu, 2015).

Whereas the C-Y model is designed to simulate the continuing yielding of joints under stress which has a more constant and accurate modification from elastic to plastic behaviour. It also provides a advancing failure and yielding of joints more effectively, (ITASCA, 2024).

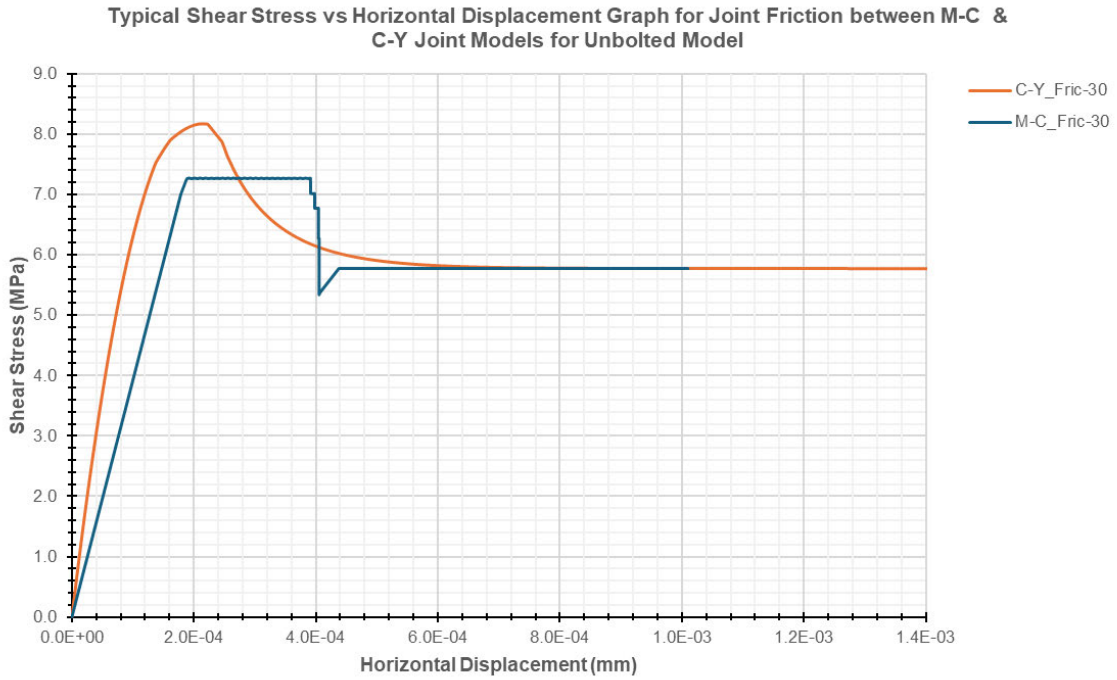

Figure 100: Presents the graph of Shear Stress vs the Horizontal Displacement for Joint Friction for unbolted model

Figure 100 shown the comparison of shear stress for both the models from the simulation carried out in this study, the M-C model shows a linear increase in shear stress until failure which reflects it is

simple to use as a linear failure criterion, whereas the C-Y model validates a more steady and continuous increase in shear stress resulting in the progressive yielding and non-linear behaviour of joints under stress.

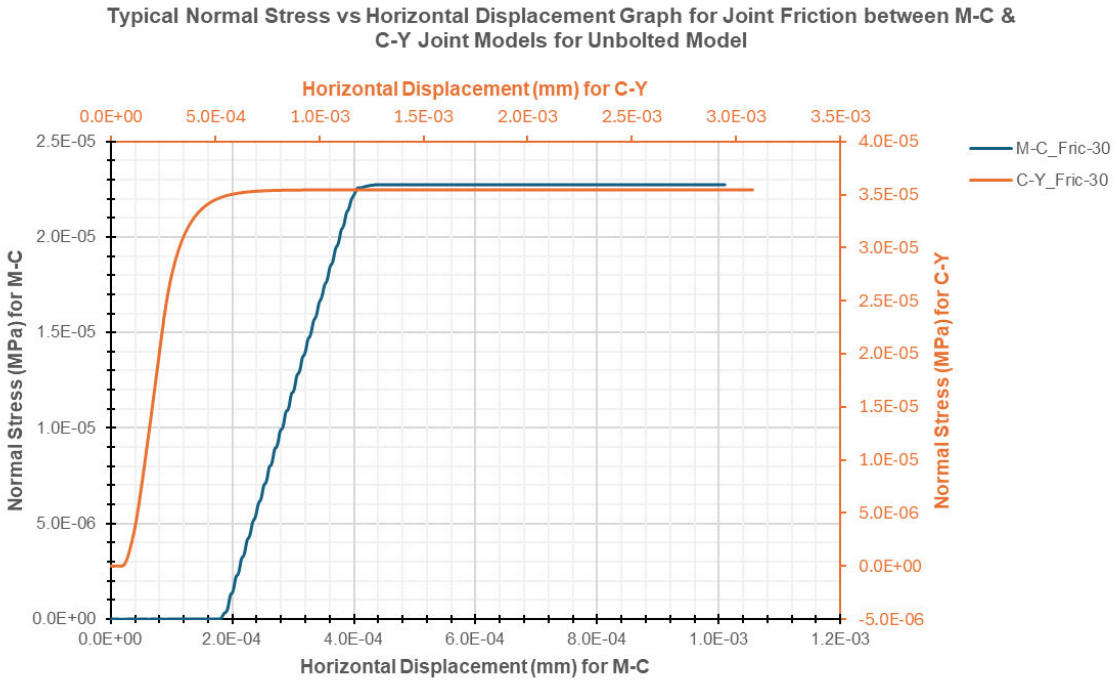

Figure 101: Presents the graph of Normal Stress vs the Horizontal Displacement for Joint Friction for unbolted model

Figure 101 shown the comparison of normal stress for both the models from the simulation carried out in this study, the M-C model shows a linear increase in normal stress until failure which reflects it is simple to use as a linear failure criterion.

On the other hand, C-Y model reveals a more regular and continuous increase in normal stress due to the progressive yielding and non-linear behaviour of joints under stress.

These graphs reveal that the C-Y model aligns more directly with experimental data from the past studies and provide accurate illustration of joint behaviour in any given circumstances.

4.4.8 Comparison between Mohor Coulomb (M-C) and Continuously Yielding (C-Y) Joint Models Simulation for Bolted Model

As for the bolted models for both M-C and C-Y, it has a comprehensive approach to simulate in UDEC for the reinforcement effects of rock bolts under CNL conditions. M-C model can be effective for preliminary assessment but not for detailed analysis, as it may not completely analyse the increased shear strength and displacement provided by bolting system in highly irregular joints, (P. Barsanescu, 2015).

Comparing this with C-Y model, as its capability to interpret for non-linear behaviour and joint roughness which can estimate higher shear and normal stress values and greater displacement before the failure. Hence, this model is more efficient in simulating the improved shear resistance due to bolting in rough joints, (ITASCA, 2024).

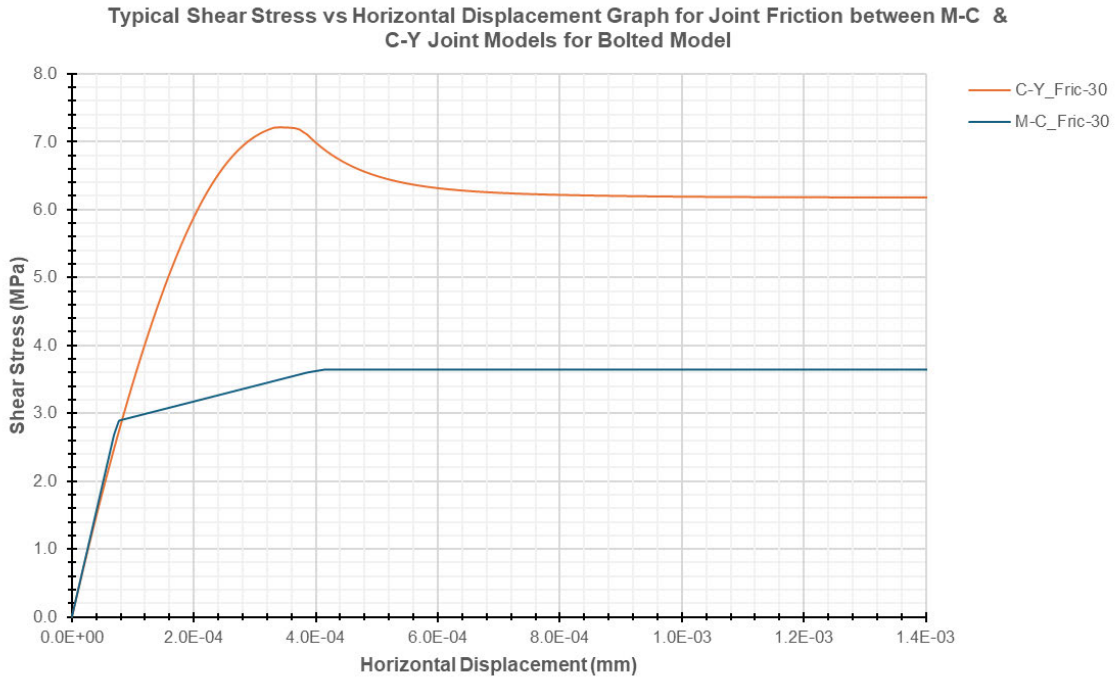

Figure 102: Presents the graph of Shear Stress vs the Horizontal Displacement for Joint Friction for bolted model

Figure 102 shows the graphs for the shear stress for the comparison of M-C and C-Y models simulations with the introduction of rock bolts under CNL conditions. The M-C model shows a linear increase in shear stress before the failure which reflects it is simpler and follow a linear failure criterion.

Whereas the C-Y model explains a steady and continuous increase in shear stress which has a progressive yielding and non-linear behaviour of bolted joints under stress.

These graphic relationships reveals that the C-Y model is closer with experimental data caried out in the past studies and provides accurate interpretation of an enhanced system of shear resistance due to bolting.

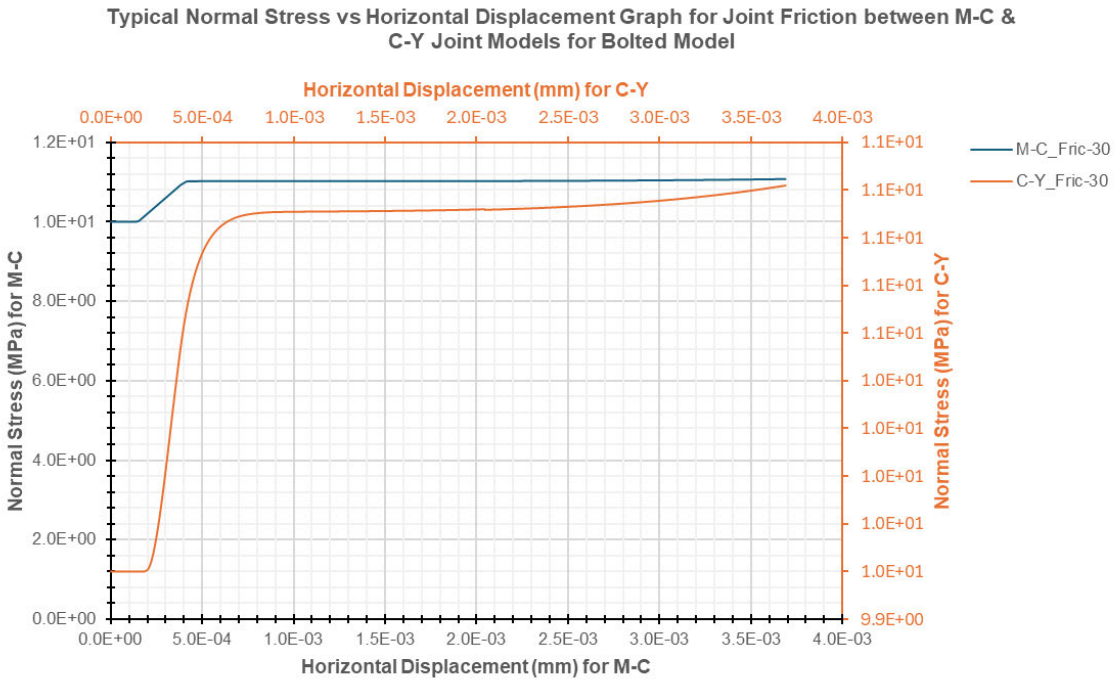

Figure 103: Presents the graph of Normal Stress vs the Horizontal Displacement for Joint Friction for bolted model

Figure 103 shows the graphs for normal stresses for the comparison of M-C and C-Y models simulations with the introduction of rock bolts under CNL conditions, which shows an increase in normal stress with horizontal displacement.

This increase is due to the rock bolts enhances the restraint of the joint surfaces which increases the frictional resistance and the normal stress as displacement proceeds.

These graphic relationships reveals that the C-Y model is closer with experimental data caried out in the past studies and provides accurate interpretation of an enhanced system of shear resistance due to bolting.

4.4.9 Summary of Comparison between M-C and C-Y

In general, the C-Y model concludes that the with this mode predicts a larger deformations and more accurate failure modes for both unbolted and bolted situations due to its capability to provide justification for the non-linear increase in shear strength with normal stress and joint roughness. Whereas the M-C model is easier to use which provides a simpler and more consecutive estimate of joint stability, (P. Barsanescu, 2015).

With comparison of the results obtained from this study the shear and normal stress against horizontal displacement show that the C-Y model provides a closer match to experimental data of past studies and in relation to a higher displacements and importance of its strength in simulating joint behaviour with varying conditions, (ITASCA, 2024).

5 Reference

(n.d.).

Indraratna B, Haque A & Aziz N. (1999). *Shear behaviour of idealized infilled joints under constant normal stiffness.* 49, 331–355. [CrossRef]: Géotechnique.

Johnston I.W, Lam T.S.K, & Williams A.F. Sr. . (1987). *Constant normal stiffness direct shear testing for socketed pile design in weak rock.* 37, 83–89. [CrossRef]: Géotechnique.

A.M. Crawford & J.H. Curran. (1981). *The influence of shear velocity on the frictional resistance of rock discontinuities.* London, Ontario: International Journal of Rock Mechanics and Mining Sciences & Geomechanics Abstracts.

Abdullah R. A, Fowell R. J & Murphy W. (2010). *Selecting Shear Strength Models For Joints - Experience With Modeling of Complex Rock Slope Failure In UDEC.* International Society for Rock Mechanics and Rock Engineering. .

Adachi, T. K. (1999). *Shear Behavior of Rock Joints In Consideration of Material Friction And Joint Surface Roughness.* International Society for Rock Mechanics and Rock Engineering and some solutions, Journal of Rock Mechanics and Geotechnical Engineering, 5(4), 249-264.

ASTM, D. (2016). *Standard Test Method for Performing Laboratory Direct Shear Strength Tests of Rock Specimens Under Constant Normal Force.* West Conshohocken, PA: ASTM International, 5607-16.

Azuar J. J, Dardaine M, & Pellet F. (1979). Le renforcement des massifs rocheux par armatures passives. *In Proceedings of the 4th International Congress on Rock Mechanics (ISRM)*, (pp. Vol. 1, pp. 23-30). Montreux.

B Indraratna. (2008). *Shear strength model for overconsolidated clay-infilled idealised rock joints.* Sydney: ResearchGate.

Babanouri, N. (2011). *Overconsolidation effect on shear behavior of rock joints.* International Journal of Rock Mechanics and Mining Sciences - INT J ROCK MECH MINING SCI.

Bandis. S, Lumsden. A C & Barton, N R. (1981). *Experimental studies of scale effects on the shear behaviour of rock joints.* International Journal of Rock Mechanics and Mining Sciences & Geomechanics Abstracts, Volume 18, Issue 3, Page 45.

Barton. (1971).

Barton N. R. (1976). *The shear strength of rock and rock joints.* DOI:10.1016/0148-9062(76)90003-6: International Journal of Rock Mechanics and Mining Sciences & Geomechanics Abstracts 13(9):255-279.

Barton, N & V. Choubey. (1977). *The shear strength of rock joints in theory and practice.* Rock mechanics, 10(1-2), 1-54.

Barton, N. (1973). *Review of a new shear-strength criterion for rock joints.* New York, N.Y: Engineering Geology, Volume 7, Issue 4, 1973, Pages 287-332.

Barton, N. (2018, November 2). *Barton-Bandis Criterion*. Retrieved from Springer Nature Link: https://doi.org/10.1007/978-3-319-73568-9_25

Charlie Li. (2017, May). *Principles of rockbolting design*. Retrieved from ResearchGate: DOI: 10.1016/j.jrmge.2017.04.002

Chen W & Li L. (2015). Experimental study on the mechanical behavior of rock bolts under combined pull and shear loads. *International Journal of Rock Mechanics and Mining Sciences*, 78, 1-10.

Cundall, P. &. (1990). *Numerical simulation of fault instabilities with the continuously-yielding joint model.* Proceedings of the 2nd International Conference on Rockburst and Seismicity in Mines, University of Minnesota .

Daniil Iakovlev. (2015). Comparison of Barton-Bandis and Mohr-Coulomb models for use in discontinuity shear stability analysis. *Academia.edu*, p. https://www.academia.edu/80588121/Comparison_of_Barton_Bandis_and_Mohr_Coulomb_models_for_use_in_discontinuity_shear_stability_analysis?auto=download.

Davis H.E, Holtz W.G & Housel W.S. (1951). *In Triaxial Testing of Soils and Bitminous Mixtures.* West Conshohocken, PA, USA, pp. 180–191.: ASTM International.

De Beer. (1950). *I.E.E. The cell-test.* Géotechnique.

Dight P. M. (1982). *Improvements to the Stability of Open Pit Walls. PhD.* Melbourne, Australia.: Monash University.

Edelbro, C. (2009). *Numerical modelling of observed fallouts in hard rock masses using an instantaneous cohesion-softening friction-hardening model.* Tunnelling and Underground Space Technology.

Franklin J.A, Kanji M.A, Herget G, Ladanyi B, Drozd K, Dvorak A, Egger P, Kutter H, & Rummel F; et al. (1974 – 2006). *Suggested methods for determining shear strength. Int Soc Rock Mech Commission on Testing Methods. In The Complete ISRM Suggested Methods for Rock Characterization, Testing and Monitoring:.* Ulusay, R., Hudson, J.A., Eds: ISRM.

Fuller P. G & Cox W. R. (1978). Behavior of Fully Grouted Rock Bolts in Shear. *In Proceedings of the 19th U.S. Symposium on Rock Mechanics (USRMS)*, (pp. Paper Number: ARMA-78-0004). Reno, Nevada.

Gerdeen J. C, Weaver T. A., & Heasley K. A. (1977). *Design Criteria for Roof Bolting Plans Using Fully Resin-Grouted Nontensioned Bolts to Reinforce Bedded Mine Roof.* Michigan Technological Univ., Houghton. Dept. of Mechanical Engineering and Engineering Mechanics.; Bureau of Mines, Washington, DC.: National Technical Reports Library.

Gerdeen, J.C., et al. (1977). Design Criteria for Roof Bolting Plans Using Fully Resin-Grouted Nontensioned Bolts to Reinforce Bedded Mine Roof. *USBM*, pp. Contract No. JO366004, Michigan Technological University, Vol. IV.

Gonzalez de Vallejo, L. L. (2011). *Geological engineering.* Leiden: CRC Press/Balkema.

Goodman R.E. (1976). *Methods of Geological Engineering in Discontinuous Rocks.* St. Paul, MN, USA; p. 472.: West Publishing Company.

Goodman, R. (1993). *Engineering geology; rock in engineering construction.* New York: Wiley.

Grawira Ganjur Giwangkara1, A. M. (2020). *Analysis of Internal Friction Angle and Cohesion Value for.* Skudai, Johor, Malaysia: Journal of Advanced Civil and Environmental Engineering.

Gregory L. Hempen. (2018, January 1). Blasting. *Encyclopedia of Engineering Geology*, pp. pp 62–63.

Haas C. J. (1976). Behavior of Fully Grouted Rock Bolts in Shear. *In Proceedings of the 17th U.S. Symposium on Rock Mechanics (USRMS)*, (pp. Paper Number: ARMA-76-0003). Snowbird, Utah.

Haque, A & Indraratna, B . (2000). *Shear Behaviour of Rock Joints.* Rotterdam Netherland: A A Balkema.

Hempen, G. (2018, November 2). *Blasting*. Retrieved from Springer Nature Link: https://doi.org/10.1007/978-3-319-73568-9_30

Indraratna, B. (2013). *Shear behaviour of rock joints with unsaturated infill.* Géotechnique.

Indraratna, S. T. (2015). *A review of shear strength models for rock joints subjected to constant normal stiffness.* Wollongong: Journal of Rock Mechanics and Geotechnical Engineering.

ISRM, & Franklin J.A, K. M. (1974 - 2007). *Suggested methods for determining shear strength. Int Soc Rock Mech Commission on Testing Methods. In The Complete ISRM Suggested Methods for Rock Characterization, Testing and Monitoring.* Ulusay, R., Hudson, J.A., Eds.; ISRM: Ankara, Turkey, pp. 165–176.: ISRM.

Itasca. (2019). *UDEC — Universal Distinct Element Code, Ver. 7.0.* Minneapolis: Itasca.: Itasca Consulting Group, Inc.

Itasca. (2024, February 25). Continuously Yielding Joint Model In 3DEC. *3DEC © 2019, Itasca*.

ITASCA. (2024, Novemeber 3). *Continuously Yielding Joint Model In 3DEC*. Retrieved from ITASCA: https://docs.itascacg.com/3dec700/3dec/docproject/source/theory/cyjoint/cyjoint.html

Itasca. (2024, February 25). Joints. *3DEC © 2019, Itasca*.

Itasca. (2024, Februray 25). Mohr-Coulomb Joint Model In 3DEC. *3DEC © 2019, Itasca*.

Itasca. (2024). *Structural Elements*. Retrieved from Itasca: https://docs.itascacg.com/3dec700/3dec/docproject/source/theory/3dectheory/theory_sels.html

ITASCA, Version 9.1.13. (2024, November 2). *Mohr-Coulomb Joint Model In 3DEC*. Retrieved from ITASCA: https://docs.itascacg.com/itasca910/3dec/docproject/source/theory/mohrcoulomb/mohrcoulomb.html

Jan Nemcik, Ali Mirzaghorbanali & Naj Aziz . (2013, December 6). An Elasto-Plastic Constitutive Model for Rock Joints Under Cyclic Loading and Constant Normal Stiffness Conditions. *Geotechnical and Geological Engineering*, pp. Volume 32, pages 321–335.

Jie Liu, Jiahong Wu, Xiaoshuang Li, He Zhang & Yanbin Song. (2022, February 7). Numerical Simulation on Shear Behavior of Double Rough Parallel Joints Under Constant Normal Stiffness Boundary Condition. *Advances in Modeling, Assessment, and Prevention of Geotechnical and Geological Disasters*.

Johnston, I.W.; Lam, T.S.K.; Williams, A.F., Sr. Constant normal stiffness direct shear testing for socketed pile design in weak rock. (1987). *Constant normal stiffness direct shear testing for socketed pile design in weak rock.* 37, 83–89. [CrossRef]: Géotechnique.

Jun Wang, Derek B. Apel, Huawei Xu & Chong Wei . (2022, November 22). Evaluation of the performance of yielding rockbolts during rockbursts using numerical modeling method. *International Journal of Coal Science & Technology* , p. Volume 9.

Jung-Wook Park, Yong-Ki Lee, Jae-Joon Song & Byung-Hee Choi . (2013, January 29). A Constitutive Model for Shear Behavior of Rock Joints Based on Three-Dimensional Quantification of Joint Roughness. *Springer Nature Link*, pp. Volume 46, pages 1513-1537.

Kelleg. (2024, November 11). *How do Rock Bolts Stabilize a Slope?* Retrieved from Kelleg: https://kellegdrill.com/rock-bolts-stabilize-a-slope/

Kim M.M & Ko H-Y. (1979). *Multistage triaxial testing of rocks.* 2, 98–105. [CrossRef]: ASTM Geotech. Test. J.

Kovari K & Tisa A. (1975). *Multiple failure state and strain controlled triaxial tests.* 7, 17–33. [CrossRef]: Rock Mech. Rock Eng.

L. Jing, O. Stephansson & E. Nordlund . (1993, July). Study of rock joints under cyclic loading conditions. *Rock Mechanics and Rock Engineering*, pp. Volume 26, pages 215–232.

Lambe T.W, Whitman, R.V. (1969). *Soil Mechanics.* New York, NY, USA: Wiley.

Li, C. C. (2010). Rockbolting in High-Stress Rock. *In Proceedings of the 5th International Symposium on Ground Support in Mining and Underground Construction*, 305-320.

Liu He, Zhiming Zhao, Jiayi Chen & Diyi Liu . (2020, April 23). Empirical Shear Strength Criterion for Rock Joints Based on Joint Surface Degradation Characteristics During Shearing. *Rock Mechanics and Rock Engineering*, pp. Volume 53, pages 3609–3624.

Mahdi Saadat . (2019). *The Performance of Fully Grouted Rock Bolts Subjected to Combined Pull and Shear Loads Under Constant Normal Stiffness Condition .* Adelaide : School of Civil, Environmental and Mining Engineering, the University of Adelaide .

Mahmoud B, Behzad N, Javad T. & Mohsen S B. (2020, July 11). *Comparison of experimental and empirical methods for estimating the shear strength of rock joints based on the statistical approach*. Retrieved from Springer Nature Link: https://doi.org/10.1007/s12665-020-09080-6

Mahmoud Behnia, Behzad Nateghpour, Javad Tavakoli & Mohsen Sharifi Broujerdi . (2020, July 11). Comparison of experimental and empirical methods for estimating the shear strength of rock joints based on the statistical approach. *Environmental Earth Sciences*, pp. Volume 79, article number 361.

Malavika Varma, V. B. Maji & A. Boominathan . (2024, February 18). Response Analysis of Rock Mass and Support Under Dynamic Loading. *Indian Geotechnical Journal* .

Manuel J.A. Leal Gomes, C. D. (2009). *An Experimental Study on Scale Effects in Rock Mass Joint Strength.* University of Brasília, Brazil: SOILS and ROCKS, An International Journal of Geotechnical and Geoenvironmental Engineering.

Mohammad Reza Shahverdiloo & Shokrollah Zare . (2021, September 28). Studying the normal stress influential factor on rock joint stiffness using CNL direct shear test. *Arabian Journal of Geosciences*, pp. Volume 14, article number 2082.

Mohammad Reza Shahverdiloo & Shokrollah Zare. (2021, September 28). Studying the normal stress influential factor on rock joint stiffness using CNL direct shear test. *Arabian Journal of Geosciences*, pp. Volume 14, article number 2082.

Muralha J. (2007). *Stress paths in laboratory joint shear tests. In Proceedings of the 11th International Society for Rock Mechanics (ISRM) Congress.* Lisbon, Portugal, London, UK, pp. 431–434.: 9–13; Taylor & Francis Group:.

Muralha J, Grasselli G, Tatone B, Blümel M, Chryssanthakis P & Yujing J. (2014). *ISRM suggested method for laboratory determination of the shear strength of rock joints: Revised version.* 47, 291–302. [CrossRef]: Rock Mech. Rock Eng.

N Barton & R Olsson . (2001). *An improved model for hydromechanical coupling during shearing of rock joints.* International Journal of Rock Mechanics & Mining Sciences.

N. Barton & S. Bandis. (1982). *Effect of block size on the shear behavior of jointed rocks.* Aristotle University of Thessaloniki: https://www.researchgate.net/publication/280021212.

N. Barton. (1982). *Modelling Rock Joint Behavior From In-situ Block Test: Implicaions for Nuclear Waste Repository Design.* Salt Lake City, Utah: ONWI.

Nicholas R. MacDonald, Timothy R. M. Packulak and Jennifer J. Day. (2023). *A Critical Review of Current States of Practice in Direct Shear Testing of Unfilled Rock Fractures Focused on Multi-Stage and Boundary Conditions.* Kingston, ON K7L 3N6, Canada: Department of Geological Sciences and Geological Engineering, Queen's University.

Nicholas R. MacDonald,Timothy R. M. Packulak & Jennifer J. Day. (2023, November 2). *A Critical Review of Current States of Practice in Direct Shear Testing of Unfilled Rock Fractures Focused on Multi-Stage and Boundary Conditions*. Retrieved from www.mdpi.com: https://doi.org/10.3390/geosciences13060172

Nick Barton, C. W. (2023). *Advances in joint roughness coefficient (JRC) and its engineering applications.* Høvik, Oslo, Norway: Journal of Rock Mechanics and Geotechnical Engineering.

Obert L, Brady B.T, & Schmechel F.W. (1976). *The Effect of Normal Stiffness on the Shear Resistance of Rock.* 8, 57–72: Rock Mech.

P. Barsanescu. (2015, April 25). Extension of Mohr-Coulomb Theory for Ductile Materials. *Experimental Mechanics* , pp. Volume 55, pages 1389–1393.

Packulak T.R.M. (2018). *Laboratory Investigation of Shear Behaviour in Rock Joints under Varying Boundary Conditions.* Kingston, ON, Canada, Available online: https://qspace.library.queensu.ca/handle/1974/24827(: Master's Thesis, Department of Geological Sciences and Geological Engineering, Queen's University.

Packulak T.R.M, & Day J.J. (2022). *Enhancement of constant normal stiffness direct shear testing protocols for determining geomechanical properties of fractures.* 59, 1643–1659. [CrossRef]: Can. Geotech. J.

Palmström A. (2001). *In-Situ Characterization of Rocks.* Övre Smestad vei 35e, N-0378 Oslo, Norway: Chapter 2 of the book, In-Situ Characterization of rocks.

Patton F.D. . (1966). *Multiple modes of shear failure in rock. Proc. 1st Congr. .* Lisbon, pp. 509-513: ISRM.

Pells, P. J. N. (1974). *Rock Mechanics and Engineering Geology in the Design of Underground Openings.* Sydney: PhD Thesis, University of Sydney.

Poeck, E. C. (2016). *Analyzing the potential for unstable mine failures with the calculation of released energy in numerical models.* Colorado: Colorado School of Mines.

R. A. Abdullah, R. J. Fowell & W. Murphy. (2010, June 15-18). Selecting Shear Strength Models For Joints - Experience With Modeling of Complex Rock Slope Failure In UDEC. *ISRM International Symposium - EUROCK 2010*, pp. Lausanne, Switzerland.

Richard E. Goodman. (1991). *Introduction to Rock Mechanics, 2nd Edition.* Wiley.

Ripley C.F & Lee K.L. (1961). *Sliding friction tests on sedimentary rock specimens. In Proceedings of the 7th International Congress on Large Dams.* Rome, Italy, 26 June–1 July 1961; pp. 657–671.

S. Bjurstroem. (1974). Shear strength of hard rock joints reinforced by grouted untensioned bolts. *Engineering, Geology*, DOI:10.1016/0148-9062(75)90705-6, Corpus ID: 115959082.

Saeb S & Amadei B. (1992). *Modelling rock joints under shear and normal loading.* 29, 267–278. [CrossRef]: Int. J. Rock Mech. Min. Sci. Geomech. Abstr.

Shrivastava, A.K & Rao, K.S. (2010, December 16-18). Numerical Simulation of Direct Test for Rock. *Indian Geotechnical Conference – 2010, GEOtrendz*.

Skinas, C. A. (1990). *Experimental investigations and modelling of rock joint behaviour under constant stiffness.* Loen, pp. 301-308. Rotterdam: Balkema: Proc. Int. Conf. on Rock Joints.

Solak, K.C., Tuncay, E. (2023, November 2). *An evaluation on Barton-Bandis shear strength criterion for discontinuities in weak materials under low normal stresses*. Retrieved from Springer Nature Link: https://doi.org/10.1007/s10064-023-03434-7

Spang, K & Egger, P. (1990). Action of fully-grouted bolts in jointed rock and factors of influence. *Rock Mechanics and Rock Engineering* , Volume 23, pages 201–229.

St. John, C. M., & Van Dillen, D. E. (1983). Rockbolts: A New Numerical Representation and Its Application in Tunnel Design. *In Proceedings of the 24th U.S. Symposium on Rock Mechanics (USRMS), College Station* (pp. In Proceedings of the 24th U.S. Symposium on Rock Mechanics (USRMS), College Station). Texas: Paper Number: ARMA-83-0003.

Stout, K. S. (1975). *Soil and Rock Mechanics Illustrated.* (96), 187.

Sui-Min H, Amitava G, Asadul H. C & Mikko P. A. (1993). *Evaluation of Rock Joint Models and Computer Code UDEC Against Experimental Results.* San Antonio, Texas: Center for Nuclear Waste Regulatory Analyses.

Sui-Min H, Amitava G, Asadul H. C. & Mikko P. A. (1993). *Evaluation of Rock Joints Model and Computer Code UDEC Against Experimental Results.* San Antonio, Texas: Center for Nuclear Waste Regulatory Analyses.

Sunhao Zhang, Yujing Jiang, Hengjie Luan, Bo Li, Jianrong Liu & Changsheng Wang . (2024, July 22). Study on Shear Mechanical Characteristics of Rock Joints Under Different Anchorage Lengths. *Rock Mechanics and Rock Engineering* , pp. Volume 57, pages 9959–9981.

Tanimoto C, K. K. (1996). *The experimental study of the shear behaviour of natural rock joint in consideration of joint roughness.* Rock Mechanics, 1619-1625.
Taylor D.W. (1951). *A triaxial shear investigation on a partially saturated soil.* West Conshohocken, PA, USA, pp. 180–191.: ASTM International.
Thirukumaran, S. (2014). *Shear strength of degradable rock joints.* Wollongong: University of Wollongong.
Thomas Frühwirt, Daniel Pötschke & Heinz Konietzky . (2021, April 7). Simulation of direct shear tests using a forces on fracture surfaces (FFS) approach. *Environmental Earth Sciences* , pp. Volume 80, article number 312.
Y. Tasaku, Y. Jiang, Y. Tanahashi & B. Li. (2008). *Estimating The Influence of Surface Characteristics Of Rock Joints On Shear Behavior.* Nagasaki University.
Yinge Zhu, Gang Wang, Anqi Li, Huiyuan Chen, Tingfang Liu & Hui Guan . (2022, November 15). Effects of Joint Roughness, Shear Rate, and Normal Stress on Shear Behavior and Acoustic Emission Characteristics in Two Parallel Coplanar Intermittently Jointed Rock: An Experimental Study. *Rock Mechanics and Rock Engineering*, pp. Volume 56, pages 1289–1303.
Yong-Ki Lee, Jung-Wook Park & Jae-Joon Song. (2013, November 2). *Model for the shear behavior of rock joints under CNL and CNS conditions*. Retrieved from ScienceDirect: https://doi.org/10.1016/j.ijrmms.2014.05.005
Younkin G.W. (2003). *Industrial servo control systems fundamentals and applications.* Inc: New York, NY, USA, p. 384.: In Revised and Expanded, 2nd ed.; Marcel Dekker.
Yu Chen & Haodong Xiao . (2024, February 5). State-of-the-art on the anchorage performance of rock bolts subjected to shear load. *International Journal of Coal Science & Technology*, pp. Volume 11, article number 9.
Zhao J. (1997a). Joint Roughness Coefficient (JRC) and Joint Matching Coefficient (JMC) for Estimating the Peak Shear Strength of Rock Joints. *Rock Mechanics and Rock Engineering*, 30(3), 135-153.
Zhao J. (1997b). A Modified JRC-JCS Model for Rock Joint Shear Strength. *International Journal of Rock Mechanics and Mining Sciences*, 34(2), 173-180.
Zhezhe Zhang, Baohua Guo, Shengjin Cheng, Pengbo Zhong & Chuangwei Zhu. (2024, September 19). Experimental study on shear mechanical properties of concrete joints under different unloading stress paths. *Plos One, Article*, p. https://doi.org/10.1371/journal.pone.0310694.

Appendix A

UDEC Coding for Barton-Bandis Joint Model for CNL Conditions

A.1 BB Joint Model

(Note: The following codes are adopted from the UDEC manual version 7.0)

```
block config barton-bandis
block tolerance corner-round-length 0.001
block create polygon -0.05 -0.1 -0.05 0.1 0.25 0.1 0.25 -0.1
block cut crack -0.05 0 0.25 0
block cut crack 0 0 0 0.1
block cut crack 0.2 0 0.2 0.1
block delete range pos-x -0.05 0 pos-y 0 0.1
block delete range pos-x 0.2 0.25 pos-y 0 0.1
;
block zone gen quad 0.4 0.11 range pos-x -0.05 0.25 pos-y -0.1 0
block zone gen quad 0.07 0.11 range pos-x 0 0.2 pos-y 0 0.1
block zone group 'block'
group zone 'block' range pos-x -5E-2,0.25 pos-y -0.1,0.1
block property material 1 density 2.60e3 bulk 45000 shear 30000
;
; B-B joint model
block contact cmodel assign barton-bandis
block contact property st-normal 40000 st-shear 40000 jrco 8 jcso 30
sigmac 50 lo 0.1 phir 20
block contact cmodel default barton-bandis
;
; apply boundary conditions
block gridpoint apply velocity-x 0 range pos-x -0.06 -0.04 pos-y -1 1
block gridpoint apply velocity-x 0 range pos-x 0.24 0.26 pos-y -1 1
block gridpoint apply velocity-y 0 range pos-x -1 1 pos-y -0.11 -0.09
; apply normal load
block edge apply stress 0 0 -10 range pos-x -1 1 pos-y 0.09 0.11
;
block solve
;
; functions to calculate average joint stresses
; and average joint displacements
```

```
;
call 'BB.FIN'
;
fish define av_str
whilestepping
sstav = 0.0
njdil = 0.0
njusc = 0.0
ncon = 0
jl = 0.2 ; joint length
ic = block.contact.head
loop while ic # 0
ncon = ncon+1
sstav = sstav + block.contact.force.shear(ic)
cmext = block.contact.extension(ic)
njdil = njdil + fmem(cmext+$bb_dil)
njusc = njusc + fmem(cmext+$bb_usc)
ic = block.contact.next(ic)
endloop
if ncon # 0
sstav = sstav / jl
njdil = njdil / ncon
njusc = njusc / ncon
endif
end
fish callback 0 av_str
;
block contact reset displacement
block gridpoint init displacement-x 0
block gridpoint init displacement-y 0
hist reset
;
hist interval 1
fish hist @sstav
fish hist @njdil
fish hist @njusc
;
```

```
;
;*****************************************************************************
;rockblot
block struct rockbolt create begin 0.1,0.2 end 0.1,-0.20 seg 1 prop 50
block struct rockbolt prop 20 cross-sectional-area 5E-4 coupling-
cohesion-normal 1E5 coupling-friction-normal 45 coupling-stiffness-normal
2E7 coupling-cohesion-shear 1E5 coupling-friction-shear 45 coupling-
stiffness-shear 2E7 density 1E-3 young 2E11 moi 2E-8 perimeter 8E-2
tension-failure-strain 0.2 yield-tension 2.25E5 yield-compression 2.23E5
*****************************************************************************
;
; apply shear load by imposing x-velocity on top block
block gridpoint apply velocity-x 0.01 range pos-x -.01 .21 pos-y -.01 .11
;
block cycle 1000
;
his write 1 file 'sstav.his'
his write 2 file 'njdil.his'
his write 3 file 'njusc.his'
```

Appendix B

UDEC Coding for Mohor Coulomb Joint Model for CNL Conditions

B.1 MCJM

(Note: The following codes are adopted from the UDEC manual version 7.0)

```
; create shear test model
model title 'direct shear test'
block tolerance corner-round-length 0.001
block tolerance minimum-edge-length 0.002
block create polygon -5E-2 -0.1 -5E-2 0.1 0.25 0.1 0.25 -0.1
block cut crack -1 0 1 0
block cut crack 0 0.1 0 0
block cut crack 0.2 0.1 0.2 0
block delete range pos-x -5E-2 0 pos-y 0 0.1
block delete range pos-x 0.2 0.25 pos-y 0 0.1
block zone gen quad 0.4 0.11 range pos-x 0 1 pos-y -1 0
block zone gen quad 0.07 0.11 range pos-x 0 1 pos-y 0 1
block zone group 'block'
block zone cmodel assign elastic density 2.6E-3 bulk 4.5E4 shear 3E4
range group 'block'
;
; Coulomb joint model
block contact group 'joint'
block contact cmodel assign area stiffness-shear 4E4 stiffness-normal 4E4
friction 30 dilation 6 dilation-limit 4E-4 range group 'joint'
; new contact default
block contact cmodel default area stiffness-shear 4E4 stiffness-normal 4E4
friction 30 dilation 6 dilation-limit 4E-4
; set add_dil on
;
block gridpoint apply velocity-x 0 range pos-x -0.06 -0.04 pos-y -1 1
block gridpoint apply velocity-x 0 range pos-x 0.24 0.26 pos-y -1 1
block gridpoint apply velocity-y 0 range pos-x -1 1 pos-y -0.11 -0.09
; apply normal load
block edge apply stress 0 0 -10 range pos-x -1 1 pos-y 0.09 0.11
;
block cycle 1000
;
```

```
; functions to calculate average joint stresses
; and average joint displacements
;
fish define ini_jdisp
njdisp0 = 0.0
sjdisp0 = 0.0
ic = block.contact.head
loop while ic # 0
njdisp0 = njdisp0 + block.contact.disp.normal(ic)
sjdisp0 = sjdisp0 + block.contact.disp.shear(ic)
ic = block.contact.next(ic)
endloop
end
@ini_jdisp
;
fish define av_str
whilestepping
sstav = 0.0
nstav = 0.0
njdisp = 0.0
sjdisp = 0.0
ncon = 0
jl = 0.2 ; joint length
ic = block.contact.head
loop while ic # 0
ncon = ncon+1
sstav = sstav + block.contact.force.shear(ic)
nstav = nstav + block.contact.force.normal(ic)
njdisp = njdisp + block.contact.disp.normal(ic)
sjdisp = sjdisp + block.contact.disp.shear(ic)
ic = block.contact.next(ic)
endloop
if ncon # 0
sstav = sstav / jl
nstav = nstav / jl
njdisp = (njdisp-njdisp0) / ncon
sjdisp = (sjdisp-sjdisp0) / ncon
```

```
endif
end
fish callback 0 av_str
;
block contact reset displacement
block gridpoint init displacement-x 0
block gridpoint init displacement-y 0
hist reset
;
hist interval 1
fish history @sstav
fish history @nstav
fish history @njdisp
fish history @sjdisp
;hist name 1 label 'Shear Stress'
;hist name 3 label 'Normal Displacement'
;hist name 4 label 'Shear Displacement'
;
*********************************************************************************
;rockblot
block struct rockbolt create begin 0.1,0.2 end 0.1,-0.20 seg 1 prop 50
block struct rockbolt prop 20 cross-sectional-area 5E-4 coupling-
cohesion-normal 1E5 coupling-friction-normal 45 coupling-stiffness-normal
2E7 coupling-cohesion-shear 1E5 coupling-friction-shear 45 coupling-
stiffness-shear 2E7 density 1E-3 young 2E11 moi 2E-8 perimeter 8E-2
tension-failure-strain 0.2 yield-tension 2.25E5 yield-compression 2.23E5
*********************************************************************************
; apply shear load by imposing x-velocity on top block
block gridpoint apply velocity-x 0.01 range pos-x -.01 .21 pos-y -.01 .11
;
block cycle 6500
;
;plot hold hist -1 vs 4
;plot hold hist 3 vs 4
;
;his write 1 file 'sstav.his'
;his write 2 file 'nstav.his'
;his write 3 file 'njdisp.his'
```

```
;his write 4 file 'sjdisp.his'
;
model save 'cy_1.sav'
;
return
```

Appendix C

UDEC Coding for Continuous Yielding Model for CNL Conditions

C.1 CYJM

(Note: The following codes are adopted from the UDEC manual version 7.0)

```
config udm
block tolerance corner-round-length 0.001
block create polygon -0.05 -0.1 -0.05 0.1 0.25 0.1 0.25 -0.1
block cut crack -1 0 1 0
block cut crack 0 0.1 0 0
block cut crack 0.2 0.1 0.2 0
block delete range pos-x -0.05 0 pos-y 0 0.1
block delete range pos-x 0.2 0.25 pos-y 0 0.1
;
block zone gen quad 0.4 0.11 range pos-x 0 1 pos-y -1 0
block zone gen quad 0.07 0.11 range pos-x 0 1 pos-y 0 1
;
block property material 1 density 2.60e-3
block property material 1 bulk 4000 shear 3000
block domain property material 1 capillary-gamma 3000
;
; C-Y joint model (JOINT model cy)
block contact cmodel assign continuously-yielding
block contact cmodel default continuously-yielding
block contact property stiffness-normal 100000 stiffness-shear 100000
exponent-normal 0.0 exponent-shear 0.0 friction 30 friction-initial 59.3
roughness 1.0e-4
;
block gridpoint apply velocity-x 0 range pos-x -0.06 -0.04 pos-y -1 1
block gridpoint apply velocity-x 0 range pos-x 0.24 0.26 pos-y -1 1
block gridpoint apply velocity-y 0 range pos-x -1 1 pos-y -0.11 -0.09
; apply normal load
block edge apply stress 0 0 -10 range pos-x -1 1 pos-y 0.09 0.11
;
block cycle 1000
;
```

```
; functions to calculate average joint stresses
; and average joint displacements
;
fish define ini_jdisp
njdisp0 = 0.0
sjdisp0 = 0.0
ic = block.contact.head
loop while ic # 0
njdisp0 = njdisp0 + block.contact.disp.normal(ic)
sjdisp0 = sjdisp0 + block.contact.disp.shear(ic)
ic = block.contact.next(ic)
endloop
end
@ini_jdisp
;
fish define av_str
whilestepping
sstav = 0.0
nstav = 0.0
njdisp = 0.0
sjdisp = 0.0
ncon = 0
jl = 0.2 ; joint length
ic = block.contact.head
loop while ic # 0
ncon = ncon+1
sstav = sstav + block.contact.force.shear(ic)
nstav = nstav + block.contact.force.normal(ic)
njdisp = njdisp + block.contact.disp.normal(ic)
sjdisp = sjdisp + block.contact.disp.shear(ic)
ic = block.contact.next(ic)
endloop
if ncon # 0
sstav = sstav / jl
nstav = nstav / jl
njdisp = (njdisp-njdisp0) / ncon
sjdisp = (sjdisp-sjdisp0) / ncon
```

```
endif
end
fish callback 0 av_str
;
block contact reset displacement
block gridpoint init displacement-x 0
block gridpoint init displacement-y 0
hist reset
;
hist interval 1
fish history @sstav
fish history @nstav
fish history @njdisp
fish history @sjdisp
;hist name 1 label 'Shear Stress'
;hist name 3 label 'Normal Displacement'
;hist name 4 label 'Shear Displacement'
;
*********************************************************************************
;rockblot
block struct rockbolt create begin 0.1,0.2 end 0.1,-0.20 seg 1 prop 50
block struct rockbolt prop 20 cross-sectional-area 5E-4 coupling-
cohesion-normal 1E5 coupling-friction-normal 45 coupling-stiffness-normal
2E7 coupling-cohesion-shear 1E5 coupling-friction-shear 45 coupling-
stiffness-shear 2E7 density 1E-3 young 2E11 moi 2E-8 perimeter 8E-2
tension-failure-strain 0.2 yield-tension 2.25E5 yield-compression 2.23E5
*********************************************************************************
;
; apply shear load by imposing x-velocity on top block
block gridpoint apply velocity-x 0.01 range pos-x -.01 .21 pos-y -.01 .11
;
block cycle 6500
;
;plot hold hist -1 vs 4
;plot hold hist 3 vs 4
;
;his write 1 file 'sstav.his'
;his write 2 file 'nstav.his'
```

```
;his write 3 file 'njdisp.his'
;his write 4 file 'sjdisp.his'
;
model save 'cy_1.sav'
;
Return
```

Appendix D

UDEC Simulation for Barton-Bandis Joint Model (B-B) with Unbolted and Bolted Joint for CNL Conditions

D.1 Comparison of Joint Roughness for Shear Stresses

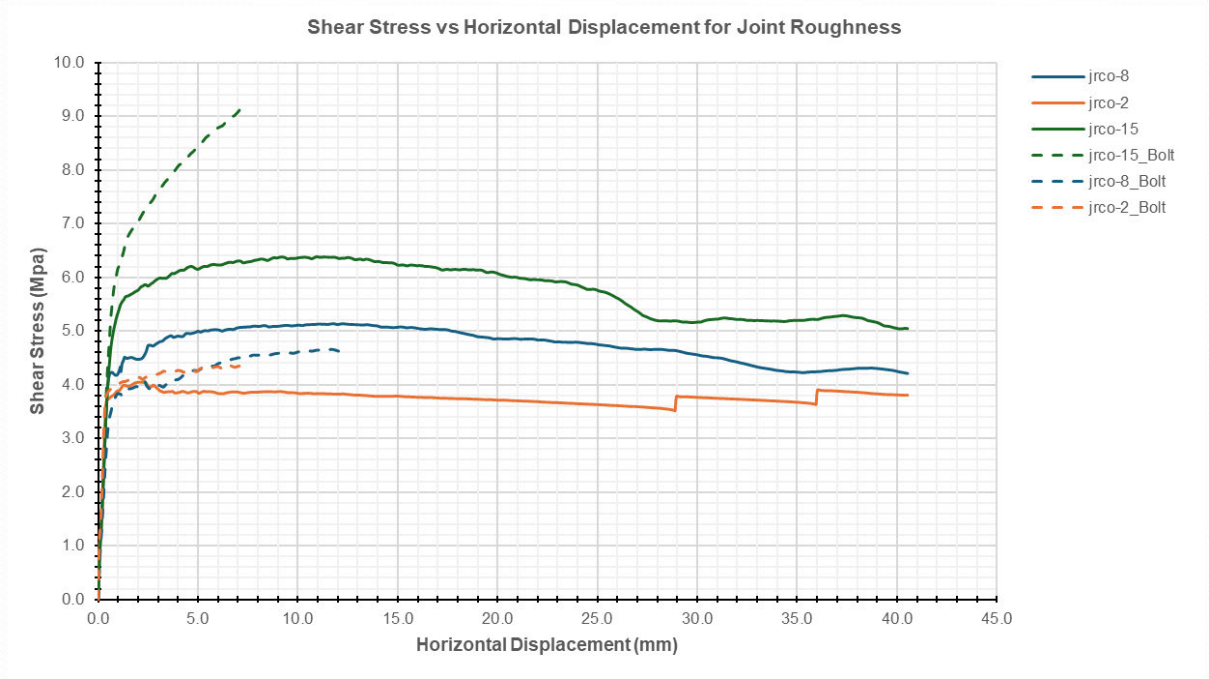

D.2 Comparison of Joint Roughness for Normal Stresses

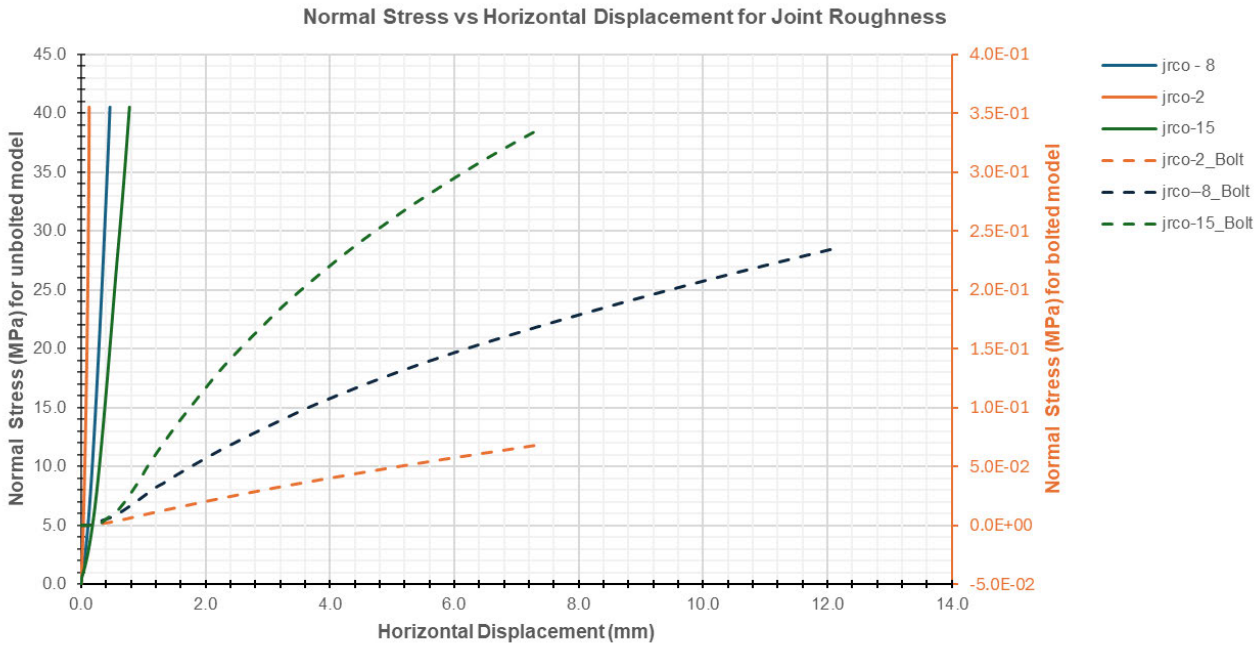

D.3 Comparison of Compressive Strength for Shear Stresses

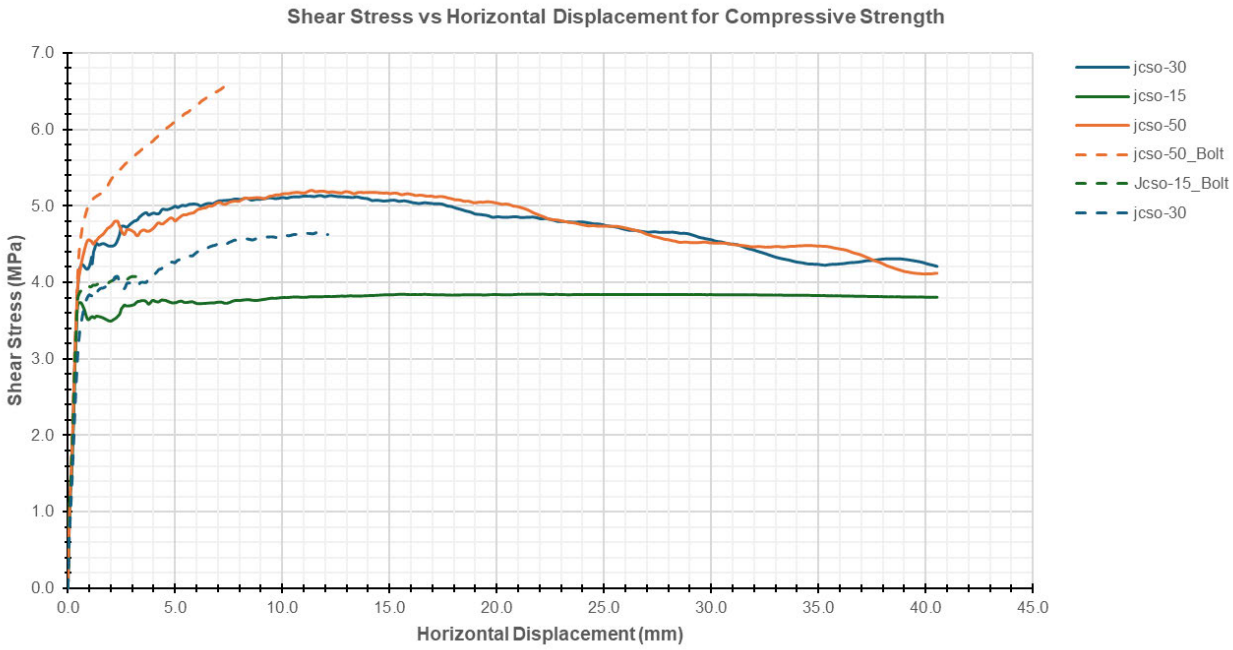

D.4 Comparison of Compressive Strength for Normal Stresses

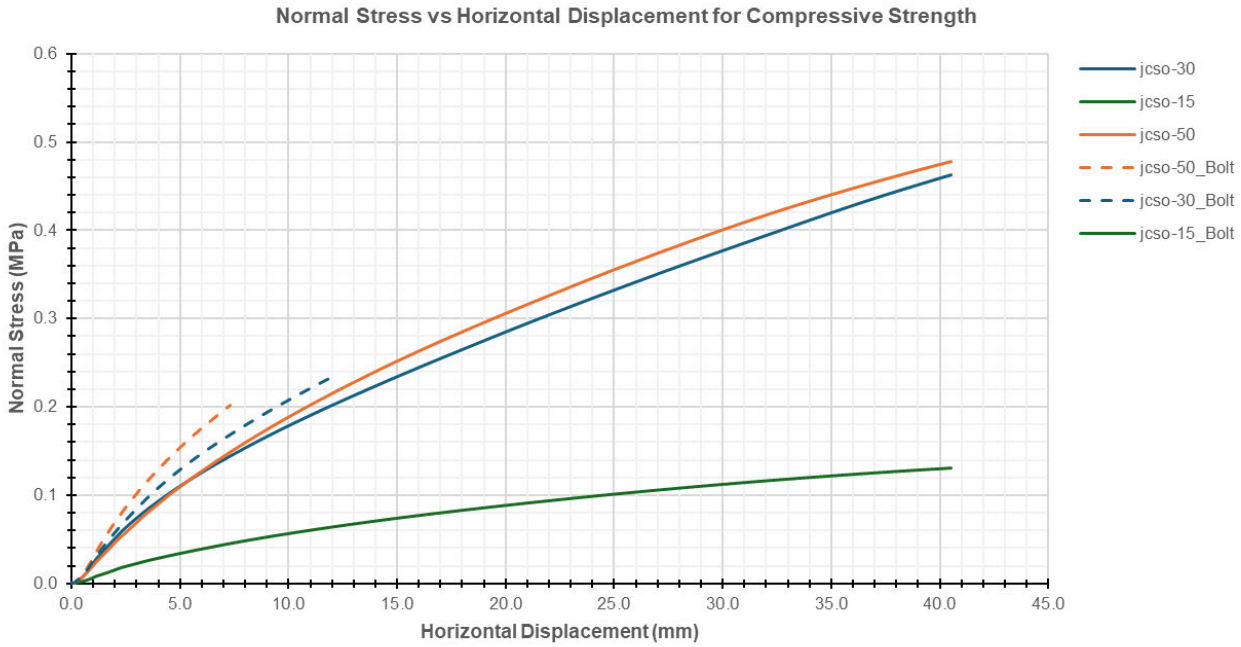

D.5 Comparison of Varies Normal Load for Shear Stresses

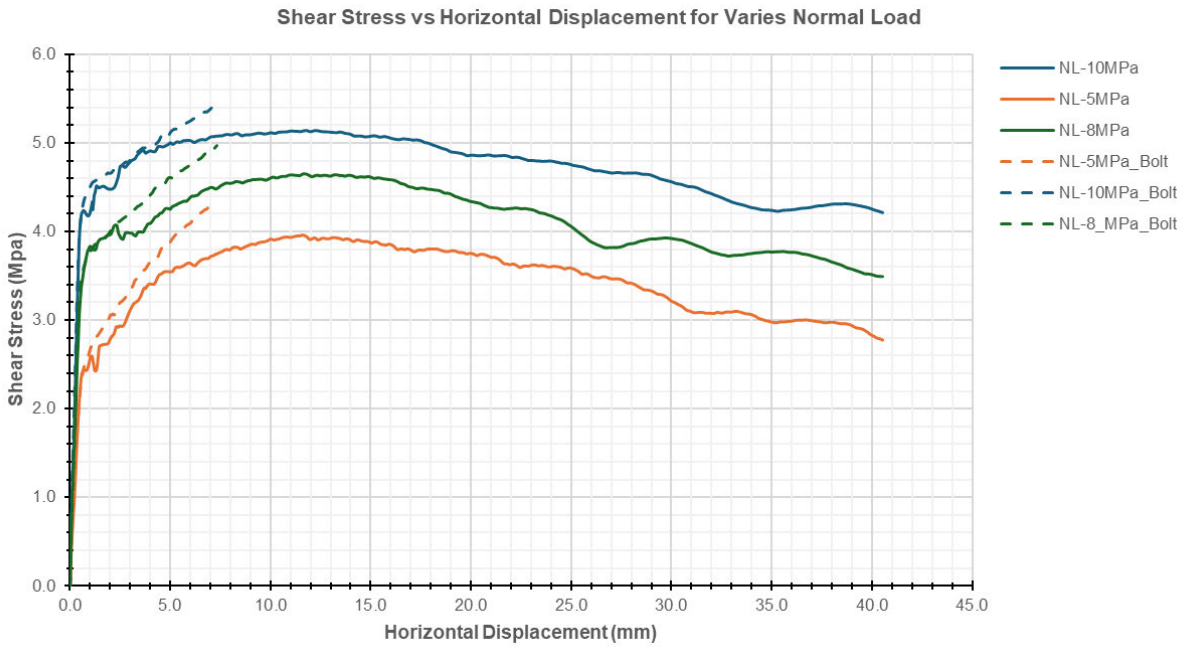

D.6 Comparison of Varies Normal Load for Normal Stresses

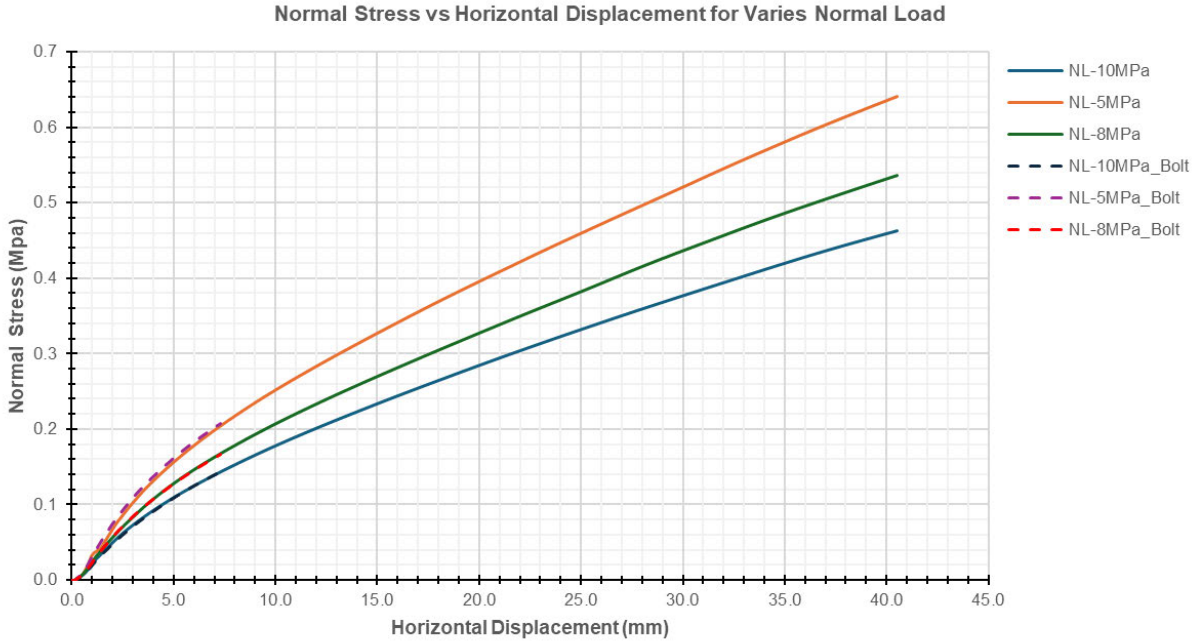

Appendix E

UDEC Simulation for Continuously Yielding Joint Model (C-Y) with Unbolted and Bolted Joint for CNL Conditions

E.1 Comparison of Joint Roughness for Shear Stresses

E.2 Comparison of Joint Roughness for Normal Stresses

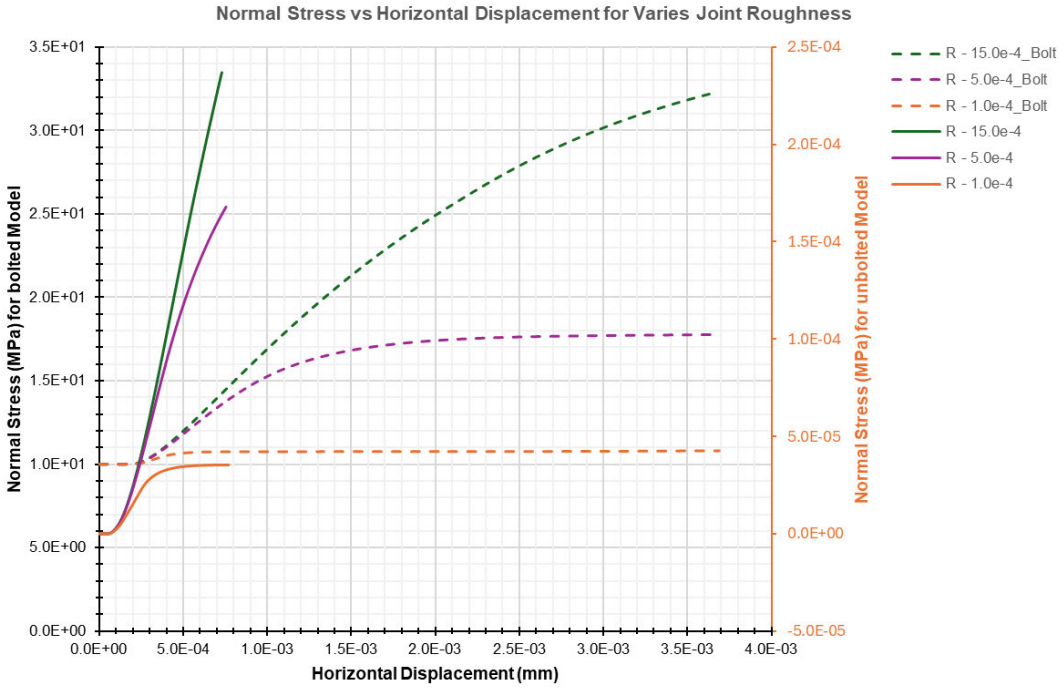

E.3 Comparison of Joint Friction Angle for Shear Stresses

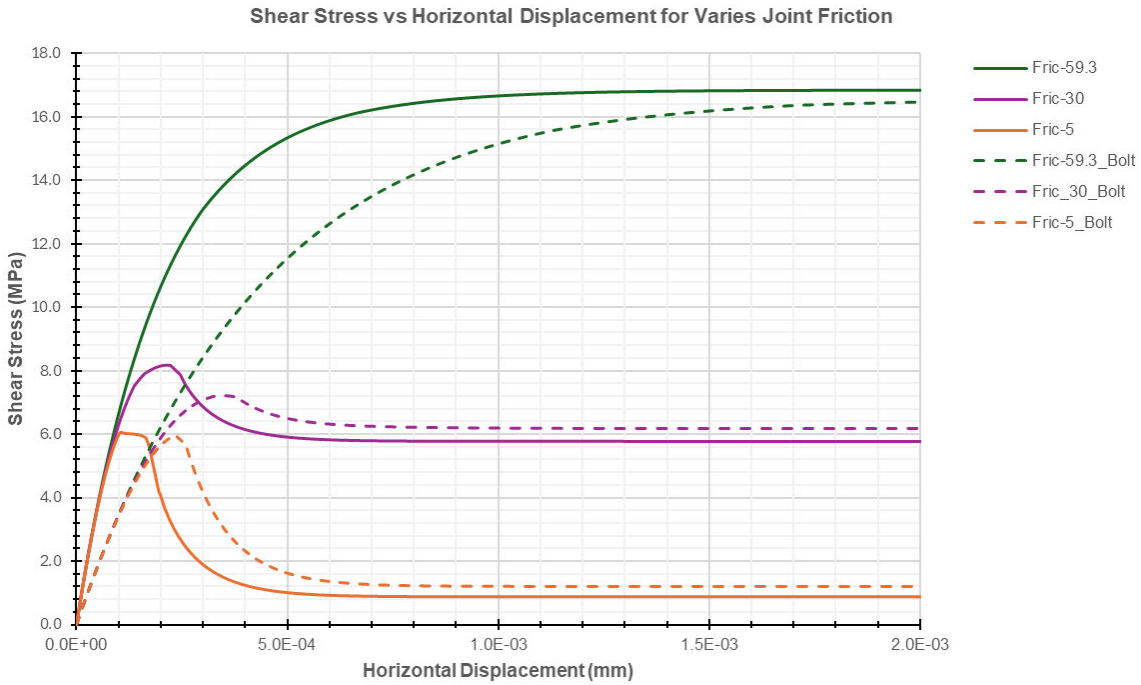

E.4 Comparison of Joint Friction Angle for Normal Stresses

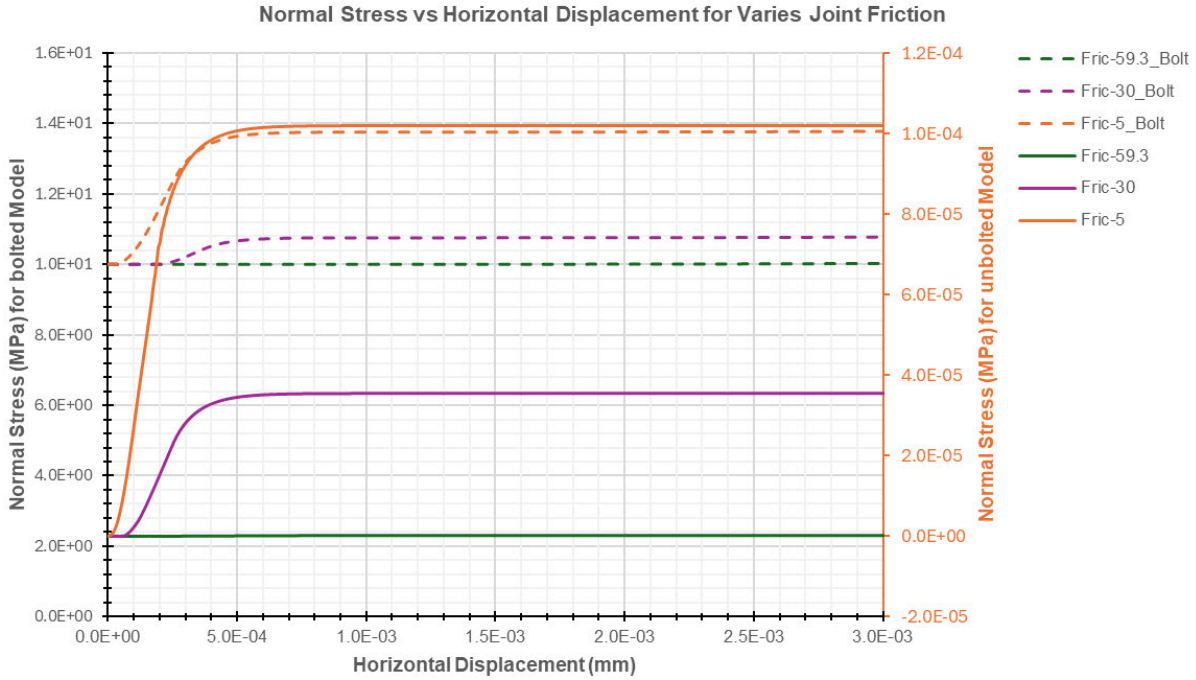

E.5 Comparison of Varies Normal Loads for Shear Stresses

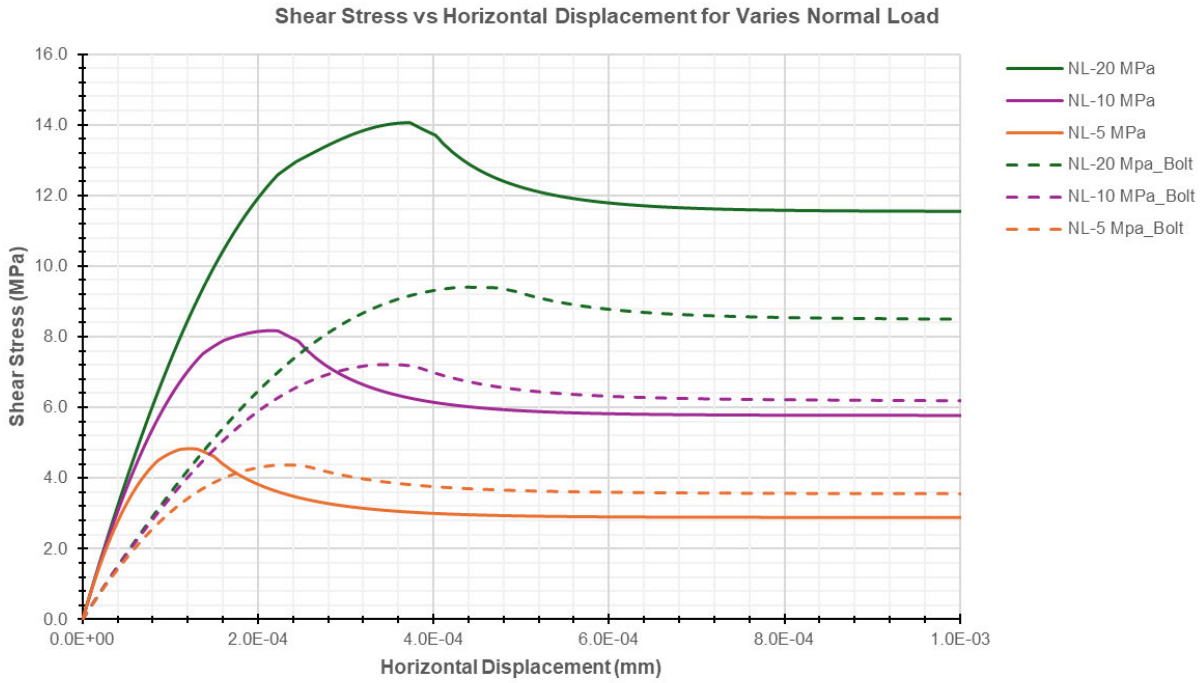

E.6 Comparison of Varies Normal Loads for Normal Stresses

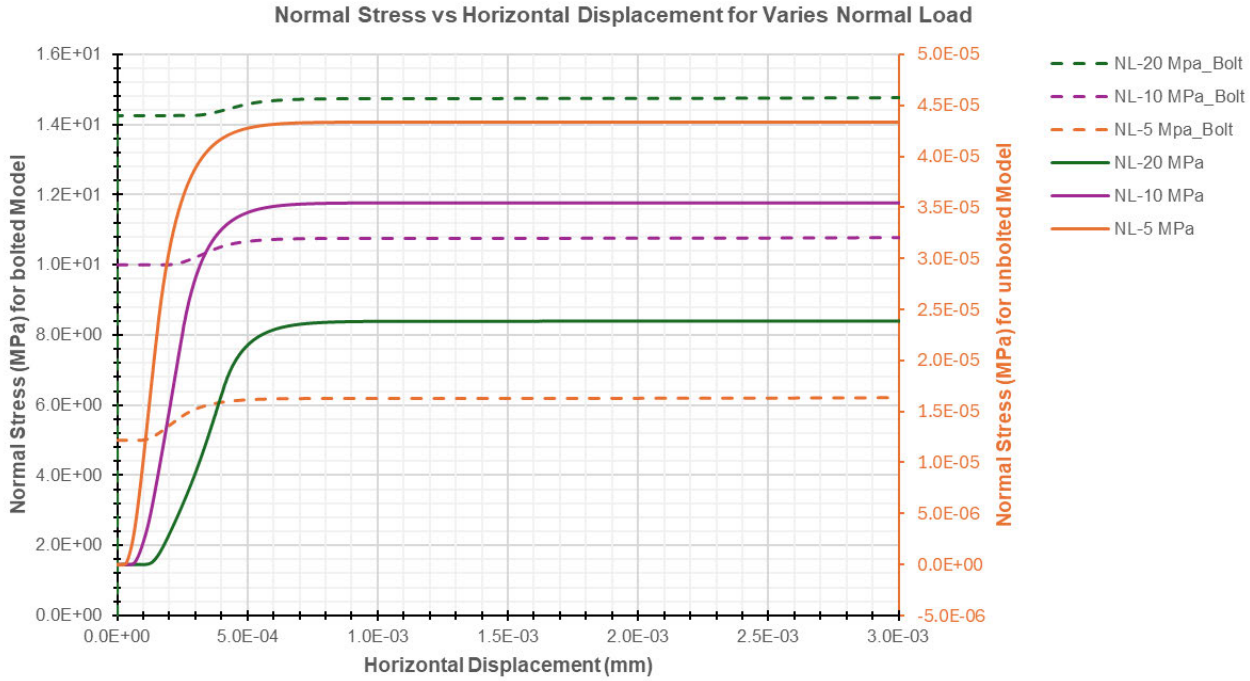

Appendix F

UDEC Simulation for Mohor Coulomb Joint Model (M-C) with Unbolted and Bolted Joint for CNL Conditions

F.1 Comparison of Joint Friction for Shear Stresses

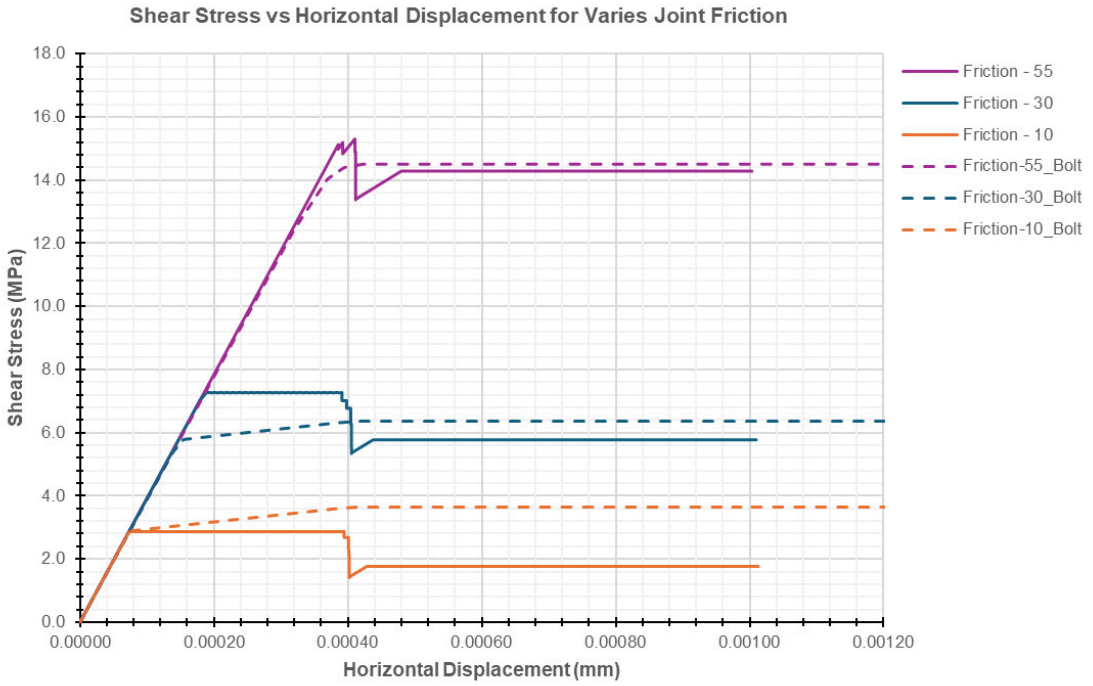

F.2 Comparison of Joint Friction for Normal Stresses

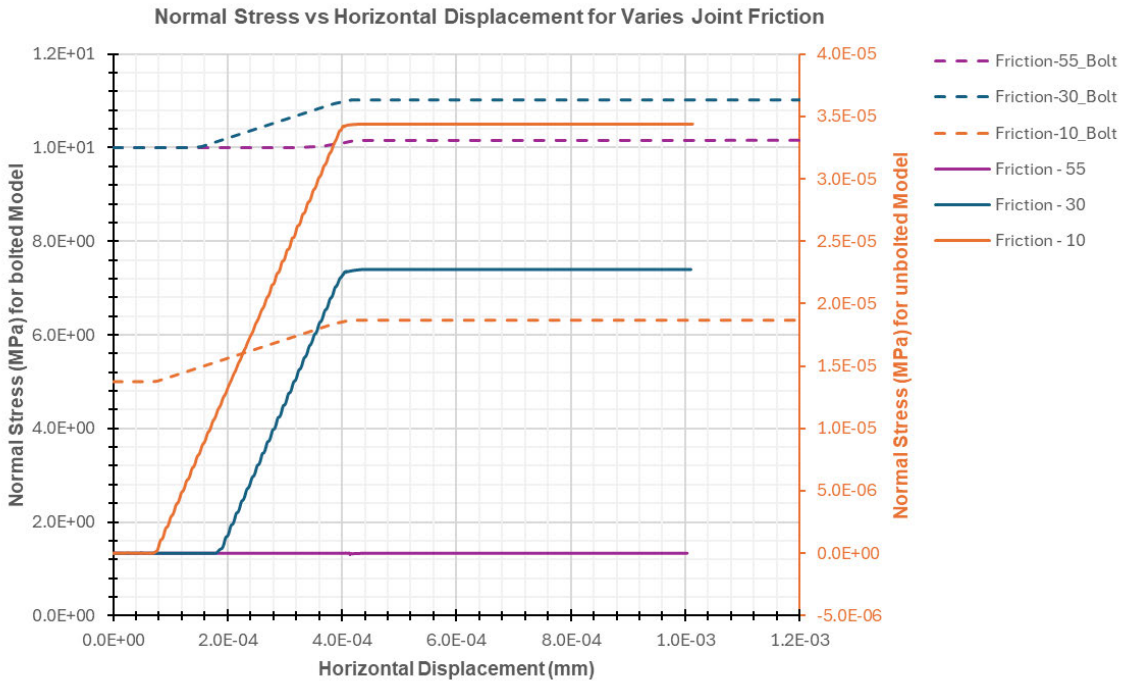

F.3 Comparison of Joint Dilation for Shear Stresses

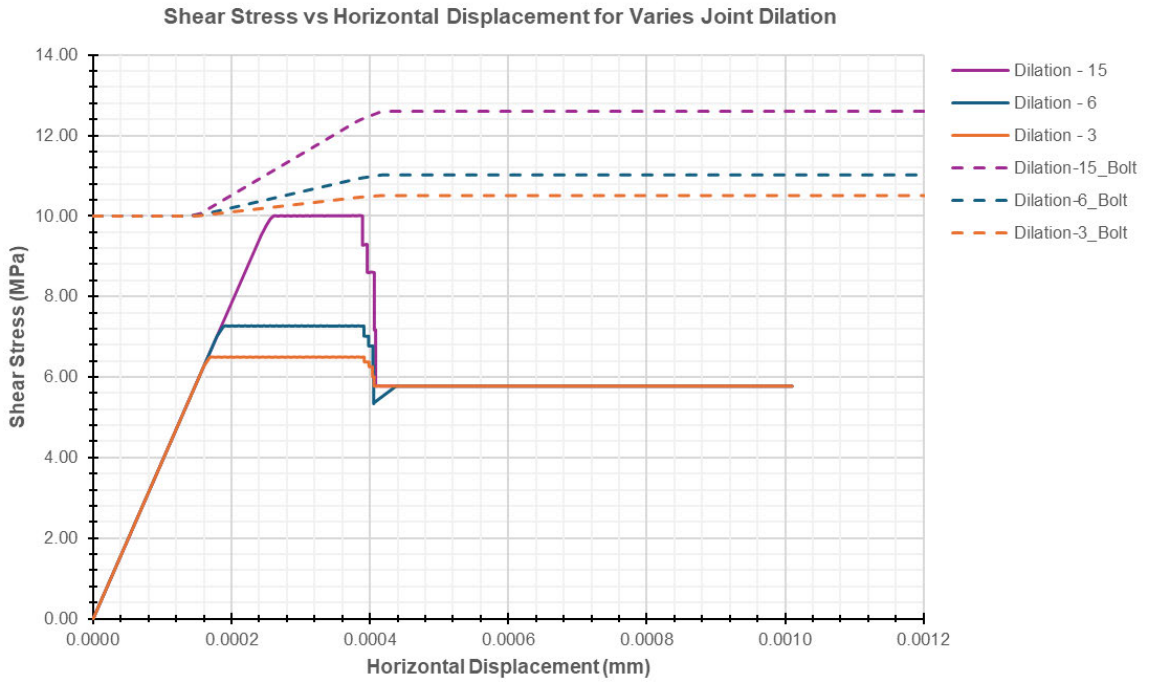

F.4 Comparison of Joint Dilation for Normal Stresses

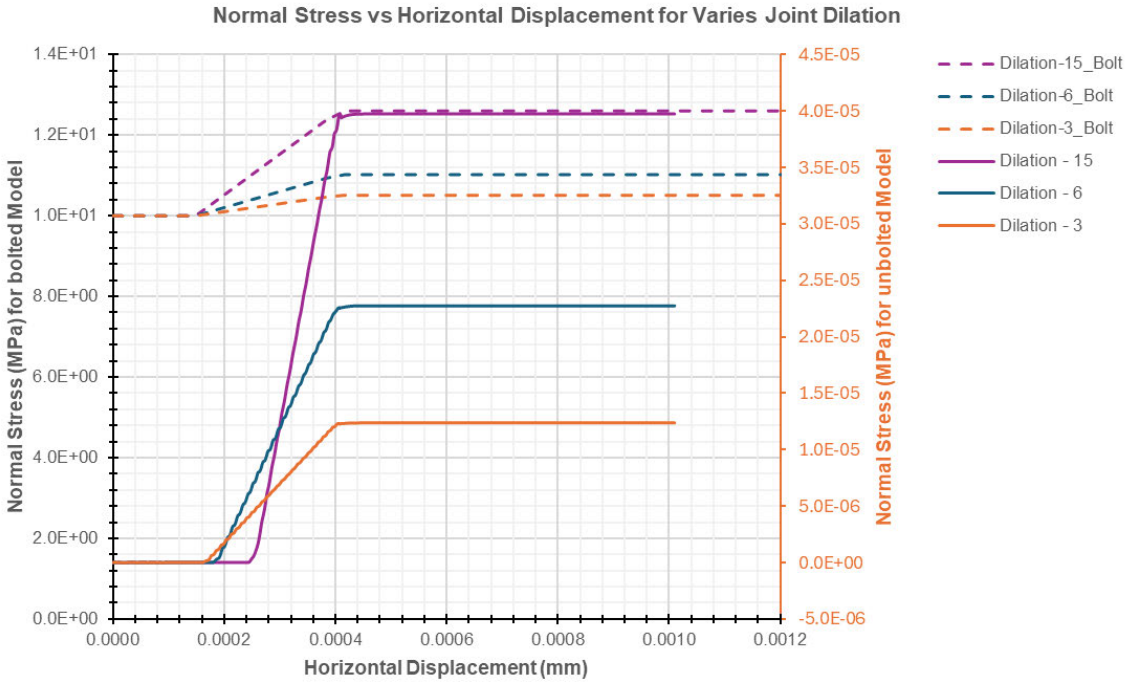

F.5 Comparison of Varies Normal Load for Shear Stresses

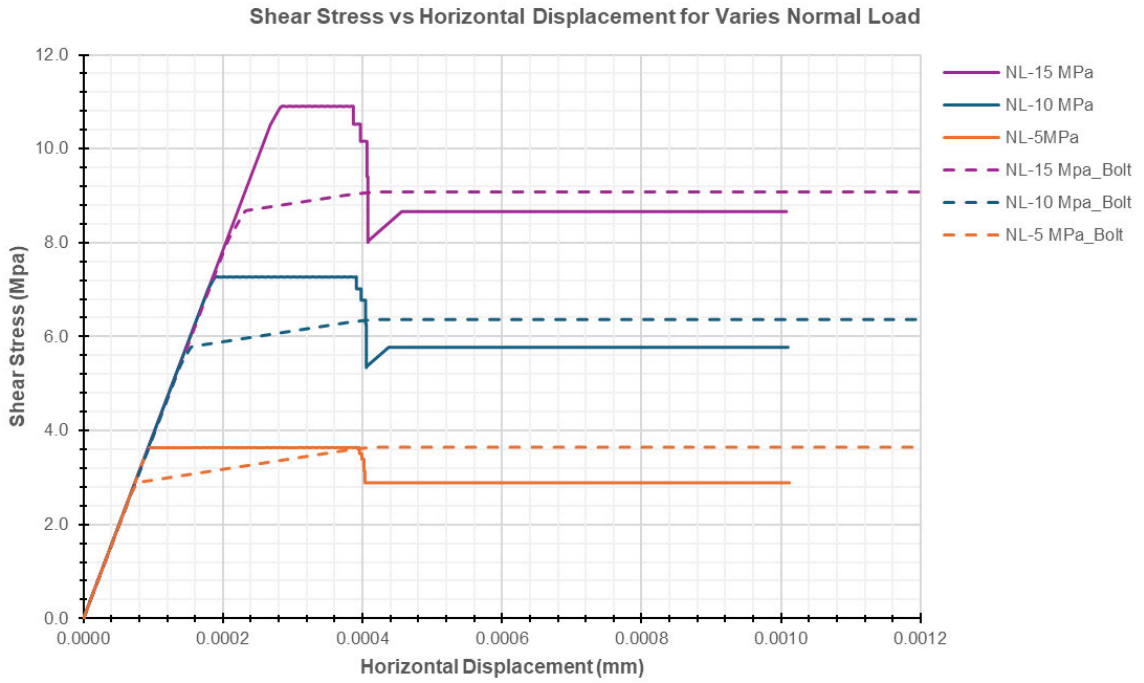

F.6 Comparison of Varies Normal Load for Normal Stresses

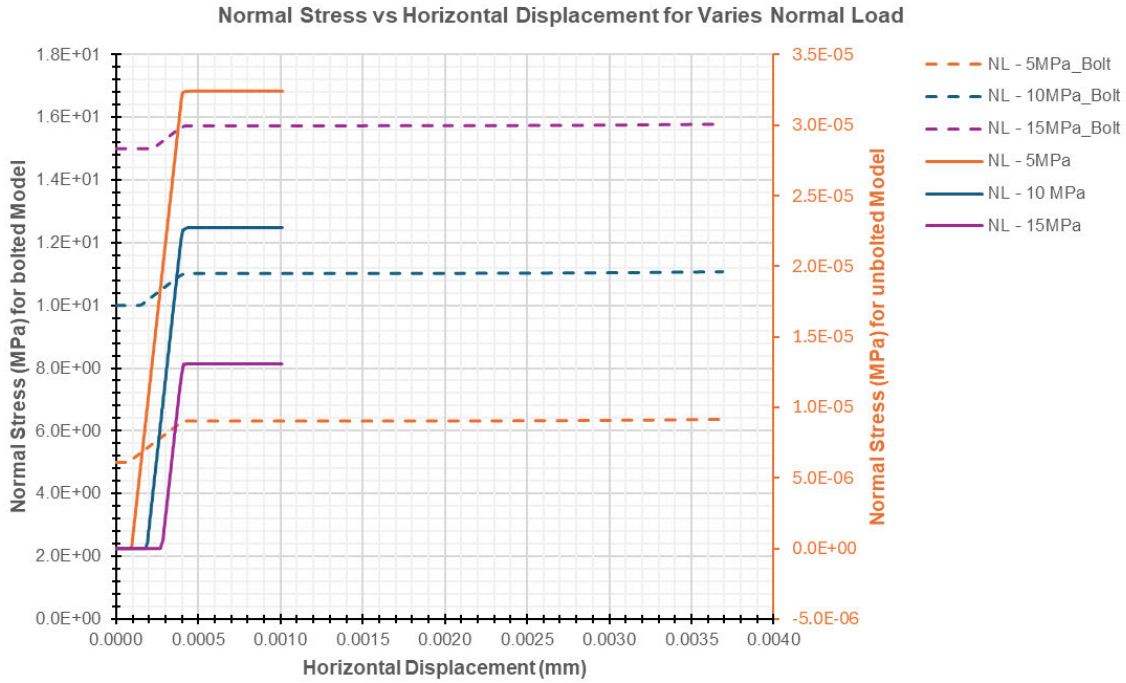

This page intentionally left blank